Response Spectra
for
Seismic Analysis and Design

by

Bo Li

A thesis
presented to the University of Waterloo
in fulfilment of the
thesis requirement for the degree of
Doctor of Philosophy
in
Civil Engineering

Waterloo, Ontario, Canada, 2015

Author's Declaration

I hereby declare that I am the sole author of this thesis. This is a true copy of the thesis, including any required final revisions, as accepted by my examiners.

I understand that my thesis may be made electronically available to the public.

Abstract

Earthquakes are one of the greatest natural disasters to human life and properties. Following lessons from previous earthquake disasters, the performance-based seismic design is increasingly accepted by engineers to prevent seismic disasters. In performance-based seismic design, realistic and reliable design response spectra are required to reliably and accurately predict responses of designing structures. However, the mostly used ground response spectra, i.e., Newmark design spectrum and Uniform Hazard Spectrum on soil surface, and floor response spectrum constructed by current methods do not properly meet the requirements of performance-based seismic design:

1. Newmark design spectrum exhibits lower amplitudes at high frequencies and higher amplitudes at low frequencies. Thus, it cannot realistically and reliably reflect seismic features of target sites.

2. Variability of soil parameters, nonlinear property of soils, and vector-valued seismic site response analysis are not integrated into the process of constructing Uniform Hazard Spectrum on soil surface in modern methodologies. Thus, the desired design response spectrum is not realistically and reliably represented.

3. An efficient method to generate probabilistic floor response spectrum considering random ground motions has not been addressed. The direct spectra-to-spectra method to generate floor response spectrum is superior to the time history analysis method in efficiency. However, this method is not applicable currently to generate probabilistic floor response spectrum.

The objective of this study is bridge the gap between performance-based seismic design and realistic design response spectra.

1. Considering the problem of Newmark design spectrum, this study establishes a system of site design spectrum coefficients to modify the Newmark design spectrum. The modified Newmark design spectrum could more realistically and reliably represent seismic features of target sites.

2. To obtain more realistic and reliable Uniform Hazard Spectrum on soil surface, this study integrates the variability of soil parameters, the nonlinear property of soils, and the vector-valued seismic site response analysis into the process of constructing Uniform Hazard Spectrum on soil surface.
3. This study investigates contribution of ground motions (i.e., tuning cases) to the uncertainty of floor response spectrum, and established the statistical relationship between t-response spectrum and ground response spectrum. Using this statistical relationship, probabilistic floor response spectrum by the direct spectra-to-spectra method considering random ground motions could be constructed.

With results of this study, the most economic solution to the balance between the safety and economy is expected to reliably obtain for performance-based seismic design for the nuclear industry.

Acknowledgments

I would like to express my gratitude to my supervisors, Professor Wei-Chau Xie and Professor Mahesh D. Pandey, whose support, encouragement, and guidance from the initial and final level enabled me to complete this thesis. I would like to thank Professors Wei-Ya Xu, Giovanni Cascante, Dipanjan Basu, Kumaraswamy Ponnambalam for the serving as my thesis committee members, and for their insightful comments and cares for my research.

A very special thanks goes out to Dr. Jack W. Baker from the Department of Civil and Environmental Engineering at the Stanford University for providing the MATLAB code of ground motion prediction equations. With his help, I could easily finish my computer code to perform PSHA for soil sites.

Thanks also go to my friends and colleagues, Dr. Tian-Jin Cheng, Dr. Dong-Liang Lu, Dr. Shun-Hao Ni, Dr. Jian Deng, Dr. De-Yi Zhang, Dr. Zhao-Liang Wang, Dr. Xu-Fang Zhang, Dr. Yu-Song Xue, Dr. Yi Zhuang, Wei Jiang, Zhen Cai, Sen Long, Qing-Xiang Meng, Chao Wu, Fan Li and other graduate students in the Department of Civil and Environmental Engineering.

The financial support by the Natural Sciences and Engineering Research Council of Canada (NSERC) and the University Network of Excellence in Nuclear Engineering (UNENE) in the form of a Research Assistantship is greatly appreciated.

Lastly and most importantly, I would like to thank my parents, without their decades of material aids and spiritual supports, I cannot go from primary school to postgraduate school, and I cannot finish this thesis.

Contents

List of Figures

Nomenclature

AEC	Atomic Energy Commission
CENA	Central and Eastern North America
DBE	Design Based Earthquake
DOF	Degree-Of-Freedom
DRS	Design Response Spectra
FRS	Floor Response Spectrum
GMPE	Ground-Motion Prediction Equation
GRS	Ground Response Spectrum
NEHRP	National Earthquake Hazard Reduction Program
NEP	non-exceedance probability
NGA	Next Generation Attenuation
NPP	Nuclear Power Plant
PEER	Pacific Earthquake Engineering Research
PGA	Peak Ground Acceleration
PGD	Peak Ground Displacement
PGV	Peak Ground Velocity
PSD	Power Spectral Density
PSHA	Probabilistic Seismic Hazard Analysis
P-BSD	Performance-Based Seismic Design
SDOF	Single Degree-of-Freedom
SEAOC	Structural Engineers Association of California
SHD	Seismic Hazard Deaggregation

SRSS	square root of the sum of the squares
SSC	Structure, System, or Component
SSE	Safe Shutdown Earthquake
tRS	t-Response Spectrum
UHS	Uniform Hazard Spectrum
USGS	U.S. Geological Survey
USNRC	U.S. Nuclear Regulatory Commission
WNA	Western North America

CHAPTER 1

Introduction

In Section 1.1, the seismic analysis and design in engineering is introduced, and several relative issues are discussed. Based on the problems discussed in Section 1.1, the objectives of this study are presented in Section 1.2. The organization of this thesis is then presented in Section 1.3.

1.1 Overview

Earthquakes are one of the greatest natural disasters to human life and properties. Historically, hundreds of thousands of people were injured or died during earthquakes, such as Kanto Earthquake in 1923, Tangshan Earthquake in 1976, and Tohoku Earthquake in 2011. Disasters by earthquakes are almost all due to the effects of earthquake forces on structures and failure of the ground that supports these structures. To prevent seismic disasters, people need to properly design structures that could resist the damage or failure caused by earthquakes.

In 1995, Structural Engineers Association of California (SEAOC) developed conceptual framework of performance-based seismic engineering (Committee, 1995). Under this framework, designing structures needs to satisfy seismic performance within established levels of risk. After 1995, Performance-Based Seismic Design (P-BSD) has been introduced in many regular building standards (FEMA, 1997; FEMA, 2000; ATC, 1996; IBC, 2000), and nuclear building standards (USNRC, 2007a; ANS, 2004; ASCE, 2005).

For critical buildings, such as Nuclear Power Plants (NPPs), reliable design response spectrum considering detailed information of specific target sites, such as local soil conditions, seismic configurations, and dynamic characteristics of designing structures, is required for seismic analysis and design with specified approaches, such as P-BSD.

Design response spectrum is one of the useful tools of earthquake engineering for analysis and design. Different types of design response spectra in engineering are presented in Figure 1.1:

- Design response spectrum at bedrock reflects characteristics of ground motions propagating from seismic sources to bedrock. For structures designed on the bedrock, this type of design response spectrum should be used.
- Design response spectrum at a control point under the soil surface reflects characteristics of ground motions propagating from seismic sources to bedrock then to the control point under the soil surface.

  In nuclear power plants, foundations of structures are usually embedded in soil, at least to some extent. For many cases, the conditions of embedment are complicated. For example, structures are not supported uniformly around their circumferences because of adjacent structures and cuts in the soil, such as for transportation, pipe tunnels, etc. Foundation embedment has a significant effect on soil-structure interaction: in comparison with a surface foundation, both the foundation input motion and the foundation impedances change for an embedded foundation. For vertically propagating waves, a horizontal shear wave produces both a horizontal translation and rotation of the embedded massless foundation; a vertical compression wave produces a vertical translation and rocking of the embedded massless foundation. In general, the amplitude of a foundation input motion for embedded foundations is less than that for surface foundations, especially in the high-frequency range. Structural responses are thus reduced for embedded foundations.

  For nuclear power plants, during the seismic design of a soil-foundation-structure system, if the foundation is embedded under the soil surface, design response spectra at the control point under the soil surface—where the foundation level is—should be used.

However, location of the foundation is not always known at the time when the design response spectrum is constructed (USNRC, 2007A). Thus, design response spectra at several depths of the site profile need to be established considering the free-field ground response; the effect of soil-structure interaction is not considered. In addition, because soil parameters usually exhibit large variabilities, it causes uncertainty of the design response spectra at various depths of the site profile. Thus, probabilistic design response spectrum at a control point under the soil surface may be required to accurately reflect the seismic hazards at corresponding locations.

- Design response spectrum on the soil surface reflects characteristics of ground motions propagating from seismic sources to bedrock then to soil surface. For structures designed on the soil surface, this type of design response spectrum should be used.
- Floor response spectrum (FRS) reflects dynamic characteristics of the supporting structures under specific levels of seismic excitations. When designing secondary structures or equipment mounted on the supporting structures, this type of design response spectrum should be used.

These four types of design response spectra can be categorized as two general design response spectra: ground response spectrum (GRS) and floor response spectrum (in-structure response spectrum). GRS is used to analyze and design structures directly contacted with the ground, such as bedrock or soil surface. Construction of GRS does not consider any information of designing structures. FRS is used to analyze and design equipment or secondary structures mounted on supporting structures. FRS can be considered as a GRS filtered by the supporting structure. Thus, FRS reflects dynamic characteristics of supporting structures and spectral characteristics of GRS.

1.1.1 Performance-Based Seismic Engineering

Having investigated the great economic losses in previous earthquakes, such as the 1989 Loma Prieta Earthquake with more than $10 billion losses (Bertero, 1992), and the 1994 Northridge Earthquake with over $20 billion losses (Goltz, 1994), people began to realize the critical role of facility-performance that plays in maintaining the operational and safe

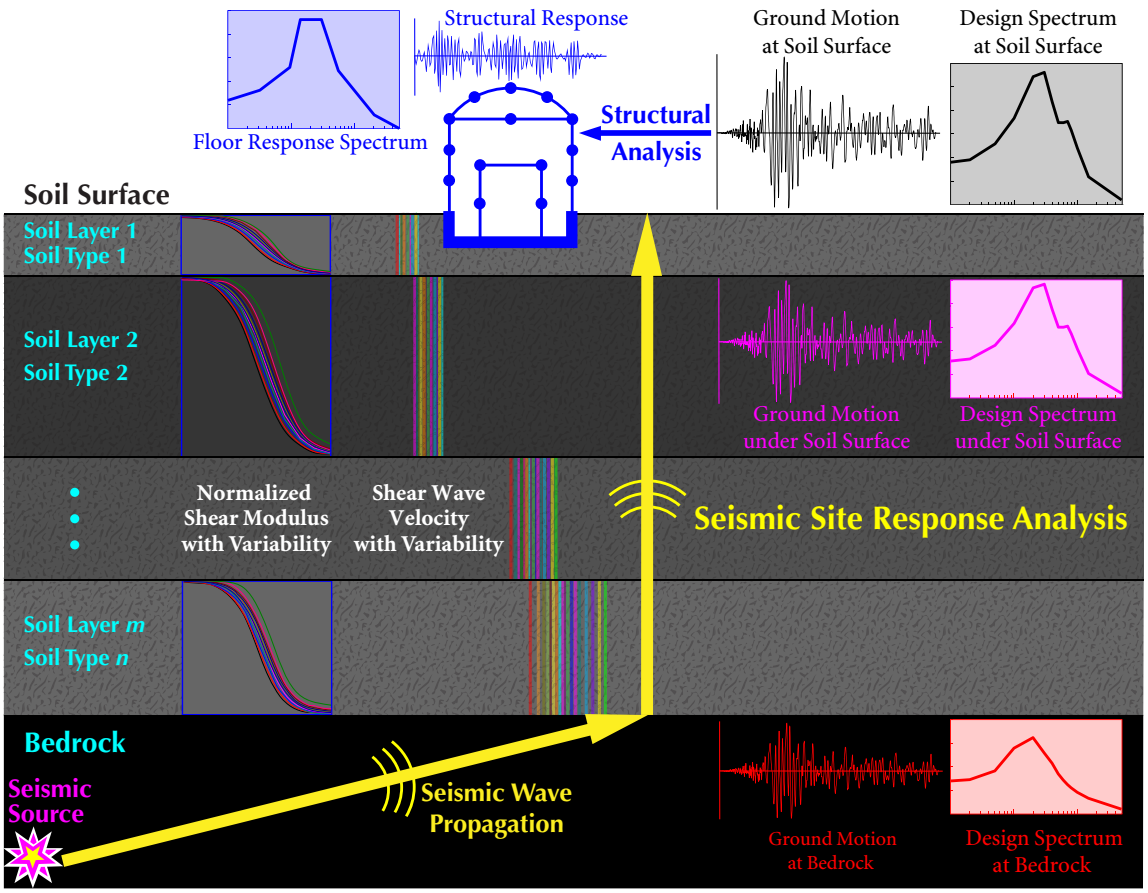

Figure 1.1 Design response spectra in earthquake engineering

function of entire systems, such as a building, during and after earthquakes (Bertero, 1992; Goltz, 1994; Bertero, 2000).

Following lessons from previous earthquakes with great economic losses, the original strength- and ductility-based design is not practically and reliably applicable to the design of new buildings; the P-BSD is increasingly accepted by engineers. In P-BSD, performance objectives describe the acceptable risk of different levels of structural or nonstructural damages caused by a specified level of seismic hazards. For different types of structures, different design criteria are used by selecting different performance objectives. Performance objectives are developed by linking a performance level to a specified level of seismic hazards. Performance levels describe the limiting values of measurable structural response parameters, such as interstory drift indexes, floor accelerations, and floor velocity. After selecting

performance levels, the associating limiting values become the acceptability criteria to be checked in the later stages of the design (Bozorgnia and Bertero, 2004). In order to reliably describe the performance levels, the theory of probability is introduced by Cornell and Krawinkler (Cornell and Krawinkler, 2000) into P-BSD. Under a specific design criterion, structures should be designed to satisfy the acceptable probability of measurable structural responses exceeding their corresponding limiting vales under a specified level of seismic hazards (failure probability). In determining the acceptable probability, a balance between safety and economy needs to maintain considering a variety of factors, such as the importance of structures, the economic condition of owners, and the society's needs. Thus, a most economic solution to the balance between safety and economy needs to obtain.

In order to obtain a most economic solution, an accurate and reliably prediction of the failure probability is required. To accurately predict the failure probability of structures, accurate and realistic prediction of structure responses, for which a realistic and reliable input design earthquake, e.g, design response spectrum, is an essential prerequisite, is required. Thus, a realistic and reliable design response spectrum is preliminarily important to P-BSD.

In nuclear industry, the philosophy of P-BSD is implemented to perform seismic design of safety-related Structures, Systems, and Components (SSCs) (ASCE, 2005). A structure refers to a collection of elements to provide support or enclosure, such as the supporting buildings, a system refers to a collection of components assembled to perform a certain function, such as piping, and a component refers to a mechanical or electrical equipment, such as a heat exchanger (ASCE, 2005). For SSCs standing on the ground, such as a reactor hall, a Design Based Earthquake (DBE) is required for design and analysis, while for SSCs mounted on supporting buildings, such as a heat exchanger, a FRS is required for design and analysis. Therefore, accurate and realistic DBE and FRS become crucial to the P-BSD of nuclear facilities.

1.1.2 Ground Response Spectrum for Seismic Analysis and Design

In earthquake engineering, the most important characteristics of ground shaking are the amplitude and the frequency content. In seismic analysis and design, these two characteristics are reduced to the spectral shape and the spectral amplitude of design response spectra. Effects of spectral amplitudes and spectral shapes on dynamic responses of structures have been recognized (Baker and Cornell, 2006; Seifried and Baker, 2014; McGuire, Silva, and Costantino, 2001; ASCE, 2010; Chopra, 2011). Previous studies (Baker and Cornell, 2006; Boore and Atkinson, 2008; Trifunac, 1976; Trifunac, 1989; Kramer, 1996; Bommer and Acevedo, 2004; Stewart, Chiou, Bray, *et al.*, 2001) implied that spectral shapes and spectral amplitudes are influenced by earthquake magnitudes, source-to-site distances, local site conditions, and fault types. Among these factors, earthquake magnitudes and local site conditions greatly affect spectral shapes of a design response spectrum (Kramer, 1996; Bommer and Acevedo, 2004; Stewart, Chiou, Bray, *et al.*, 2001). Therefore, GRS used for analysis and design should possibly consider these two factors affecting spectral shapes and spectral amplitudes of design response spectra.

Site-independent design response spectrum for NPPs

The concept of elastic response spectrum was first proposed by Biot (Biot, 1933; Biot, 1941). Housner used this concept and developed the first seismic design response spectrum in 1959 (Housner, 1959; Housner, 1970) (called Housner's design spectrum) by averaging and smoothing the response spectra of eight ground motions, i.e., two horizontal components of ground motions recorded during the earthquakes of 1934 and 1940 in EI Centro, the earthquake of 1949 in Olympia, the earthquake of 1952 in Taft. In addition, response spectra of the eight ground motions were anchored to Peak Ground Acceleration (PGA) of 0.2 *g*. For design response spectra corresponding to other PGAs, one only needs to multiply the initial design response spectrum by the ratio of the desired PGA to 0.2 *g*.

In Housner's design spectrum, only PGA is used to quantify the damage potential of earthquakes. However, at very high frequencies, the spectral accelerations of response spectrum approach GPA, whereas at other frequencies, the spectral accelerations of response

spectrum are quite different from PGA. Thus, using a fixed spectral shape and scaling it with a single parameter, i.e., PGA, is not conceptually justified; the variation of spectral shapes due to some other factors, such as earthquake magnitudes, source-to-site distances, and local site conditions, should be considered.

During 1970s, Atomic Energy Commission (AEC) funded two studies—one by John A. Blume and Associates (Blume *et al.*, 1973) and the other by N. M. Newmark Consulting Engineering Services (Newmark *et al.*, 1973B)—to develop design response spectra for NPPs.

In Blume's research group, they used a statistical analysis of 31 ground motions and computed response spectra of these ground motions. Using a set of amplification factors corresponding to four controlling frequencies, Blume *et al.* recommended the 84.1% non-exceedance probability horizontal and vertical design response spectra for the nuclear industry. These design response spectra are used in the Standard U.S. Nuclear Regulatory Commission (USNRC) R.G. 1.60 (USNRC, 2014) for seismic design of nuclear structures.

In Newmark's research group, they observed that some spectral ordinates are affected more by Peak Ground Velocity (PGV) or Peak Ground Displacement (PGD) than by PGA. For a given response spectrum, there are three sensitive regions: acceleration sensitive region in high frequency band, velocity sensitive region in intermediate frequency band, and displacement sensitive region in low frequency band. Based on spectrum amplification factors in different sensitive regions for various damping ratios, Newmark and Hall (Hall, Mohraz, and Newmark, 1976; Newmark and Hall, 1982) proposed a smooth elastic design spectrum, i.e., Newmark design spectrum, which has been widely used in many building standards, such as ASCE 4-98 (ASCE, 2000), DOE-STD-1023-2002 (DOE, 2002), and CSA N289.3-10 (CSA, 2010). One previous study (Newmark *et al.*, 1973A) showed that the design response spectra recommended by Blume's research group and those by Newmark's research group are in substantial agreement.

Construction of Newmark design spectrum requires spectrum amplification factors and ground motions parameters (i.e., PGA, PGV, and PGD). In Newmark *et al.* (Newmark *et al.*, 1973B), 28 horizontal and 14 vertical ground motions were used to determine the probability distributions of horizontal and vertical spectrum amplification factors, respec-

tively. For sites lacking information about PGA, PGV, and PGD, relationships among these three ground motion parameters were recommended (Hall, 1982; Newmark and Hall, 1982): $v/a = 48$ (in/sec)/g for competent soil sites and $v/a = 36$ (in/s)/g for rock sites, and $ad/v^2 = 6.0$ for all types of sites, where a, v and d represent PGA, PGV, and PGD, respectively. In Newmark design spectrum, acceleration-amplification factor α_{A}, velocity-amplification factor α_{V}, and displacement-amplification factor α_{D} characterize the spectral amplitude in the high frequency range, in the intermediate frequency range, and in the low frequency range, respectively. The relationships among ground motion parameters mainly characterize the spectral shape.

Because the ratios v/a and ad/v^2 recommended by Newmark do not consider earthquake magnitudes, and spectrum amplification factors recommended by Newmark do not consider local soil conditions and earthquake magnitudes, the problem of Newmark design spectrum has been caused. Previous studies (Dunbar and Charlwood, 1991; Mohraz, 1976; Mohraz, 1978; Mohraz, 1992) specified that Newmark design spectrum exhibits lower amplitudes at high frequencies and higher amplitudes at low frequencies in comparison with response spectra developed by the statistical method. To perform P-BSD, more accurate and realistic Newmark design spectra characterizing the earthquake features of target sites are required.

The Housner's design spectrum, design spectrum in USNRC R.G. 1.60, and Newmark design spectrum are grouped as site-independent design response spectrum because they are obtained by statistical analysis of a certain suite of ground motions independent of target sites.

Site-specific design response spectrum for NPPs

The site-independent design response spectra discussed above represent design earthquakes for generic site conditions, such as soil sites or rock sites, without considering the detailed information of target sites. For critical structures, such as nuclear structures, a design response spectrum that covers detailed seismic information (such as site- and region-specific geological, seismological, and geotechnical characteristics) of target sites may be required to do performance-based seismic design and analysis (USNRC, 2007A).

With respect to a specific target site, a design response spectrum considering (1) regional seismicity, tectonic setting, and geology; (2) expected recurrence rates and maximum magnitude of events on known seismic sources; (3) site location with respect to known seismic sources and ground motion attenuation with distance; (4) near-source effects; and (5) subsurface characteristics, is called site-specific design response spectrum (Villaverde, 2009). Site-specific design response spectrum is exclusively used for the design of structures on the specific site, different from site-independent design response spectrum mentioned above.

The Probabilistic Seismic Hazard Analysis (PSHA) is an acceptable method to construct site-specific design response spectrum. The framework of PHSA was first proposed by C. A. Cornell (Cornell, 1968) in 1968. Following Cornell's work on integrating contributions to the seismic risk of a site, the concept of Uniform Risk Absolute Acceleration Spectra (which is called Uniform Hazard Spectrum nowadays) was first proposed by Anderson and Trifunac (Anderson and Trifunac, 1977; Anderson and Trifunac, 1978). After that, the nuclear industry (EPRI, 1986) and the USNRC (USNRC, 1994) systematically investigated the seismic hazard, developed a methodology to perform PSHA, and used the PSHA methodology to estimate seismic hazards for sites of NPPs in the Central and Eastern United States. In 1997, USNRC R.G. 1.165 (USNRC, 1997) implemented the latest PSHA methodology to determine the Safe Shutdown Earthquake (SSE) in the form of Uniform Hazard Spectrum (UHS).

Recently, several nuclear standards (ASCE, 2005; USNRC, 2007a; USNRC, 2007c) specify UHS for seismic design and analysis. In PSHA, the Ground Motion Prediction Equation (GMPE) is required to characterize seismic waves propagating from seismic sources to the target site. GMPEs are usually valid to describe the attenuation relation of ground motions propagating from seismic sources to rock sites, but they are usually invalid for soil sites due to the generic soil instead of site-specific soil used. Thus, to construct UHS on soil sites, PSHA for soil sites integrating seismic site response analysis and PSHA for rock sites is required.

For critical structures, such as nuclear structures, rock is usually defined as a geotechnical material whose shear-wave velocity is greater than 2.8 km/sec for sites in the Central and Eastern North America (USNRC, 2007a). In practice, most NPPs are located at soil sites

according to the definition of rock sites in nuclear industries. Therefore, how to construct reliable and accurate soil UHS is important for the P-BSD.

1.1.3 Floor Response Spectrum for Seismic Analysis and Design

Secondary systems are components, such as heat exchangers and piping systems, mounted on the floors of supporting structures that are not part of the main structural system for the supporting structures. Secondary systems maintain functional, safe, and operational performance of the entire primary-secondary system, particularly under the event of extreme loads such as earthquakes. Previous engineering experiences (Bozorgnia and Bertero, 2004; Villaverde, 2009) showed that the damage of secondary systems usually causes great injuries and financial loss.

Two special physical characteristics of secondary systems make them vulnerable to earthquake excitations. They are (Bozorgnia and Bertero, 2004; Villaverde, 1997):

- Most secondary systems are attached to the elevated parts of supporting structures. Thus, their responses depend on responses of the supporting structure on which they are mounted; not only ground motions at the base of the supporting structure but also amplified motions due to dynamic characteristics of the supporting structure affect responses of secondary systems.
- Because their masses are much smaller than those of the supporting structure on which they are mounted, and their stiffness is also much lower than that of the supporting structure as a whole, their natural frequencies are in many instances close to the natural frequencies of their supporting structure, which is called the tuning case (Asfura and Kiureghian, 1986) in engineering. As a result, they may be subjected to remarkably resonant vibrations.

Because of these special physical characteristics, the seismic responses of secondary systems are different from those of primary systems.

In the analysis of seismic responses of secondary systems, a decoupled approach is usually used; the secondary systems and their supporting structure are analyzed separately

(USNRC, 1978). Advantages of the decoupled approach used for the analysis of secondary systems include:

- Seismic responses of nuclear facility structures are usually analyzed by mathematical models. Because a large number of degrees of freedom in mathematical models are required due to the complicated and large structures in the analysis, some problems, such as ill-conditioning of the resulting stiffness matrix, usually arise from the single mathematical model representing the entire structure system. Therefore, it is quite necessary to divide the whole structure system into several separate systems for the seismic response analysis.
- The decoupled approach increases the efficiency of preliminary design of secondary systems. During preliminary design of secondary systems, if a change is introduced into parameters of the secondary systems or the secondary systems are replaced, only secondary systems need to be reanalyzed if the decoupled approach is used, in comparison with the combined approach, which needs to reanalyze the entire primary-secondary systems every time a change in parameters of the secondary systems or replacement of the secondary systems, and serious problems of schedule and efficiency are caused because of very expensive computation.

Thus, equipment and supporting structures are usually modelled and analyzed separately in engineering, if the equipment—actually, most of the equipment—having relatively small mass in comparison with that of the supporting structures has negligible interaction effects with the supporting structures. For such analysis, a GRS is first used as the input seismic excitation to do seismic analysis to the supporting structure, and obtain the FRS. Using the FRS as the input seismic excitation to the equipment, seismic response analysis for the equipment is then performed. These two separate analyses are shown in Figure 1.2.

Because FRS reflects dynamic characteristics of the supporting structures under specific earthquake excitations, the uncertainty of FRS stems from the supporting structures (e.g., material properties) and earthquake excitations. Previous studies (Padgett and DesRoches, 2007; Kappos, 2001) showed that ground motions most unpredictably and significantly

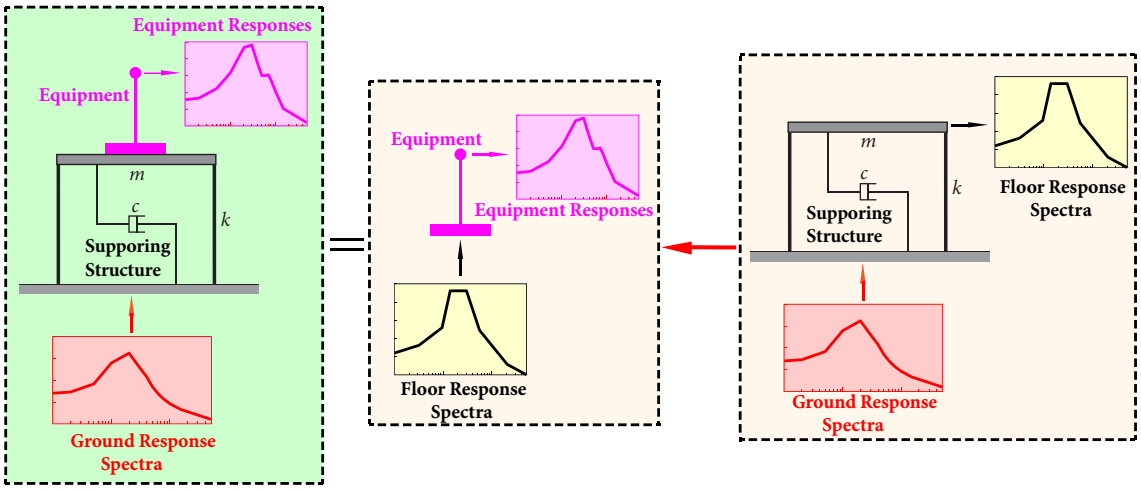

Figure 1.2 Separate analyses for the equipment and the supporting structure

affect the uncertainty of dynamic responses of structures. Thus, contribution of ground motions to the uncertainty of FRS should be considered in generating probabilistic FRS.

For two ground motions respectively spectrum-compatible with a target GRS, if they are used as input motions to a supporting structure, two different FRS could be obtained from the two ground motions. This is because some characteristics of ground motions affecting dynamic responses of structures (Hancock and Bommer, 2007; Kennedy, 1984; Kennedy, 1989), such as duration, phasing characteristics, and Fourier power spectrum characteristics, could be different, even if both of them are spectrum-compatible with the same target ground response spectrum. The uncertainty of such characteristics causes the uncertainty of FRS.

Two methods are usually used to generate FRS in engineering. The first method is the time-history analysis method (Adam and Fotiu, 2000; USNRC, 1978; Scanlan, 1974). Given a ground acceleration time history spectrum-compatible with a target GRS, acceleration time history of the supporting structure at various floors or other equipment-support locations of interest can be calculated by dynamic analysis of the supporting structure. Then, using the acceleration time history of the supporting structure, a FRS can be generated. However, because only one acceleration time history is not acceptable for design purpose, it is necessary to generate a FRS from an average or envelope to many floor response spectra from

many different ground acceleration time histories. To generate probabilistic FRS, a large number of ground acceleration time histories spectrum-compatible with the target GRS are required (Ardakan, 2006), and low efficiency is therefore caused.

The second method for generating FRS is the direct spectra-to-spectra method (Jean-pierre and Livolant, 1977; Singh, 1975; Singh, 1980). Given a GRS, the FRS is generated using response spectrum method or any variant of it to determine—in terms of the given GRS and the dynamic characteristics of the supporting structure—the maximum acceleration response of a simple oscillator attached to the structural floor for which a FRS is desired. In using the direct spectra-to-spectra method to generate FRS, spectral acceleration of FRS under the tuning cases (i.e., the frequency and damping ratio of a single degree-of-freedom (SDOF) oscillator is equal to those of a SODF supporting structure) cannot deterministically be evaluated accurately, which mainly comprises the contribution of ground motions to the uncertainty of FRS. Approaches to obtain probabilistic FRS using the direct spectra-to-spectra method were investigated in previous studies (Lilhanand, Wing, and Tseng, 1985; Paskalov and Reese, 2003; Igusa and Kiureghian, 1985), but the contribution of tuning cases to the uncertainty of FRS was not discussed. Thus, to obtain probabilistic FRS considering the uncertainty from ground motions, the contribution of tuning cases to the uncertainty of FRS needs to be investigated.

1.2 Objectives of This Study

The overall objective of this study is to bridge the gap between P-BSD for nuclear facilities and realistic design response spectrum. The specific objectives of this study are:

- Considering the problem of Newmark design spectrum, this study uses a large number of ground motions recorded at different types of sites to establish a system of site design spectrum coefficients to overcome the problem of Newmark design spectrum, which leads to more realistic and reliable Newmark design spectrum for P-BSD.
- Considering requirements of constructing accurate and realistic soil UHS for a target site with detailed information for P-BSD, this study proposes a probabilistic framework

to integrate the uncertainties from seismic sources and local site conditions into soil UHS.

- Considering requirements of constructing probabilistic FRS using the direct spectra-to-spectra method, this study discusses the t-response spectrum (tRS), which deals with equipment-structure resonance or tuning, and investigates the contribution of tuning cases to the uncertainty of FRS. Using a large number of ground motions recorded at different categories of sites, this study further establishes the statistical relationship between tRS and GRS, which are required to generate probabilistic FRS consider uncertainty from ground motions.

1.3 Organization of This Study

In Chapter 2, the Newmark design spectrum is introduced, and the problem of Newmark design spectrum—exhibiting lower amplitudes at high frequencies and higher amplitudes at low frequencies—is discussed, and reasons causing the problem are investigated. To resolve the problem of Newmark design spectrum, a wide range of ground motions recorded at three types of sites are selected. Using these ground motions, influences of the average shear-wave velocity V_{s30}, earthquake magnitudes, and source-to-site distances on the ratios v/a and ad/v^2 (where a is the PGA, v is the PGV, and d is the PGD) are studied, and spectrum amplification factors are statistically calculated. Spectral bounds for the combinations of three site categories and two cases of earthquake magnitudes (small and large) are estimated. A system of site design spectrum coefficients for the three site categories considering earthquake magnitudes is recommended to overcome the problem of Newmark design spectrum, and more realistic Newmark design spectrum is constructed using the site design spectrum coefficients.

In Chapter 3, a probabilistic framework is proposed to perform PSHA for soil sites and construct soil UHS. In this framework, the variability of soil parameters, the nonlinear property of soils, and the vector-valued seismic site responses analysis are comprehensively integrated into PSHA for soil sites. Because local soil conditions greatly affect ground motions propagating from bedrock to soil surface, the evaluation of ground motions at the

soil surface needs to consider effects of the local soil conditions. GMPEs using the generic soil to characterize local soil conditions are possible to estimate ground motions at the soil surface, but the estimation is not acceptable for critical structures because of lacking accuracy. Therefore, site amplification is used to modify the bedrock GMPEs to make them suitable for soil sites. Based on the modified GMPEs, PSHA for soil sites are performed accurately, and the framework to construct acceptable soil UHS is proposed.

In Chapter 4, the concept of tRS is first proposed, and physical meanings of tRS and GRS are compared and discussed. To establish the probabilistic FRS by the direct spectra-to-spectra method, the statistical relationship between tRS and GRS is required.

Based on different suites of horizontal and vertical ground motions selected at different types of sites, simulation results are employed to establish statistical relationships between tRS and GRS. It is observed that the influence of site conditions on horizontal statistical relationship is negligible, whereas the effect of site conditions on vertical statistical relationship cannot be ignored. Considering the influence of site conditions, horizontal statistical relationship suitable for all site conditions and vertical statistical relationships suitable for hard sites and soft sites, respectively, are established. The horizontal and vertical statistical relationships are suitable to estimate tRS for design spectra in USNRC R.G. 1.60 and NUREG/CR-0098, UHS in Western North America (WNA), or any GRS falling inside the valid coverage of the statistical relationship.

For UHS with significant high frequency spectral accelerations, such as UHS in Central and Eastern North America (CENA), an amplification ratio method is proposed to estimate tRS.

In Chapter 5, some conclusions from this study and directions for further research are presented.

CHAPTER 2

Newmark Design Spectra Considering Earthquake Magnitudes and Site Categories

Elastic design spectra constructed by Newmark-Hall approach (Newmark design spectra) have been implemented in many building standards, especially in building standards for critical structures, such as nuclear power plants. Previous studies showed that Newmark design spectra exhibit lower amplitudes at high frequencies and higher amplitudes at low frequencies.

To resolve this problem, this study considers a wide range of ground motions recorded at three types of sites, i.e., B sites, C sites, and D sites according to National Earthquake Hazards Reduction Program (NEHRP) site classification criteria. Using different suites of ground motions for different site categories, influences of the average shear-wave velocity V_{s30}, earthquake magnitudes, and source-to-site distances on the ratios v/a and ad/v^2 (where a is the peak ground acceleration, v is the peak ground velocity, and d is the peak ground displacement) are studied, and spectrum amplification factors are statistically calculated. Spectral bounds for the combinations of three site categories and two cases of earthquake magnitudes (small and large) are estimated. Site design spectrum coefficients for the three site categories considering earthquake magnitudes are recommended. The site design spectrum coefficients are used to modify the spectral values of Newmark design spectra in the

acceleration sensitive, velocity sensitive, and displacement sensitive regions. Comparison among the modified Newmark design spectra by site design spectrum coefficients in this study, Newmark design spectra, and the modified Newmark design spectra by site design spectrum coefficients in Mohraz's study reveals that the site design spectrum coefficients obtained in this study are suitable to overcome the problem of Newmark design spectra mentioned in previous studies.

2.1 Introduction

During late 1960s and early 1970s, Newmark and Hall (Newmark, Blume, and Kapur, 1973A; Newmark and Hall, 1969) observed that some spectral ordinates are affected more by Peak Ground Velocity (PGV) or Peak Ground Displacement (PGD) than by Peak Ground Acceleration (PGA). For a given response spectrum, there are three sensitive regions: acceleration sensitive region in high frequency band, velocity sensitive region in intermediate frequency band, and displacement sensitive region in low frequency band. Based on spectrum amplification factors in different sensitive regions for various damping ratios, Newmark and Hall (Hall, Mohraz, and Newmark, 1976; Newmark and Hall, 1982) proposed a smooth elastic design spectrum, i.e., Newmark design spectrum. Many nuclear building standards, such as ASCE 4-98 (ASCE, 2000), DOE-STD-1023-2002 (DOE, 2002), GB 50276-97 (SPC, 1997), NS-TAST-GD-013 (ONR, 2014) and CSA N289.3-10 (CSA, 2010), adopt Newmark design spectra. Many regular building standards, such as ASCE 7-10 (ASCE, 2010), FEMA 356 (FEMA, 2000), and IBC (IBC, 2012), also adopt the Newmark design spectra but with some modifications.

Construction of Newmark design spectrum requires spectrum amplification factors and ground motions parameters. Spectrum amplification factors are calculated using many typical ground motions. In Newmark *et al.* (Newmark *et al.*, 1973B), 28 horizontal and 14 vertical ground motions were used to determine the probability distributions of horizontal and vertical spectrum amplification factors, respectively. Information of the 28 horizontal ground motions used in Newmark's study is listed in Table 2.1. Newmark *et al.* (Newmark *et al.*, 1973B) found that the velocity- and acceleration-amplification factors

obtained using ground motions with PGA $> 0.1g$ are smaller than those obtained using all 28 ground motions. It was concluded that "the strong motion data clearly indicate a decrease in amplification, especially for the velocity and acceleration regions, as compared to the case where low intensity excitation is included." Hence, 8 ground motions listed in Table 2.1 with PGA $< 0.1g$ were not used when calculating the spectrum amplification factors recommended to building standards. By comparing horizontal spectrum amplification factors with vertical spectrum amplification factors, Newmark concluded that vertical design spectra can be taken as 2/3 of horizontal design spectra in Western United States.

In determining Newmark design spectra, ground motion parameters, i.e., PGA, PGV, and PGD, are also required. For sites lacking such information, relationships among these three ground motion parameters were recommended (Hall, 1982; Newmark and Hall, 1982): $v/a = 48$ (in/sec)/g for competent soil sites, and $v/a = 36$ (in/s)/g for rock sites. To calculate PGD, the ratio $ad/v^2 = 6.0$ is recommended for all types of sites, where a, v and d represent PGA, PGV, and PGD, respectively.

However, previous studies (Mohraz, 1976; Mohraz, 1978; Mohraz, 1992) showed that these relationships greatly influence the spectral shape and spectral amplitude of Newmark design spectra. Further study (Dunbar and Charlwood, 1991) also showed that the relationships among PGA, PGV, and PGD recommended by Newmark can lead to significant magnitude bias in the resulting design spectra as these relationships strongly depend on earthquake magnitudes.

Previous studies (Dunbar and Charlwood, 1991; Mohraz, 1976; Mohraz, 1978; Mohraz, 1992) concluded that Newmark design spectra exhibit lower amplitudes at high frequencies and higher amplitudes at low frequencies in comparison with response spectra developed by the statistical method. These discrepancies have been explained on the grounds that spectrum amplification factors are biased toward the spectra of large-amplitude earthquakes: large-magnitude earthquakes generate ground motions rich in low frequencies, while small-magnitude earthquakes generate ground motions rich in high frequencies. The bias toward large-magnitude earthquakes is due to the fact that seven of the nine earthquakes used in calculating spectrum amplification factors have magnitudes larger than 6.0. This bias is also due to the fact that most of the ground motions considered were recorded on alluvial

Table 2.1 28 ground motions used by Newmark in 1973

Earthquake Event	Date	Station Name	Component	Magnitude	R_{rup} (km)	Site condition	PGA (g)
San Francisco	22/03/1957	1117 Golden Gate Park	GGP010	5.3	8.0	USGS(A)	0.095
San Francisco	22/03/1957	1117 Golden Gate Park	GGP100	5.3	8.0	USGS(A)	0.112
San Fernando	09/02/1971	Old Ridge Route	ORR021	6.6	24.9	USGS(B)	0.324
San Fernando	09/02/1971	Old Ridge Route	ORR291	6.6	24.9	USGS(B)	0.268
San Fernando	09/02/1971	126 Lake Hughes #4	L04111	6.6	24.2	USGS(B)	0.192
San Fernando	09/02/1971	126 Lake Hughes #4	L04201	6.6	24.2	USGS(B)	0.153
Imperial Valley	19/05/1940	117 El Centro Array #9	I-ELC180	7.0	8.3	USGS(C)	0.313
Imperial Valley	19/05/1940	117 El Centro Array #9	I-ELC270	7.0	8.3	USGS(C)	0.215
Northwest Calif	08/10/1951	1023 Ferndale City Hall	B-FRN224	5.8	56	USGS(C)	0.105
Northwest Calif	08/10/1951	1023 Ferndale City Hall	B-FRN314	5.8	56	USGS(C)	0.110
Kern County⋆	21/07/1952	Hollywood Stor FF	HOL090	7.4	120.5	USGS(C)	0.044
Kern County⋆	21/07/1952	Hollywood Stor FF	HOL180	7.4	120.5	USGS(C)	0.057
Kern County⋆	21/07/1952	Hollywood Stor Lot	PEL090	7.4	120.5	USGS(C)	0.042
Kern County⋆	21/07/1952	Hollywood Stor Lot	PEL180	7.4	120.5	USGS(C)	0.058
Eureka	21/12/1954	CA-Federal Building	N11W	6.6	23.5	USGS(C)	0.153
Eureka	21/12/1954	CA-Federal Building	N79E	6.6	23.5	USGS(C)	0.258
Northern Calif	21/12/1954	1023 Ferndale City Hall	H-FRN044	6.5	31.5	USGS(C)	0.159
Northern Calif	21/12/1954	1023 Ferndale City Hall	H-FRN314	6.5	31.5	USGS(C)	0.189
El Alamo⋆	09/02/1956	117 El Centro Array #9	ELC180	6.8	130	USGS(C)	0.033
El Alamo⋆	09/02/1956	117 El Centro Array #9	ELC270	6.8	130	USGS(C)	0.052
Hollister⋆	09/04/1961	1028 Hollister City Hall	B-HCH181	5.6	12.6	USGS(C)	0.074
Hollister	09/04/1961	1028 Hollister City Hall	B-HCH271	5.6	12.6	USGS(C)	0.196
Borrego Mtn	09/04/1968	117 El Centro Array #9	A-ELC180	6.8	46	USGS(C)	0.130
Borrego Mtn⋆	09/04/1968	117 El Centro Array #9	A-ELC270	6.8	46	USGS(C)	0.057
San Fernando	09/02/1971	279 Pacoima Dam	PCD164	6.6	2.8	USGS(C)	1.226
San Fernando	09/02/1971	279 Pacoima Dam	PCD254	6.6	2.8	USGS(C)	1.160
San Fernando	09/02/1971	15250 Ventura Blvd	N11E	6.6	23.4	USGS(C)	0.225
San Fernando	09/02/1971	15250 Ventura Blvd	N79W	6.6	23.4	USGS(C)	0.149

⋆ Ground motions not considered in calculating spectrum amplification factors due to PGA $< 0.1g$.

sites, because earthquake response spectra at soil sites tend to exhibit these characteristics in comparison with those at rock sites.

To resolve the problem of Newmark design spectra, Mohraz (Mohraz, 1976) considered a total of 54 earthquake records from 54 stations recorded during 16 earthquakes. These records were divided into four categories: 25 records observed on alluvium deposits, 13 records observed on rock deposits, 7 records observed on less than 30 feet of alluvium underlain by rock deposits, and 9 records observed on 30 to 200 feet of alluvium underlain by rock deposits. The average v/a, ad/v^2, and spectrum amplification factors for the four categories were calculated. Site design spectrum coefficients were recommended by Mohraz to overcome the problem of Newmark design spectra.

Malhotra (Malhotra, 2006) proposed an improved method to develop spectrum amplification factors based on the approach of constructing Newmark design spectra from ground motion parameters—PGA, PGV, and PGD —and spectrum amplification factors. A method to normalize earthquake response spectra was first proposed to avoid *a priori* assumption of three sensitive regions of response spectra used by Newmark in developing spectrum amplification factors. The normalized response spectra of 63 ground motions were calculated and the probability distributions of spectrum amplification factors were obtained. The median acceleration- and velocity-amplification factors obtained are close to those in Newmark's study, but the median displacement-amplification factors are significantly different from those in Newmark's study. Malhotra also concluded that the effects of site conditions on spectrum amplification factors are statistically insignificant for both horizontal and vertical motions. Finally, Malhotra suggested improved methods to construct design response spectra in three regular building standards: IBC (2003), ASCE 7 (2002), and FEMA 356 (2000).

In Mohraz's studies (Mohraz, 1976; Mohraz, 1992) and Malhotra's study (Malhotra, 2006), a small number of ground motions were used in an attempt to resolve the problem of Newmark design spectra. In this study, a wide range of ground motions observed at three types of sites, i.e., B sites, C sites, and D sites following the National Earthquake Hazard Reduction Program (NEHRP) site classification criteria (ASCE, 2010; IBC, 2012), are used. Influences of the parameter V_{s30}, earthquake magnitudes, and source-to-site distances on

the ratios v/a and ad/v^2 are analyzed, and the average ratios v/a and ad/v^2 considering site categories (B, C, and D sites) and earthquake magnitudes (small earthquakes with $M \leqslant 6.0$ and large earthquakes with $M > 6.0$) are estimated. The spectrum amplification factors in Newmark's study were re-estimated to validate the method of developing spectrum amplification factors in this study. Using the ground motions recorded at these three types of sites, spectrum amplification factors considering site categories and earthquake magnitudes are developed. Based on the average ground motion parameters, i.e., d, v, and a, and 84.1% spectrum amplification factors, spectral bounds for the three site categories considering earthquake magnitudes are obtained. Comparing spectral bounds in this study with those in Newmark's study (Newmark, Blume, and Kapur, 1973A; Newmark and Hall, 1982), a system of site design spectrum coefficients considering earthquake magnitudes and site categories is constructed. These site design spectrum coefficients are used to overcome the problem of Newmark design spectra by modifying spectral values in acceleration sensitive, velocity sensitive, and displacement sensitive regions. Finally, examples of the modified Newmark design spectra by the site design spectrum coefficients in this study are compared with Newmark design spectra to verify the validity of the new results.

The site design spectrum coefficients in this study are different from those in Mohraz's study (Mohraz, 1976): (1) The scope of ground motions is different. Mohraz (Mohraz, 1976) considered a total of 54 ground motions from 16 earthquake events. This study considers a wide range of ground motions: 81 ground motions observed at B sites (rock sites), 210 ground motions observed at C sites, and 300 ground motions observed at D sites; (2) Site classification criteria are different. In Mohraz' study, sites were classified according to the depth of alluvium underlain by rock deposits. However, this site classification criterion is not used any more in current building standards. Instead, new site classification criterion based on the parameter V_{s30} is used to classify sites in current building standards, which is used in this study; and (3) In Mohraz's study, earthquake magnitudes were not considered in establishing site design spectrum coefficients. In this study, using a large number of ground motions recorded during more than 100 earthquake events around the world covering a wide range of earthquake magnitudes, influences of earthquake magnitudes on response spectra are considered in constructing the system of site design spectrum coefficients.

This study focuses on resolving the problem of horizontal Newmark design spectra. Therefore, the average ratios v/a and ad/v^2, spectrum amplification factors, and Newmark design spectra mentioned in this study only refer to horizontal earthquakes. The vertical design spectra can be taken as 2/3 of horizontal design spectra.

It should be noted that the Uniform Hazard Spectrum (UHS) based on Probabilistic Seismic Hazard Analysis (PSHA) has been widely used by nuclear industry in United States, which paves the way for probabilistic seismic design and analysis. However, UHS is very conservative and not a good representative of a suitable target earthquake spectrum (McGuire, 1995; Baker, 2010). Thus, UHS is not accepted in some countries. For example, the UK regulator, HMNII (Her Majesty's Nuclear Installations Inspectorate), does not adopt UHS. As stated in the Nuclear Safety Technical Assessment Guide (ONR, 2014), "*ONR (HMNII) has accepted the principle of UHS spectra. However, ONR (HMNII) has not accepted any UHS spectra for design purposes because of concern about the deliberate avoidance of conservatism*". In countries like Canada, United Kingdom, and China, Newmark design spectra or modified Newmark design spectra (CSA, 2010; ONR, 2014; SPC, 1997) are still used for analysis and design of nuclear power plants. In addition, Newmark spectra, such as those in NUREG/CR-0098 (Newmark and Hall, 1978), are also used as review level earthquakes in seismic margin assessment in nuclear industry in Canada.

2.2 Tripartite Response Spectra

Using the relationships between pseudo-acceleration, pseudo-velocity, and pseudo-displacement, it is convenient to plot a response spectrum in tripartite. If a spectral pseudo-velocity is defined as

$$\mathrm{PSV}(\omega,\zeta)=\left|\int_0^t \ddot{u}_g(\tau)\mathrm{e}^{-\zeta\omega(t-\tau)}\sin\omega(t-\tau)\mathrm{d}\tau\right|_{\max}, \tag{2.2.1}$$

then, for small damping ratios, one has

$$\mathrm{PSA}(\omega,\zeta)=\omega\cdot\mathrm{PSV}(\omega,\zeta), \tag{2.2.2}$$

$$\mathrm{PSD}(\omega,\zeta)=\frac{\mathrm{PSV}(\omega,\zeta)}{\omega}, \tag{2.2.3}$$

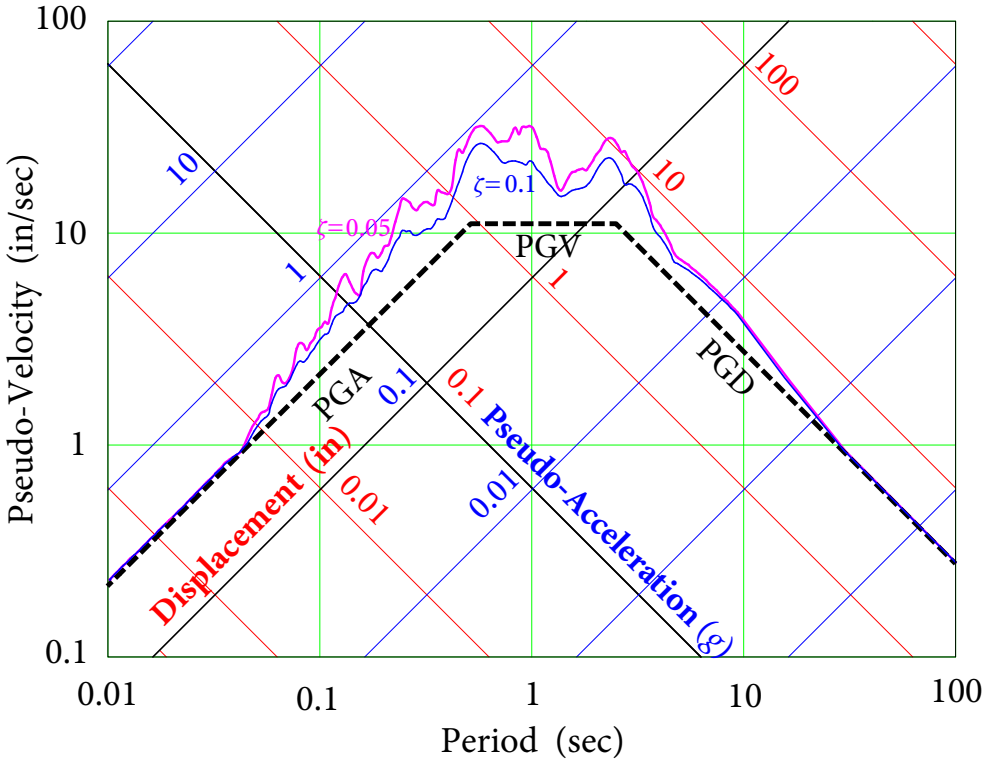

Figure 2.1 Tripartite response spectra (damping ratios $\zeta = 0.05$ and $\zeta = 0.1$) of El Centro earthquake

where ω is circular frequency, ζ is damping ratio, $\mathrm{PSV}(\omega, \zeta)$, $\mathrm{PSA}(\omega, \zeta)$, and $\mathrm{PSD}(\omega, \zeta)$ denote the pseudo-velocity, pseudo-acceleration, and pseudo-displacement, respectively, and $\ddot{u}_g$ is the ground acceleration.

From equations (2.2.1) to (2.2.3), a tripartite response spectrum of a ground motion can be plotted. Tripartite response spectra for one El Centro record are shown in Figure 2.1. This figure demonstrates that response spectral ordinates in short period (high frequency) band largely depend on PGA, response spectral ordinates in intermediate period (intermediate frequency) band largely depend on PGV, and response spectral ordinates in long period (low frequency) band largely depend on PGD. The entire period range of a response spectrum is divided into three regions: an acceleration sensitive region, a velocity sensitive region, and a displacement sensitive region, as shown in Figure 2.2. α_{A}, α_{V}, and α_{D} are the amplification factors of PGA, PGV, and PGD, respectively.

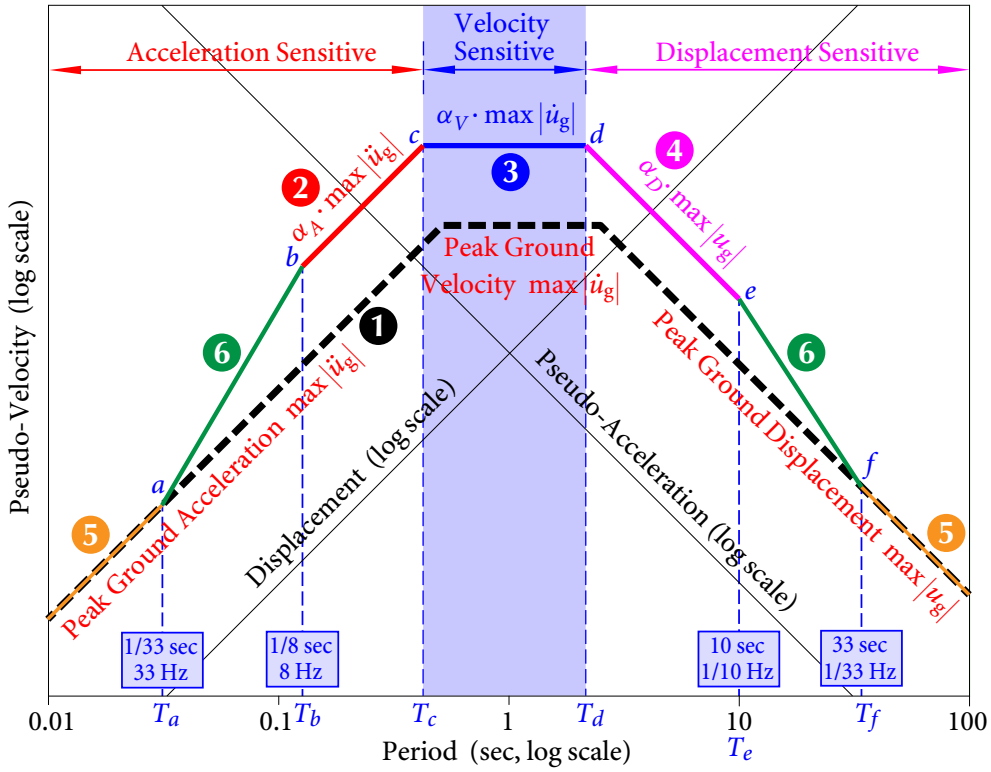

Figure 2.2 Newmark design spectra

2.3 Selected Ground Motions

To determine the average ratios v/a and ad/v^2, and spectrum amplification factors for a given type of site conditions, ground motions observed at sites with similar site conditions are required. Ground motions are selected following the criteria:

- Ground motions with PGA less than 0.05 g are excluded. The limit of 0.05 g is usually used to classify strong earthquake records (Mohraz, 1976). In comparison, reference (Ritcher, 1958) showed that 0.1g can be defined as the damaging acceleration to weak structures. Considering that weak ground motions usually have great spectrum amplification factors (Hall *et al.*, 1976), ground motions with PGA somewhat less than the damage threshold 0.1g are necessary.
- Ground motions with complete information, including three components (two horizontal components and one vertical component) and site classifications are considered.

Only one horizontal component randomly selected from the two horizontal components is used in this study.

- In order to study characteristics of response spectra at frequencies higher than 33 Hz, only ground motions with usable frequency greater than 33 Hz are selected.
- Pulse-like ground motions are excluded due to their special characteristics.

Following these selection criteria, 81 ground motions (including 33 ground motions recorded during small earthquakes, i.e., magnitude $M \leqslant 6$, and 48 ground motions recorded during large earthquakes, i.e., magnitude $M > 6$) recorded at B sites, 210 ground motions (including 64 ground motions recorded during small earthquakes and 146 ground motions recorded during large earthquakes) recorded at C sites, and 300 ground motion (including 117 ground motions recorded during small earthquakes and 183 ground motions recorded during large earthquakes) recorded at D sites are selected. Respectively comparing 5% damping ratio response spectra of the selected ground motions at B sites, C sites, and D sites with those of the 28 ground motions in Newmark's study, as shown in Figures 2.3 to 2.8, it is revealed that

- 50% and 84.1% response spectra of the 28 ground motions from Newmark's study remarkably exhibit lower amplitudes at high frequencies, and higher amplitudes at lower frequencies, in comparison with 50% and 84.1% response spectra of the selected ground motions recorded at B sites during large and small earthquakes, and C sites and D sites during small earthquakes.
- 50% and 84.1% response spectra of the 28 ground motions from Newmark's study exhibit similar spectral shapes with the 50% and 84.1% response spectra of the selected ground motions recorded at C sites and D sites during large earthquakes. This is because these ground motions and the majority of the 28 ground motions have similar characteristics.

Using these selected ground motions at different types of sites, the average ratios v/a and ad/v^2, and spectrum amplification factors for the three site categories are calculated in following sections.

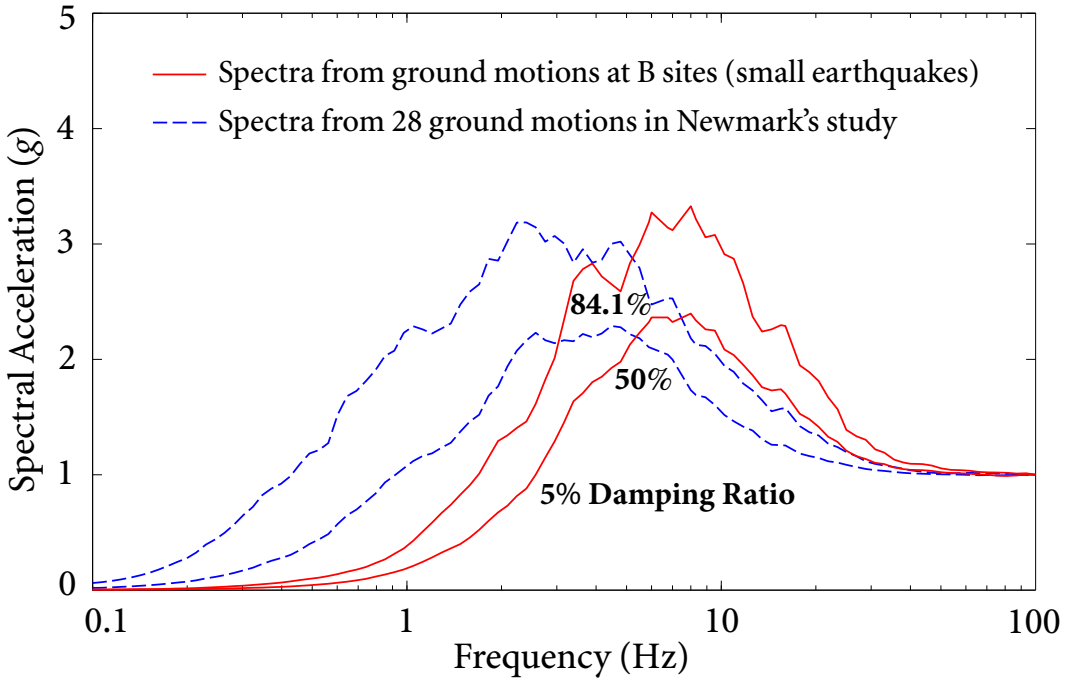

Figure 2.3 Comparison between response spectra of 33 selected ground motions recorded at B sites during small earthquakes and those of 28 ground motions in Newmark's study

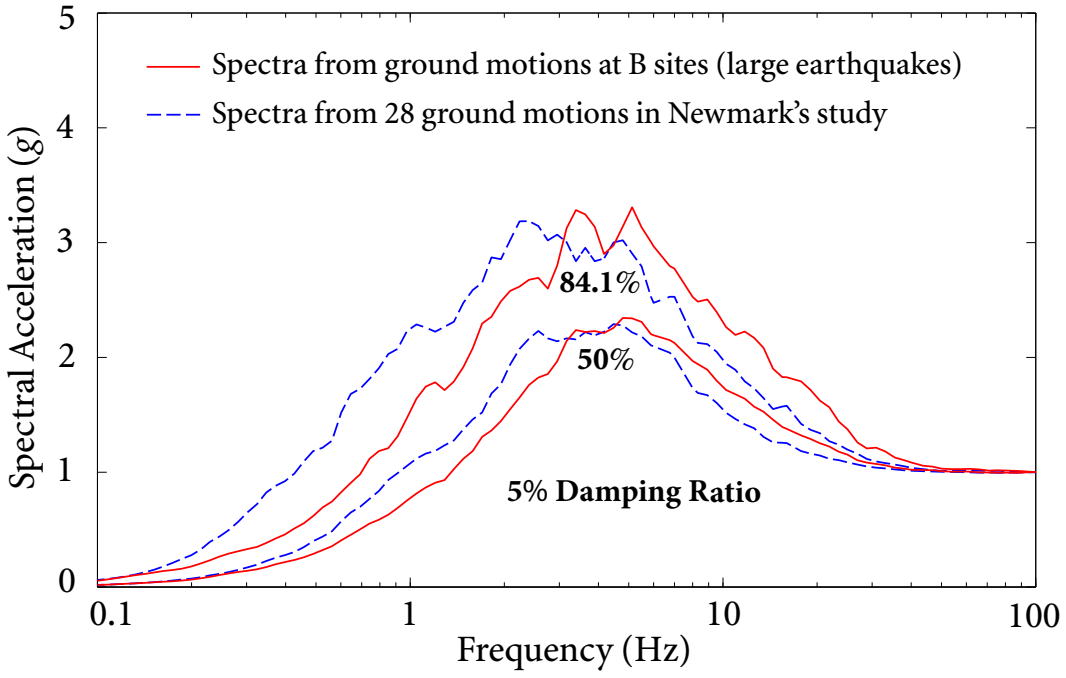

Figure 2.4 Comparison between response spectra of 48 selected ground motions recorded at B sites during large earthquakes and those of 28 ground motions in Newmark's study

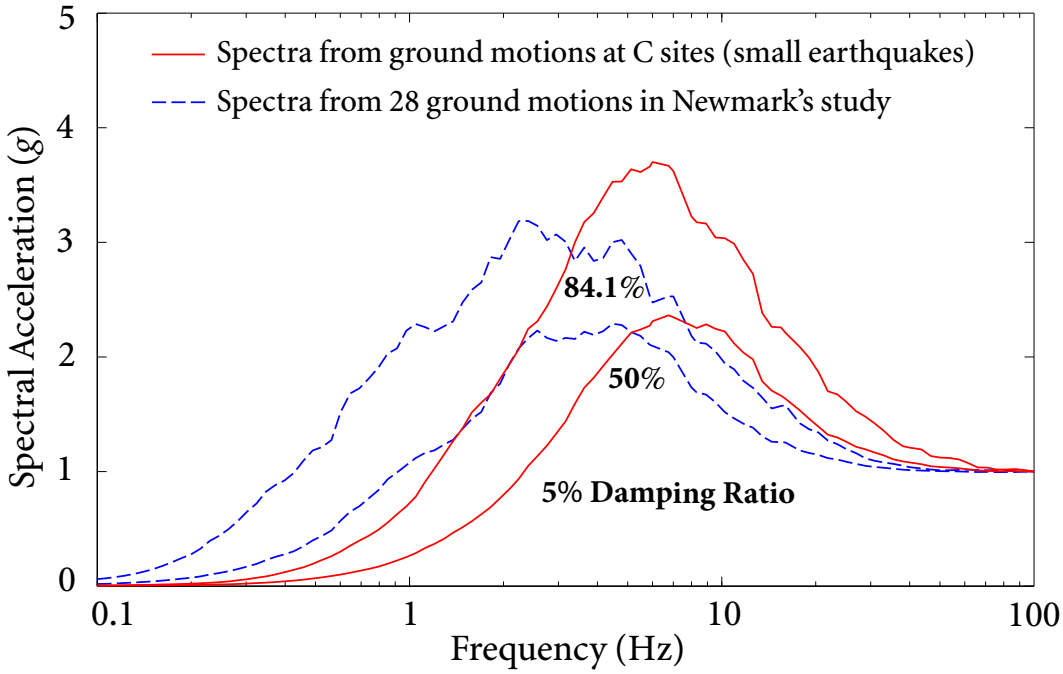

Figure 2.5 Comparison between response spectra of 64 selected ground motions recorded at C sites during small earthquakes and those of 28 ground motions in Newmark's study

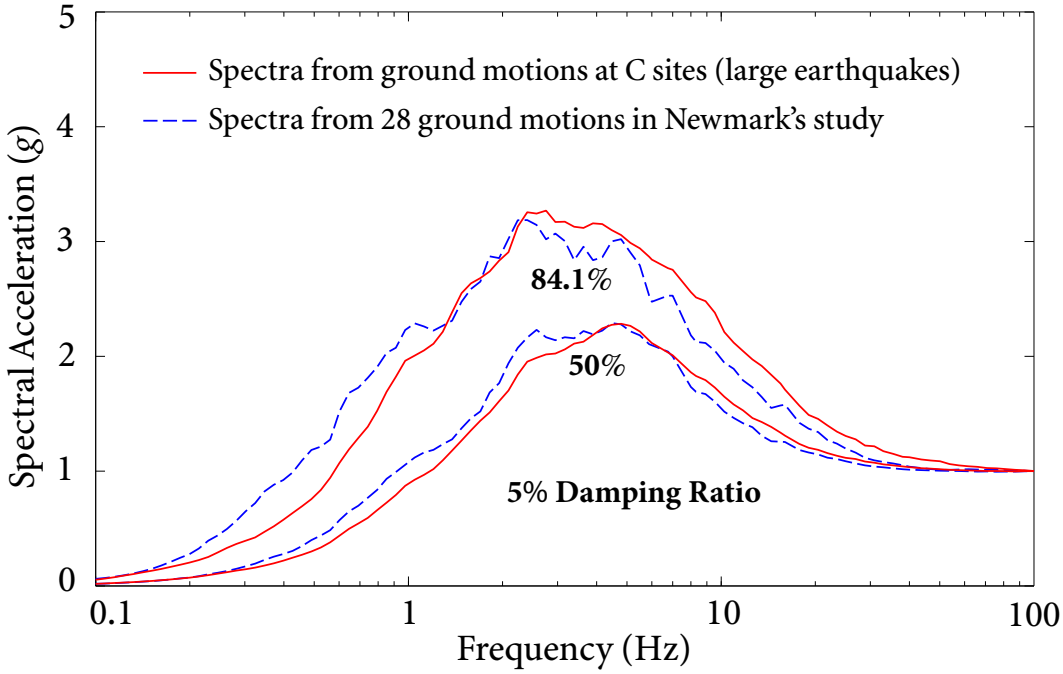

Figure 2.6 Comparison between response spectra of 146 selected ground motions recorded at C sites during large earthquakes and those of 28 ground motions in Newmark's study

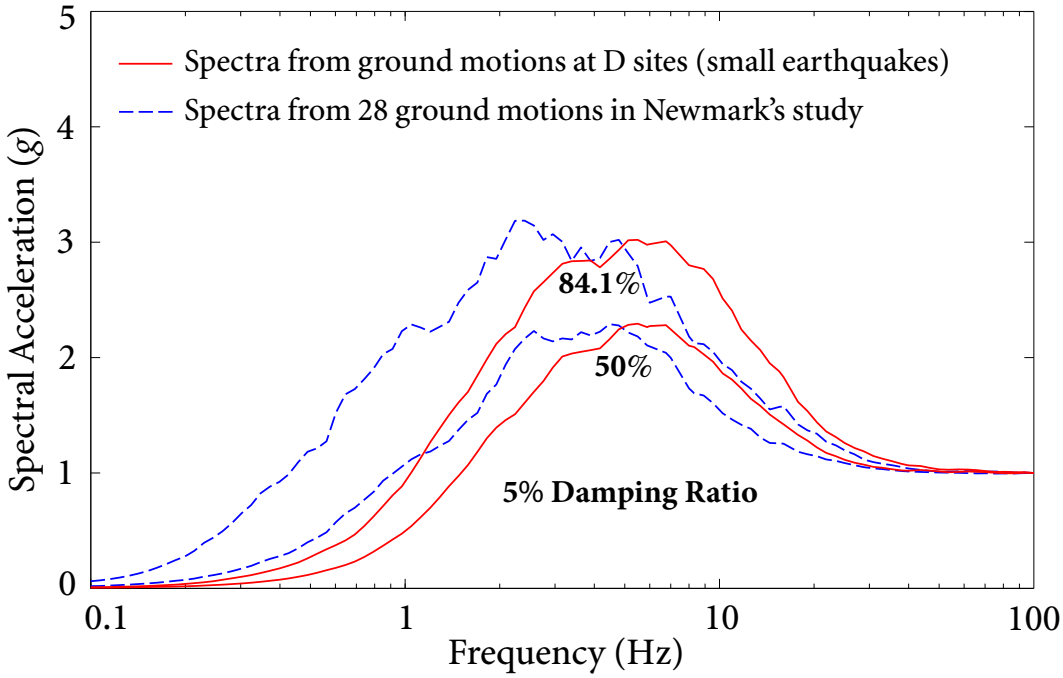

Figure 2.7 Comparison between response spectra of 117 selected ground motions recorded at D sites during small earthquakes and those of 28 ground motions in Newmark's study

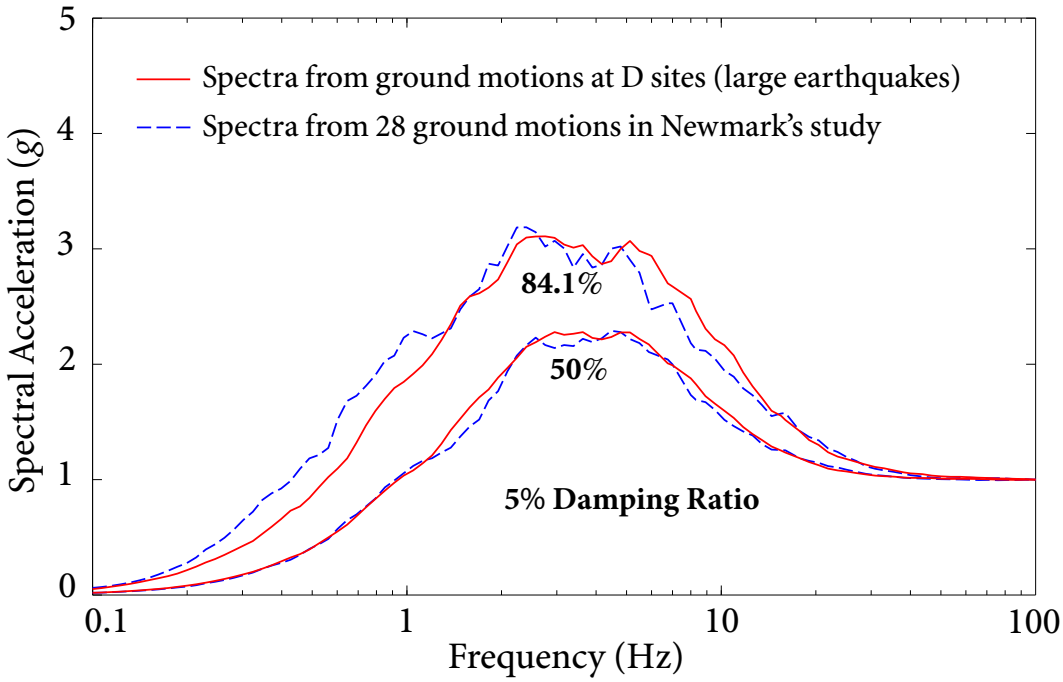

Figure 2.8 Comparison between response spectra of 183 selected ground motions recorded at D sites during large earthquakes and those of 28 ground motions in Newmark's study

2.4 Statistical Analysis of Ground Motion Parameters

Newmark design spectra exhibiting lower amplitudes at high frequencies and higher amplitudes at low frequencies are mainly caused by the v/a and ad/v^2 ratios recommended by Newmark (Dunbar and Charlwood, 1991; Hall, 1982; Mohraz, 1976; Newmark and Hall, 1982; Villaverde, 2009). These ratios were based on 22 ground motions recorded at soil sites and 6 ground motions recorded at rock sites. All of these 28 ground motions were from California earthquakes that were predominantly of magnitudes 6 to 7 with source-to-site distances from 10 to 50 km; 8 of the 28 ground motions were recorded during the 1971 M6.6 San Fernando Earthquake. Therefore, the application of these ratios should be limited to the West Coast of United States (Hall *et al.*, 1976).

To obtain more suitable ratios v/a and ad/v^2, Mohraz (Mohraz, 1976) used twice as many ground motions, but the number of ground motions is still small—only 54 ground motions. To determine these ratios for different site categories, the limited 54 ground motions were divided into four groups: 25 ground motions observed on alluvium deposits, 13 ground motions observed on rock deposits, 7 ground motions and 9 ground motions, respectively, observed on less than 30 feet of alluvium underlain by rock deposits and on 30 to 200 feet of alluvium underlain by rock deposits. Moreover, the site classification criteria in Mohraz's study are not consistent with those used in current building standards.

Considering the problem discussed above in previous studies (Dunbar and Charlwood, 1991; Mohraz, 1976; Mohraz, 1978; Mohraz, 1992), in this study a wide range of ground motions observed at three different types of sites are used: 81 ground motions recorded at B sites (rock sites), 210 ground motions recorded at C sites, and 300 ground motions recorded at D sites. Details of these three suites of ground motions are listed in the appendix. All of these motions are selected from the PEER Strong Motion Database and the European Strong Motion Database (Ambraseys *et al.*, 2002). Ground motions selected from these two databases have been processed (filtering and baseline correction) consistently and reliably by the supplying agencies (Ambraseys, Smit, Douglas, *et al.*, 2004; PEER, 2010).

Previous studies (Mohraz, 1992; Riddell and Newmark, 1979) showed that the ratios v/a and ad/v^2 depend on earthquake magnitudes, source-to-site distances, and durations of

earthquake records, and site conditions of recording stations. But these influences have not been generally quantified, even though Mohraz quantified the influence of source-to-site distances on these ratios based on ground motions observed during the Loma Prieta Earthquake of October 17, 1989 (Mohraz, 1992), and quantified the influence of site conditions based on a limited number of ground motions (Mohraz, 1976).

In current building standards, the average shear-wave velocity between 0 and 30 meters depth V_{s30} is usually used to categorize local site conditions (ASCE, 2010; IBC, 2012; Wills, Petersen, Bryant, *et al.*, 2000). The influences of V_{s30} on the ratios v/a and ad/v^2 are unclear. This study divides the three suites of ground motions into eight groups according to the V_{s30} value of recording stations. A total number of 571 ground motions are divided into eight groups; 20 ground motions recorded at rock sites without specific values of V_{s30} are excluded from the eight groups.

Table 2.2 Average ratios v/a and ad/v^2 for different V_{s30} ranges

V_{s30} (m/sec)	Number of Motions	v/a (in/sec)/g	ad/v^2
180 − 300	155	37	3.0
301 − 400	214	31	3.1
401 − 500	72	36	3.6
501 − 600	21	36	3.6
601 − 700	42	28	4.6
701 − 900	39	25	4.3
901 − 1100	19	31	4.1
> 1100	9	34	3.2

The ratios v/a and ad/v^2 for different V_{s30} ranges are listed in Table 2.2, which shows that the influence of V_{s30} on these ratios is not remarkable. Even though these ratios change with V_{s30}, there is no clear trend with the change; the average ratios v/a of six groups fall within the narrow range between 31 and 37 (in/sec)/g, and the average ratios ad/v^2 of another six groups fall within the range of 3.0 to 4.1. This phenomenon is caused by the fact that V_{s30} is a weak proxy to seismic amplification of sites (Castellaro, Mulargia, and Rossi, 2008; Lee and Trifunac, 2010). The frequency-dependent seismic amplification characterizes the change of frequency contents and amplitudes of ground motions on the ground surface due

to the local soil deposit sitting on the bedrock (Kramer, 1996). This change further affects PGA and, especially, PGV and PGD of ground motions on the ground surface. Because V_{s30} is an unreliable parameter to describe seismic amplification, the relation between V_{s30} and the ratios v/a and ad/v^2 is weak.

The impacts of earthquake magnitude M and source-to-site distance R on the ratios v/a and ad/v^2 have been discussed in previous studies (Mohraz, 1976; Mohraz, 1992; Riddell and Newmark, 1979). However, the impacts have not been generally quantified. Based on a large number of ground motions observed at three site categories, the average ratios v/a and ad/v^2 of ground motions recorded during small near-field (SN) earthquakes ($M \leqslant 6$ and $R \leqslant 40$ km), small far-field (SF) earthquakes ($M \leqslant 6$ and $R > 40$ km), large near-field (LN) earthquakes ($M > 6$ and $R \leqslant 40$ km), and large far-field (LF) earthquakes ($M > 6$ and $R > 40$ km) are, respectively, calculated and listed in Table 2.3.

For a same site category, comparing the average ratios v/a for the SN group with the SF group, or the LN group with the LF group, it is seen that the difference between the average ratios v/a in the SN group and in the SF group, or in the LN group and in the LF group is quite small. Hence, the influence of R on the average ratio v/a is small, and M dominates the average ratio v/a. Similarly, comparing the average ratios ad/v^2 for the SN group with the SF group, or the LN group with the LF group, it is observed that the difference between the average ratios ad/v^2 in the SN and SF groups, or in the LN and LF groups is small, except between the SN and SF groups of B sites (this may be due to the small number of ground motions in the SN and SF groups of B sites). Similar conclusion can be drawn: the influence of R on the average ratio ad/v^2 is small, and M dominates the average ratio ad/v^2. It is also observed that the average ratios v/a and ad/v^2 of large earthquakes are greater than those of small earthquakes. In order to obtain conservative results, the greater ratios in the SN and SF groups are recommended for small earthquakes, and the greater ratios in the LN and LF groups are recommended for large earthquakes, as shown in the columns of "Recommended Value" in Table 2.3.

For a certain earthquake category, the recommended ratio v/a of soft ground is greater than that of firm ground. This is consistent with Newmark's study (Newmark *et al.*, 1973B) and Mohraz's study (Mohraz, 1976). The ratio v/a characterizes intermediate-frequency

Table 2.3 Average ratios v/a and ad/v^2 for three site categories

Site Category	Statistical Analysis				Recommended Value		
	Group	Number of Records	v/a (in/sec)/g	ad/v^2	Earthquake Category	v/a (in/sec)/g	ad/v^2
B Sites	SN	29	16	2.35	Small M	16	3.94
	SF	4	14	3.94			
	LN	30	32	5.02	Large M	38	5.12
	LF	18	38	5.12			
C Sites	SN	58	18	2.51	Small M	19	2.51
	SF	6	19	2.50			
	LN	100	37	4.26	Large M	40	4.26
	LF	46	40	3.88			
D Sites	SN	112	24	2.28	Small M	28	2.28
	SF	5	28	2.24			
	LN	102	38	3.61	Large M	43	3.67
	LF	81	43	3.67			

"SN", "SF", "LN", and "LF" represent small near-field, small far-field, large near-field, and large far-field earthquakes, respectively. "Small M" means $M \leqslant 6.0$, and "Large M" means $M > 6.0$.

contents of ground motions. The larger the value of ratio v/a, the more intermediate-frequency contents the ground motion contains. However, the recommended ratio ad/v^2 of soft ground is smaller than that of firm ground. This is different from the conclusions in Newmark's study (Newmark *et al.*, 1973B), but is almost consistent with the conclusions in Mohraz's study (Mohraz, 1976). For a given a, both v and d of soft ground are, nearly to the same extent, greater than those of firm ground, respectively. As a result, the ratio ad/v^2 of firm ground is greater than that of soft ground.

2.5 Spectrum Amplification Factors

The construction of Newmark design spectra requires spectrum amplification factors and ground motion parameters PGA, PGV, and PGD. As shown in Figure 2.2, the acceleration-amplification factor α_A, velocity-amplification factor α_V, and displacement-amplification factor α_D represent ratios of the computed response spectra to the peak ground motions for acceleration, velocity, and displacement, respectively. The spectrum amplification factors are estimated by statistical analysis based on a suite of ground motions.

To statistically determine spectrum amplification factors, relative response values rather than absolute response values are required. Because different ground motions have different PGA, PGV, and PGD values, normalization of ground motions is required to eliminate the effects of ground motion parameters. If ground motions are normalized to PGA, the variation of spectrum amplification factors is small in the high frequency band, but quite large in the low frequency band; whereas if ground motions are normalized to PGD, the variation of spectrum amplification factors is small in the low frequency band, but quite large in the high frequency band. If ground motions are normalized to PGV, the variation of spectrum amplification factors is nearly constant over the whole frequency range; however, the variations of spectrum amplification factors in the high frequency band and the low frequency band are larger than those of ground motions normalized to PGA and PGD, respectively.

Therefore, prior to statistically determining spectrum amplification factors, ground motions are normalized by PGA in the high frequency band, by PGV in the intermediate frequency band, and by PGD in the low frequency band (Hall, Mohraz, and Newmark, 1976; Newmark, Hall, and Mohraz, 1973B).

2.5.1 Procedure for Developing Spectrum Amplification Factors

Suppose that Q (where $Q > 1$) ground motions are used to statistically determine spectrum amplification factors. At a given frequency, the amplification factors are assumed to follow normal distributions.

The displacement, velocity, and acceleration sensitive frequency bands used for calculating spectrum amplification factors are chosen and listed in Table 2.4. Different sensitive frequency bands are chosen for these three suites of ground motions in this study by considering the approach of constructing Newmark design spectra in building standards (CSA, 2010; Newmark and Hall, 1978; DOE, 2002; Riddell and Newmark, 1979), spectral shapes of the three suites of ground motions, and sensitive frequency bands in previous studies (Hall, Mohraz, and Newmark, 1976; Mohraz, 1976).

Table 2.4 Three sensitive regions in Newmark's study and this study

Sensitive Regions	Groups of Motions	
	Newmark's Study⋆	This Study†
Displacement Frequency Band	0.2 to 0.4 Hz	0.1 to 0.3 Hz
Velocity Frequency Band	0.4 to 2.0 Hz	0.3 to 3.0 Hz
Acceleration Frequency Band	2.0 to 6.0 Hz	3.0 to 8.0 Hz

⋆ includes 20 or 28 ground motions in Newmark *et al.* (1973B)

† includes 81, 210, 300 ground motions, respectively, recorded at B, C, and D sites

Referring to the procedure used by Newmark (Newmark *et al.*, 1973B) in developing spectrum amplification factors, the steps and formulations for determining α_{A} in this study are presented in the following. The steps and formulations for determining α_{V} and α_{D} in this study are similar to those of α_{A}.

1. For a damping value ζ_k, the acceleration-amplification factor at frequency f_i for the jth ground motion normalized by PGA is

$$\alpha_{\mathrm{A},j}(\zeta_k, f_i) = \frac{S_{\mathrm{A},j}(\zeta_k, f_i)}{\mathrm{PGA}}, \quad i = 1, 2, \ldots, N_{\mathrm{A}}, \quad k = 1, 2, \ldots, K. \tag{2.5.1}$$

2. The mean value and standard deviation of $\alpha_{\mathrm{A}}(\zeta_k, f_i)$ at frequency f_i can be determined from the Q sample values $\alpha_{\mathrm{A},j}(\zeta_k, f_i)$, $j = 1, 2, \ldots, Q$:

$$\begin{aligned} \mu_{\alpha_{\mathrm{A}}}(\zeta_k, f_i) &= \frac{1}{Q}\sum_{j=1}^{Q} \alpha_{\mathrm{A},j}(\zeta_k, f_i), \\ \sigma^2_{\alpha_{\mathrm{A}}}(\zeta_k, f_i) &= \frac{1}{Q-1}\sum_{j=1}^{Q} \left[\alpha_{\mathrm{A},j}(\zeta_k, f_i) - \mu_{\alpha_{\mathrm{A}}}(\zeta_k, f_i)\right]^2. \end{aligned} \tag{2.5.2}$$

3. The median $\alpha_{\mathrm{A}}^{50\%}(\zeta_k, f_i)$ and the mean-plus-one-sigma (84.1% non-exceedance probability) value $\alpha_{\mathrm{A}}^{84.1\%}(\zeta_k, f_i)$ can be determined from the normal distribution:

$$\alpha_{\mathrm{A}}^{50\%}(\zeta_k, f_i) = \mu_{\alpha_{\mathrm{A}}}(\zeta_k, f_i), \quad \alpha_{\mathrm{A}}^{84.1\%}(\zeta_k, f_i) = \mu_{\alpha_{\mathrm{A}}}(\zeta_k, f_i) + \sigma_{\alpha_{\mathrm{A}}}(\zeta_k, f_i). \tag{2.5.3}$$

4. The median $\alpha_{\mathrm{A}}^{50\%}(\zeta_k)$ and the mean-plus-one-sigma value $\alpha_{\mathrm{A}}^{84.1\%}(\zeta_k)$ are obtained by averaging the corresponding values in the acceleration sensitive frequency band:

$$\alpha_{\mathrm{A}}^{50\%}(\zeta_k) = \frac{1}{N_{\mathrm{A}}}\sum_{i=1}^{N_{\mathrm{A}}} \alpha_{\mathrm{A}}^{50\%}(\zeta_k, f_i), \quad \alpha_{\mathrm{A}}^{84.1\%}(\zeta_k) = \frac{1}{N_{\mathrm{A}}}\sum_{i=1}^{N_{\mathrm{A}}} \alpha_{\mathrm{A}}^{84.1\%}(\zeta_k, f_i). \tag{2.5.4}$$

5. For K damping values, regression analysis is applied to $\alpha_{\mathrm{A}}^{50\%}(\zeta_k)$ and $\alpha_{\mathrm{A}}^{84.1\%}(\zeta_k)$, respectively, to obtain statistical relationships $\alpha_{\mathrm{A}}^{50\%}(\zeta)$ and $\alpha_{\mathrm{A}}^{84.1\%}(\zeta)$.

2.5.2 Re-estimate Spectrum Amplification Factors in NUREG/CR-0098

Many nuclear building standards, such as ASCE 4-98 (ASCE, 2000), and DOE-STD-1023-2002 (DOE, 2002), adopt the spectrum amplification factors in Newmark's study (Newmark, Blume, and Kapur, 1973A; Newmark, Hall, and Mohraz, 1973B) to construct Newmark design spectra. The spectrum amplification factors are re-estimated based on the 20 ground motions used in Newmark *et al.* (Newmark *et al.*, 1973B) to validate the method in this study.

The results are shown in Table 2.5, in comparison with those from Newmark's study (Newmark, Blume, and Kapur, 1973A; Newmark, Hall, and Mohraz, 1973B). It is easily seen

that the differences between the two results are quite small, with the maximum relative error being 5%. The small discrepancy could be caused by the difference in the ground motions. Newmark performed baseline correction and digital filtering to the 20 ground motions in his study, because these ground motions obtained from Department of Commerce or the California Institute of Technology were raw data (Newmark *et al.*, 1973B). Since the original ground motions used by Newmark cannot be obtained, the 20 ground motions used in this study are obtained from the Pacific Earthquake Engineering Research Center (PEER) Strong Motion Database and the Center for Engineering Strong Motion Data. The ground motions from PEER Strong Motion Database have been performed baseline correction and filtered by the supplying agency (PEER, 2010), while the two ground motions from the Center for Engineering Strong Motion Data are raw data and are processed in this study prior to use. The data processing methods used by Newmark are different from those used by the supplying agency or those used in this study, resulting in different characteristics of ground motions. Values of PGA, PGV, and PGD of the 20 ground motions used by Newmark are not consistent with those obtained in the current ground motion databases due to different processing methods. As a result, the different processing methods cause the small discrepancy in the spectrum amplification factors. Moreover, as discussed in Newmark *et al.* (Newmark *et al.*, 1973B), the numbers of discrete frequencies N_A, N_V, and N_D in the acceleration sensitive, velocity sensitive, and displacement sensitive regions, respectively, and the values of the frequencies also have an effect on the spectrum amplification factors.

From the re-estimated spectrum amplification factors, regression analysis is performed, as shown in Figures 2.9, and equations for spectrum amplification factors for different damping ratios are obtained. Comparison of equations for spectrum amplification factors between this study and Newmark's study (Newmark and Hall, 1982) is presented in Table 2.6 and Figure 2.10, which shows very small difference between the two results for various damping ratios. The small difference validates the statistical method used in this study.

Table 2.5 Spectrum amplification factors from this study and those from Newmark's study

Damping ζ(%)	Study	μ (50%)			$\mu+\sigma$(84.1%)		
		α_A	α_V	α_D	α_A	α_V	α_D
0.5	T	3.66	2.51	1.95	5.10	3.71	2.88
	N	3.68	2.59	2.01	5.10	3.84	3.04
2	T	2.77	2.06	1.70	3.74	2.92	2.42
	N	2.74	2.03	1.63	3.66	2.92	2.42
5	T	2.12	1.69	1.46	2.76	2.31	1.99
	N	2.12	1.65	1.39	2.71	2.30	2.01
10	T	1.66	1.40	1.24	2.08	1.84	1.60
	N	1.64	1.37	1.20	1.99	1.84	1.69

"T" denotes this study, while "N" denotes Newmark's study.

Table 2.6 Equations for spectrum amplification factors

AF	Study	μ (50%)	$\mu+\sigma$ (84.1%)
α_A	T	$3.21-0.67\ln\zeta$	$4.41-1.01\ln\zeta$
	N	$3.21-0.68\ln\zeta$	$4.38-1.04\ln\zeta$
α_V	T	$2.28-0.37\ln\zeta$	$3.31-0.62\ln\zeta$
	N	$2.31-0.41\ln\zeta$	$3.38-0.67\ln\zeta$
α_D	T	$1.82-0.24\ln\zeta$	$2.64-0.42\ln\zeta$
	N	$1.82-0.27\ln\zeta$	$2.73-0.45\ln\zeta$

"T" denotes this study, while "N" denotes Newmark's study.

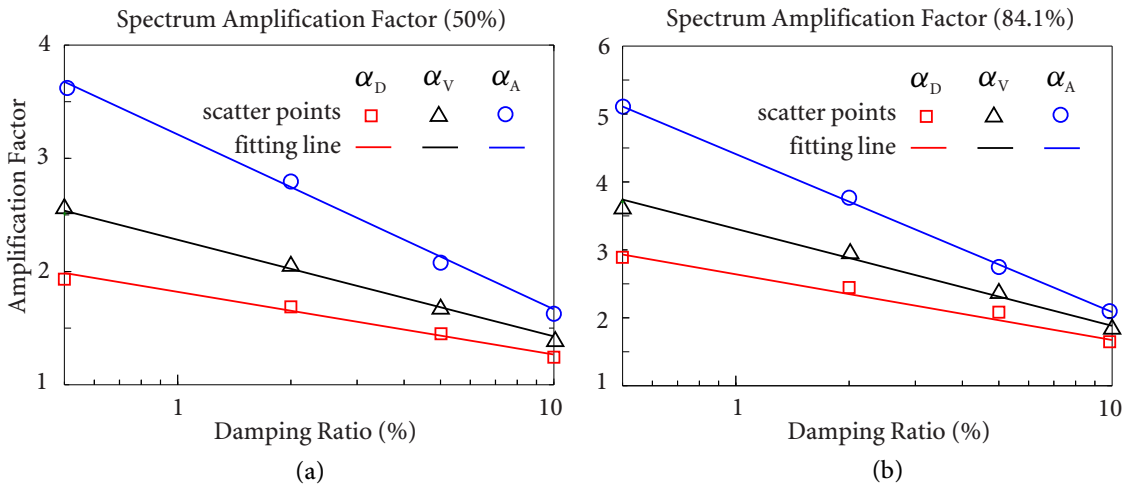

Figure 2.9 Spectrum amplification factors regression analysis: (a) for 50%; (b) for 84.1%

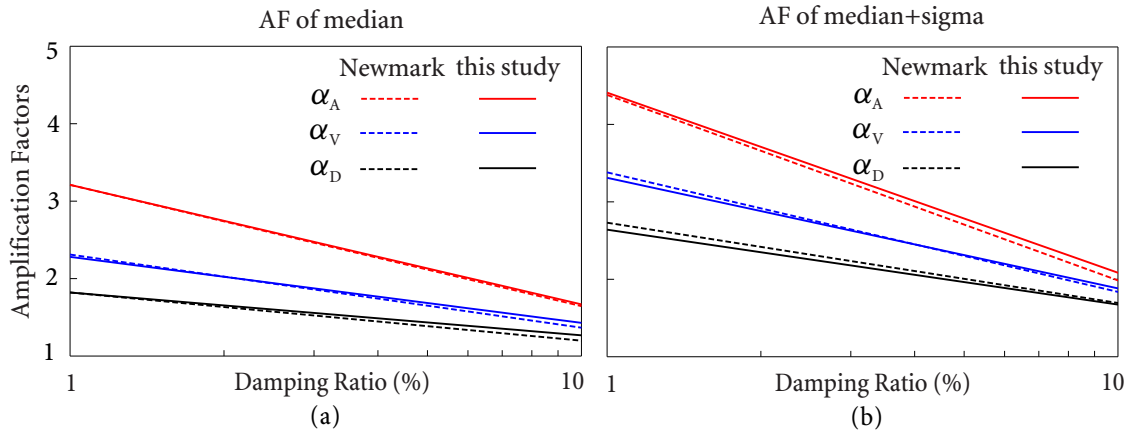

Figure 2.10 Comparison between spectrum amplification factors of various damping ratios from this study and those from Newmark's study: (a) for 50%; (b) for 84.1%

2.5.3 Spectrum Amplification Factors for Different Site Conditions

Following the procedure presented in Section 2.5.1, the median and 84.1 percentile of spectrum amplification factors with seven damping ratios (i.e., 0.5%, 1%, 2%, 3%, 5%, 7%, and 10%) considering site categories and earthquake magnitudes are statistically determined based on the three suites of ground motions at B sites, C sites, and D sites. For the same site category, ground motions are divided into two groups: small M with $M \leqslant 6.0$, and large M with $M > 6.0$; spectrum amplification factors for the two groups are listed in Tables 2.7 to 2.9. The results show that the influence of earthquake magnitudes on spectrum amplification factors is significant, especially for velocity- and displacement-amplification factors. Generally, for the same site category and damping ratio, spectrum amplification factors in the group of large M are greater than those in the group of small M, except for some cases with high damping ratios. This further verifies the significant magnitude bias of spectrum amplification factors in Newmark's study (Newmark, Blume, and Kapur, 1973A; Newmark, Hall, and Mohraz, 1973B).

2.5.4 Design Spectral Bounds

Two factors cause Newmark design spectra exhibiting lower amplitudes at high frequencies and higher amplitudes at low frequencies (Dunbar and Charlwood, 1991; Hall, 1982; Mohraz, 1976; Newmark and Hall, 1982; Villaverde, 2009). The first factor is the ratios v/a and ad/v^2 recommended by Newmark, which do not consider earthquake magnitudes, and the other factor is the spectrum amplification factors recommended by Newmark, which do not consider site categories and earthquake magnitudes. In order to resolve the problem of Newmark design spectra, the design spectral bounds of acceleration, velocity, and displacement for small earthquakes and large earthquakes of three site categories are estimated based on the average ratios of v/a and ad/v^2 in Table 2.3 and the 84.1 percentile spectrum amplification factors in Tables 2.7 to 2.9.

Table 2.7 Summary of spectrum amplification factors for B sites

Damping	Earthquake	Acceleration		Velocity		Displacement	
(% of critical)	Category	50%	84.1%	50%	84.1%	50%	84.1%
0.5	Small M	3.50	5.14	1.79	2.46	1.28	1.75
	Large M	4.25	5.98	2.53	3.61	2.35	3.47
1	Small M	3.16	4.53	1.71	2.30	1.26	1.70
	Large M	3.66	5.04	2.31	3.24	2.25	3.28
2	Small M	2.75	3.85	1.61	2.11	1.23	1.64
	Large M	3.06	4.12	2.05	2.82	2.09	3.00
3	Small M	2.48	3.42	1.54	1.99	1.21	1.58
	Large M	2.71	3.60	1.89	2.56	1.96	2.77
5	Small M	2.15	2.89	1.45	1.82	1.17	1.49
	Large M	2.31	3.01	1.68	2.23	1.77	2.44
7	Small M	1.92	2.55	1.37	1.69	1.13	1.41
	Large M	2.05	2.63	1.53	2.02	1.61	2.17
10	Small M	1.70	2.22	1.29	1.55	1.05	1.29
	Large M	1.81	2.28	1.38	1.79	1.40	1.84

For PGA $a = 1\,g$, PGV v and PGD d are estimated from average ratios of v/a and ad/v^2 in Table 2.3. The spectral bounds are estimated from the product of ground motion parameters (a, v, and d) and corresponding 84.1 percentile spectrum amplification factors.

In this study, spectral bounds for the three site categories with seven damping ratios are estimated considering earthquake magnitudes. Because the influence of earthquake magnitudes on the ratios v/a and ad/v^2 and spectrum amplification factors is remarkable, spectral bounds for small M are determined using the ground motion parameters and the 84.1 percentile spectrum amplification factors for small M, while spectral bounds for large M are determined using the ground motion parameters and the 84.1 percentile spectrum amplification factors for large M. Results of the spectral bounds are shown in Table 2.10.

From the discrete spectral bounds in Table 2.10, linear regression using the least-square method is performed to spectral bounds versus damping ratios, and the results are shown in Figures 2.11 to 2.13. Spectral bounds with any damping ratio ranging from 0.5% to 10% could be estimated from the fitting straight line in the log-log plots. Figures 2.11 to

Table 2.8 Summary of spectrum amplification factors for C sites

Damping	Earthquake	Acceleration		Velocity		Displacement	
(% of critical)	Category	50%	84.1%	50%	84.1%	50%	84.1%
0.5	Small M	3.81	5.62	2.14	3.22	1.25	1.70
	Large M	4.21	6.12	2.64	3.96	2.31	3.44
1	Small M	3.40	4.93	1.99	2.93	1.23	1.65
	Large M	3.60	5.10	2.40	3.54	2.21	3.26
2	Small M	2.92	4.16	1.83	2.59	1.21	1.59
	Large M	2.99	4.12	2.12	3.05	2.07	2.99
3	Small M	2.62	3.68	1.72	2.37	1.19	1.53
	Large M	2.64	3.58	1.94	2.74	1.95	2.77
5	Small M	2.24	3.08	1.58	2.10	1.16	1.45
	Large M	2.24	2.96	1.70	2.35	1.77	2.44
7	Small M	1.99	2.70	1.47	1.91	1.11	1.36
	Large M	2.00	2.59	1.54	2.09	1.61	2.18
10	Small M	1.75	2.33	1.35	1.70	1.03	1.22
	Large M	1.78	2.24	1.37	1.82	1.40	1.84

Table 2.9 Summary of spectrum amplification factors for D sites

Damping	Earthquake	Acceleration		Velocity		Displacement	
(% of critical)	Category	50%	84.1%	50%	84.1%	50%	84.1%
0.5	Small M	3.71	5.32	2.31	3.35	1.45	2.11
	Large M	4.25	6.04	2.94	4.42	2.41	3.71
1	Small M	3.31	4.63	2.14	3.03	1.42	2.03
	Large M	3.62	5.03	2.64	3.89	2.30	3.49
2	Small M	2.87	3.89	1.94	2.66	1.38	1.91
	Large M	3.01	4.06	2.29	3.30	2.14	3.17
3	Small M	2.59	3.45	1.81	2.42	1.34	1.82
	Large M	2.66	3.52	2.07	2.93	2.01	2.92
5	Small M	2.25	2.92	1.65	2.13	1.28	1.68
	Large M	2.26	2.92	1.80	2.48	1.82	2.56
7	Small M	2.03	2.58	1.53	1.94	1.22	1.56
	Large M	2.02	2.55	1.62	2.19	1.66	2.28
10	Small M	1.80	2.24	1.40	1.73	1.12	1.39
	Large M	1.80	2.22	1.43	1.90	1.45	1.93

Table 2.10 Spectral bounds for unit (1.0 *g*) peak ground acceleration

Site Category	Damping Ratio (% of critical)	Small *M*			Large *M*		
		accel. (*g*)	veloc. (in/sec)	displ. (in)	accel. (*g*)	veloc. (in/sec)	displ. (in)
B Sites	0.5	5.14	39.36	4.64	5.98	137.18	67.46
	1	4.54	36.84	4.52	5.04	123.44	63.88
	2	3.85	33.76	4.35	4.12	107.16	58.33
	3	3.43	31.85	4.20	3.61	97.38	53.92
	5	2.89	29.12	3.95	3.01	84.74	47.44
	7	2.55	27.13	3.75	2.64	76.78	42.28
	10	2.22	24.80	3.42	2.28	68.02	35.77
C Sites	0.5	5.62	61.18	4.77	6.12	158.40	61.28
	1	4.94	55.73	4.65	5.11	141.81	58.09
	2	4.16	49.21	4.46	4.12	122.00	53.26
	3	3.68	45.19	4.31	3.58	109.67	49.39
	5	3.08	39.90	4.07	2.96	94.00	43.47
	7	2.71	36.35	3.83	2.59	83.82	38.88
	10	2.33	32.30	3.42	2.24	72.80	32.78
D Sites	0.5	5.32	93.80	10.71	6.04	194.48	68.81
	1	4.64	84.88	10.30	5.04	171.59	64.86
	2	3.89	74.48	9.69	4.06	145.20	58.79
	3	3.45	67.98	9.24	3.53	129.21	54.32
	5	2.92	59.64	8.53	2.92	109.12	47.48
	7	2.58	54.32	7.94	2.56	96.55	42.31
	10	2.24	48.44	7.05	2.22	83.60	35.80

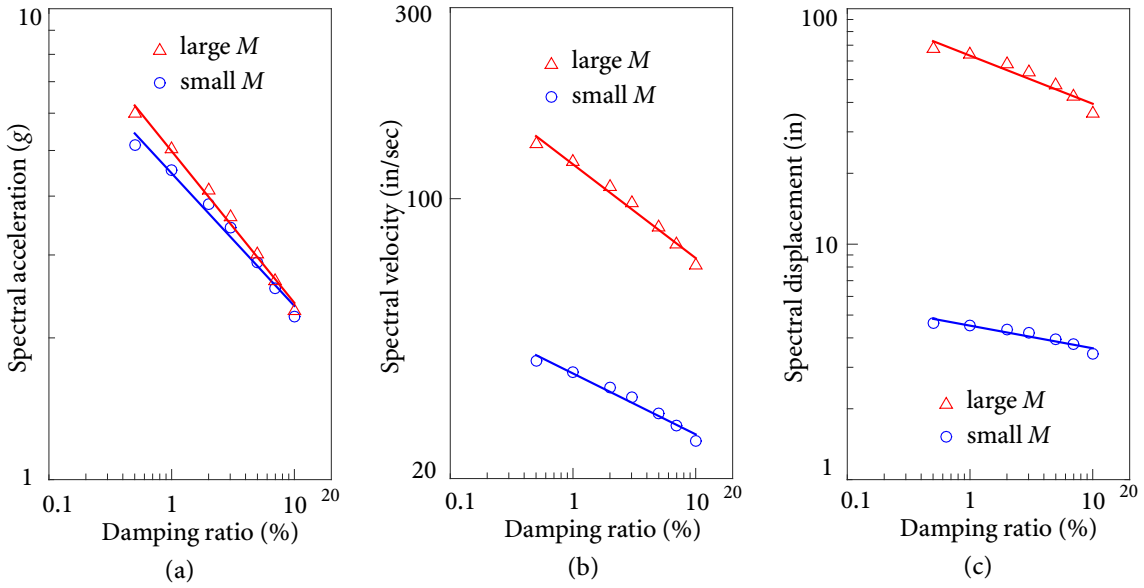

Figure 2.11 Spectral bounds for B sites

2.13 reveal that earthquake magnitudes significantly affect spectral bounds of the three site categories, especially the spectral bounds for velocity and displacement. One reason for the relatively small influence of earthquake magnitudes on the spectral bounds for acceleration is that only the variation of acceleration-amplification factors is considered and the PGA is assumed to be 1.0 g without variation, whereas for velocity and displacement, both variations of ground motion parameters, i.e., v and d, and velocity- and displacement-amplification factors are considered. Therefore, the influence of earthquake magnitudes on the spectral bounds for acceleration is much smaller than that on the spectral bounds for velocity and displacement under the case of deterministic PGA.

Generally, the spectral bounds for large earthquakes are greater than those for small earthquakes, except the spectral bounds of acceleration for C sites and D sites with high damping ratios. Because the ratios v/a and ad/v^2, and spectrum amplification factors in Newmark's study (Newmark *et al.*, 1973B) were estimated predominately based on large earthquakes, Newmark design spectra would be too conservative to sites dominated by small earthquakes.

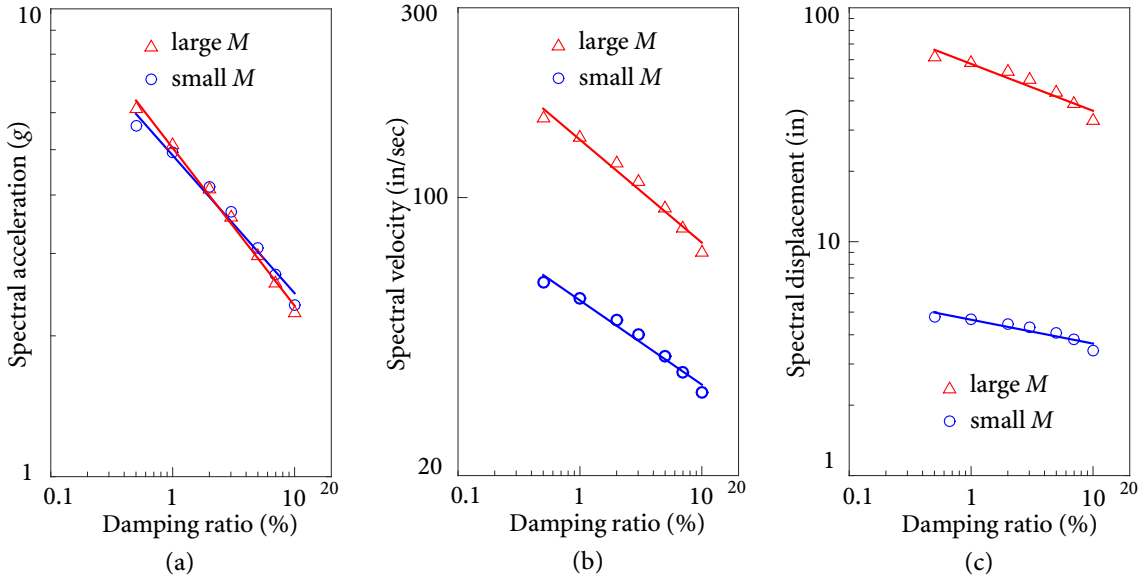

Figure 2.12 Spectral bounds for C sites

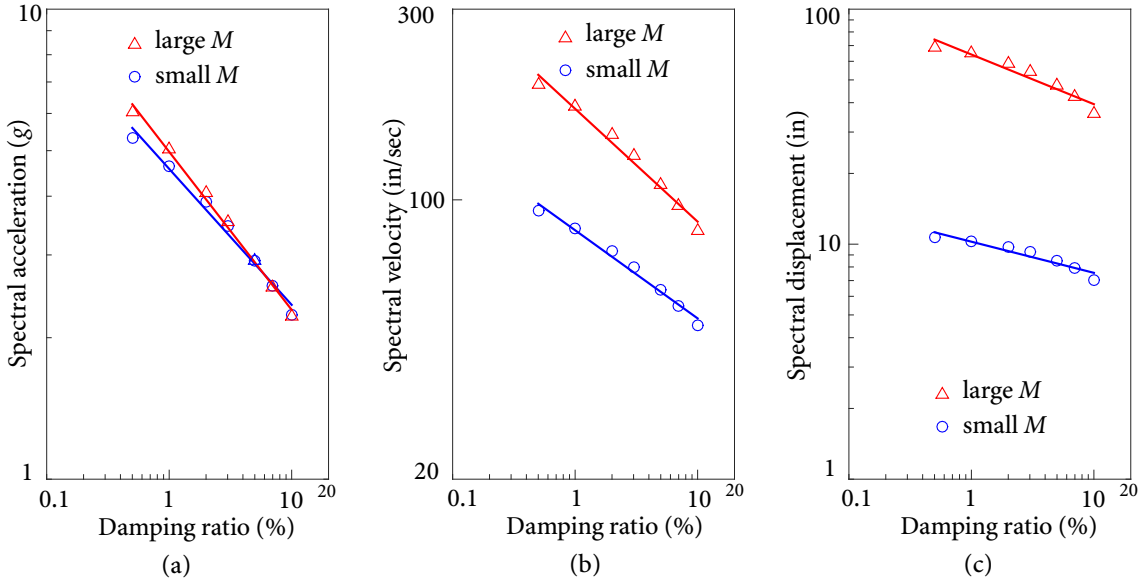

Figure 2.13 Spectral bounds for D sites

2.6 Site Design Spectrum Coefficients

Considering the problem of Newmark design spectra discussed in Section 2.1 and referring to the idea of applying site design spectrum coefficients to modify Newmark design spectra in Mohraz's study (Mohraz, 1976), a system of site design spectrum coefficients considering site categories and earthquake magnitudes is developed in this study.

Spectral bounds for Newmark design spectra can be estimated using the recommend v/a and ad/v^2 ratios, and the 84.1 percentile spectrum amplification factors in Newmark's study (Newmark, Blume, and Kapur, 1973A; Newmark, Hall, and Mohraz, 1973B). For a unit peak ground acceleration, velocity v and displacement d are estimated from the recommended v/a and ad/v^2 ratios. The product of ground motion parameters (a, v, and d) and the 84.1 percentile spectrum amplification factors yields spectral bounds for Newmark design spectra, as shown in Table 2.11.

In this study, B sites are considered to be rock sites, C sites and D sites are considered to be soil sites. For each damping ratio, the ratios of spectral bounds for B sites in Table 2.10 to spectral bounds for rock sites in Table 2.11, the ratios of spectral bounds for C sites and D sites in Table 2.10 to spectral bounds for soil sites in Table 2.11, are respectively

Table 2.11 Spectral bounds for unit (1.0 g) PGA for Newmark design spectra

Damping Ratio (% of critical)	Rock Sites			Soil Sites		
	accel. (g)	veloc. (in/sec)	displ. (in)	accel. (g)	veloc. (in/sec)	displ. (in)
0.5	5.10	138.24	61.21	5.10	184.32	108.81
1	4.38	121.68	54.96	4.38	162.24	97.71
2	3.66	105.12	48.72	3.66	140.16	86.62
3	3.24	95.04	45.10	3.24	126.72	80.18
5	2.71	82.80	40.47	2.71	110.40	71.94
7	2.36	74.88	37.25	2.36	99.84	66.22
10	1.99	66.24	34.03	1.99	88.32	60.49

calculated and presented in Table 2.12. As shown in Table 2.12, for the same site category and earthquake category (small earthquakes or large earthquakes), the ratios are nearly constant for various damping ratios, and mean ratio of the seven damping ratios are calculated. Table 2.12 reveals that

- for all types of sites, Newmark design spectra are unconservative in the high frequency region;
- for all types of sites dominated by small earthquakes with magnitudes $M \leqslant 6.0$, Newmark design spectra are too conservative in the intermediate and low frequency regions;
- for rock sites dominated by large earthquakes, Newmark design spectra are unconservative in all frequency bands, especially in the high frequency band and the low frequency band;
- for soil sites dominated by large earthquakes, Newmark design spectra are almost conservative in the intermediate or low frequency regions.

Using the mean ratios of spectral bounds in this study to spectral bounds for Newmark design spectra in Table 2.12, a system of site design spectrum coefficients is established, as listed in Table 2.13, by slightly adjusting the mean ratios in Table 2.12. For a given site category dominated by a certain earthquake category (small earthquakes or large earthquakes), the design response spectrum could be constructed by multiplying Newmark design spectral values in the acceleration sensitive, velocity sensitive, and displacement sensitive regions by the corresponding site design spectrum coefficients.

Comparing site design spectrum coefficients for different cases in Table 2.13 demonstrates that coefficients for D sites dominated by large earthquakes are relatively close to 1. These coefficients are reasonable considering the characteristics of the ground motions used in Newmark's study (Newmark, Blume, and Kapur, 1973A; Newmark, Hall, and Mohraz, 1973B; Newmark and Hall, 1982). The characteristics of the majority of ground motions in Newmark's study are similar to those of the ground motions recorded at D sites during large earthquakes ($M > 6.0$) in this study. As a result, the site design spectrum coefficients for D sites dominated by large earthquakes are relatively close to 1.

Table 2.12 Ratios of spectral bounds in this study to those for Newmark design spectra

Site Category	Damping Ratio(%)	*M*	accel.	veloc.	displ.	*M*	accel.	veloc.	displ.
B Sites	0.5	Small	1.01	0.28	0.08	Large	1.17	0.99	1.10
	1		1.04	0.30	0.08		1.15	1.01	1.16
	2		1.05	0.32	0.09		1.13	1.02	1.20
	3		1.06	0.34	0.09		1.11	1.02	1.20
	5		1.07	0.35	0.10		1.11	1.02	1.17
	7		1.08	0.36	0.10		1.12	1.03	1.14
	10		1.12	0.37	0.10		1.15	1.03	1.05
			Mean	**1.06**	**0.33**	**0.09**	**Mean**	**1.13**	**1.02**	**1.15**
C Sites	0.5	Small	1.10	0.33	0.04	Large	1.20	0.86	0.56
	1		1.13	0.34	0.05		1.17	0.87	0.59
	2		1.14	0.35	0.05		1.13	0.87	0.61
	3		1.14	0.36	0.05		1.10	0.87	0.62
	5		1.14	0.36	0.06		1.09	0.85	0.60
	7		1.15	0.36	0.06		1.10	0.84	0.59
	10		1.17	0.37	0.06		1.13	0.82	0.54
			Mean	**1.14**	**0.35**	**0.05**	**Mean**	**1.13**	**0.85**	**0.59**
D Sites	0.5	Small	1.04	0.51	0.10	Large	1.18	1.06	0.63
	1		1.06	0.52	0.11		1.15	1.06	0.66
	2		1.06	0.53	0.11		1.11	1.04	0.68
	3		1.06	0.54	0.12		1.09	1.02	0.68
	5		1.08	0.54	0.12		1.08	0.99	0.66
	7		1.09	0.54	0.12		1.08	0.97	0.64
	10		1.13	0.55	0.12		1.12	0.95	0.59
			Mean	**1.08**	**0.53**	**0.11**	**Mean**	**1.12**	**1.01**	**0.65**

Table 2.13 A system of site design spectrum coefficients in this study

Site Category	Earthquake Category	Coefficients		
		c_A	c_V	c_D
B Sites	Small M	1.15	0.40	0.15
	Large M	1.15	1.00	1.15
C Sites	Small M	1.15	0.40	0.15
	Large M	1.15	0.85	0.60
D Sites	Small M	1.10	0.55	0.15
	Large M	1.10	1.00	0.65

c_A, c_V, and c_D denote site design spectrum coefficients for acceleration, velocity, and displacement, respectively.

The main reasons that the acceleration and displacement coefficients for D sites dominated by large earthquakes are different from 1 are

- Different methods were used to process the ground motions (baseline correction and filtering) in Newmark's study and in this study, which have a great effect on the time histories of displacement (Newmark *et al.*, 1973B), especially for PGD. This would contribute to the discrepancy in displacement coefficients.
- A minority of ground motions used in Newmark's study are different from the 183 ground motions (see ground motions of LN group and LF group for D sites in Table 2.3) used in this study in term of site categories and earthquake magnitudes. Some ground motions used in Newmark's study were recorded at stations classified as A sites and B sites by USGS site classification criteria, and six ground motions were also recorded during small earthquakes. Characteristics of these ground motions are different from those of the 183 ground motions recorded at D sites during large earthquakes ($M > 6.0$) used in this study.

Table 2.14 lists the site design spectrum coefficients from Mohraz's study (Mohraz, 1976). In Mohraz's study, the ratio $v/a = 28$ in/sec (Mohraz, 1976; Newmark, Blume, and Kapur, 1973A) was used to estimate ground motion parameters for rock sites, whereas $v/a = 36$

in/sec is used in building standards (ASCE, 2000; CSA, 2010) for rock sites. The entries in boldface denote site design spectrum coefficients corresponding to $v/a = 36$ in/sec for rock sites.

Table 2.14 Site design spectrum coefficients by Mohraz

Site Category	Coefficients		
	c_A	c_V	c_D
Rock	1.05	0.5 (**0.64**)	0.5 (**0.83**)
Less than 30 ft of Alluvium underlain by Rock	1.20	0.75	0.75
30 to 200 ft of Alluvium underlain by Rock	1.20	0.75	0.75

The entries in boldface denote site design spectrum coefficients are correspond to $v/a = 36$ in/sec for rock sites.

The following conclusions can be drawn by comparing site design spectrum coefficients in this study and those in Mohraz's study.

- Both coefficients show that Newmark design spectra exhibit lower amplitudes in the high frequency region.
- Not considering earthquake magnitudes in site design spectrum coefficients will lead to very conservative Newmark design spectra if the sites of interest are dominated by small earthquakes.
- Differences exist between the site design spectrum coefficients for soil sites in Mohraz's study and in this study, which may be due to different number of ground motions used to estimate the coefficients, different site classification criteria, and different methods in dealing with earthquake magnitudes in the two studies.
- Remarkable differences exist between site design spectrum coefficients for rock sites in Mohraz's study and in this study. The remarkable difference could be explained as follows. First, Mohraz used only 9 ground motions observed at rock sites to estimate the coefficients, whereas 81 ground motions were used in this study, which would lead

to more reliable results. Second, Mohraz did not consider earthquake magnitudes in developing the site design spectrum coefficients.

2.7 Examples of Design Response Spectra

In the current procedure (Chopra, 2011; DOE, 2002) for constructing Newmark design spectra, spectral values in the acceleration sensitive, the velocity sensitive, and the displacement sensitive regions are obtained by $\alpha_A \cdot \text{PGA}$, $\alpha_V \cdot \text{PGV}$, and $\alpha_D \cdot \text{PGD}$, respectively, while in the modified Newmark design spectra, the corresponding values are modified by the site design spectrum coefficients as $c_A \cdot (\alpha_A \cdot \text{PGA})$, $c_V \cdot (\alpha_V \cdot \text{PGV})$, and $c_D \cdot (\alpha_D \cdot \text{PGD})$, respectively. Note that only the spectral values in the acceleration sensitive, the velocity sensitive, and the displacement sensitive regions are modified. Since the fundamental frequencies of many structures, especially for nuclear power plants, fall within the acceleration sensitive and velocity sensitive regions, spectral values in these two sensitive regions are crucial in design.

Using the site design spectrum coefficients obtained in this study, the 5% damping-ratio modified Newmark deign spectra at the non-exceedance level of 84.1% with PGA anchored at 0.3 g are shown in Figures 2.14 to 2.19 for B sites, C sites, and D sites, respectively. Newmark design spectra, the modified Newmark design spectra by coefficients in Mohraz's study, the design response spectrum in USNRC R.G. 1.60 (USNRC, 2014) and 84.1% response spectra by statistical analyses are also shown for comparison. The 84.1% response spectra are used as benchmarks, which are obtained by scaling all the ground motions in the group to PGA $= 0.3\,g$, calculating the 84.1% response spectrum for 5% damping ratio.

In Figures 2.14 to 2.19, only spectral values corresponding to periods less than 10 sec are presented, because the site design spectrum coefficients only modify Newmark design spectral values in the three sensitive regions. The following conclusions can be drawn:

- The problem of Newmark design spectra exhibit lower amplitude in short period (high frequency) regions and higher amplitude in long period (low frequency) regions can be easily observed.

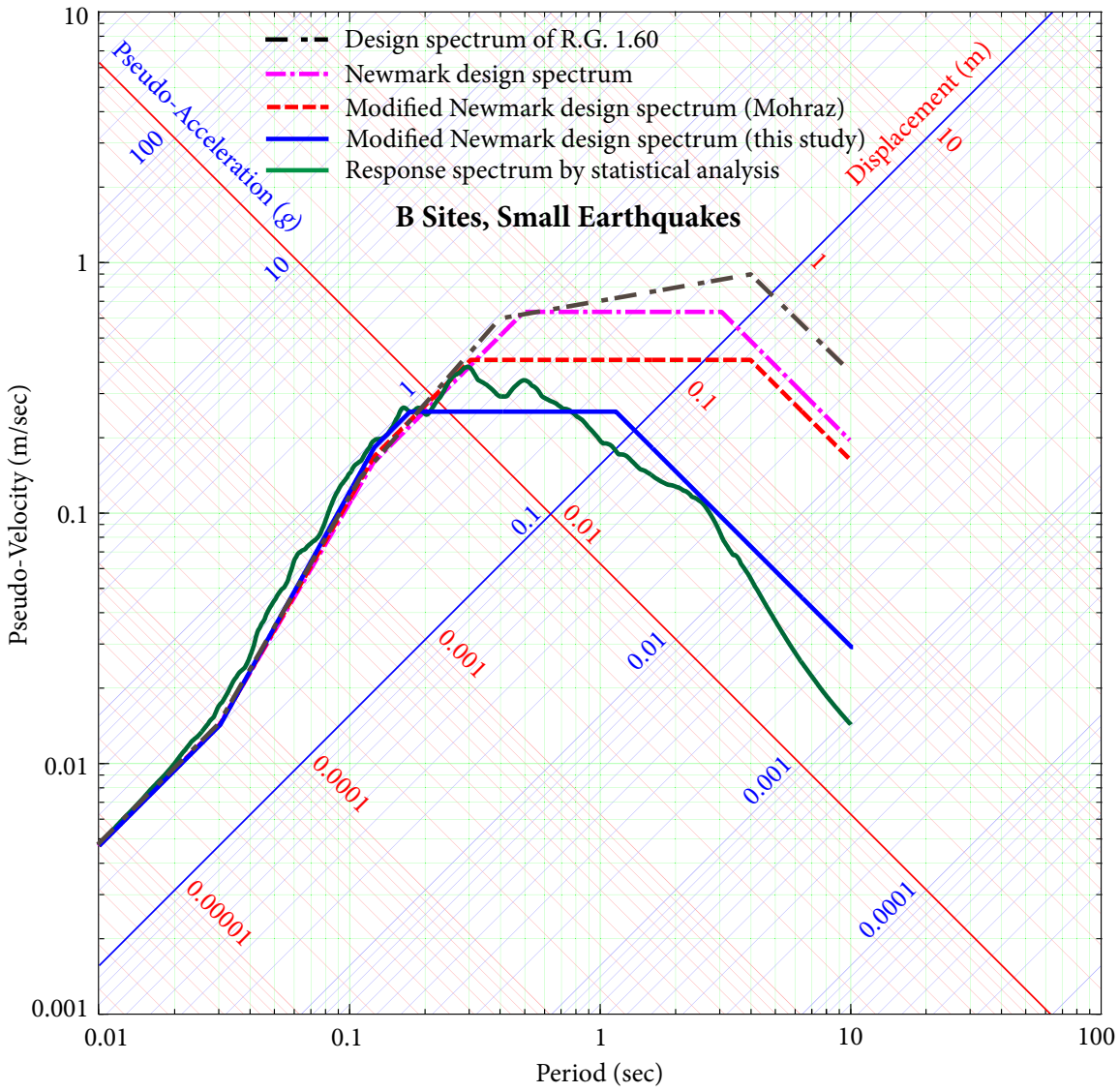

Figure 2.14 The 5% damping-ratio design spectra for B sites dominated by small earthquakes

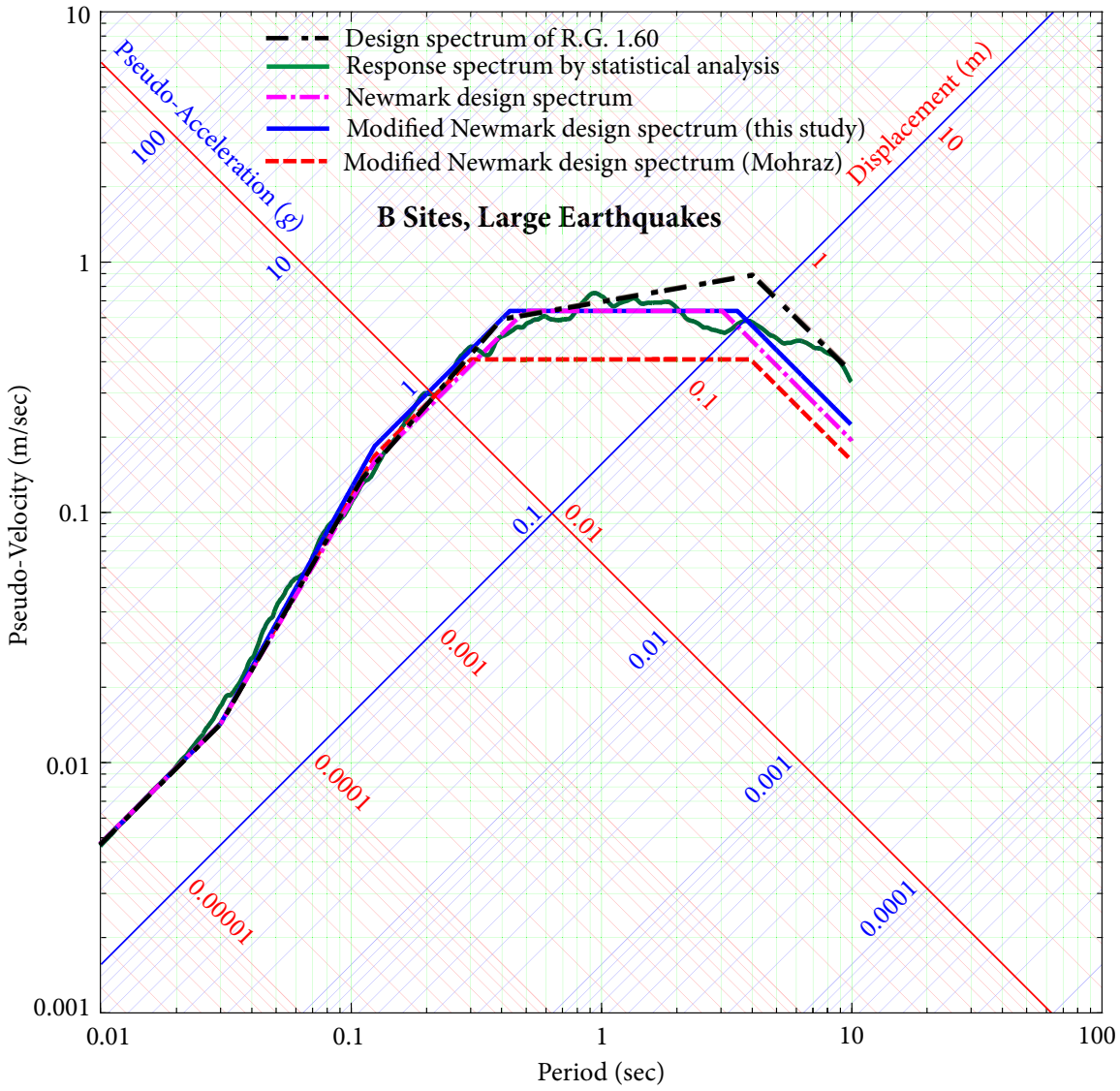

Figure 2.15 The 5% damping-ratio design spectra for B sites dominated by large earthquakes

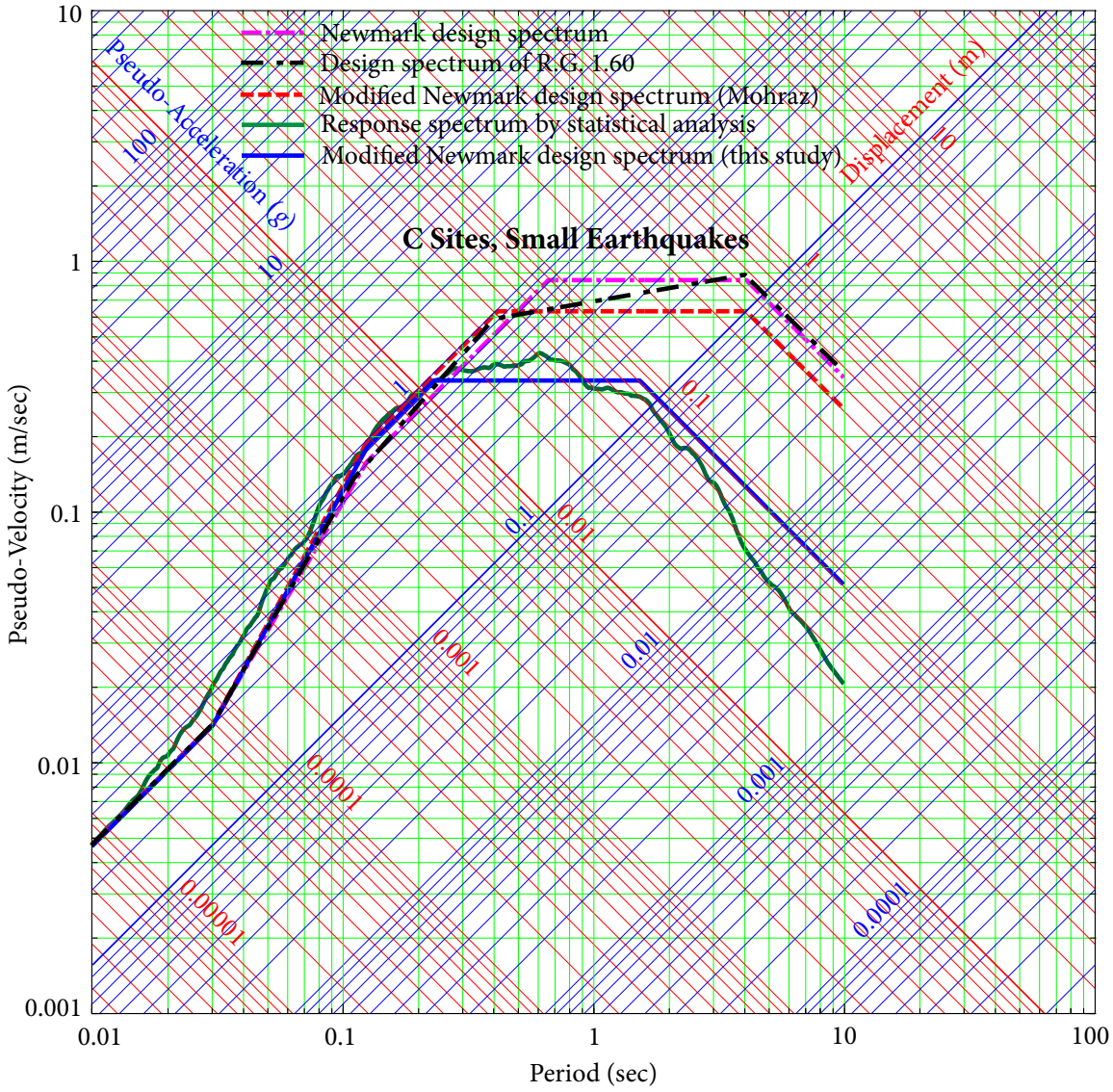

Figure 2.16 The 5% damping-ratio design spectra for C sites dominated by small earthquakes

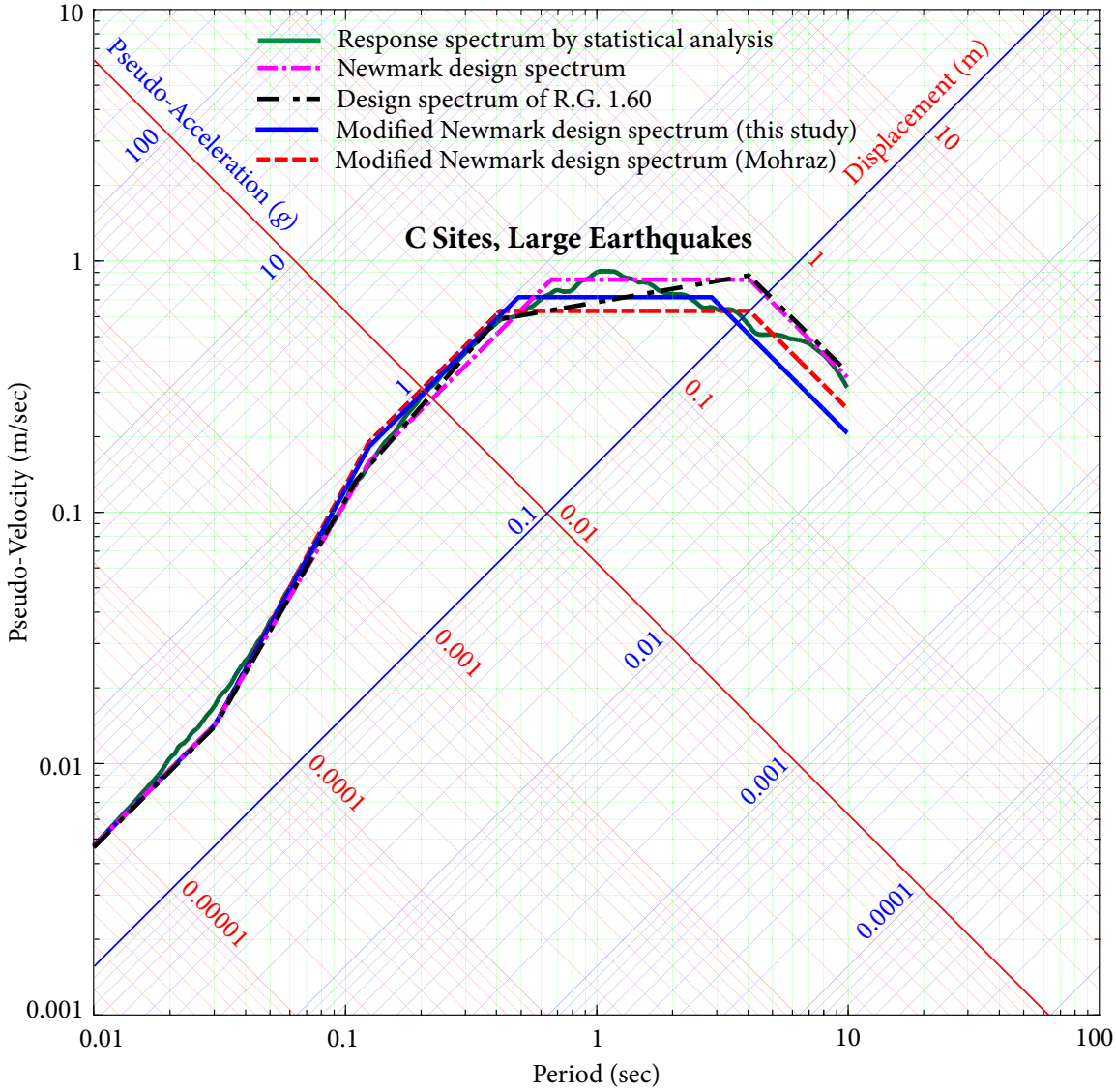

Figure 2.17 The 5% damping-ratio design spectra for C sites dominated by large earthquakes

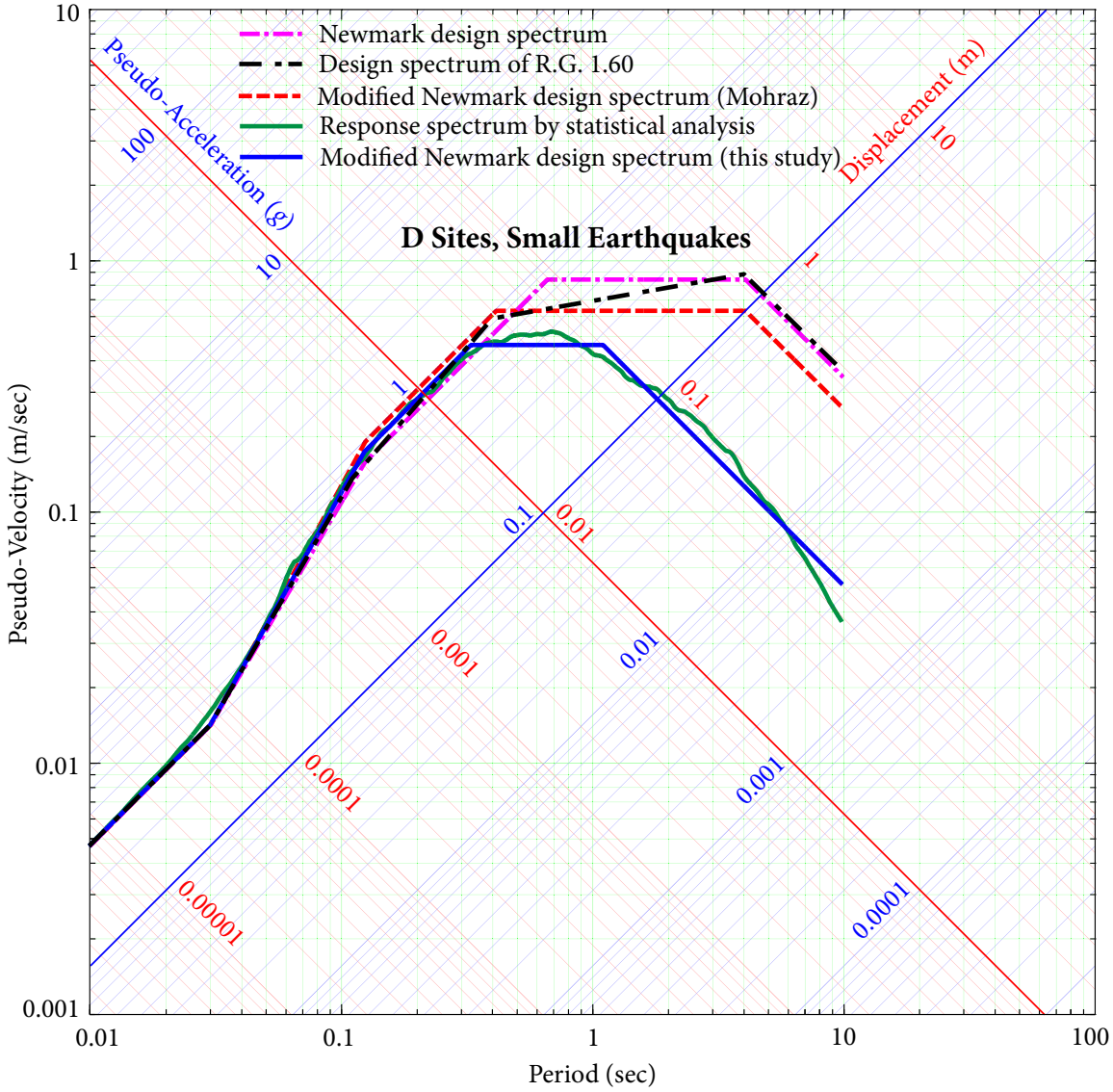

Figure 2.18 The 5% damping-ratio design spectra for D sites dominated by small earthquakes

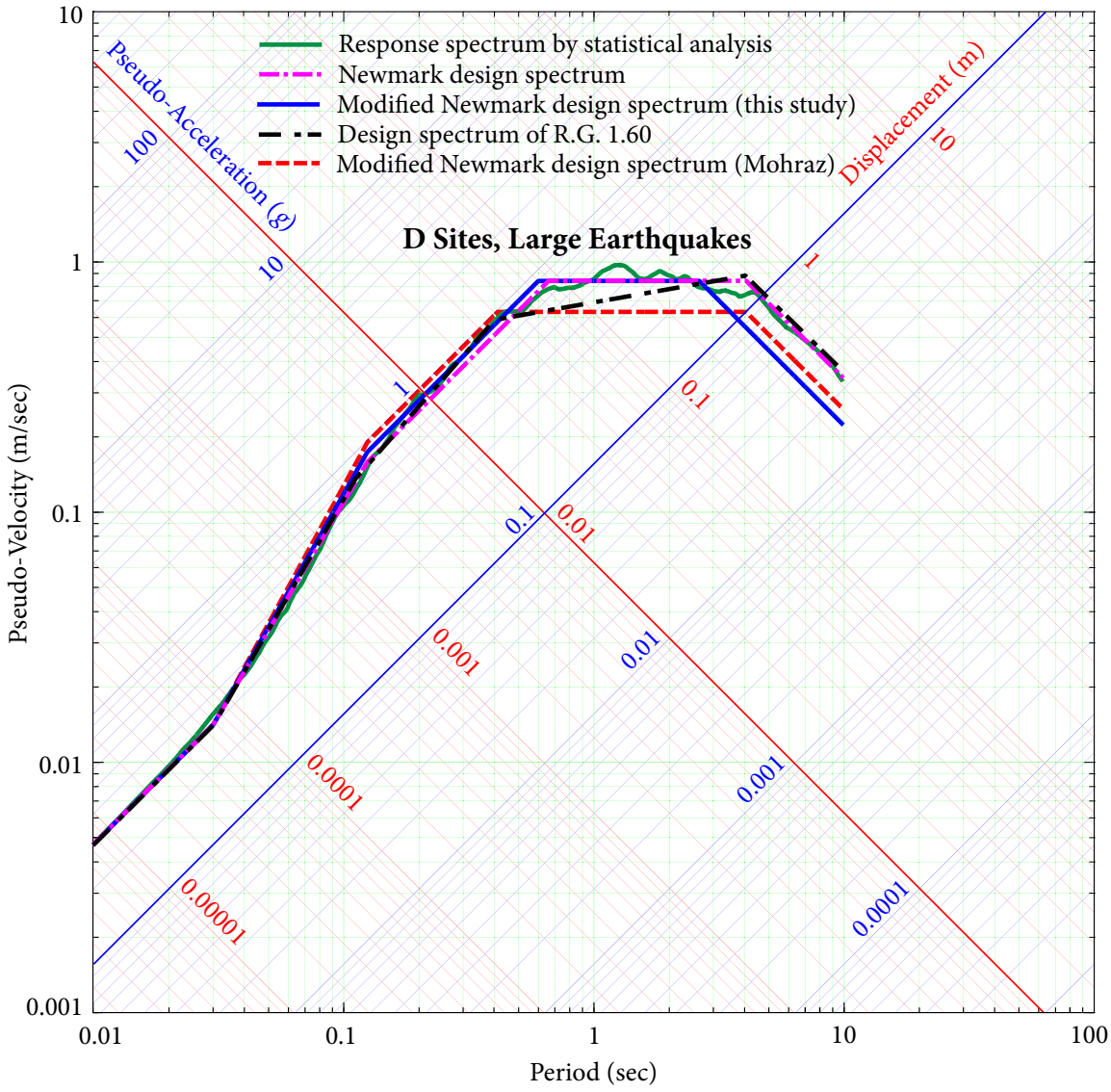

Figure 2.19 The 5% damping-ratio design spectra for D sites dominated by large earthquakes

- The design spectrum in USNRC R.G. 1.60 presents the similar problem of Newmark design spectra: lower amplitude in short period (high frequency) regions and higher amplitude in long period (low frequency) regions.
- *In cases of small earthquakes*: Newmark design spectra, the design spectrum in USNRC R.G. 1.60, and the modified Newmark design spectra by coefficients in Mohraz's study are too conservative in the intermediate and the long period regions, Newmark design spectra and the design spectrum in USNRC R.G. 1.60 tend to be lower at short periods, especially in the acceleration sensitive region. This may be due to the ground motions from predominately large earthquakes used in Newmark's study, Blume's study (Newmark *et al.*, 1973A) (the design spectrum in USNRC R.G. 1.60 was from Blume's study in 1973, in which 31 ground motions were used to develop this design spectrum) and Mohraz's study.
- *In cases of large earthquakes*:
  - In the short period region, especially in the acceleration sensitive region, of design spectra, Newmark design spectra and design spectrum in USNRC R.G. 1.60 tend to be slightly lower. The modified Newmark design spectra by coefficients in this study match better with the 84.1% benchmark response spectra than the modified Newmark design spectra by coefficients in Mohraz's study do, although the difference is small.
  - In the intermediate period region of design spectra, the modified Newmark design spectra by coefficients in Mohraz's study are significantly lower.
  - In the long period region of design spectra for C sites and D sites, the difference between the modified Newmark design spectra by coefficients in Mohraz's study and those by coefficients in this study is small, but both are lower than the 84.1% benchmark response spectra. The 84.1% benchmark response spectra are statistically determined from response spectra of ground motions normalized to PGA that have great variation in the long period region, whereas the 84.1% design spectra in the long period regions are estimated ($\alpha_D \cdot \text{PGD}$ or $c_D \cdot \alpha_D \cdot \text{PGD}$) based on response spectra of ground motions normalized to PGD that have small variation in the long period region. The non-exceedance probability 84.1% (mean-plus-

one-sigma) reflects the extent of variation. Therefore, the 84.1% benchmark response spectra tend to be much greater in the displacement sensitive region in comparison with 84.1% the "correct" Newmark design spectra discussed in this study; it is reasonable that the modified Newmark design spectra are lower than the 84.1% benchmark response spectra in the long period region.

2.8 Summary

In this chapter, 81 ground motions recorded at B sites, 210 ground motions recorded at C sites, and 300 ground motions recorded at D sites are used to establish a system of site design spectrum coefficients considering earthquake magnitudes and site categories. Using the site design spectrum coefficients to modify the Newmark design spectra resolves the problem of Newmark design spectra: exhibiting lower amplitudes at high frequencies and higher amplitudes at low frequencies in comparison with response spectra generated by the statistical method.

To establish the system of site design spectrum coefficients, the average ratios v/a and ad/v^2 for three site categories are estimated. It is found that influences of the parameter V_{s30} on these ratios are negligible, which may be due to the fact that V_{s30} is a weak proxy to seismic amplification of sites. In order to find parameters that greatly influence the ratios v/a and ad/v^2, the impacts of earthquake magnitude M and source-to-site distance R are analyzed. It is observed that the influence of R on these ratios is small, while the influence of M on these ratios is remarkable. The results also show that the ratios v/a and ad/v^2 for large earthquakes ($M > 6$) are greater than those for small earthquakes ($M \leqslant 6$).

As the ratios v/a and ad/v^2, and spectrum amplification factors together cause the problem of Newmark design spectra, this study further determines statistically the spectrum amplification factors of the three site categories considering earthquake magnitudes. The spectrum amplification factors in Newmark's study are re-estimated to validate the method used in this study. Spectrum amplification factors of the three site categories are then determined statistically for large earthquakes ($M > 6.0$) and small earthquakes ($M \leqslant 6.0$) to account for the effect of earthquake magnitudes. It is shown that, for the same site cat-

egory and damping ratio, spectrum amplification factors of large earthquakes are greater than those of small earthquakes except a few cases with high damping ratios. This further verifies the significant magnitude bias of spectrum amplification factors in Newmark's study.

Design spectral bounds for the three site categories and two cases of earthquake magnitudes are estimated using unit PGA $a = 1\ g$ (with v, and d determined from the average ratios v/a and ad/v^2) and 84.1% spectrum amplification factors. The ratios of the estimated spectral bounds to the spectral bounds for Newmark design spectra are calculated for different site categories and various damping ratios. It is found that the ratios are almost independent of damping values. Considering the independence, mean ratios of the estimated spectral bounds to the spectral bounds for Newmark design spectra over different damping values are calculated. Based on the mean ratios, a system of site design spectrum coefficients considering site categories and earthquake magnitudes is established to modify the spectral values of Newmark design spectra in the acceleration sensitive, velocity sensitive, and displacement sensitive regions. This modification overcomes the problem of Newmark design spectra.

Examples of 5% damping-ratio Newmark design spectra and the modified Newmark design spectra by different coefficients at the non-exceedance level of 84.1% with PGA anchored at 0.3 g are constructed. The following conclusions can be drawn:

- For sites dominated by small earthquakes, Newmark design spectra and the modified Newmark design spectra by the coefficients in Mohraz's study are too conservative in the intermediate and the low frequency regions.
- For all site categories and earthquake magnitudes, Newmark design spectra tend to be lower at high frequencies and higher at low frequencies.
- For sites dominated by large earthquakes, the modified Newmark design spectra by coefficients in Mohras's study tend to be lower in the intermediate frequency region.
- The modified Newmark design spectra by coefficients in this study can better match the benchmark response spectra, especially for spectra values in the acceleration sensitive and the velocity sensitive regions. This is crucial because the fundamental frequencies of many critical structures fall within these two regions.

Because of the wide range of ground motions used in this study to establish the system of site design spectrum coefficients and the good match between the modified Newmark design spectra and the benchmark response spectra in the important regions, the system of site design spectrum coefficient in this study is suitable to overcome the problem of Newmark design spectra.

2.9 Appendix

Table 2.15 Earthquake events considered for B sites

No.	Earthquake	Year	No. of Stations	Magnitude
1	San Francisco	1957	1	5.3
2	Lytle Creek	1970	1	5.3
3	San Fernando	1971	2	6.6
4	Hollister	1974	1	5.2
5	Northern Calif	1975	1	5.2
6	Friuli	1976	1	6.5
7	Friuli-1	1976	1	5.2
8	Friuli-2	1976	1	6.0
9	Friuli-3	1976	1	4.5
10	Friuli-4	1976	1	5.3
11	Tabas	1978	1	7.3
12	Coyote Lake	1979	2	5.7
13	Montenegro	1979	2	5.4
14	Montenegro-1	1979	1	5.8
15	Irpinia-Italy	1980	2	6.9
16	Irpinia,Italy-1	1980	3	6.2
17	Anza (Horse Cany)	1980	1	4.9
18	Morgan Hill	1984	2	6.2
19	Kremidia	1984	1	5.0
20	N. Palm Springs	1986	4	6.0
21	Whittier Narrows	1987	4	6.0
22	Whittier Narrows-1	1987	2	5.3
23	Kalamata	1987	1	5.3
24	Loma Prieta	1989	6	6.9
25	Sierra Madre	1991	2	5.6
26	Landers	1992	1	7.3
27	Northridge	1994	14	6.7
28	Northridge-1	1994	3	5.3
29	Kozani	1995	1	6.5
30	Kalamata	1997	1	6.4
31	Strofades	1997	1	6.6
32	Strofades-1	1997	1	5.0
33	Bovec	1998	1	4.3
34	Duzce-Turkey	1999	3	7.1
35	Chi-Chi-Taiwan	1999	3	7.6
36	Kocaeli-Turkey	1999	3	7.5
37	Izmit	1999	1	7.6
38	Izmit -1	1999	1	5.8
39	Denali-Alaska	2002	1	7.9
40	Bingol	2003	1	6.3

Table 2.16 Earthquake events considered for C sites

No.	Earthquake	Year	No. of Stations	Magnitude
1	Parkfield	1966	1	6.2
2	Lytle Creek	1970	2	5.3
3	San Fernando	1971	10	6.6
4	Sitka-Alaska	1972	1	7.7
5	Oroville	1975	8	4.7
6	Oroville-1	1975	1	4.4
7	Friuli-Italy	1976	1	6.5
8	Friuli-Italy-1	1976	2	5.9
9	Gazli-USSR	1976	1	6.8
10	Coyote Lake	1979	3	5.7
11	Norcia Italy	1979	1	5.9
12	Imperial Valley	1979	1	6.5
13	Livermore	1980	2	5.8
14	Mammoth Lakes	1980	1	6.1
15	Mammoth Lakes-1	1980	1	5.7
16	Mammoth Lakes-2	1980	1	4.8
17	Irpinia-Italy	1980	4	6.9
18	Irpinia-Italy-1	1980	2	6.2
19	Coalinga	1983	22	6.4
20	Coalinga-1	1983	1	5.1
21	Coalinga-2	1983	9	5.2
22	Coalinga-3	1983	5	5.8
23	Morgan Hill	1984	6	6.2
24	Nahanni-Canada	1985	2	6.8
25	N. Palm Springs	1986	12	6.1
26	Whittier Narrows	1987	19	6.0
27	Whittier Narrows-1	1987	3	5.3
28	Loma Prieta	1989	28	6.9
29	Big Bear	1992	1	6.5
30	Northridge	1994	27	6.7
31	Kobe-Japan	1995	1	6.9
32	Kocaeli-Turkey	1999	4	7.5
33	Duzce-Turkey	1999	10	7.1
34	Hector Mine	1999	5	7.1
35	Chi-Chi- Taiwan	1999	4	6.2
36	Chi-Chi-Taiwan-1	1999	1	5.9
37	Anza	2001	1	4.9
38	Gilroy	2002	3	4.9
39	Yorba Linda	2002	1	4.3
40	Denali-Alaska	2002	2	7.9

Table 2.17 Earthquake events considered for D sites

No.	Earthquake	Year	No. of Stations	Magnitude
1	Kern County	1952	1	7.4
2	Parkfield	1966	2	6.2
3	San Fernando	1971	3	6.6
4	Managua-Nicaragua	1972	1	6.2
5	Point Mugu	1973	1	5.7
6	Friuli-Italy	1976	2	6.5
7	Friuli-Italy-1	1976	1	5.9
8	Coyote Lake	1979	3	5.7
9	Imperial Valley	1979	14	6.5
10	Imperial Valley-1	1979	12	5.0
11	Livermore	1980	3	5.8
12	Livermore-1	1980	3	5.4
13	Anza (Horse Canyon)	1980	1	5.2
14	Mammoth Lakes	1980	2	6.1
15	Mammoth Lakes-1	1980	2	5.7
16	Mammoth Lakes-2	1980	4	5.9
17	Mammoth Lakes-3	1980	3	5.7
18	Mammoth Lakes-4	1980	4	5.9
19	Victoria-Mexico	1980	2	6.3
20	Irpinia-Italy	1980	1	6.9
21	Westmorland	1981	4	5.9
22	Mammoth Lakes	1983	2	5.3
23	Coalinga	1983	19	6.4
24	Coalinga-1	1983	6	5.1
25	Coalinga-2	1983	1	5.4
26	Coalinga-3	1983	2	5.2
27	Coalinga-4	1983	4	5.8
28	Morgan Hill	1984	11	6.2
29	Hollister	1986	2	5.5
30	Mt. Lewis	1986	1	5.6
31	N. Palm Springs	1986	11	6.1
32	Chalfant Valley	1986	3	5.8
33	Chalfant Valley-1	1986	6	6.2
34	Imperial Valley	1979	1	6.5
35	Chalfant Valley	1986	1	6.2
36	Chalfant Valley-1	1986	2	5.4
37	Whittier Narrows	1987	30	6.0
38	Whittier Narrows-1	1987	6	5.3
39	Superstition Hills	1987	1	6.2
40	Superstition Hills-1	1987	2	6.5
41	Spitak-Armenia	1988	1	6.8
42	Loma Prieta	1989	21	6.9
43	Cape Mendocino	1992	2	7.0
44	Landers	1992	19	7.3
45	Big Bear	1992	10	6.5
46	Northridge	1994	28	6.7
47	Kobe-Japan	1995	3	6.9
48	Dinar-Turkey	1995	1	6.4
49	Kocaeli-Turkey	1999	6	7.5
50	Upland	1990	1	5.6
51	Manjil-Iran	1990	1	7.4
52	Sierra Madre	1991	2	5.6
53	Northridge-1	1994	1	5.1
54	Northridge-2	1994	12	5.3
55	Little Skull Mtn-NV	1992	1	5.7
56	Hector Mine	1999	11	7.1

C H A P T E R 3

Uniform Hazard Spectra on Soil Surface

This chapter presents a probabilistic framework to perform Probabilistic Seismic Hazard Analysis (PSHA) for soil sites. In this framework, the soil parameter variabilities, the nonlinear property of soils, and the vector-valued seismic site responses analysis comprehensively integrate into PSHA for soil sites. Because local soil conditions greatly affect ground motions propagating from bedrock to soil surface, the evaluation of ground motions at the soil surface needs to consider effects of the local soil conditions. Ground Motion Prediction Equations (GMPEs) using the generic soil to characterize local soil conditions are possible to estimate ground motions at the soil surface, but the estimation is not acceptable for critical structures because of lacking accuracy. Therefore, site amplification is used to modify the bedrock GMPEs to make them suitable for soil sites. Based on the modified GMPEs, PSHA for soil sites are performed accurately and methods to construct acceptable soil UHS are proposed. Using an example soil site, influences of soil parameter variabilities and soil nonlinear responses on spectral shapes and spectral amplitudes of design spectra are discussed.

3.1 Introduction

For critical structures, such as Nuclear Power Plants (NPPs), rock is usually defined as a geotechnical material whose shear-wave velocity is greater than 2.8 km/sec for sites in the Central and Eastern North America (USNRC, 2007a). The design spectra used to perform seismic design of structures should reflect seismic characteristics of the target site; structures built on rock site should be designed by a design spectrum for rock sites, while structures built on soil sites should be designed by a design spectrum for soil sites. In practice, most NPPs are located at soil sites according to the definition of soil sites in nuclear industries (ASCE, 2005). The design spectra for soil sites are commonly required for the seismic design of NPPs.

In the seismic design of NPPs, Safe Shutdown Earthquakes (SSEs) are determined based on an evaluation of the maximum earthquake potential considering the regional and local geology, seismology, and specific characteristics of local subsurface materials. SSEs play a crucial role in the seismic resistant design of NPPs (ASCE, 2005) and are usually represented by Design Response Spectra (DRS), such as Uniform Hazard Spectra (UHS). When incident bedrock motions propagate from bedrock to the soil surface, the soil deposit changes characteristics of the ground motions; the extent of this change largely depends on features of the incident bedrock motions and characteristics of the local soil deposit. Thus, differences between Uniform Hazard Spectra at soil sites (soil UHS) and Uniform Hazard Spectra at rock sites (rock UHS) are caused and governed by this change.

Ground Motion Prediction Equations (GMPEs) are necessary for the construction of UHS. Some empirical GMPEs (Abrahamson and Silva, 1997; Campbell and Bozorgnia, 2003; Boore and Atkinson, 2008) for soil sites could be used to construct the soil UHS in the same way as constructing the rock UHS. These attenuation relationships in the empirical GMPEs are based on ground motion data recorded at stiff and generally deep soil sites, and use generic soils to characterize various practical soil sites. Since these empirical GMPEs are constrained by the ground motion data that they used to develop their attenuation relationships, it is only appropriate to use the attenuation relationships to probabilistically estimate ground motions at the soil surface above a similar soil deposit with consideration

of the effects of differences between the practical site-specific profile and the generic profile used in the estimation (ANS, 2008). This requirement actually greatly restricts the usage of empirical GMPEs to construct the soil UHS. Furthermore, for shallow soil profiles above a bedrock where there is a pronounced shear-wave velocity contrast between the soil and the bedrock, strong site response effects are caused, and estimation of ground motions at the soil surface by empirical GMPEs is quite not suitable (ANS, 2008). Thus, the soil UHS determined by empirical GMPEs using the generic soils are unacceptable for critical structures, such as NPPs and large dams.

To construct the acceptable soil UHS for NPPs, an early method suggested multiplying the rock UHS by a deterministic (usually the mean or median) site amplification and obtain the soil UHS, which is similar with the current method used in building standards (ASCE, 2005; USNRC, 2007A). The single value of site amplification used in this method implies that there is no uncertainty in the calculation of site amplification. However, research showed (Regnier *et al.*, 2008) that site amplification of a soil site is affected by many factors: the incident bedrock motion, the shear-wave velocity, the soil normalized shear modulus, the damping ratio, and the thickness of soil layers, most of which are uncertain. Therefore, the exceedance levels of ground motions at the soil surface calculated by the early method are unknown, non-uniform and inconsistent over all the controlling periods, and generally nonconservative. This would lead to inaccurate and unrealistic prediction of structure responses in performance-based seismic design, which has been introduced in many regular building standards (FEMA, 1997; FEMA, 2000; ATC, 1996; IBC, 2000), and nuclear building standards (USNRC, 2007A; ANS, 2004; ASCE, 2005).

To overcome this problem, McGuire *et al.* (McGuire *et al.*, 2001) have suggested that site amplification be used to modify the bedrock GMPEs into site-specific attenuation relations prior to perform PSHA for soil sites. Based on this idea, several methods have been proposed to perform PSHA for soil sites. Tsai (Tsai, 2000) proposed a method to calculate Peak Ground Acceleration (PGA) at the soil surface, and obtained several conclusions: (1) nonlinear site effects play a crucial role in the calculation of annual probability of exceedance for PGA at the soil surface, and failure to consider nonlinearity of soils may dramatically distort the soil-hazard curve and may not always lead to conservative estimates; (2) the

linear analysis is unable to appropriately describe the nonlinear characteristics of a soil site; (3) the annual probability of exceedance for PGA at the soil surface calculated by nonlinear seismic site response analysis cannot be facilitated by GMPEs method, due to the loss of detailed site information in GMPEs method; and (4) the result of annual probability of exceedance for PGA greatly depends on the standard deviation of the site amplification.

Cramer (Cramer, 2003) also proposed an equation to calculate the soil-hazard curve following the suggestions of McGuire. By applying the proposed equation to two sites, Cramer concluded that using the proposed method can make about a 10% difference or even larger in ground motion estimates over simply multiplying a bedrock probabilistic ground motion by a mean site amplification.

Bazzurro and Cornell (Bazzurro and Cornell, 2004A; Bazzurro and Cornell, 2004B) used Monte Carlo simulation to study the effects of soil parameter uncertainties and input motion uncertainties on site amplification at the soil surface. Based on two different example soil sites, they developed site amplification models for the two example sites, modified bedrock GMPEs and proposed equations to perform PSHA for soil sites. Using the proposed equations, soil UHS for the two example sites are constructed.

This chapter provides a probabilistic framework to construct soil UHS by PSHA for soil sites. Three issues should be considered in PSHA for soil sites: the variability of soil parameters, the nonlinear property of soils, and the vector-valued site response analysis method (Li *et al.*, 2012). In this study, the vector-valued seismic site response analysis considering the variability of soil parameters and the nonlinear property of soils is performed, and site amplification regression model for a specific soil site is obtained by regression analysis. Using the site amplification regression model, the bedrock GMPEs are first modified, and the modified GMPEs valid for the specific soil site are obtained. Using the modified GMPEs, PSHA for soil sites are performed, based on which soil UHS is constructed.

3.2 Local Site Conditions

During many earthquakes, the local geology and soil conditions profoundly influenced the important characteristics, i.e., amplitude, frequency content, and duration, of the strong

ground motions. The extent of their influences depends on the geometry and property of the subsurface materials, the topography of the sites, and the characteristic of the underlying ground motions. One-dimensional seismic site response analysis is usually used in practice based on three assumptions (Kramer, 1996):

- all boundaries are horizontal;
- the response of a soil deposit is predominantly caused by SH-waves propagating vertically from the underlying bedrock;
- the soil and bedrock surfaces extend infinitely in the horizontal direction.

3.2.1 Soil Parameters Affecting Seismic Site Response

It is widely accepted that shear-wave velocity, soil normalized shear modulus, and soil damping ratio greatly affect the seismic response of a soil site (Kramer, 1996; Hashash, Groholski, Phillips, *et al.*, 2011; Villaverde, 2009; Hashash and Park, 2001).

Zhang and Andrus (Zhang *et al.*, 2005) showed that there is a relation between soil normalized shear modulus $G/G_{\max}$ and damping ratio ξ:

$$\xi - \xi_{\min} = f(G/G_{\max}) = 10.6(G/G_{\max})^2 - 31.6(G/G_{\max}) + 21, \tag{3.2.1}$$

$$\xi_{\min} = \xi_{\min 1}\left(\frac{\sigma'_{\mathrm{m}}}{P_{\mathrm{a}}}\right)^{-\frac{k}{2}}. \tag{3.2.2}$$

The parameters $\xi_{\min 1}$ and k are determined by the soil types. P_{a} is equal to 100 kPa; equation (3.2.2) converts $\xi_{\min 1}$ to $\xi_{\min}$ for σ'_{m} other than 100 kPa.

Based on these two equations, soil damping curves can be generated from the normalized shear modulus reduction curves.

3.2.2 Uncertainty of Soil Properties

Uncertainties pervade in many aspects of geotechnical earthquake engineering. The uncertainties in geotechnical properties of soils can be formally classified as *aleatory uncertainty* and *epistemic uncertainty*. *Aleatory uncertainty* represents the natural randomness of soil properties. It results from inherent variability of soil properties, which is the consequence of natural geologic process that continually modify the properties of soils in situ. *Epistemic*

uncertainty represents the uncertainty due to the lack of knowledge and shortcomings in measurement or calculation. It results from equipment errors, procedural-operator errors, random testing effects, and transformation uncertainties.

Previous studies (Toro, 1993; Lumb, 1966) showed that the variability of soil parameters can be modeled by either normal distribution or lognormal distribution. The Electric Power Research Institute (Toro, 1993) tested soil samples from more than 200 different sites. The testing results showed that both shear-wave velocity and normalized shear modulus conform to lognormal distribution. Another laboratory testing results on natural soils indicated that most soil properties can be considered as random variables conforming to normal distribution (Lumb, 1966). Examples of randomized normalized shear modulus with average coefficients of variation 0.12 and randomized shear-wave velocity with average coefficients of variation 0.3 are shown in Figure 3.1.

The variabilities of normalized shear modulus, damping ratio, and shear-wave velocity vary with soil types, depths of soil samples, and values of the shear strain, which is another source of uncertainties in PSHA for soil sites. A completely probabilistic seismic hazard analysis is created by integrating the variabilities in both seismic sources and soil parameters into the whole analysis process.

In seismic site response analysis, soil parameters with variability are first randomized independently. These randomized soil parameters are then randomly paired with each other to obtain random profiles. For example, if 30 random profiles are to be created, the following steps will be required.

- Generate independently 30 sets of randomized normalized shear modulus, and 30 randomized shear-wave velocity profiles.
- Randomly pair the 30 sets of randomized normalized shear modulus with the 30 randomized shear-wave velocity profiles (one set of randomized normalized shear modulus with one randomized shear-wave velocity profile).
- 30 random profiles are generated that follow the distributions of the normalized shear modulus and the shear-wave velocity.

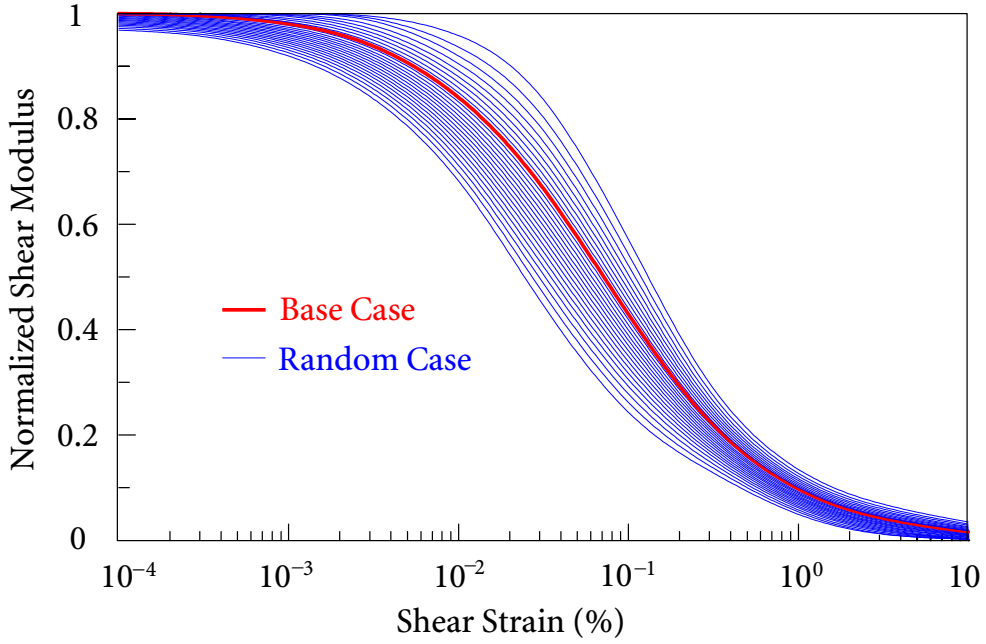

(a) normalized shear modulus

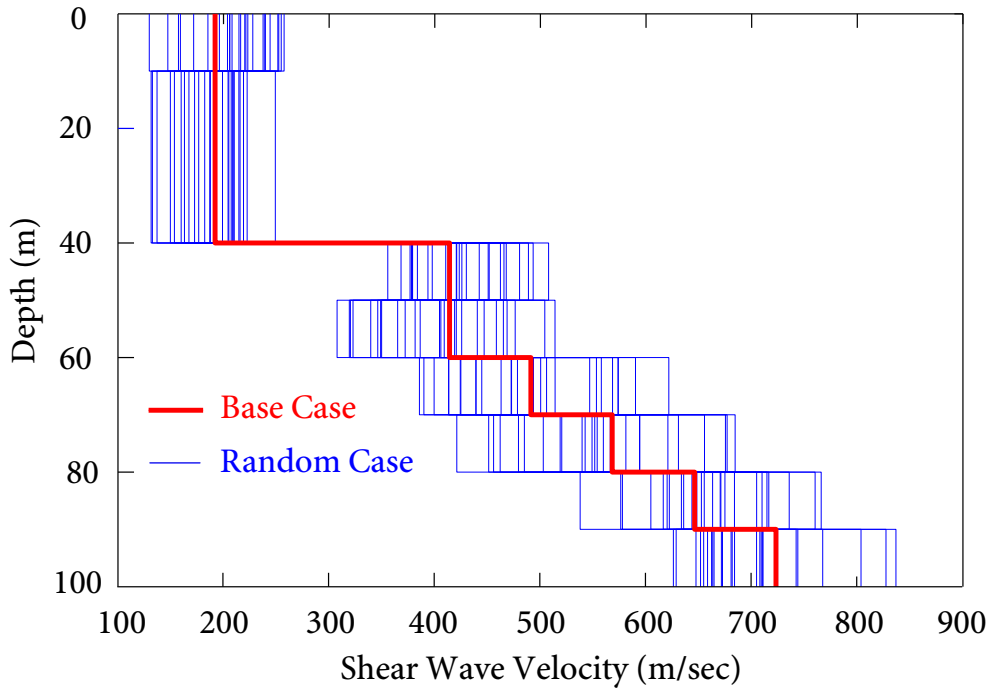

(b) shear-wave velocity

Figure 3.1 Randomized soil parameters

3.3 Seismic Site Response Analysis

The computer program *DEEPSOIL* (Hashash *et al.*, 2011) is used to simulate seismic site responses. Soil nonlinear models relatively accurately characterize dynamic behaviors of soil under low to high ground motion intensities. Serval soil nonlinear models have been proposed in the past (Kondner, 1963; Idriss, Dobry, and Sing, 1978; Streeter, Wylie, and Richart, 1974; Faccioli, Santoyo, and Leon, 1973; Iwan, 1967; Hashash and Park, 2001), among which the Modified Konder and Zelasko (MKZ) model is usually used (Hashash and Park, 2001). Research has shown that the MKZ model is able to predict ground motions at the soil surface better than the equivalent linear model (Li, 2010). The MKZ model is used by *DEEPSOIL* to describe the soil stress-strain relationship under seismic excitations in simulating seismic site responses.

Seismic waves generated from earthquake fault ruptures usually propagate from bedrock to soil surface. Due to effects of soil deposits, characteristics of ground motions at the soil surface are changed in comparison with those at the bedrock. Prediction of these changes requires seismic site response analysis, which is affected by many factors, such as soil profiles, soil parameters, and incident bedrock motions at the bedrock; most of these factors are uncertain. Therefore, methods of probabilistic analysis are applied to the seismic site response analysis.

At a specific soil site, if G_k is taken as a response measure of the soil site corresponding to a vibration period T_k, its probability is given by

$$p(g_k) = \int_{-\infty}^{\infty} p(g_k | i_m) f_{I_m}(i_m) \mathrm{d}i_m, \tag{3.3.1}$$

where I_m is the incident bedrock motion intensity measure, $p(g_k | i_m)$ is the probability of response measure equal to g_k given i_m, and $f_{I_m}(i_m)$ is the probability density function of I_m. Since only one incident bedrock motion intensity measure is used to predict the response measure, this analysis method is called scalar site response analysis.

Due to uncertainties in incident bedrock motions, using only one incident bedrock motion intensity measure to predict seismic response of soil sites cannot give satisfactory results. Therefore, multiple incident bedrock motion intensity measures are required to

improve the accuracy of scalar site response analysis. Using multiple incident bedrock motion intensity measures, the probability of G_k corresponding to vibration period T_k is given by

$$p(g_k) = \int_{-\infty}^{\infty} \int_{-\infty}^{\infty} \cdots \int_{-\infty}^{\infty} p(g_k \mid i_{m1}, i_{m2}, \ldots, i_{mn}) \\ f_{I_{m1} I_{m2} \cdots I_{mn}}(i_{m1}, i_{m2}, \ldots, i_{mn}) \mathrm{d}i_{m1} \mathrm{d}i_{m2} \cdots \mathrm{d}i_{mn}, \quad (3.3.2)$$

where $I_{m1}, I_{m2}, \ldots, I_{mn}$ are incident bedrock motion intensity measures, and $f_{I_{m1} I_{m2} \cdots I_{mn}}(i_{m1}, i_{m2}, \ldots, i_{mn})$ is the joint probability density function. Since multiple incident bedrock motion intensity measures are used to predict the response measure, this analysis method is called vector-valued site response analysis.

3.3.1 Selection of Ground Motions

Selection of ground motions is a crucial part for this research, because the ground motions selected are used as incident bedrock motions at the base of soil deposits to perform seismic site response analysis and to predict ground motions at the soil surface. Appropriate ground motions could represent characteristics of seismic sources around the site of interest, and lead to reliable and realistic prediction of site responses. Several selection criteria are applied to select appropriate ground motions for this research:

- The earthquake magnitude M and source-to-site distance R of the selected ground motions should roughly match M and R of the seismic sources around the site of interest. Since large far-field earthquakes produce long-period dominant ground motions, and small near-field earthquakes produce short-period dominant ground motions, selected ground motions with M and R significantly different from those of the seismic sources could overdrive or underdrive soil deposits.
- Since a soil deposit is sitting on a bedrock, incident bedrock motions at the base of the soil deposit possess the characteristics of ground motions observed at rock sites, which have higher high-frequency amplitudes than the ground motions observed at soil sites. Therefore, the selected ground motions should be recorded at "rock" sites according to the U.S. Geological Survey (USGS) or Geomatrix classification criteria, which are

ground motions recorded at sites with V_{s30} greater than 750 m/sec (USGS criteria) or classified as *A* (Geomatrix criteria). However, because of the limited number of ground motions satisfy these criteria, ground motions recorded at soft rock sites (with values of V_{s30} between 360 m/sec and 750 m/sec) are also selected. Using ground motions recorded at soft rock sites does not invalidate statistical findings of this research on the variability of site amplifications caused by the variability of incident bedrock motions (Bazzurro and Cornell, 2004B).

- To ensure that the ground motion signal is correct up to the period of 5 sec, the lowest usable frequencies of the selected ground motions should be possibly lower than 0.2 Hz. This issue is important to the seismic response of soil sites, because when the soil undergoes cyclic degradation, its effective vibration period increases.
- Some exclusion criteria are also applied. Ground motions observed at dam crests, toes, or abutment are excluded, because they contain effects of these structures.

3.3.2 Site Amplification

Local site effects on ground responses can be evaluated using *site amplification*, which is defined as the ratio of an intensity value of a ground motion at a target site to the intensity value of the ground motion at a reference site underneath the target site. In this research, spectral acceleration is taken as the ground motion intensity measure; a soil site is taken as the target site; and a rock site is taken as the reference site. Site amplification plays a crucial role in the prediction of ground motions at the target site. Since statistically robust empirical evaluations of site amplification cannot generally be performed on a practical site accurately due to the generic soil used, accurate site-specific amplifications considering the detailed site information are required.

There are many factors affecting the site amplification of a soil site (Regnier *et al.*, 2008), including the input motion, the shear-wave velocity, the soil normalized shear modulus, the damping ratio, and the thickness of soil layers. Research has showed that the greatest influence comes from the input motion (Rogers *et al.*, 2007), on whose amplitude and frequency content the site amplification depends. Therefore, in site amplification regression analysis,

predictor variables are selected from input motion intensities; effects of the uncertainties in the soil parameters are absorbed in the site amplification residuals, which always reflect the composite effects of a large number of factors not considered in the regression model.

GMPEs are usually valid to describe the attenuation relation of ground motions propagating from seismic sources to rock sites, but they are usually invalid for soil sites due to the generic soil instead of site-specific soil used. The site amplification in this study, which includes the variabilities in both the seismic sources and the soil properties, can be used to modify bedrock GMPEs in order to provide new attenuation relations valid for soil sites with modified uncertainties. Thus, PSHA for soil sites can be performed accurately results based on the modified GMPEs.

3.3.3 Regression Analysis

Regression analysis is a statistical methodology that establishes a statistical relationship between a dependent variable (response variable) and one or more independent variables (predictor variables). A statistical relationship, unlike a functional relation, is not perfect. In general, the observations for a statistical relation do not fall exactly on the curve of the relationship. Residuals are introduced in the regression model to describe deviations of the response variable observations from the fitted function.

The construction of a regression model involves the selections of predictor variables and functional form for the regression relation.

Selection of Predictor Variables

In reality, there are numerous factors affecting the response variable, but only a limited number of predictor variables should be included in a regression model. A set of predictor variables selected for the regression model should be "good" to some extent for the purpose of analysis. A major consideration in selecting predictor variables is the extent to which a chosen variable contributes to reducing the remaining variation of the response variable after allowance is made for the contributions of other predictor variables that have tentatively been included in the regression model (Neter *et al.*, 1996). The predictor variables should not be highly correlated with each other to avoid multicollinearity effects. However, if values

of predictor variables, for which inferences are to be made, follow the same multicollinearity pattern as the data, on which the regression model is based, the presence of serious multicollinearity often does not affect the usefulness of the fitting model for estimating response or making predictions (Neter, Kutner, Wasserman, *et al.*, 1996; Johnson, 1991).

For a small number of potential predictor variables, *all-possible-regressions procedure* (Neter *et al.*, 1996) could be used to select the "good" subset of predictor variables according to some criteria, such as coefficient of determination, R^2, from the pool of potential predictor variables. Usually, the higher the value of R^2, the better the subset of predictor variables is. However, an overfitted regression model should be avoided. Although it could give a high value of R^2, it may also cause a larger variance of the estimated parameters than that of a simpler regression model.

Selection of Functional Form for Regression Relations

The selection of functional form of regression relation is tied to the selection of predictor variables. Sometimes, previous research may indicate a functional form. More frequently, the functional form of the regression relation is not known in advance, and must be decided empirically based on the data collected. Linear or quadratic regression functions are often used as satisfactory first approximations to regression functions of unknown nature (Neter *et al.*, 1996). In most cases, these simple regression functions may be used even when previous research provides a functional form, especially when the known functional form is complex but can be reasonably approximated by a linear or quadratic regression function.

The selection of functional form is directly related to scalar and vector-valued site amplification regression analyses in this research. As mentioned in Section 3.3, there are two different methods to perform site response analysis: scalar site response analysis and vector-valued site response analysis. Accordingly, the corresponding site amplification regression analyses are scalar site amplification regression analysis and vector-valued site amplification regression analysis, respectively, which will be discussed in the following.

Scalar Site Amplification Regression Analysis

Since site amplification is period-dependent, the regression analysis is done period-by-period to predict the mean site amplification at different periods.

The scalar site response analysis uses a single parameter of input motions to predict responses of the soil deposit. Accordingly, this parameter of input motions is taken as the predictor variable for the scalar site amplification regression analysis.

Previous studies (Abrahamson and Silva, 1997; Bazzurro and Cornell, 2004B; Cramer, 2003) show that the period-dependent site amplification, $A(T)$, strongly depends on spectral acceleration of input motions. Abrahamson *et al.* (Abrahamson and Silva, 1997) proposed an equation of site amplification by regression analysis based on strong ground motions observed at different sites,

$$\ln A(T) = a_{10} + a_{11} \ln(\mathrm{PGA}_{\mathrm{rock}} + c_5), \tag{3.3.3}$$

where $\mathrm{PGA}_{\mathrm{rock}}$ is the peak ground motion of input motions at the bedrock, a_{10}, a_{11}, and c_5 are the regression coefficients.

In the site amplification regression analysis in this research, the functional form follows equation (3.3.3). For the scalar site amplification regression analysis, the general quadratic functional form is expressed as:

$$\ln A(T_i) = c_0 + c_1 \ln S_a(T_k) + c_2 [\ln S_a(T_k)]^2 + \tau_{\mathrm{soil}} + \tau_{\mathrm{motion}} + \varepsilon_{\mathrm{r}}, \tag{3.3.4}$$

where A is the site amplification, T_i is a vibration period at which site amplification is regressed, T_k is another vibration period (T_i may be equal to T_k), $S_a(T_k)$ is the spectral value of the input motions at vibration period T_k, τ_{soil} denotes the random effects in the soil properties, τ_{motion} denotes the random effects in the input motions, and ε_{r} denotes the remaining errors.

The three error components are assumed to be independent and normally distributed with zero means and variances σ^2_{soil}, $\sigma^2_{\mathrm{motion}}$, and σ^2_{r}, respectively. The three error components can also be lumped into a combined residual, $\varepsilon_{\ln A}$.

Vector-Valued Site Amplification Regression Analysis

The vector-valued site response analysis uses multiple parameters of input motions to predict responses of the soil deposit. Accordingly, the multiple parameters of input motions are taken as the predictor variables for the vector-valued site amplification regression analysis. As all the predictor variables are logarithmically transformed before construction of the regression model, their interaction effects are eliminated in the transformed functional form.

The general quadratic functional form for vector-valued regression analysis is

$$\begin{aligned}\ln A(T_i) = c_0 + c_{11}\ln S_a(T_1) + c_{12}\ln S_a(T_2) + \cdots + c_{1n}\ln S_a(T_n) \\ + c_{21}[\ln S_a(T_1)]^2 + c_{22}[\ln S_a(T_2)]^2 + \cdots + c_{2n}[\ln S_a(T_n)]^2 + \varepsilon_{\ln A},\end{aligned} \quad (3.3.5)$$

where $S_a(T_1), S_a(T_2), \ldots, S_a(T_n)$ are the spectral acceleration values of input motions at vibration periods $T_1, T_2, \ldots, T_n$, respectively, and $\varepsilon_{\ln A}$ is the combined residual.

3.4 Uniform Hazard Spectra on Soil Sites

Uniform Hazard Spectra on soil sites (soil UHS) and on rock sites (rock UHS) possess different spectral shapes and spectral amplitudes, which are caused by the local soil site effects. Although GMPEs for soil sites could be used to construct soil UHS in the same way as constructing rock UHS, they use the generic soil instead of site-specific soil in their attenuation relations. Thus, soil UHS determined by GMPEs for soil sites are usually not accurate enough. Site amplification taking account of specific soil site effects is used to modify the bedrock GMPEs in order to provide new attenuation relations valid for soil sites with modified uncertainties. Then, PSHA for soil sites can be performed more accurately, based on which accurate soil UHS considering detailed site information are constructed.

3.4.1 PSHA for Soil Sites

The vector-valued site amplification regression analysis is much better than the scalar site amplification regression analysis. Thus, the vector-valued site amplification regression model is used in this study to modify the bedrock GMPEs.

Consider a specific soil site in a region where there are N_S potential seismic sources, and take $S_a(T_k)$ as the single parameter of ground motions at the soil surface. For a given spectral acceleration value at the bedrock corresponding to period T_k, denoted by x_k, the probability $P\{S_a(T_k) \geqslant s_k\}$ is equal to the probability $P\{A_k \geqslant s_k/x_k\}$. Thus, the annual probability of $S_a(T_k)$ exceeding a specified value of s_k is expressed as

$$\lambda_{s_k} = P\{S_a(T_k) \geqslant s_k\} = \int_0^\infty \int_0^\infty \int_0^\infty P\{A_k \geqslant s_k/x_k \mid x_k, \text{pga}, z_2\} \left\{ \sum_{i=1}^{N_S} \nu_i \int_0^\infty \int_0^\infty f_{X_k,\text{PGA},Z_2 \mid M,R}(x_k, \text{pga}, z_2 \mid m, r) f_M(m) f_R(r) \text{d}m \, \text{d}r \right\}_i \text{d}x_k \, \text{d}(\text{pga}) \, \text{d}z_2, \quad (3.4.1)$$

where A_k is the site amplification at period T_k, PGA is the peak ground acceleration of input motions at the bedrock, Z_2 is spectral acceleration of input motions at the bedrock averaged over the second resonant vibration period range (i.e., the first resonant frequency vibration period range) of soil columns, $f_{X_k,\text{PGA},Z_2 \mid M,R}(x_k, \text{pga}, z_2 \mid m, r)$ is the multivariate lognormal probability density function of x_k, pga, and z_2 conditional on m and r. Given a pair of m and r, a vector of the natural logarithm of spectral accelerations at multiple periods has been empirically tested to follow multivariate normal distribution (Jayaram and Baker, 2008).

In equation (3.4.1), the term $P\{A_k \geqslant s_k/x_k \mid x_k, \text{pga}, z_2\}$ is used to modify the bedrock GMPEs. $\ln A_k$ follows normal distribution with mean $\mu_{\ln A_k}$ and standard deviation $\sigma_{\ln A_k}$, both of which are obtained from site amplification regression models.

The probability of A_k exceeding the value of s_k/x_k given x_k, pga, and z_2 is calculated by

$$P\{A_k \geqslant s_k/x_k \mid x_k, \text{pga}, z_2\} = \int_{s_k/x_k}^\infty f_{A_k \mid X_k,\text{PGA},Z_2}(a_k \mid x_k, \text{pga}, z_2) \text{d}a_k. \quad (3.4.2)$$

In equation (3.4.1), the joint probability density function $f_{X_k,\text{PGA},Z_2 \mid M,R}(x_k, \text{pga}, z_2 \mid m, r)$ is obtained from the bedrock GMPEs. As it involves the joint distribution of X_k, PGA, and Z_2, their correlations are needed. The correlation coefficients between spectral values at any two periods have been calculated by Baker and Jayaram (Baker and Jayaram, 2009) on the basis of four Next Generation Attenuation (NGA) Models and the Pacific Earthquake Engineering Research Center (PEER) strong ground motion database. These correlation coefficients are suitable for periods from 0.01 sec to 10 sec, as shown in Figure 3.2.

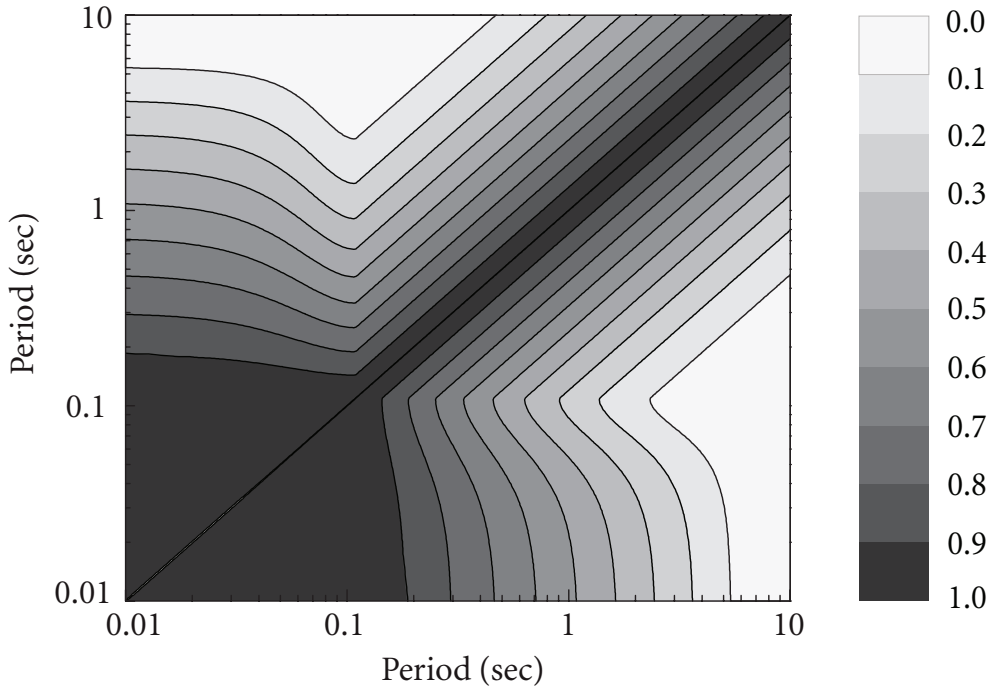

Figure 3.2 The correlation of spectral acceleration at multiple periods

The correlation coefficient between spectral value at a single period $S_a(T)$ and an average spectral value over n periods, $S_a^{\text{avg}}(T_1, T_2, \ldots, T_n)$, can be calculated by (Baker and Cornell, 2006) the formula

$$\rho_{\ln S_a(T),\, \ln S_a^{\text{avg}}(T_1,T_2,\ldots,T_n)} = \frac{\sum_{i=1}^{n} \rho_{\ln S_a(T),\, \ln S_a(T_i)} \sigma_{\ln S_a(T_i)}}{\sqrt{\sum_{i=1}^{n}\sum_{k=1}^{n} \rho_{\ln S_a(T_k),\, \ln S_a(T_i)} \sigma_{\ln S_a(T_i)} \sigma_{\ln S_a(T_k)}}}, \tag{3.4.3}$$

where $\rho_{\ln S_a(T_k),\, \ln S_a(T_i)}$ denotes the correlation coefficient between $\ln S_a(T_k)$ and $\ln S_a(T_i)$, and $\sigma_{\ln S_a(T_i)}$ denotes standard deviation of $\ln S_a(T_i)$.

Having obtained the mean annual rate of exceedance of spectral acceleration $S_a(T_k)$ in equation (3.4.1), the temporal uncertainties of the occurrence of such earthquakes are modelled using Poisson process (Kramer, 1996). The probability of at least one event occurring, i.e., at least one event of spectral acceleration $S_a(T_k)$ exceeding s_k during time period t is given by

$$P\left\{S_a(T_k) \geqslant s_k\right\} = 1 - \mathrm{e}^{-\lambda_{s_k} t}. \tag{3.4.4}$$

In most earthquake engineering practices, the time period t is taken as one year or 50 years. In this study, the time period t is taken as one year. When the values of the mean rate of exceedance in equation (3.4.1) is small, which is almost always the case in reality, the mean rate of exceedance and the probability of exceedance are numerically identical. The commonly used terminology of "annual probability of exceedance" is employed directly for λ_{s_k} in equation (3.4.1) in this context instead of the mean rate of exceedance.

3.4.2 Generation of Soil UHS

The framework of the scalar PSHA for soil sites was described in Section 3.4.1. For a specified probability level of exceedance p, the value of target spectral acceleration s_k, with the probability of $S_a(T_k)$ exceeding s_k equal to p, can be determined from the seismic hazard curve. A plot of the thresholds $s_k\,(k=1,2,\ldots,n)$ for a number of controlling periods $T_1, T_2, \ldots, T_n$ gives the soil UHS. Since the probability of exceedance p of spectral acceleration at each controlling period is constant, the spectrum is called "uniform hazard". Figure 3.3 illustrates the determination of soil UHS from seismic hazard curves on the soil surface.

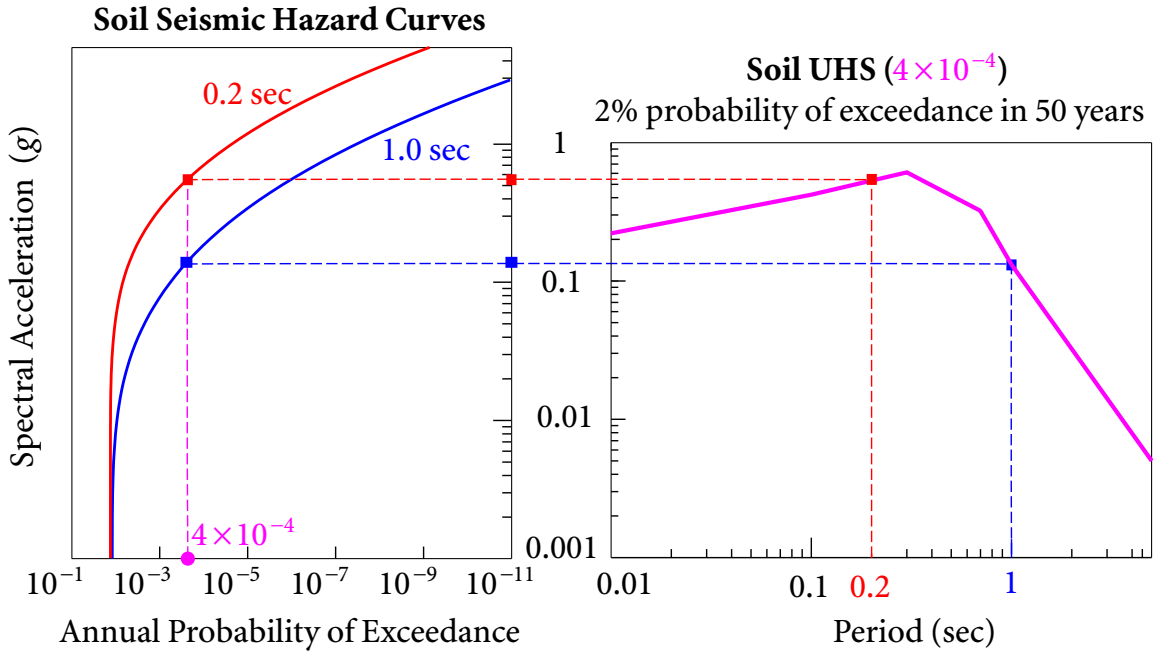

Figure 3.3 Determine soil UHS using soil seismic hazard curves

3.4.3 Seismic Hazard Deaggregation

The PSHA procedures described in Section 3.4.1 are able to compute the annual probability of exceedance at a particular site based on the aggregate risk from potential earthquakes of many different magnitudes occurring at many different source-to-site distances. The annual probability of exceedance computed in a PSHA, therefore, is not associated with a particular earthquake magnitude or source-to-site distance.

In some cases, it may be necessary to estimate the most likely earthquake magnitude and the source-to-site distance in order to select appropriate ground motions, or determine a representative (beta) earthquake (McGuire, 1995) for seismic response analysis of structures. Thus, Seismic Hazard Deaggregation (SHD), which identifies the typical magnitude and source-to-site distance of earthquakes making the largest contributions to a specified probability of exceedance, is necessary.

Due to effects of a soil site sitting on a bedrock, which could change the important characteristics—frequency content, duration and amplitude—of ground motions, results of SHD at soil sites are different from those at rock sites. Since seismic hazards at short periods are dominated by small near-field earthquakes, and seismic hazards at long periods are dominated by large far-field earthquakes (McGuire, 1995), the hazard contribution from large far-field earthquakes tends to be greater for soil sites than for rock sites due to effects of local soil conditions.

According to the formulation of PSHA for soil sites in equation (3.4.1), the annual probability of exceeding a spectral acceleration value s_k at period T_k for the intervals $[m_l, m_{l+1}]$ and $[r_j, r_{j+1}]$ is given by

$$\lambda_{s_k,j,l} = \int_0^\infty \int_0^\infty \int_0^\infty \bar{P}\{A_k \geqslant s_k / x_k \,|\, x_k, \text{pga}, z_2\} \left\{ \sum_{i=1}^{N_S} \nu_i \int_{r_j}^{r_{j+1}} \int_{m_l}^{m_{l+1}} f_{X_k,\text{PGA},Z_2\,|\,M,R}(x_k, \text{pga}, z_2 \,|\, m, r) f_M(m) f_R(r) \mathrm{d}m \,\mathrm{d}r \right\}_i \mathrm{d}x_k \,\mathrm{d}(\text{pga}) \,\mathrm{d}z_2. \quad (3.4.5)$$

Dividing these annual probabilities of exceedance level $\lambda_{s_k,j,l}$ for different m-r intervals by the total annual probability of exceedance λ_{s_k} in equation (3.4.1), relative hazard contributions corresponding to different m-r can be calculated.

Based on relative hazard contributions of different *m*-*r* intervals, the weighted mean values of magnitude and distance that contribute to the target probability of exceedance, λ_{s_k}, can be calculated

$$\overline{M}_{s_k} = \sum_{l=1}^{m_n-1} \sum_{j=1}^{r_n-1} \frac{m_l + m_{l+1}}{2} \cdot \frac{\lambda_{s_k,j,l}}{\lambda_{s_k}}, \quad \overline{R}_{s_k} = \sum_{j=1}^{r_n-1} \sum_{l=1}^{m_n-1} \frac{r_j + r_{j+1}}{2} \cdot \frac{\lambda_{s_k,j,l}}{\lambda_{s_k}}, \tag{3.4.6}$$

where m_n and r_n are the numbers of intervals for m and r, respectively.

From SHD described above, the characteristic earthquake ($\overline{M}_{s_k}$ and $\overline{R}_{s_k}$) is determined in an average sense. In order to determine the beta earthquake for a specific soil site, it is necessary to determine the characteristic occurrence rate $\overline{\nu}_{s_k}$ using a similar method in the sense of weighted average

$$\overline{\nu}_{s_k} = \sum_{i=1}^{N_S} \nu_i \cdot \frac{\lambda_{s_k,i}}{\lambda_{s_k}}. \tag{3.4.7}$$

For engineering structures, 0.1 sec and 1.0 sec usually represent the short period and the long period, respectively. If the result of SHD at $T_1 = 0.01$ sec is $\{\overline{M}_{s_1}, \overline{R}_{s_1}, \text{and } \overline{\nu}_{s_1}\}$, and the result of SHD for $T_2 = 1.0$ sec is $\{\overline{M}_{s_2}, \overline{R}_{s_2}, \text{and } \overline{\nu}_{s_2}\}$, where s_1 and s_2 are corresponding to the annual probability level of exceedance p at T_1 and T_2, respectively, then the beta earthquake (McGuire, 1995) can be expressed as

$$M_\beta = \frac{1}{2}(\overline{M}_{s_1} + \overline{M}_{s_2}), \quad R_\beta = \frac{1}{2}(\overline{R}_{s_1} + \overline{R}_{s_2}), \quad \nu_\beta = \frac{1}{2}(\overline{\nu}_{s_1} + \overline{\nu}_{s_2}). \tag{3.4.8}$$

Previous studies (McGuire, 1995; Ni, Zhang, Xie, and Pandey, 2012) showed that the results of PSHA by the beta earthquake match quite well with those obtained by considering all potential earthquakes generated from seismic sources around the site.

In reality, for different probability levels of exceedance p, the resulting earthquake events from SHD vary in a small range at the same period (Halchuk and Adams, 2004). Thus, the spectral accelerations on different probability levels of exceedance at the same period T_k can be induced approximately by the same earthquake event ($\overline{M}_{s_k}$, $\overline{R}_{s_k}$ and $\overline{\nu}_{s_k}$). The selection of target probability level of exceedance p does not affect the ability of the beta earthquake to represent all potential earthquakes of the site.

3.5 Numerical Application

The soil site at Charleston, South Carolina, as shown in Figure 3.4, is used as an example site for which the soil UHS is constructed using the probabilistic framework proposed aforementioned in this study. Site profile of the Charleston Site is shown in Figure 3.5. The parameter V_s in this figure represents the best estimate of shear-wave velocity.

Previous studies have been performed to analyze the seismic activity near this site. The Charleston earthquake in 1886 with magnitude around 7.3 was the strongest historic earthquake in the eastern United States (Andrus *et al.*, 2003). One study (Talwani and Cox, 1985) from field evidence and radiocarbon dates showed that at least two earthquakes with magnitudes greater than 6.2 preceded the 1886 event in the past 3000 to 3700 years near this site. Another study (Amick and Gelinas, 1991) showed that, during the last 2000 to 5000 years, large earthquakes with magnitudes greater than 5.4 may be happened exclusively in South Carolina by analyzing the spacial distribution of seismically induced liquefaction features along the Atlantic seaboard. Referring to the document published by U.S. Geological Survey (USGS) (Petersen *et al.*, 2008), it can be concluded that earthquakes near this site should mainly be with magnitude from 6.0 to 7.5, and source-to-site distance from 0 to 80 km.

The bedrock GMPEs proposed by Boore and Atkinson (Boore and Atkinson, 2008)—characterizing ground motions propagating from seismic sources to the bedrock underneath the Charleston Site—are first modified by the site amplification regression model for the soil site, and then the modified GMPEs valid to characterize ground motions propagating from seismic sources to bedrock then to the soil surface are obtained. Then, using the modified GMPEs, the PSHA for the soil site are performed more accurately and soil UHS is constructed.

Two different numerical characterizations of the soil site are used in this study: base case, with deterministic soil parameters whose values are equal to their best engineering estimates (such as the mean values or median values of soil parameters), and random case, with uncertain soil parameters. PSHA for soil sites under the base case only considers the uncertainty from seismic sources, while PSHA for soil sites under the random case considers the uncertainties from both seismic sources and soil parameters. These two cases are used

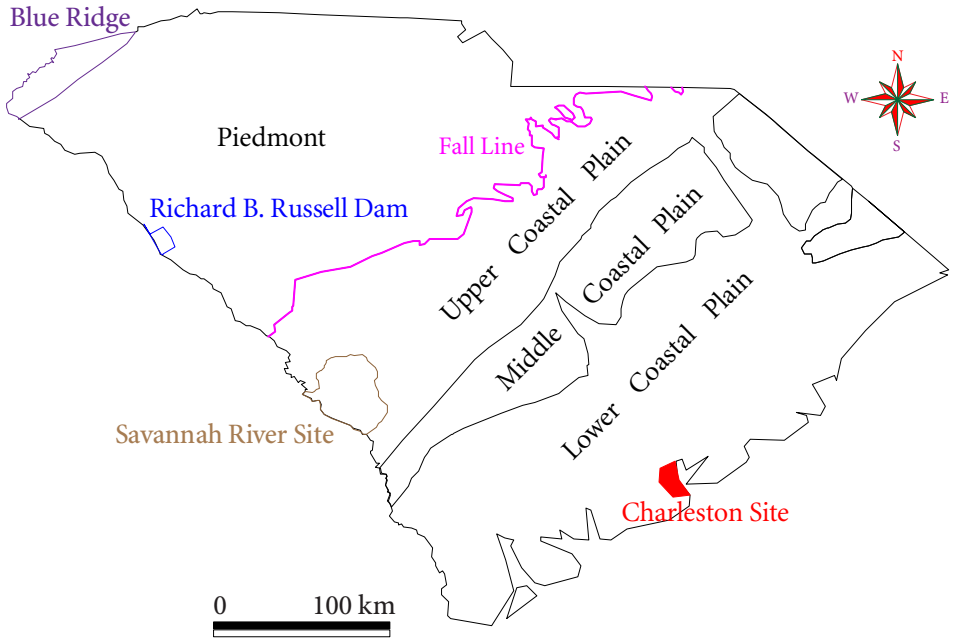

Figure 3.4 Map of the Charleston, South Carolina (modified from Andrus *et al.* 2003)

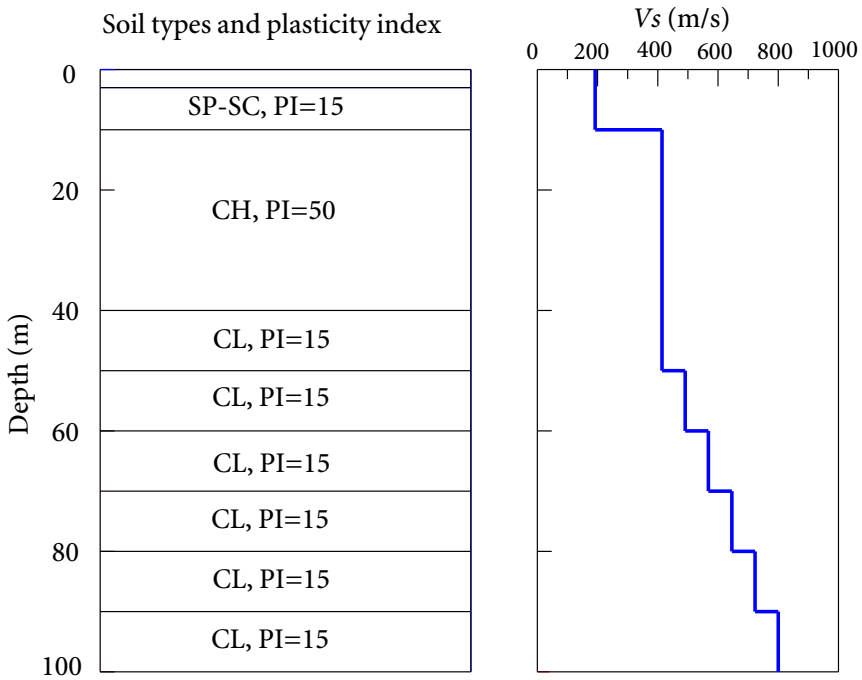

Figure 3.5 Site profile of the Charleston Site, South Carolina. PI represents plastic index, SP-SC, CH, and CL represent types of soils according to the Unified Soil Classification System (ASTM, 2011)

to study influences of the uncertain seismic sources and the uncertain soil parameters on the results of PSHA for soil sites.

According to the ground motion selection criteria, 65 ground motions are selected as input motions for the seismic site response analysis. The 5%-damped response spectra of the 65 ground motions are shown in Figure 3.6, and the scattergram of magnitudes and source-to-site distances of the 65 ground motions is shown in Figure 3.7. Figure 3.7 shows that most of the ground motions are selected from earthquake events with magnitudes from 6.5 to 7.5, and source-to-site distance from 0 to 80 km. Detailed earthquake events of the 65 ground motions are listed in Table 3.1.

Combining the 30 random profiles with the 65 ground motions, a total of $65 \times 30 = 1950$ random cases are generated. The computer program *DEEPSOIL* is used to simulate the seismic site responses. Based on the simulation results, site amplification spectra are computed, as shown in Figure 3.8. It can be seen that there are two resonant period ranges, 0.6 sec to 0.8 sec and 0.2 sec to 0.4 sec, corresponding to the first resonant vibration period range and the second resonant vibration period range of the soil columns, respectively.

In this example, the contributions of the uncertain seismic sources and the uncertain soil properties to the variability of site amplification are shown in Figure 3.9. From this figure, it can be seen that the contributions of soil parameter uncertainty to the variability of site amplification is greater in the period range of 0.2 sec to 1.2 sec than other periods due to the uncertain resonant periods of soil columns, which are related to linear responses of soils under low to medium input motion intensities and nonlinear responses of soils under high input motion intensities. Under low to medium input motion intensities, soils usually exhibit linear properties, and the uncertainty in resonant periods of a soil deposit is mainly caused by the uncertainty of shear-wave velocity. Thus, the uncertainty of shear-wave velocity dominates the contributions of soil parameter uncertainty to the variability of the site amplification under low to medium input motion intensities. Under high input motion intensities, soils exhibit stiffness degradation, represented by normalized shear modulus reduction curves, and resonant periods of a soil deposit shift. The extent of the resonant period shift is determined both by the input motion intensities and the normalized shear modulus reduction curves. Because of the uncertainty of normalized shear modulus, the

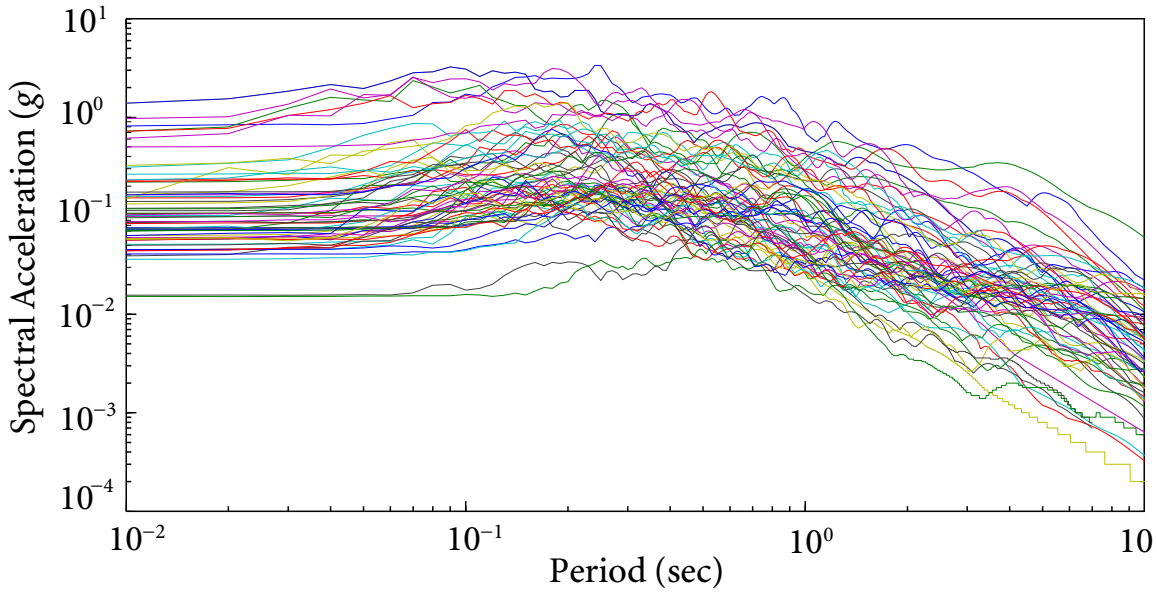

Figure 3.6 Response spectra of the 65 ground motions

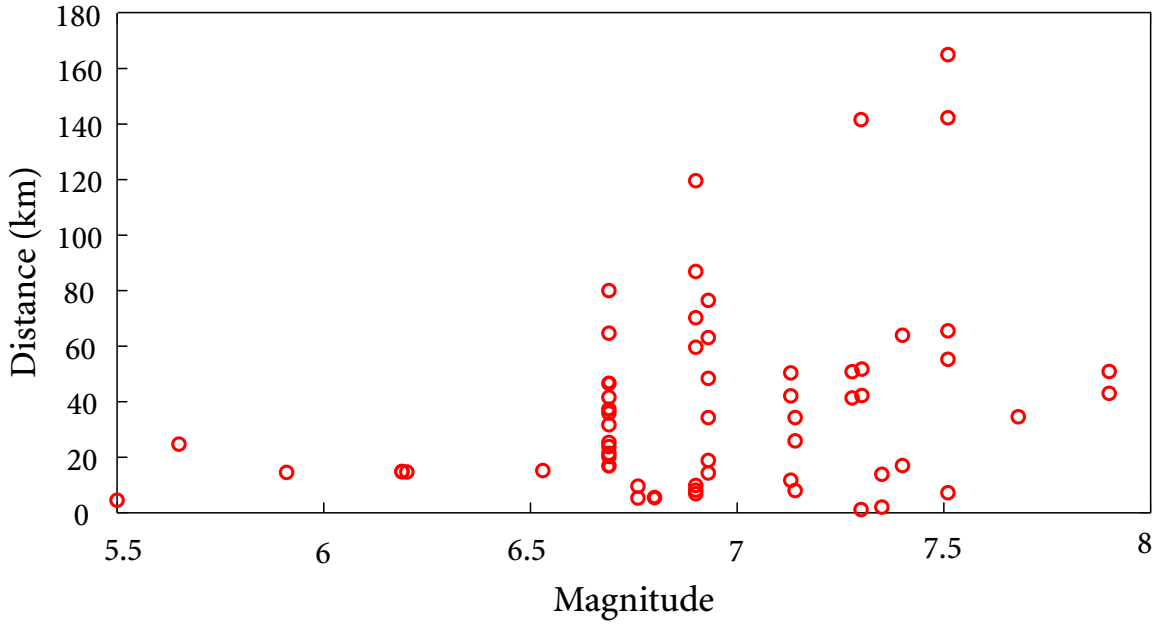

Figure 3.7 Scattergram of M and R of the 65 ground motions

Table 3.1 65 selected ground motions

Earthquake Event	Year	Station Name	Component	Magnitude	R_{rup} (km)	V_{s30} (m/s)	Lowest Freq. (HZ)	PGA (g)
San Fernando	1971	Isabella Dam	ISD284	6.61	131	684.9	0.12	0.82
Sitka	1972	Sitka Observatory	212V5090	7.68	34.6	659.6	0.08	0.22
Gazli	1976	Karakyr	GAZ090	6.8	5.5	659.6	0.06	0.15
Friuli	1976	San Rocco	B-SRO000	5.91	14.5	659.6	0.12	0.10
Tabas	1978	Dayhook	DAY-LN	7.35	13.9	659.6	0.12	0.06
Tabas	1978	Tabas	TAB-LN	7.35	2	766.8	0.06	0.06
Imperial Valley	1979	Cerro Prieto	H-CPE237	6.53	15.2	659.6	0.12	0.14
Irpinia	1980	Auletta	A-AUL000	6.9	9.6	1000	0.12	0.08
Irpinia	1980	Bagnoli Irpinio	A-BAG000	6.9	8.2	1000	0.12	0.07
Irpinia	1980	Torre Del Greco	A-TDG000	6.9	59.6	659.6	0.12	0.11
Irpinia	1980	Bisaccia	B-BIS000	6.2	14.7	1000	0.16	0.05
Morgan Hill	1984	Gilroy-Gavilan Coll.	GIL337	6.19	14.8	729.6	0.12	0.16
Morgan Hill	1984	Gilroy Array ♯1	G01230	6.19	14.9	1428	0.12	0.16
Nahanni	1985	Site 1	S1010	6.76	9.6	659.6	0.06	0.11
Nahanni	1985	Site 3	S3270	6.76	5.3	659.6	0.12	0.06
Baja California	1987	Cerro Prieto	CPE161	5.5	4.5	659.6	0.12	0.07
Loma Prieta	1989	Lower Crystal Springs Dam	CH09090	6.93	48.4	712.8	0.19	0.23
Loma Prieta	1989	SAGO South	SG3261	6.93	34.3	684.9	0.12	0.05
Loma Prieta	1989	Sierra Pt.	SSF205	6.93	63.1	1020.6	0.07	0.10
Loma Prieta	1989	S -Telegraph Hill	TLH090	6.93	76.5	712.8	0.12	0.13
Loma Prieta	1989	San Jose	SJTE315	6.93	14.7	671.8	0.06	0.04
Loma Prieta	1989	UCSC	UC2000	6.93	18.5	714	0.12	0.04
Landers	1992	E Grand Av	GRN180	7.3	141.6	A (Geo.)	0.07	0.72
Landers	1992	24 Lucerne	LCN275	7.3	1.1	A (Geo.)	0.08	0.04
Landers	1992	Poppet Flat	SIL000	7.3	51.7	A (Geo.)	0.12	0.07
Landers	1992	Silent Valley	SIL090	7.28	50.9	684.9	0.12	0.06
Landers	1992	Twentynine Palms	29P090	7.28	41.4	684.9	0.12	1.39
Landers	1992	22161 Twentynine Palms	29P000	7.3	42.2	A (Geo.)	0.12	0.12
Little Skull Mtn	1992	NTS Control Pt. 1	Lsm2000	5.65	24.7	659.6	0.12	1.39
Little Skull Mtn	1992	Las Vegas Calico Basin	Lsm6000	5.65	100.2	659.6	0.12	0.10
Northridge	1994	Antelope Buttes	ATB000	6.69	46.9	821.7	0.12	0.72
Northridge	1994	Howard Rd.	HOW330	6.69	16.9	821.7	0.12	0.16
Northridge	1994	Griffith Park Observatory	0141-360	6.69	23.8	1015.9	0.12	0.97
Northridge	1994	Wonderland Ave	WON095	6.69	20.3	1222.5	0.16	0.15
Northridge	1994	Lake Hughes ♯4	L04000	6.69	31.7	821.7	0.12	0.17
Northridge	1994	Littlerock	LIT090	6.69	46.6	821.7	0.2	0.16
Northridge	1994	Mt Wilson	MTW000	6.69	35.9	821.7	0.1	0.09
Northridge	1994	Rancho Cucamonga	CUC180	6.69	80	821.7	0.3	0.08
Northridge	1994	Lake Hughes ♯12*A*	H12090	6.69	21.4	602.1	0.12	0.23
Northridge	1994	Lake Hughes ♯9	L09000	6.69	25.4	670.8	0.1	0.61
Northridge	1994	Leona Valley ♯1	LV1000	6.69	37.2	684.9	0.2	0.06
Northridge	1994	Leona Valley ♯3	LV3000	6.69	37.3	684.9	0.2	0.09
Northridge	1994	Santa Susana Ground	5108-360	6.69	16.7	715.1	0.12	0.07
Northridge	1994	Sandberg	SAN180	6.69	41.6	821.7	0.12	0.07
Kobe	1995	MZH	MZH090	6.9	70.3	609	0.06	0.22
Kobe	1995	TOT	TOT000	6.9	119.6	609	0.06	0.31
Kobe	1995	Nishi	NIS090	6.9	7.1	609	0.12	0.50
Kobe	1995	OKA	OKA090	6.9	86.9	609	0.06	0.06
Kobe	1995	TOT	TOT090	6.9	119.6	609	0.06	0.07
Kocaeli	1999	Bursa Sivil	BRS090	7.51	65.5	659.6	0.11	0.05
Kocaeli	1999	Eregli	ERG090	7.51	142.3	659.6	0.06	0.11
Kocaeli	1999	Maslak	MSK000	7.51	55.3	659.6	0.11	0.04
Kocaeli	1999	Maslak	MSK090	7.4	63.9	A (Geo.)	0.03	0.04
Kocaeli	1999	Manisa	MNS000	7.51	293.4	659.6	0.1	0.10
Kocaeli	1999	Izmit	IZT090	7.51	7.2	811	0.12	0.32
Kocaeli	1999	Tekirdag	TKR180	7.51	165	659.6	0.12	0.05
Hector Mine	1999	Hector	HEC000	7.13	11.7	684.9	0.04	0.06
Hector Mine	1999	Joshua Tree N.M.	12647180	7.13	50.4	684.9	0.1	0.12
Hector Mine	1999	Twentynine Palms	22161360	7.13	42.1	684.9	0.07	0.06
Hector Mine	1999	Banning	12674090	7.13	83.4	684.9	0.1	0.26
Duzce	1999	Lamont 531	531-E	7.14	8	659.6	0.07	0.09
Duzce	1999	Mudurnu	MDR090	7.14	34.3	659.6	0.1	0.06
Duzce	1999	Lamont 1060	1060-E	7.14	25.9	782	0.07	0.02
Denali	2002	Carlo	5595-090	7.9	50.9	963.9	0.05	0.01
Denali	2002	R109	5596-090	7.9	43	963.9	0.07	0.02

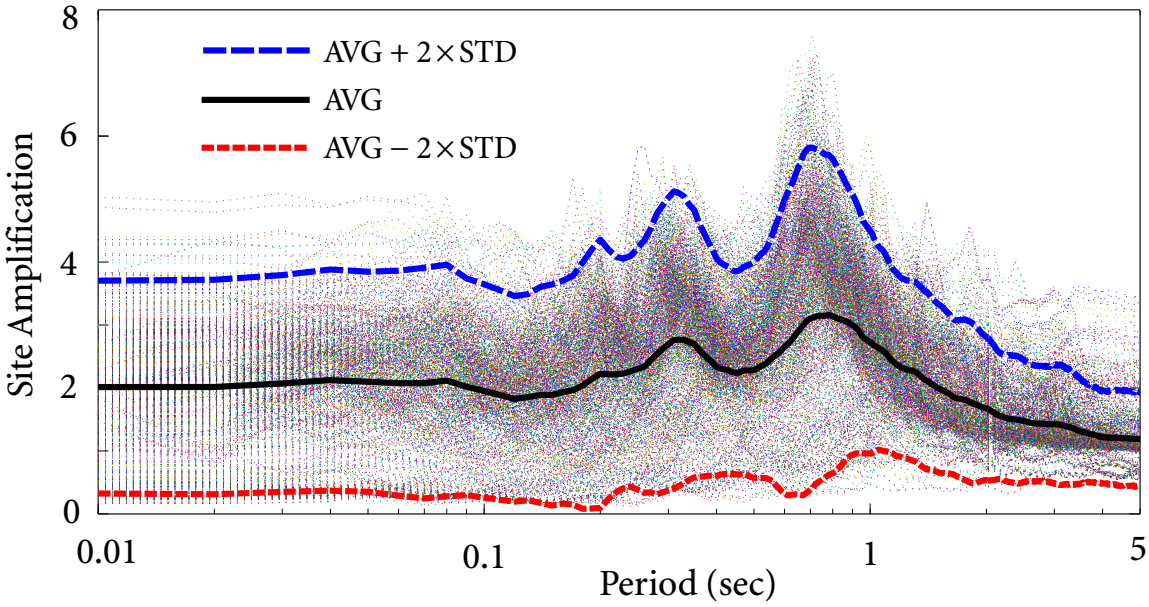

Figure 3.8 Site amplification for the soil site under 1950 random cases

extent of the resonant period shift is unknown and the eventual resonant periods of the soil deposit become uncertain. Thus, the uncertainty of normalized shear modulus dominates the contributions of soil parameter uncertainty to the variability of the site amplification under high input motion intensities. In addition, it can be seen that the uncertainty of seismic sources has a significant influence on the variability of the site amplification over the entire period range.

Based on the site amplifications computed from the simulation results, site amplification regression analysis can be performed. Four potential predictor variables are determined for the regression analysis: peak ground acceleration (spectral acceleration values at 0.01 sec) of input motions, represented by PGA, spectral acceleration of input motions at the target vibration period, represented by X, spectral acceleration of input motions averaged over the first resonant vibration period range (0.6-0.8 sec), represented by Z_1, and spectral acceleration of input motions averaged over the second resonant vibration period range (0.2-0.4 sec), represented by Z_2.

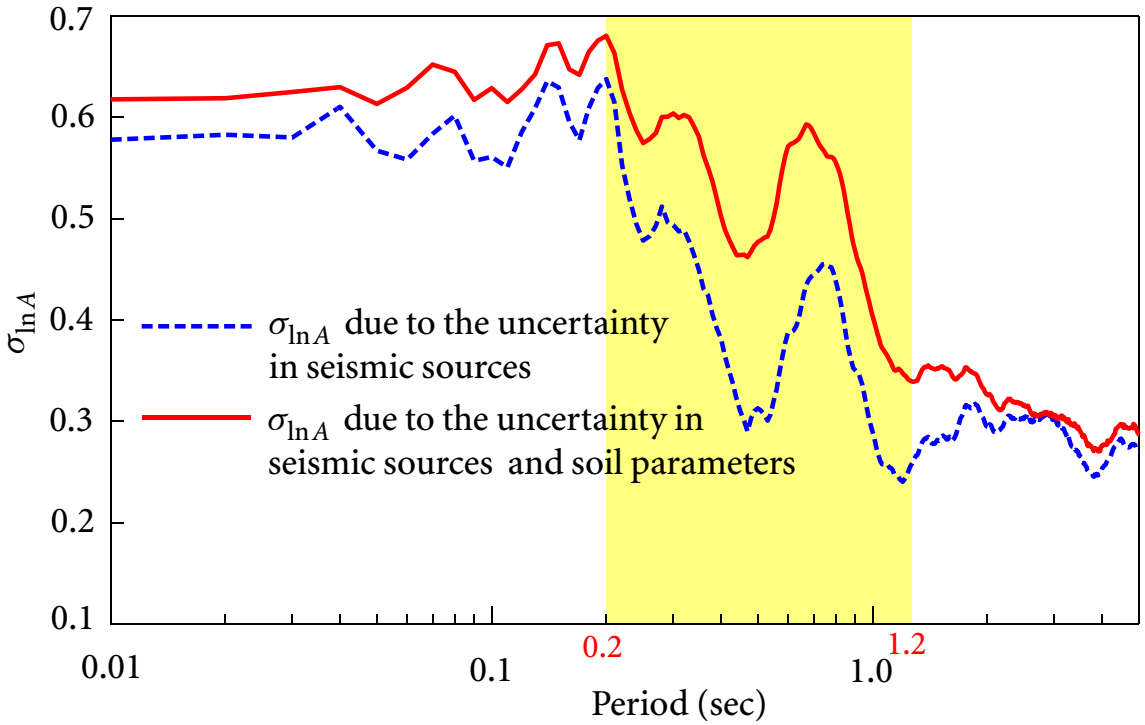

Figure 3.9 Variability of site amplification caused by different factors

The *all-possible-regression* (Neter *et al.*, 1996) method is used to select the appropriate set of predictor variables, and the coefficient of determination, R_p^2, of different sets of predictor variables are used as the criteria.

For the site amplification at 0.01 sec, values of R_p^2 of different sets of predictor variables are shown in Figure 3.10. The set of X and Z_1 or the set of X and Z_2 may be used for site amplification regression analysis at 0.01 sec. Since most of the appropriate sets of predictor variables for regression analyses for other controlling periods do not contain Z_1, the set of X and Z_2 is selected for the regression analysis at 0.01 sec, in order to reduce the total number of predictor variables used for site amplification regression analyses at all the controlling periods.

For the site amplification at 0.2 sec, values of R_p^2 of different sets of predictor variables are shown in Figure 3.10. Based on the values of R_p^2, the best set of predictor variables is the set of X, PGA, and Z_2. However, it involves three predictor variables. Furthermore, its R_p^2 value is only slightly higher than that of the set of X and PGA. Since too many predictor variables

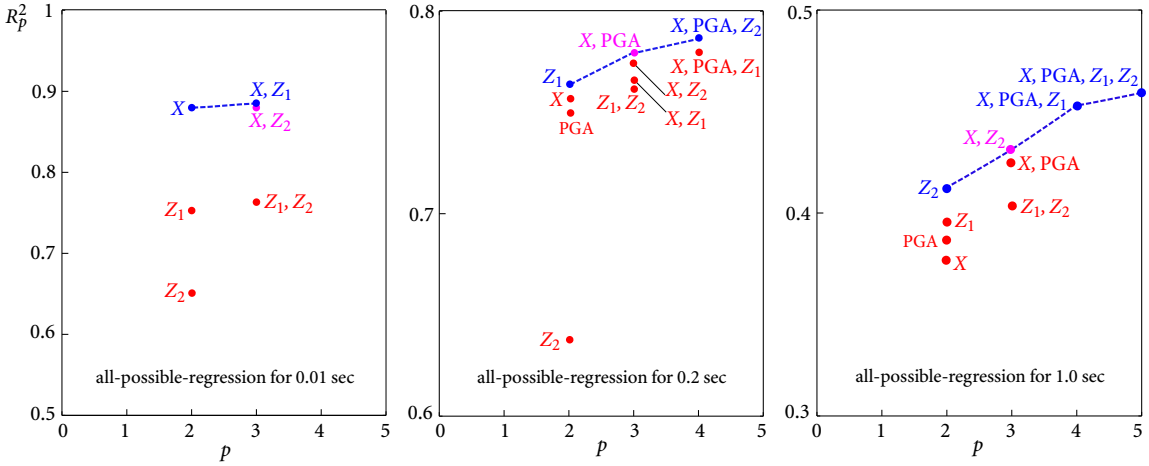

Figure 3.10 R_p^2 plot for all-possible-regression of site amplifications

may cause overfitted regression resulting in larger variance of estimated parameters (Neter *et al.*, 1996), the set of X and PGA is selected. In addition, it can be clearly seen that the value of R_p^2 for a single predictor variable, such as X, PGA, Z_1, or Z_2, is small, implying that scalar site amplification regression analysis leads to a large standard deviation.

For the site amplification at 1.0 sec, values of R_p^2 of different sets of predictor variables are shown in Figure 3.10. Based on the values of R_p^2, the best set of predictor variables is the set of X, PGA, Z_1, and Z_2. However, it involves four predictor variables. Similar to the case of 0.2 sec, in order to avoid overfitted regression and to reduce the total number of predictor variables used for site amplification regression analyses at all the controlling periods, the set of X and Z_2 is selected. It can be clearly seen that the value of R_p^2 for a single predictor variable is small, implying that scalar site amplification regression analysis leads to a large standard deviation. Therefore, vector-valued site amplification regression analysis will be used in PSHA for soil sites.

Using the same procedure, the appropriate set of predictor variables at other controlling periods are determined. The set of X and Z_2 is finally selected for site amplification regression analysis at periods 0.02 sec, 0.05 sec, 0.1 sec, 1.0 sec, 1.5 sec, and 5.0 sec, and the set of X and PGA is finally selected for site amplification regression analysis at periods 0.2 sec, 0.3 sec, 0.4 sec, 0.5 sec, 0.6 sec, 0.7 sec, and 0.8 sec. Although the correlation between X and Z_2, or X and PGA is high at some periods, they do not affect the use of the fitting model

for making predictions, because values of the predictor variables for which inferences are to be made follow the same multicollinearity pattern as the data, on which the regression model is based.

The selection of site amplification regression model refers to the functional forms proposed by Abrahamson *et al.* (Abrahamson and Silva, 1997) and Bazzurro (Bazzurro and Cornell, 2004B), and some improvements are made to establish a new regression model:

$$\ln A = c_0 + c_1 \ln X + c_2 \ln \mathrm{PGA} + c_3 \ln Z_2 + c_4 (\ln X)^2 + c_5 (\ln \mathrm{PGA})^2 + c_6 (\ln Z_2)^2, \tag{3.5.1}$$

where $c_0, c_1, \ldots, c_6$ are regression coefficients, whose values are shown in Table 3.2.

Table 3.2 Regression coefficients and standard deviation for the Charleston Site

T(sec)	c_0	c_1	c_2	c_3	c_4	c_5	c_6	$\sigma_{\ln A}$
0.01	−1.0281	−1.1678	0	0.1844	−0.1199	0	0	0.2098
0.02	−0.8877	−1.0044	0	0.0794	−0.0874	0	−0.0330	0.2123
0.05	−0.4671	−0.6859	0	−0.1584	−0.0490	0	−0.0843	0.2230
0.1	−0.3097	−0.6519	0	−0.1789	−0.0524	0	−0.0851	0.2483
0.2	−0.5493	−0.4789	−0.4929	0	−0.0701	−0.0610	0	0.3232
0.3	−0.2650	−0.5950	−0.3880	0	−0.0916	−0.0581	0	0.3121
0.4	−0.2305	−0.5373	−0.3934	0	−0.0705	−0.0880	0	0.2972
0.5	−0.2238	−0.6386	−0.2160	0	−0.1006	−0.0432	0	0.3054
0.6	−0.3324	−0.6579	−0.2832	0	−0.0963	−0.0429	0	0.3469
0.7	−0.2455	−0.5928	−0.3416	0	−0.0814	−0.0496	0	0.3518
0.8	−0.2802	−0.7701	−0.2064	0	−0.1218	−0.0196	0	0.3232
1.0	0.1947	−0.3488	0	−0.3500	−0.0587	0	−0.0704	0.3073
1.5	0.3184	−0.1341	0	−0.0259	0	0	0	0.3366
5.0	0.5042	0.1974	0	0.2068	0.0390	0	0	0.2091

3.5.1 Seismic Hazard Curves on the Soil Surface

Using equation (3.4.1), seismic hazard curves on the soil surface (soil-hazard curves) are calculated and compared with corresponding seismic hazard curves on the bedrock (rock-hazard curves), as shown in Figures 3.11 and 3.12.

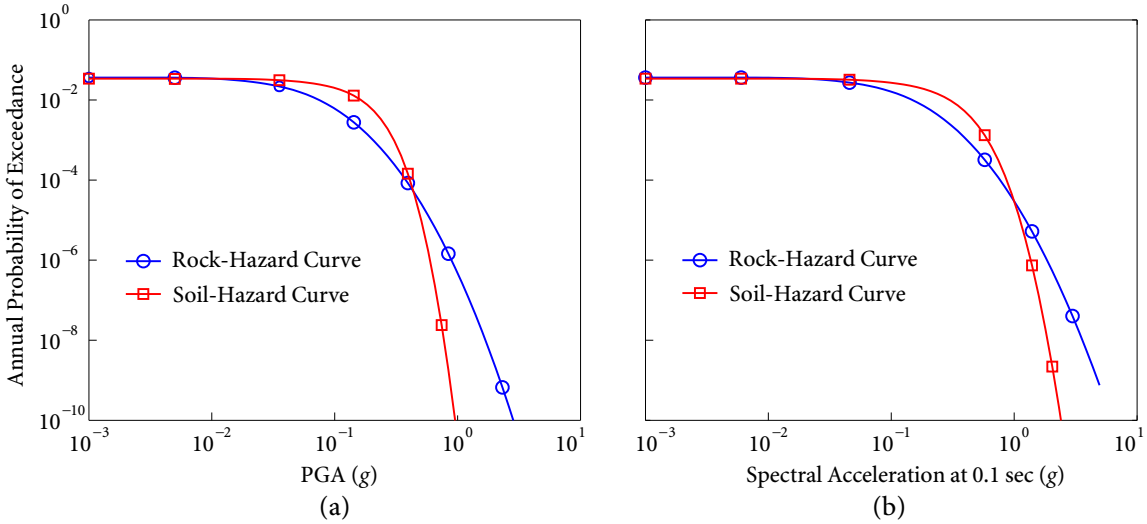

Figure 3.11 Seismic hazard curves (a) for PGA; (b) for 0.1 sec

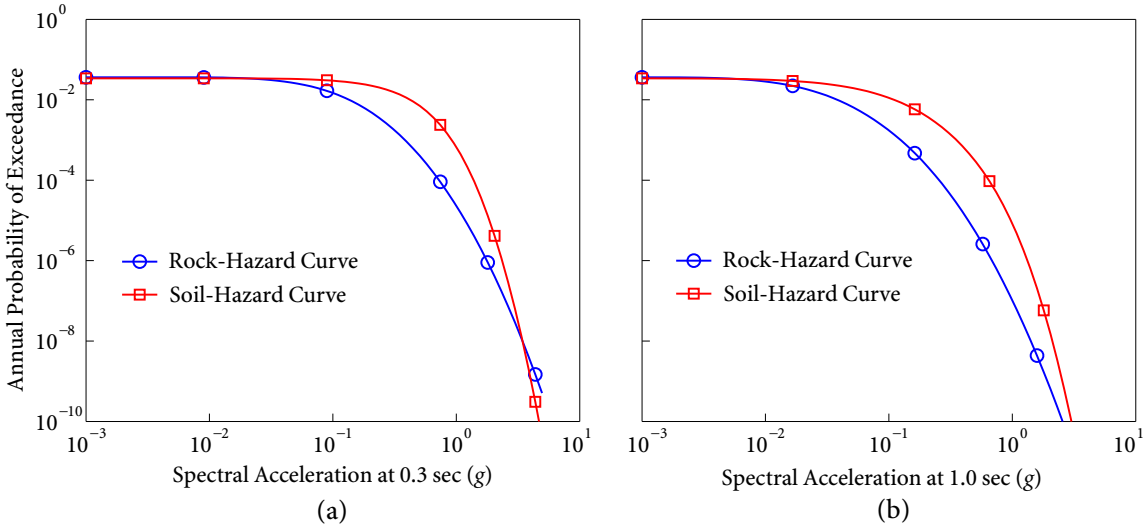

Figure 3.12 Seismic hazard curves (a) for 0.3 sec; (b) for 1.0 sec

From these figures, it is clearly seen that the soil-hazard curve is much higher than the rock-hazard curve in the medium ranges of spectral accelerations, but slightly higher or lower in the high ranges of spectral accelerations. Under low to medium incident bedrock motion intensities, seismic responses of a soil deposit increase with increment of the incident bedrock motion intensities; ground motions at the soil surface are amplified, resulting in that the soil-hazard curve is much higher than the rock-hazard curve. However, under high incident bedrock motion intensities, soils exhibit nonlinear properties and yield large shear strains. The large shear strains further increase soil damping ratio and thus reduces the intensity of ground vibrations, resulting in that the soil-hazard curve is slightly higher or lower than the rock-hazard curve.

3.5.2 Uniform Hazard Spectra on the Soil Surface

Using the seismic hazard curves at 14 controlling periods, i.e., 0.01 sec, 0.02 sec, 0.05 sec, 0.1 sec, 0.2 sec, 0.3 sec, 0.4 sec, 0.5 sec, 0.6 sec, 0.7 sec, 0.8 sec, 1.0 sec, 1.5 sec, and 5.0 sec, the soil UHS are constructed. The soil UHS and their spectral shapes are shown in Figures 3.13 to 3.16. Comparing the soil UHS and the rock UHS, it can be seen that their spectral shapes and spectral amplitudes are different. The rock UHS reflect characteristics of ground motions propagating from seismic sources to bedrock, while the soil UHS reflect characteristics of ground motions propagating from seismic sources to bedrock and then to soil surface. Because of effects of the soil deposit, amplitudes of the rock UHS at different periods are amplified with different amplification factors; the amplification factors are large at periods close to the fundament period of the soil deposit, but small at periods far from the fundamental period of the soil deposit. This contributes to the different spectral shapes and spectral amplitudes between the soil UHS and the rock UHS.

In addition, Figures 3.13 to 3.16 demonstrate that the soil UHS by the modified GMPEs (base case) are different from the soil UHS by GMPEs (base case). Because GMPEs use the generic soil instead of the site-specific soils, ground motions at the soil surface calculated by GMPEs are treated with less rigor. The modified GMPEs take account of the site-specific soils in detail; therefore, ground motions at the soil surface calculated by the modified GMPEs are highly suitable for practical application, particularly for critical structures. The

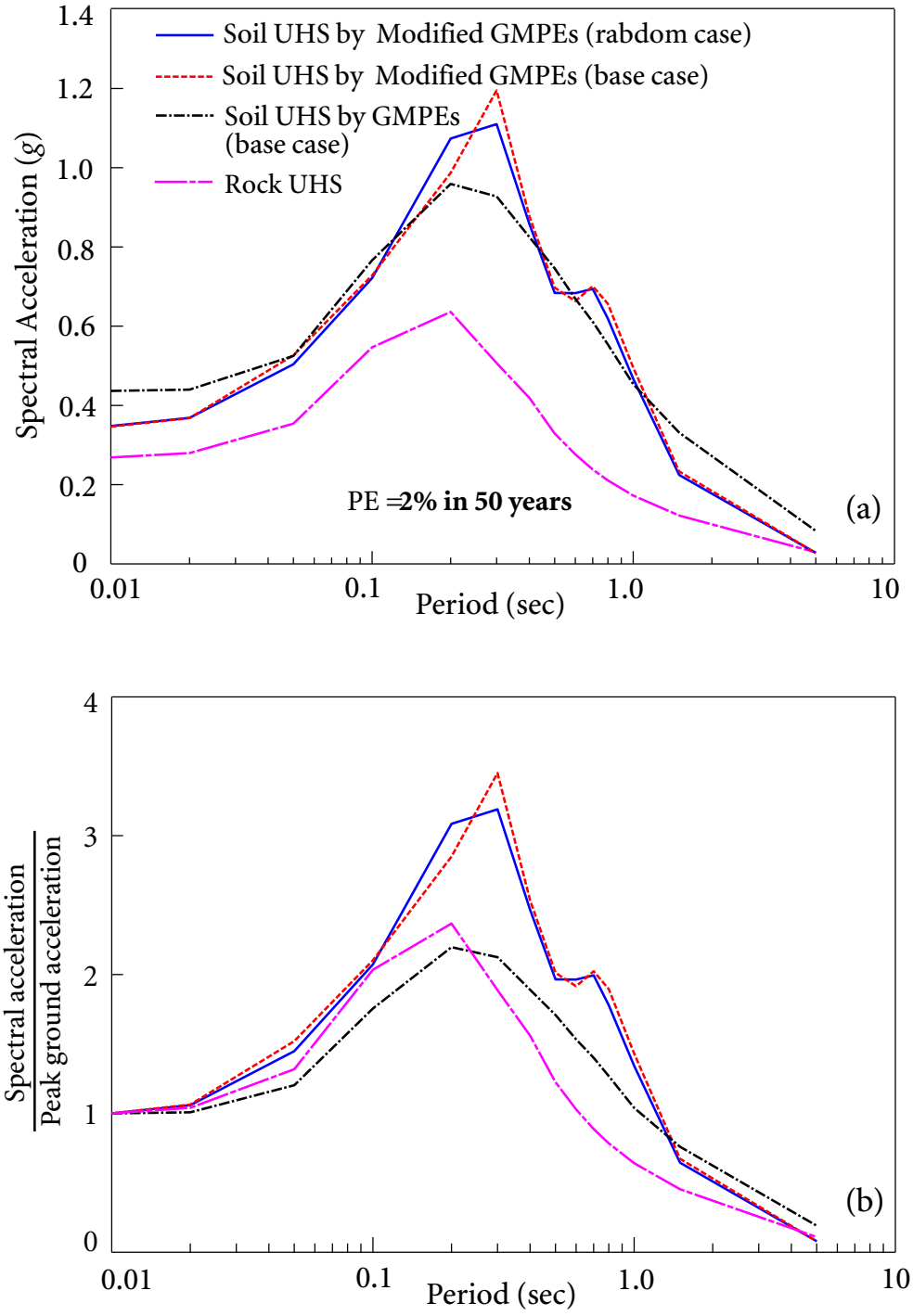

Figure 3.13 Uniform hazard spectra with 2% probability of exceedance in 50 years and their spectral shape

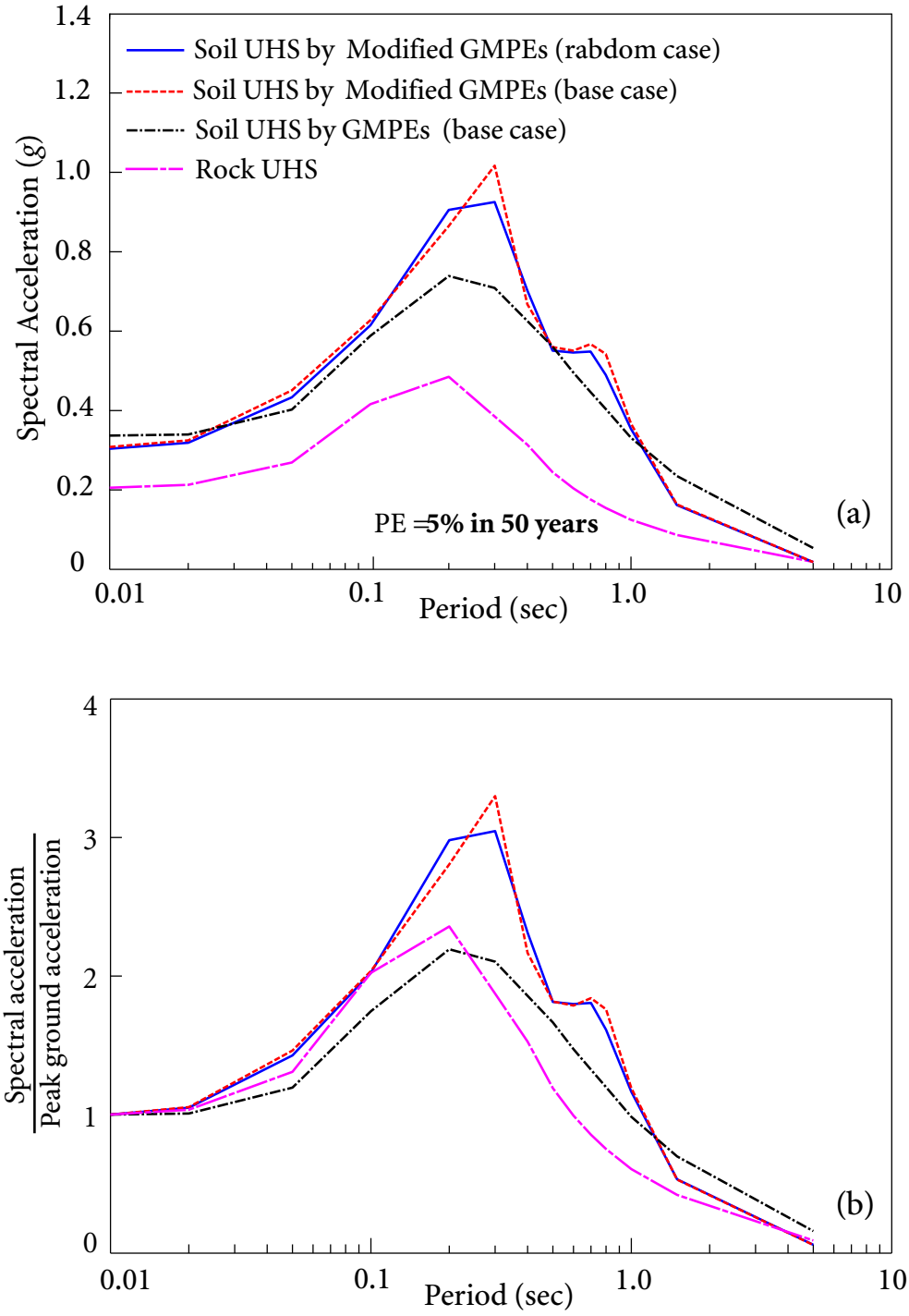

Figure 3.14 Uniform hazard spectra with 5% probability of exceedance in 50 years and their spectral shape

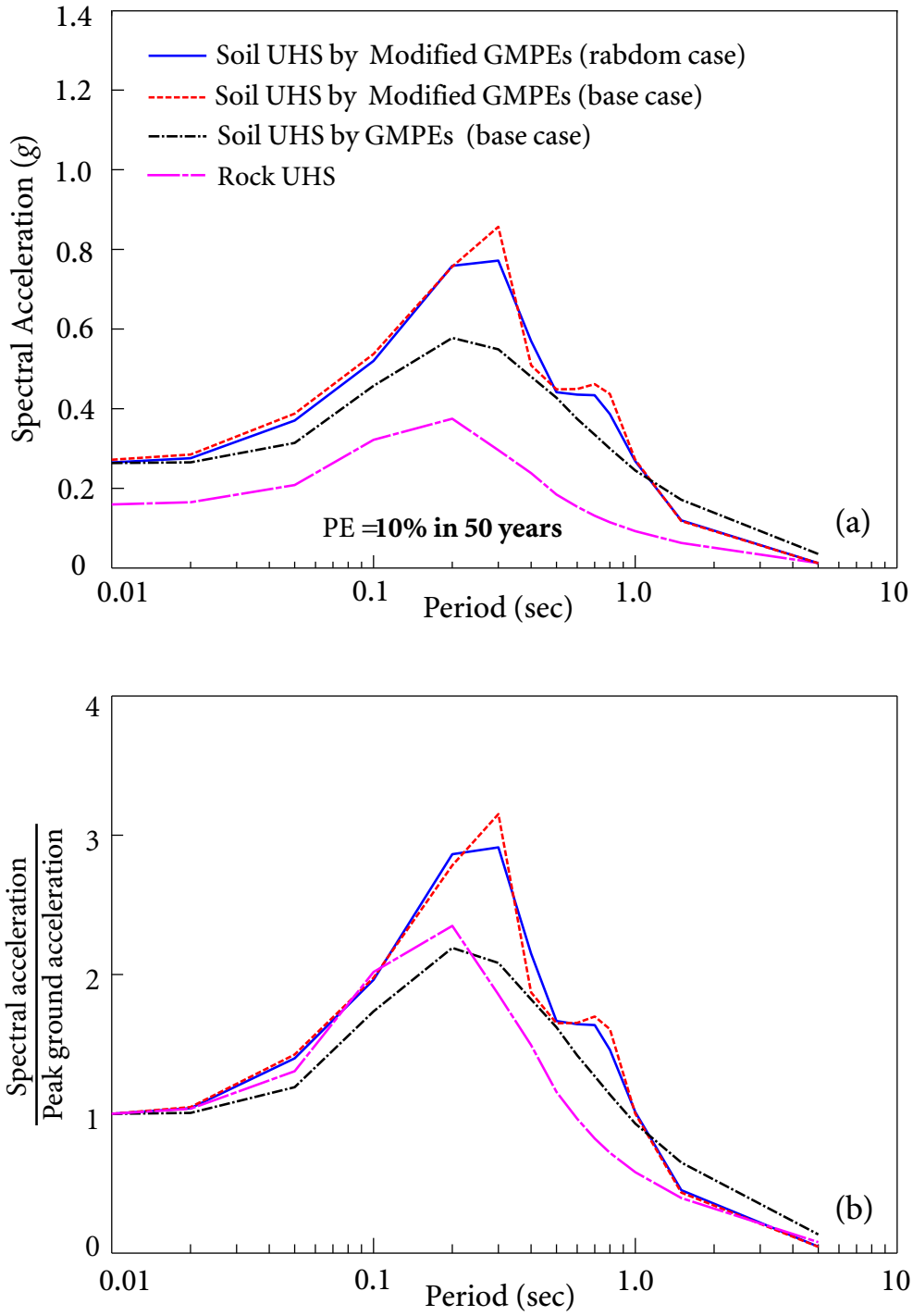

Figure 3.15 Uniform hazard spectra with 10% probability of exceedance in 50 years and their spectral shape

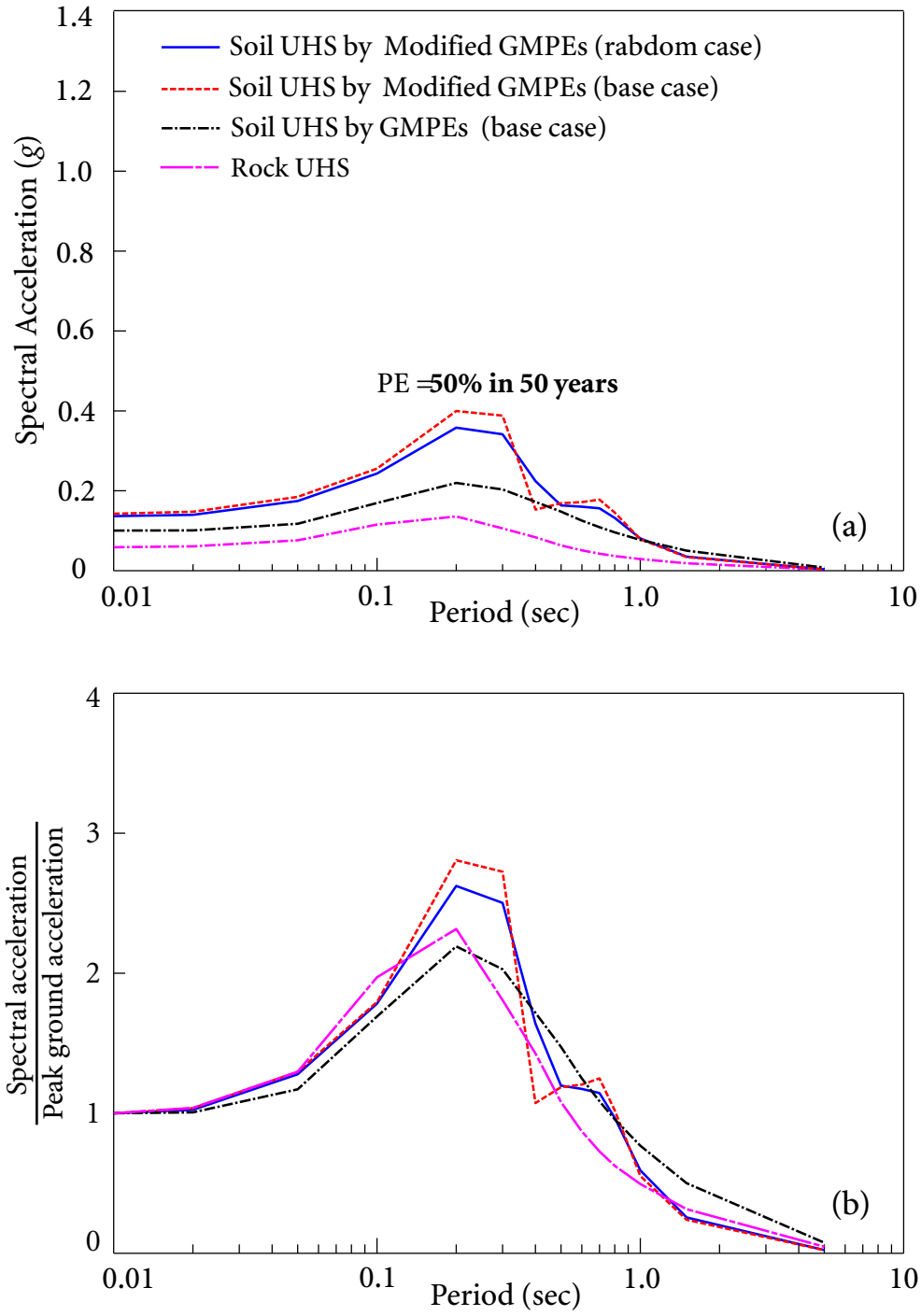

Figure 3.16 Uniform hazard spectra with 50% probability of exceedance in 50 years and their spectral shape

significant differences between the soil UHS by the modified GMPEs (base case) and those by GMPEs (base case) demonstrate that constructing soil UHS by GMPEs is not acceptable; the modified GMPEs are necessary to construct the appropriate soil UHS that are acceptable in practice.

Comparing the soil UHS by the modified GMPEs under random case and those by the modified GMPEs under base case, it can be seen that the influences of soil parameter variabilities on spectral shapes and spectral amplitudes of UHS are not very remarkable. Soil UHS under the random case and the base case have the similar spectral amplitude and spectral shape over all the controlling periods except at the period range of 0.2 sec to 0.4 sec. This is due to the resonance effects of the soil deposit. The spectral amplitudes of incident motions at the fundamental period of the soil deposit are remarkably amplified by the soil deposit. As the site profile of base case contains best estimate of soil parameters, its fundamental period is nearly constant. However, since the site profiles of random case consider soil parameter variabilities, their fundamental periods vary with the random soil parameters used to realize the site profiles. The fundamental periods range of the random site profiles in this example site vary from 0.2 sec to 0.4 sec, while the fundamental period of the base case site profile is nearly 0.3 sec. That is the reason for great difference between the soil UHS under the base case and the random case occurs at the period range of 0.2 sec to 0.4 sec.

Under high incident bedrock motion intensities, soils usually exhibit nonlinear responses and stiffness degradation, accompanying the fundamental period shift. Extent of the fundamental period shift is determined by both the incident bedrock motion intensities and the normalized shear modulus reduction curves. Because the fundamental period of the soil deposit shift, the spectral shape of UHS changes due to resonance effects of the soil deposit. Also, as soils exhibit stiffness degradation, large soil shear strain is caused. This large shear strain further increases soil damping ratio, which at last reduces the intensity of ground vibrations and spectral amplitudes of the UHS.

Based on equation (3.4.5), seismic hazard deaggregation at the soil site is conducted, and one example at 0.3 sec is shown in Figure 3.17. It can be seen that the hazard contribution at the rock site is different from that at the soil site for the same target probability level of

exceedance. The hazard contribution at the soil site from far-field earthquakes is a little greater than that at the rock site, due to the soil site effects.

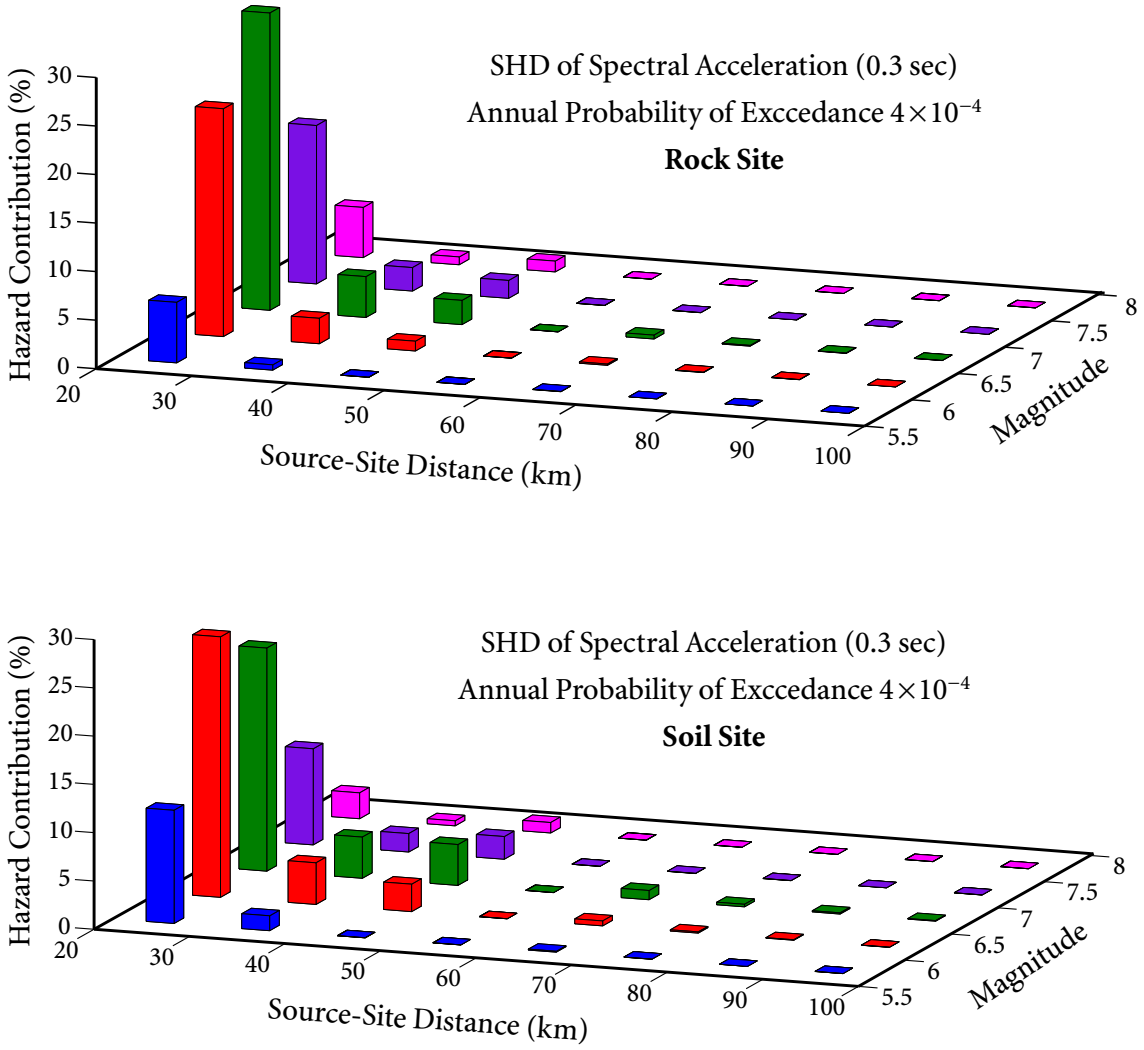

Figure 3.17 Seismic hazard deaggregation for 0.3 sec

3.6 Summary

This chapter presents a framework to perform PSHA for soil sites and generate soil UHS. Using the proposed framework, the soil UHS for the Charleston Site are constructed. Some conclusions are drawn:

- Spectral shapes and spectral amplitudes of rock UHS are greatly different from those of soil UHS. The rock UHS reflect characteristics of ground motions propagating from seismic sources to bedrock, while the soil UHS reflect characteristics of ground motions propagating from seismic sources to bedrock and then to soil surface. Therefore, the differences are caused by effects of the local soil deposit.
- The nonlinear responses of soils cannot be neglected, which could substantially affect spectral amplitudes and spectral shapes of the soil UHS.
- Seismic sources dominate the variability of the results of PSHA for soil sites, but the contribution of soil parameter uncertainty should not be neglected, which could also affect spectral shapes and spectral amplitudes of UHS.
- The soil UHS may be constructed by the GMPEs using generic soil to roughly characterize the local soil conditions. However, the significant differences between the soil UHS by the modified GMPEs (base case) and the soil UHS by GMPEs (base case) show that constructing soil UHS by GMPEs using generic soil is not acceptable in practice.

Because of the modified GMPEs' capacity to predict ground motions at the soil surface more accurately than GMPEs, the soil UHS by the modified GMPEs is highly suitable for practical application, in particular for those critical facilities that require accurate design spectra.

CHAPTER 4

Response Spectra for Equipment-Structure Resonance

When generating probabilistic floor response spectra (FRS) considering uncertainty from ground motions using the direct spectra-to-spectra method, probability distribution of t-Response Spectrum (tRS), which deals with equipment-structure resonance or tuning, corresponding to a specified Ground Response Spectrum (GRS) is required.

In this chapter, simulation results using a large number of horizontal and vertical ground motions are employed to establish statistical relationships between tRS and GRS. It is observed that the influence of site conditions on horizontal statistical relationships is negligible, whereas the effect of site conditions on vertical statistical relationships cannot be ignored. Considering the influence of site conditions, horizontal statistical relationship suitable for all site conditions and vertical statistical relationships suitable for hard sites and soft sites, respectively, are established. The horizontal and vertical statistical relationships are suitable to estimate tRS for design spectra in USNRC R.G. 1.60 and NUREG/CR-0098, Uniform Hazard Spectra (UHS) in Western North America (WNA), or any GRS falling inside the valid coverage of the statistical relationship.

For UHS with significant high frequency spectral accelerations, such as UHS in Central and Eastern North America (CENA), an amplification ratio method is proposed to estimate tRS.

Numerical examples demonstrate that the statistical relationships and the amplification ratio method are acceptable to estimate tRS with any probability for given GRS, which is required to generate probabilistic FRS considering uncertainty from ground motions using the direct method in different practical situations.

4.1 Introduction

Secondary systems are structures, equipment and components (SSCs) supported by the primary structures, such as reactor buildings and their internal structures. These secondary systems play various functions to maintain operational activities and safe shutdown of nuclear power plants.

Secondary systems are usually attached to the floors or walls of primary systems; as a result, they are subject to the vibrational motion of the floor to which they are attached, rather than subject to ground motion excitations directly. The vibration transmitted by primary structures could be amplified serval times and may damage secondary systems. Hence, the seismic input for secondary systems is not only determined by a ground motion to which the primary structure is subject, but also significantly affected by the dynamic characteristics of the supporting structure.

In order to ensure the safe design of operational and functional secondary systems, probabilistic floor response spectra are required in the design work, especially in performance-based seismic design. There are two methods for constructing floor response spectra. The first method is the time-history analysis method (USNRC, 1978; Scanlan, 1974; Adam and Fotiu, 2000): acceleration time histories compatible with ground response spectra are usually used to generate floor response spectra. The second method is the direct spectra-to-spectra method (Singh, 1975; Singh, 1980; Jeanpierre and Livolant, 1977): floor response spectra are generated directly from the given ground response spectra based on random vibration theory. Both of these two methods need to consider uncertainties in the structural frequencies due to uncertainties in the material properties of the structure and soil, and approximations in the modeling techniques used in seismic analysis. Thus, the floor response

spectra are required to be smoothed, and peaks of the floor response spectra related to each of the structural frequencies are required to be broadened (USNRC, 1978).

ASCE Standard 4-98 (ASCE, 2000) recommends that floor response spectra (FRS) be generated by time history analyses or a direct spectra-to-spectra method (Figure 4.1).

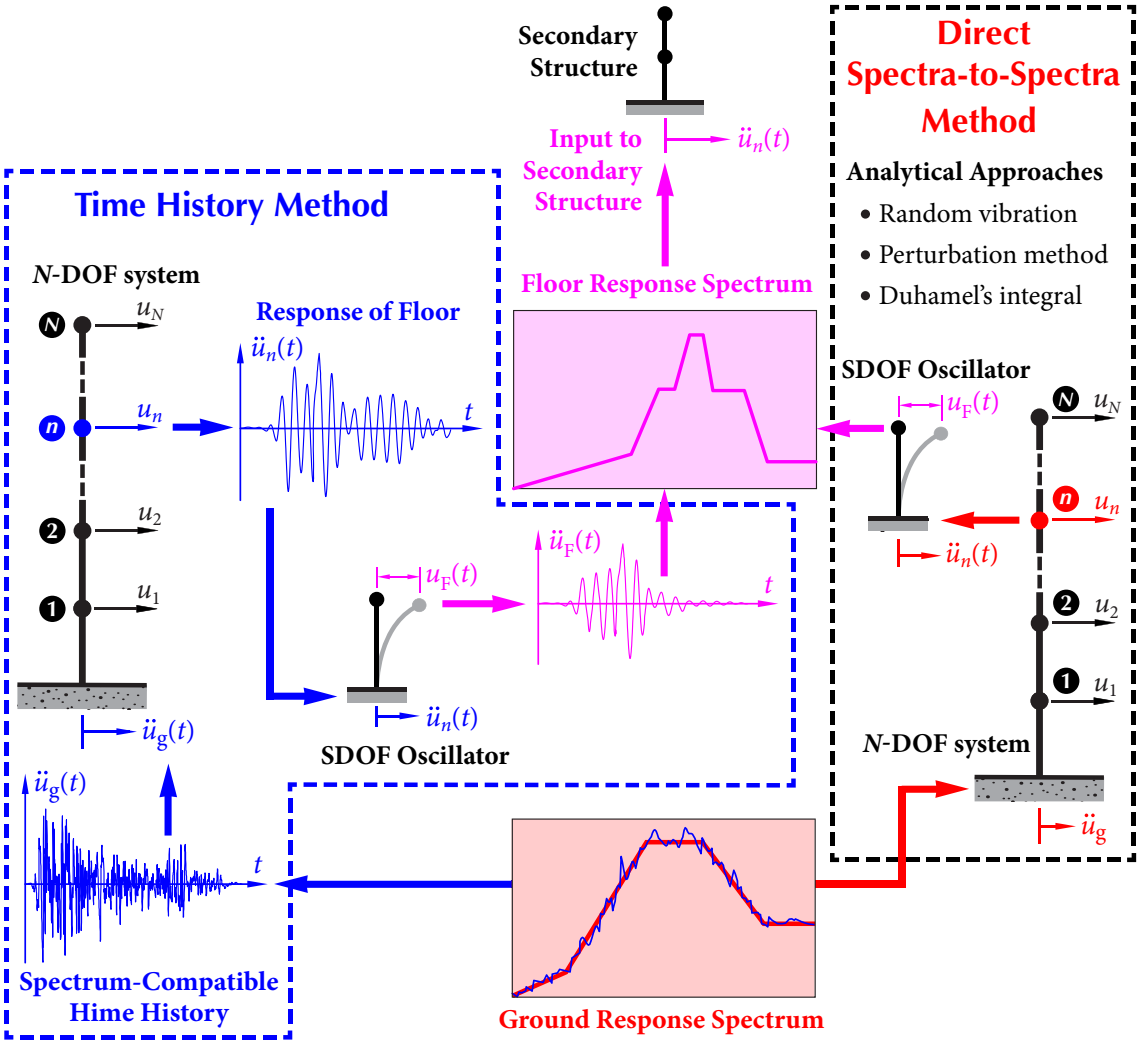

Figure 4.1 Two methods of generating floor response spectra

4.1.1 Time History Method

A dynamic analysis for a primary structure is conducted using step-by-step time integration. The time histories of responses at the floors to which secondary systems are attached are obtained and used to generate FRS. The time history analysis can give accurate responses for a given ground motion.

However, recorded ground motions representative of target sites are often not available; ground motions compatible with a target ground response spectrum are required as input for the primary structure. It has been recognized that there is significant variability in the FRS generated by the time history method, in the sense that two spectrum-compatible time histories may give significantly different FRS. Hence, if only a single ground motion is used in the time history analysis, the generated FRS is not reliable. Consequently, a number of ground motions are required to obtain a probabilistic FRS; but this procedure is not only cumbersome but also computationally expensive.

4.1.2 Direct Spectra-to-Spectra Method

The direct spectra-to-spectra method can avoid the deficiencies of the time history method by generating floor response spectra directly from ground response spectra. A modal analysis of the primary structure is performed to obtain the basic modal information of the structure, including modal frequencies, modal shapes, and modal participation factors. Response spectra of desired floors are then obtained in terms of the modal information and the prescribed ground response spectrum.

4.2 Earthquake Response Spectrum

4.2.1 Ground Response Spectrum

The calculations of an earthquake response spectrum, for assessing the impact of ground motion on structures, from available earthquake records were started by George Housner in 1941 at Caltech (Villaverde, 2009). A response spectrum gives the level of seismic force or displacement as a function of natural period (or frequency) of vibration of the structure and its damping.

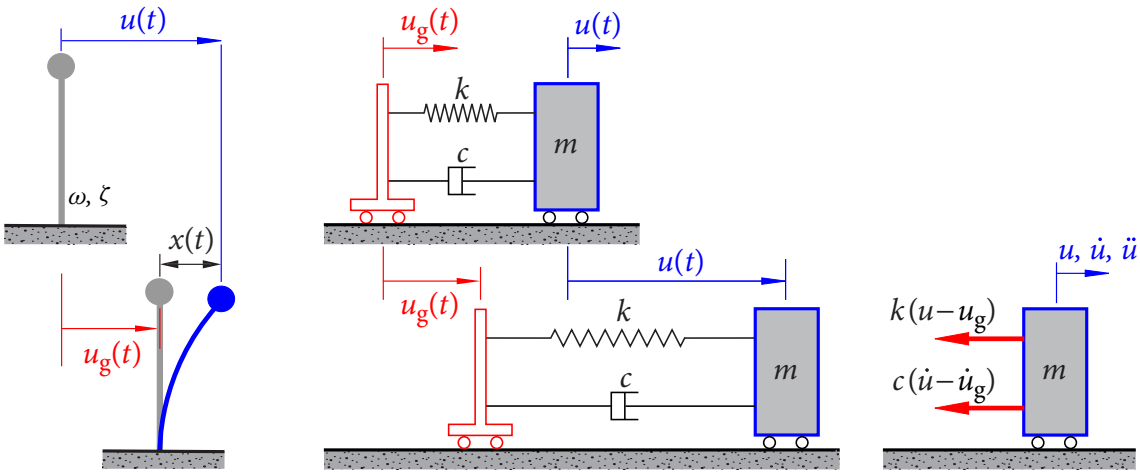

Figure 4.2 SDOF oscillator under ground excitation

Consider a SDOF oscillator with natural circular frequency ω or period T under ground excitation $u_g(t)$, as shown in Figure 4.2. The equation of motion is

$$\ddot{x}(t) + 2\zeta\omega\dot{x}(t) + \omega^2 x(t) = \frac{1}{m}F(t), \quad \omega^2 = \frac{k}{m}, \quad 2\zeta\omega = \frac{c}{m}, \tag{4.2.1}$$

where $x(t) = u(t) - u_g(t)$ is the displacement of the mass relative to the ground, $u(t)$ is the absolute displacement of the mass, and the equivalent earthquake load is $F(t) = -m\ddot{u}_g(t)$.

Using Duhamel integral (Chopra, 2011), the response of system (4.2.1) is,

$$x(t) = \int_0^t \mathrm{e}^{-\zeta\omega(t-\tau)} \frac{\sin\omega_d(t-\tau)}{m\omega_d}\left[-m\ddot{u}_g(\tau)\right]\mathrm{d}\tau. \tag{4.2.2}$$

For lightly-damped system, $\zeta \ll 1$, $\omega_d = \omega\sqrt{1-\zeta^2} \approx \omega$, and dropping the negative sign since it has no real significance with regard to earthquake excitation, equation (4.2.2) becomes

$$x(t) = \frac{1}{\omega}\int_0^t \ddot{u}_g(\tau)\sin\omega(t-\tau)\,\mathrm{e}^{-\zeta\omega(t-\tau)}\,\mathrm{d}\tau. \tag{4.2.3}$$

Taking time derivative of equation (4.2.3) gives the relative velocity

$$\dot{x}(t) = \int_0^t \ddot{u}_g(\tau)\cos\omega(t-\tau)\,\mathrm{e}^{-\zeta\omega(t-\tau)}\,\mathrm{d}\tau - \zeta\int_0^t \ddot{u}_g(\tau)\sin\omega(t-\tau)\,\mathrm{e}^{-\zeta\omega(t-\tau)}\,\mathrm{d}\tau \tag{4.2.4}$$

$$\approx \int_0^t \ddot{u}_g(\tau)\cos\omega(t-\tau)\,\mathrm{e}^{-\zeta\omega(t-\tau)}\,\mathrm{d}\tau, \quad \text{for small } \zeta. \tag{4.2.5}$$

Substituting equations (4.2.3) and (4.2.4) into (4.2.1) yields the absolute acceleration

$$\begin{aligned}\ddot{u}(t) &= \ddot{x}(t) + \ddot{u}_{\mathrm{g}}(t) = -\omega^2 x(t) - 2\zeta\omega\dot{x}(t) \\ &= \omega(2\zeta^2-1)\int_0^t \ddot{u}_{\mathrm{g}}(\tau)\sin\omega(t-\tau)\,\mathrm{e}^{-\zeta\omega(t-\tau)}\,\mathrm{d}\tau \\ &\quad - 2\zeta\omega\int_0^t \ddot{u}_{\mathrm{g}}(\tau)\cos\omega(t-\tau)\,\mathrm{e}^{-\zeta\omega(t-\tau)}\,\mathrm{d}\tau \qquad (4.2.6) \\ &\approx -\omega\int_0^t \ddot{u}_{\mathrm{g}}(\tau)\sin\omega(t-\tau)\,\mathrm{e}^{-\zeta\omega(t-\tau)}\,\mathrm{d}\tau, \quad \text{for small } \zeta. \qquad (4.2.7)\end{aligned}$$

In seismic analysis, seismic inputs are usually given in terms of Ground Response Spectra (GRS) defined as

$$\mathcal{S}_{\mathrm{A}}(\omega,\zeta) = \left|\omega\,\mathrm{e}^{-\zeta\omega t}\sin\omega t * \ddot{u}_{\mathrm{g}}(t)\right|_{\max}, \qquad (4.2.8)$$

where $\ddot{u}_{\mathrm{g}}(t)$ is the ground acceleration, and ω and ζ respectively denote the circular natural frequency and damping coefficient of a single degree-of-freedom (SDOF) oscillator mounted on the ground.

4.2.2 FRS of SDOF Primary Structure

For the special case when the primary structure is a SDOF system with circular frequency ω and damping coefficient ζ, $u(t)$ and $x(t)=u(t)-u_{\mathrm{g}}(t)$ are the absolute and relative displacements of the structure, respectively, satisfying

$$\ddot{x}(t) + 2\zeta\omega\dot{x}(t) + \omega^2 x(t) = -\ddot{u}_{\mathrm{g}}(t), \qquad (4.2.9)$$

$$\ddot{u}(t) = \ddot{x}(t) + \ddot{u}_{\mathrm{g}}(t) = -2\zeta\omega\dot{x}(t) - \omega^2 x(t). \qquad (4.2.10)$$

The motion of a SDOF oscillator with circular natural frequency ω_0 and damping coefficient ζ_0 mounted on the primary structure (Figure 4.3) is governed by

$$\ddot{x}_{\mathrm{F}} + 2\zeta_0\omega_0\dot{x}_{\mathrm{F}} + \omega_0^2 x_{\mathrm{F}} = -\ddot{u}(t), \qquad (4.2.11)$$

$$\ddot{u}_{\mathrm{F}}(t) = \ddot{x}_{\mathrm{F}}(t) + \ddot{u}(t) = -2\zeta_0\omega_0\dot{x}_{\mathrm{F}}(t) - \omega_0^2 x_{\mathrm{F}}(t), \qquad (4.2.12)$$

where $x_{\mathrm{F}}(t)=u_{\mathrm{F}}(t)-u(t)$ and $u_{\mathrm{F}}(t)$ are the relative and absolute displacements of the oscillator. The maximum absolute acceleration of the oscillator

$$\mathcal{S}_{\mathrm{F}}(\omega_0,\zeta_0) = \max\left|\ddot{u}_{\mathrm{F}}(t)\right| \qquad (4.2.13)$$

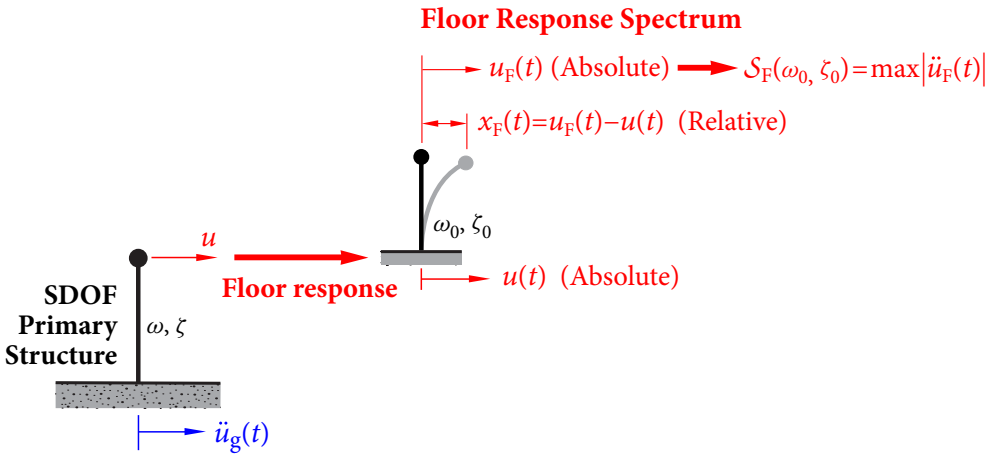

Figure 4.3 FRS of SDOF primary structure

is the floor (acceleration) response spectrum (FRS) of the SDOF primary structure.

4.3 Direct Method for Generating FRS

In this section, a direct spectra-to-spectra method for generating FRS is developed based on Duhamel's integral. To determine the probabilistic floor response spectrum by the direct spectra-to-spectra method under the tuning case, the concept of t-response spectrum is proposed, and statistical relationship between t-response spectrum and ground response spectrum is required.

4.3.1 SDOF Oscillator Mounted on SDOF Structure

Consider a SDOF oscillator mounted on a SDOF structure, as shown in Figure 4.3. Adopt the notations

$$h(t) = \mathrm{e}^{-\zeta\omega t}\frac{\sin\omega_{\mathrm{d}}t}{\omega_{\mathrm{d}}}, \qquad h^{\mathrm{c}}(t) = \mathrm{e}^{-\zeta\omega t}\frac{\cos\omega_{\mathrm{d}}t}{\omega_{\mathrm{d}}}, \qquad \omega_{\mathrm{d}} = \omega\sqrt{1-\zeta^2}, \tag{4.3.1}$$

$$h_0(t) = \mathrm{e}^{-\zeta_0\omega_0 t}\frac{\sin\omega_{0,\mathrm{d}}t}{\omega_{0,\mathrm{d}}}, \quad h_0^{\mathrm{c}}(t) = \mathrm{e}^{-\zeta_0\omega_0 t}\frac{\cos\omega_{0,\mathrm{d}}t}{\omega_{0,\mathrm{d}}}, \quad \omega_{0,\mathrm{d}} = \omega_0\sqrt{1-\zeta_0^2}. \tag{4.3.2}$$

Motion of Structure

For the SDOF system expressed by equation (4.2.9) with zero initial conditions, using Duhamel's integral (Clough and Penzien, 2003), the relative displacement $x(t)$ and the

relative velocity $\dot{x}(t)$ can be expressed as

$$x(t) = h(t) * \ddot{u}_g(t), \qquad \dot{x}(t) = \dot{h}(t) * \ddot{u}_g(t), \tag{4.3.3}$$

where $h(t)$ is the unit impulse response function of the structure and ω_d is the damped circular frequency defined by equation (4.3.1). The derivative of $h(t)$ is

$$\dot{h}(t) = -\frac{\zeta}{\sqrt{1-\zeta^2}} e^{-\zeta\omega t} \sin\omega_d t + e^{-\zeta\omega t}\cos\omega_d t = -\zeta\omega h(t) + e^{-\zeta\omega t}\cos\omega_d t. \tag{4.3.4}$$

Substituting equation (4.3.3) into (4.2.10), the absolute floor acceleration of the structure is given by

$$\ddot{u}(t) = -2\zeta\omega\dot{h}(t) * \ddot{u}_g(t) - \omega^2 h(t) * \ddot{u}_g(t). \tag{4.3.5}$$

Motion of Oscillator

The motion of the structure to which the oscillator is attached, defines the input to the SDOF oscillator with circular natural frequency ω_0 and damping coefficient ζ_0; the relative and absolute motions of the oscillator are governed by equations (4.2.11) and (4.2.12), respectively. Using Duhamel's integral and equation (4.3.5), the relative displacement $x_F(t)$ and velocity $\dot{x}_F(t)$ between the structure and the oscillator are

$$\begin{aligned} x_F(t) &= h_0(t) * \ddot{u}(t) = -2\zeta\omega h_0(t) * \dot{h}(t) * \ddot{u}_g(t) - \omega^2 h_0(t) * h(t) * \ddot{u}_g(t), \\ \dot{x}_F(t) &= \dot{h}_0(t) * \ddot{u}(t) = -2\zeta\omega\dot{h}_0(t) * \dot{h}(t) * \ddot{u}_g(t) - \omega^2\dot{h}_0(t) * h(t) * \ddot{u}_g(t), \end{aligned} \tag{4.3.6}$$

where the unit impulse response function $h_0(t)$ is defined by equation (4.3.2).

Substituting equation (4.3.6) into (4.2.12), the absolute acceleration of the oscillator is expressed as

$$\begin{aligned} \ddot{u}_F(t) &= -2\zeta_0\omega_0\dot{x}_F(t) - \omega_0^2 x_F(t) \\ &= \big[4\zeta_0\zeta\omega_0\omega \cdot \dot{h}_0(t) * \dot{h}(t) + 2\zeta_0\omega_0\omega^2 \cdot \dot{h}_0(t) * h(t) \\ &\quad + 2\zeta\omega_0^2\omega \cdot h_0(t) * \dot{h}(t) + \omega_0^2\omega^2 \cdot h_0(t) * h(t)\big] * \ddot{u}_g(t). \end{aligned} \tag{4.3.7}$$

It is easy to show that

$$h_0(t) * \dot{h}(t) = -\zeta\omega \cdot h_0(t) * h(t) + \omega\sqrt{1-\zeta^2} \cdot h_0(t) * h^c(t). \tag{4.3.8}$$

$$\dot{h}_0(t) * h(t) = -\zeta_0\omega_0 \cdot h_0(t) * h(t) + \omega_0\sqrt{1-\zeta_0^2} \cdot h(t) * h_0^{\mathrm{c}}(t), \tag{4.3.9}$$

$$\begin{aligned}\dot{h}_0(t) * \dot{h}(t) = {} & \zeta_0\zeta\omega_0\omega \cdot h_0(t) * h(t) - \zeta_0\omega_0\omega_{\mathrm{d}} \cdot h_0(t) * h^{\mathrm{c}}(t) \\ & - \zeta\omega_{0,\mathrm{d}}\omega \cdot h(t) * h_0^{\mathrm{c}}(t) + \omega_{0,\mathrm{d}}\omega_{\mathrm{d}} \cdot h_0^{\mathrm{c}}(t) * h^{\mathrm{c}}(t).\end{aligned} \tag{4.3.10}$$

Substituting equations (4.3.8) to (4.3.10) into (4.3.7) yields

$$\begin{aligned}\ddot{u}_{\mathrm{F}}(t) = \big[& (1-2\zeta_0^2-2\zeta^2+4\zeta_0^2\zeta^2)\omega_0^2\omega^2 \cdot h_0(t) * h(t) \\ & + 4\zeta_0\zeta\sqrt{(1-\zeta^2)(1-\zeta_0^2)}\,\omega_0^2\omega^2 \cdot h_0^{\mathrm{c}}(t) * h^{\mathrm{c}}(t) \\ & + 2\zeta_0\sqrt{1-\zeta_0^2}\,(1-2\zeta^2)\omega_0^2\omega^2 \cdot h(t) * h_0^{\mathrm{c}}(t) \\ & + 2(1-2\zeta_0^2)\zeta\sqrt{1-\zeta^2}\,\omega_0^2\omega^2 \cdot h_0(t) * h^{\mathrm{c}}(t) \big] * \ddot{u}_{\mathrm{g}}(t).\end{aligned} \tag{4.3.11}$$

For most SSCs in nuclear power plants, the damping coefficients ζ, $\zeta_0 < 0.1$. When t is sufficiently long, it is reasonable to assume that

$$\begin{aligned}\left|h_0(t) * h(t) * \ddot{u}_{\mathrm{g}}(t)\right|_{\max} & \approx \left|h_0^{\mathrm{c}}(t) * h^{\mathrm{c}}(t) * \ddot{u}_{\mathrm{g}}(t)\right|_{\max} \\ & \approx \left|h(t) * h_0^{\mathrm{c}}(t) * \ddot{u}_{\mathrm{g}}(t)\right|_{\max} \approx \left|h_0(t) * h^{\mathrm{c}}(t) * \ddot{u}_{\mathrm{g}}(t)\right|_{\max}.\end{aligned} \tag{4.3.12}$$

In general, the maximum values of the terms in (4.3.11) do not occur simultaneously because of the phase differences between the sine and cosine terms. The square root of the sum of the squares (SRSS) combination rule is used to calculate the maximum response. For lightly-damped systems, the values of ζ^2, ζ_0^2, and $\zeta_0\zeta$ are very small compared to 1, so that the corresponding terms are negligible. The maximum response of the oscillator is then reduced to

$$\left|\ddot{u}_{\mathrm{F}}(t)\right|_{\max} \approx \omega_0^2\omega^2 \left|h_0(t) * h(t) * \ddot{u}_{\mathrm{g}}(t)\right|_{\max}, \tag{4.3.13}$$

which is expressed analytically as a double convolution.

Denote $C(t) = h_0(t) * h(t)$. From the definition of Duhamel's integral, it is obvious that $C(t)$ is the response of an oscillator with the circular frequency ω_0 and damping coefficient ζ_0 under the excitation of $h(t)$. The equation of motion is written as

$$\ddot{C}(t) + 2\zeta_0\omega_0\dot{C}(t) + \omega_0^2 C(t) = h(t) = \frac{1}{\omega_{\mathrm{d}}}\mathrm{e}^{-\zeta\omega}\sin\omega_{\mathrm{d}}t. \tag{4.3.14}$$

The general solution for this differential equation is

$$C(t) = C_{\mathrm{C}}(t) + C_{\mathrm{P}}(t), \tag{4.3.15}$$

where

$$C_{\mathrm{C}}(t) = \mathrm{e}^{-\zeta_0\omega_0 t}\big(C_1\cos\omega_{0,\mathrm{d}}t + C_2\sin\omega_{0,\mathrm{d}}t\big), \quad \text{for } \zeta_0 < 1, \tag{4.3.16}$$

is the complementary solution with coefficients C_1 and C_2 determined by the initial conditions, and $C_{\mathrm{P}}(t)$ is a particular solution determined in the following.

4.3.2 Non-tuning Case

If $\omega \neq \omega_0$ and $\zeta \neq \zeta_0$, the right-hand side of equation (4.3.14) is not contained in the complementary solution. A particular solution $C_{\mathrm{P}}(t)$ is given by

$$C_{\mathrm{P}}(t) = \mathrm{e}^{-\zeta\omega t}\big[P_1\cos\omega_{\mathrm{d}}t + P_2\sin\omega_{\mathrm{d}}t\big], \tag{4.3.17}$$

where

$$P_1 = -\frac{r\sqrt{1-\zeta^2}\cdot A}{\omega_0^2\omega_{\mathrm{d}}\cdot\Delta}, \quad P_2 = \frac{(1-\zeta^2)\cdot B}{\omega_0^2\omega_{\mathrm{d}}\cdot\Delta}, \quad r = \frac{\omega}{\omega_0}, \tag{4.3.18}$$

and $A = 2(\zeta_0 - \zeta r)$, $B = 1 - r^2 - \zeta r\cdot A$, $\Delta = r^2\cdot A + (1-\zeta^2)\cdot B^2$. For zero initial conditions $y(0) = 0$ and $\dot{y}(0) = 0$, the coefficients C_1 and C_2 of the complementary solution are given by

$$C_1 = -P_1, \quad C_2 = -\frac{A\cdot P_1}{2\sqrt{1-\zeta_0^2}} - \frac{r\sqrt{1-\zeta^2}\cdot P_2}{\sqrt{1-\zeta_0^2}}. \tag{4.3.19}$$

Having obtained $C(t) = h_0(t) * h(t)$, the maximum absolute acceleration of the oscillator given by equation (4.3.13) is

$$\begin{aligned}\big|\ddot{u}_{\mathrm{F}}(t)\big|_{\max} = \Big|\big(&C_1\omega_0^2\omega^2\mathrm{e}^{-\zeta_0\omega_0 t}\cos\omega_{0,\mathrm{d}}t + C_2\omega_0^2\omega^2\mathrm{e}^{-\zeta_0\omega_0 t}\sin\omega_{0,\mathrm{d}}t \\ &+ P_1\omega_0^2\omega^2\mathrm{e}^{-\zeta\omega t}\cos\omega_{\mathrm{d}}t + P_2\omega_0^2\omega^2\mathrm{e}^{-\zeta\omega t}\sin\omega_{\mathrm{d}}t\big) * \ddot{u}_{\mathrm{g}}(t)\Big|_{\max}.\end{aligned} \tag{4.3.20}$$

4.3.3 Perfect-tuning Case

When $\omega_0 = \omega$ and for small damping $\zeta_0, \zeta < 0.1$, $C(t) = h_0(t) * h(t)$ becomes

$$\begin{aligned}h_0(t) * h(t) &= \int_0^t \frac{1}{\omega_0}\mathrm{e}^{-\zeta_0\omega_0(t-\tau)}\sin\omega_0(t-\tau)\cdot\frac{1}{\omega}\mathrm{e}^{-\zeta\omega\tau}\sin\omega\tau\,\mathrm{d}\tau \\ &= \frac{1}{\omega^2}\mathrm{e}^{-\zeta_0\omega t}\int_0^t \mathrm{e}^{-(\zeta-\zeta_0)\omega\tau}\sin\omega(t-\tau)\sin\omega\tau\,\mathrm{d}\tau\end{aligned}$$

$$= \frac{1}{\omega^3[4+(\zeta-\zeta_0)^2]}\left[\frac{2}{\zeta-\zeta_0}(e^{-\zeta\omega t}-e^{-\zeta_0\omega t})\cos\omega t + (e^{-\zeta\omega t}+e^{-\zeta_0\omega t})\sin\omega t\right],$$

which can be simplified to, for small damping $(\zeta-\zeta_0)^2 \to 0$,

$$h_0(t) * h(t) = \frac{1}{2\omega^3(\zeta-\zeta_0)}(e^{-\zeta\omega t} - e^{-\zeta_0\omega t})\cos\omega t + \frac{1}{4\omega^3}(e^{-\zeta\omega t} + e^{-\zeta_0\omega t})\sin\omega t$$

$$= \frac{\dot{h}(t)-\dot{h}_0(t)}{2\omega^3(\zeta-\zeta_0)} + \frac{h(t)+h_0(t)}{4\omega^2}. \tag{4.3.21}$$

Substituting equation (4.3.21) into (4.3.13) yields the maximum response of the oscillator

$$\left|\ddot{u}_F(t)\right|_{max} = \left|\frac{\omega\dot{h}(t) * \ddot{u}_g(t) - \omega\dot{h}_0(t) * \ddot{u}_g(t)}{2(\zeta-\zeta_0)} + \frac{\omega^2 h(t) * \ddot{u}_g(t) + \omega^2 h_0(t) * \ddot{u}_g(t)}{4}\right|_{max}$$

$$= \left|\frac{1}{2}\cdot\frac{\ddot{u}(t)-\ddot{u}_0(t)}{\zeta-\zeta_0} + \frac{\ddot{u}(t)+\ddot{u}_0(t)}{4}\right|_{max}, \tag{4.3.22}$$

in which the following relationships have been used

$$u(t) = h(t) * \ddot{u}_g(t),\ \ \dot{u}(t) = \dot{h}(t) * \ddot{u}_g(t),\ \ \ddot{u}(t) = \omega^2 h(t) * \ddot{u}_g(t) = \omega\dot{h}(t) * \ddot{u}_g(t). \tag{4.3.23}$$

When $\zeta_0 = \zeta$, $\ddot{u}(t) = \ddot{u}_0(t)$; the first term in equation (4.3.22), which is dominant, is undefined. For $(\zeta-\zeta_0) \to 0$, equation (4.3.22) becomes

$$\left|\ddot{u}_F(t)\right|_{max} = \frac{1}{2}\left|\frac{\partial\ddot{u}(t)}{\partial\zeta} + \ddot{u}(t)\right|_{max}. \tag{4.3.24}$$

Differentiating $\ddot{u}(t) = \omega\dot{h}(t) * \ddot{u}_g(t) = (\omega e^{-\zeta\omega t}\cos\omega t) * \ddot{u}_g(t)$ with respect to ζ gives

$$\frac{\partial\ddot{u}(t)}{\partial\zeta} = \frac{\partial[\omega\dot{h}(t) * \ddot{u}_g(t)]}{\partial\zeta} = -\omega^2 t e^{-\zeta\omega t}\cos\omega t * \ddot{u}_g(t). \tag{4.3.25}$$

Note that $\ddot{u}(t)$ can also be written as $\ddot{u}(t) = \omega^2 h(t) * \ddot{u}_g(t) = \omega e^{-\zeta\omega t}\sin\omega t * \ddot{u}_g(t)$.

Hence, in the perfect-tuning case with $\omega_0 = \omega$, $\zeta_0 = \zeta$, the FRS given by equation (4.3.24) becomes

$$\mathcal{S}_F(\omega,\zeta) = \frac{1}{2}\left|-\omega^2 t e^{-\zeta\omega t}\cos\omega t * \ddot{u}_g(t) + \omega e^{-\zeta\omega t}\sin\omega t * \ddot{u}_g(t)\right|_{max}$$

$$= \mathcal{S}_A^t(\omega,\zeta), \tag{4.3.26}$$

where $\mathcal{S}_A^t(\omega,\zeta)$ is the t-response spectrum.

4.4 GRS and tRS

In seismic design, qualification, and evaluation of critical engineering structures, such as nuclear power plants, it is crucial to determine Floor Response Spectra (FRS) at various floors where important systems, structures, and components (SSC) performing operational and safety-related functions are mounted. Seismic inputs are usually specified in terms of Ground Response Spectra (GRS) defined as

$$\mathcal{S}_{\mathrm{A}}(\omega,\zeta) = \left|\omega \mathrm{e}^{-\zeta\omega t}\sin\omega t * \ddot{u}_{\mathrm{g}}(t)\right|_{\max}, \tag{4.4.1}$$

where $\ddot{u}_{\mathrm{g}}(t)$ is the ground acceleration, ω and ζ are the circular natural frequency and damping ratio of a single degree-of-freedom (SDOF) oscillator mounted on the ground.

When the direct spectra-to-spectra method based on Duhamel integral is applied to generate FRS, the following quantity is required when the equipment and structure are in resonance (tuning)

$$\mathcal{S}^{\mathrm{t}}_{\mathrm{A}}(\omega,\zeta) = \frac{1}{2}\left|-\omega^2 t\mathrm{e}^{-\zeta\omega t}\cos\omega t * \ddot{u}_{\mathrm{g}}(t) + \omega \mathrm{e}^{-\zeta\omega t}\sin\omega t * \ddot{u}_{\mathrm{g}}(t)\right|_{\max}. \tag{4.4.2}$$

Due to the presence of a time variable t in the first convolution term, it is difficult to obtain an analytical expression for equation (4.4.2) in terms of GRS.

Analogous to GRS defined in (4.4.1), equation (4.4.2) is defined as t-Response Spectrum (tRS), in which "t" indicates "tuning" or the extra "t" term in equation (4.4.2) as compared to GRS. The concepts of GRS and tRS are illustrated in Figure 4.4. Under an earthquake excitation $\ddot{u}_{\mathrm{g}}(t)$,

- GRS $\mathcal{S}_{\mathrm{A}}(f,\zeta)$ is the maximum acceleration response of a SDOF oscillator (with frequency f and damping ratio ζ) mounted directly on ground;
- tRS $\mathcal{S}^{\mathrm{t}}_{\mathrm{A}}(f,\zeta)$ is the maximum acceleration response of a SDOF oscillator (with frequency f and damping ratio ζ) mounted on top of a SDOF structure (with the same f and ζ) that is mounted on ground. The identical SDOF oscillator and SDOF structure are uncoupled and are in *resonance* or *tuning*.

To apply the direct spectra-to-spectra method to generate probabilistic FRS considering the uncertainty from ground motions, tRS corresponding to the given GRS are required. In

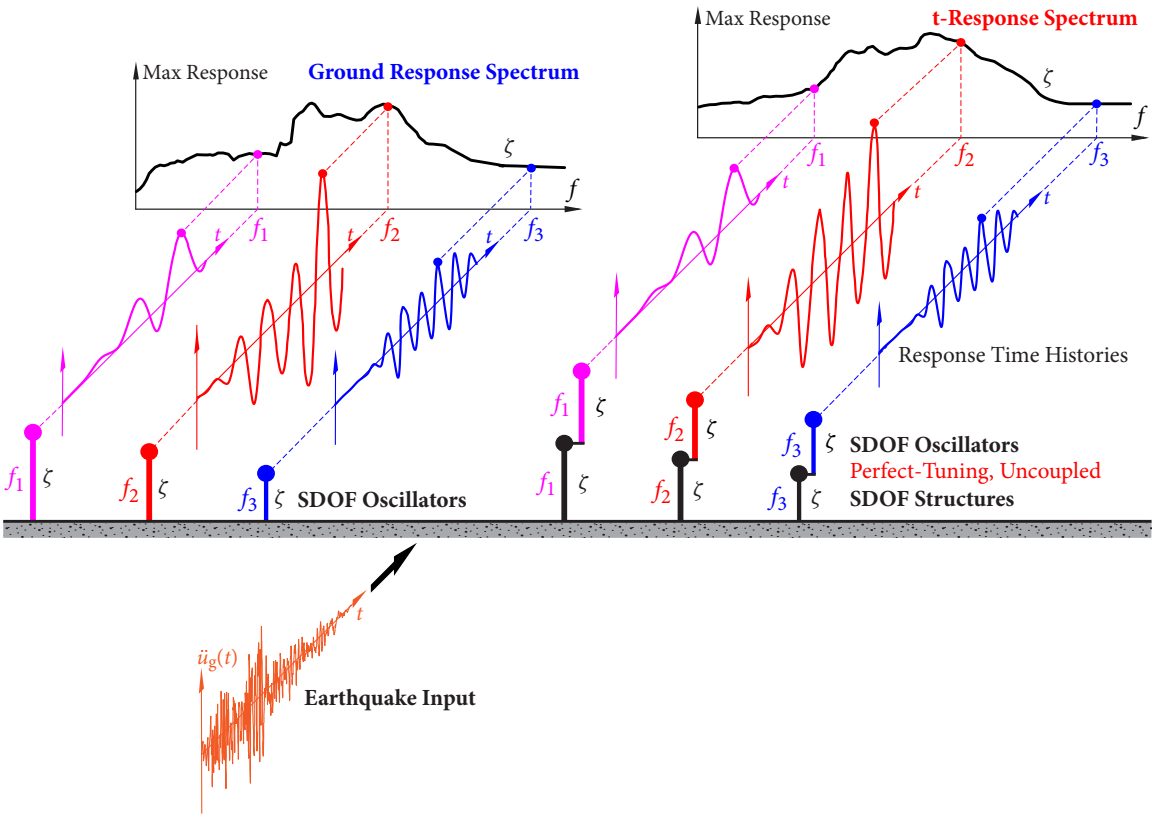

Figure 4.4 Seismic analysis methods for secondary systems

this chapter, statistical relationships between tRS and GRS are established through regression of simulation results using a large number of ground motions.

4.5 Ground Motion Selection

To determine statistical relationships between tRS and GRS, a large number of ground motions are required. In this study, ground motions recorded with different site conditions are selected by the following selection criteria:

- Ground motions with complete information, including three components (two horizontal components and one vertical component) and site classifications are considered. Only one horizontal component randomly selected from the two horizontal components is used to establish the horizontal statistical relationship between tRS and GRS,

and the corresponding vertical component is used to establish the vertical statistical relationship.

- Since the frequency range from 0.3 Hz to 24 Hz is important for structures and components of nuclear power facilities (USNRC, 2007B), Power Spectral Density (PSD) of selected ground motions should be sufficiently high in this frequency range to prevent a deficiency of power over this significant frequency band.
- Pulse-like ground motions are excluded due to their special characteristics.

Following these selection criteria, 49 horizontal and 49 vertical ground motions recorded at B sites, 154 horizontal and 154 vertical ground motions recorded at C sites, and 220 horizontal and 220 vertical ground motions recorded at D sites are selected from the PEER Strong Motion Database and the European Strong-Motion Database (Ambraseys *et al.*, 2002). The site categories B, C, and D follow the National Earthquake Hazard Reduction Program (NEHRP) site classification criteria (ASCE, 2010; IBC, 2012).

4.6 Statistical Relationships between tRS and GRS

In this section, statistical relationships between tRS and GRS are established based on ground motions recorded on different site categories, including the 28 horizontal ground motions and 14 vertical ground motions used by Newmark and Hall to develop design spectra in NUREG/CR-0098 (Newmark and Hall, 1978), 98, 308, and 440 ground motions recorded at B, C, and D sites, respectively.

Regression analysis is a statistical method that establishes a statistical relationship between a dependent variable (response variable) and one or more independent variables (predictor variables). To construct the statistical relationship between tRS and GRS, tRS and GRS of the selected ground motions are calculated first; tRS $\mathcal{S}_{\mathrm{A}}^{\mathrm{t}}(f,\zeta)$ and GRS $\mathcal{S}_{\mathrm{A}}(f,\zeta)$ are used as response variable and predictor variable, respectively. The regression model or the statistical relationship, is determined after evaluating the random relationship between $\mathcal{S}_{\mathrm{A}}^{\mathrm{t}}(f,\zeta)$ and $\mathcal{S}_{\mathrm{A}}(f,\zeta)$. Suppose the regression model is of the form

$$\ln \mathcal{S}_{\mathrm{A}}^{\mathrm{t}}(f,\zeta) = c_1(\zeta,f) + c_2(\zeta,f)\cdot \ln \mathcal{S}_{\mathrm{A}}(f,\zeta) + \varepsilon\, \sigma_{\ln \mathcal{S}_{\mathrm{A}}^{\mathrm{t}}}, \tag{4.6.1}$$

where $c_1(\zeta, f)$ and $c_2(\zeta, f)$ are coefficients of regression, ε is the number of standard deviations of a single predicted value of $\ln \mathcal{S}_{\mathrm{A}}^{\mathrm{t}}(f, \zeta)$ deviating from the mean value of $\ln \mathcal{S}_{\mathrm{A}}^{\mathrm{t}}(f, \zeta)$, and $\sigma_{\ln \mathcal{S}_{\mathrm{A}}^{\mathrm{t}}}$ is the standard deviation.

In practice, for a given GRS $\mathcal{S}_{\mathrm{A}}(\zeta, f)$, with or without a prescribed non-exceedance probability (NEP), tRS at each frequency is modelled using *lognormal distribution*. tRS $\mathcal{S}_{\mathrm{A}}^{\mathrm{t},p}(\zeta, f)$ with any NEP p corresponding to the given GRS can be estimated as:

$$\ln \mathcal{S}_{\mathrm{A}}^{\mathrm{t},p}(\zeta, f) = c_1(\zeta, f) + c_2(\zeta, f) \cdot \ln \mathcal{S}_{\mathrm{A}}(\zeta, f) + \sigma_{\ln \mathcal{S}_{\mathrm{A}}^{\mathrm{t}}}(\zeta, f) \cdot \Phi^{-1}(p). \tag{4.6.2}$$

In this section, details in determining the coefficients of regression $c_1(\zeta, f)$ and $c_2(\zeta, f)$, the standard deviation $\sigma_{\ln \mathcal{S}_{\mathrm{A}}^{\mathrm{t}}}(\zeta, f)$ are presented. The results are summarized in Table 4.2 and Tables 4.5 and 4.6, respectively, for horizontal motions and vertical motions; for frequencies not listed in these tables, the coefficients and standard deviations can be obtained using linear interpolation in the logarithmic scale of frequency.

Application of the statistical relationships between tRS and GRS is limited to GRS with PGA $= 0.3\,g$. For GRS with other values of PGA, three steps are required to calculate its tRS:

1. Apply an scale factor λ to the initial GRS, and make it PGA $= 0.3\,g$. A new GRS with PGA $= 0.3\,g$ is obtained.
2. Calculate tRS with any NEP corresponding to the new GRS by the statistical relationships between tRS and GRS.
3. Obtain tRS with any NEP corresponding to the initial GRS from multiplying the tRS calculated in step 2 by the scale factor λ in step 1.

4.6.1 Procedure to Establish Statistical Relationships between tRS and GRS

The procedure to establish the statistical relationship is as follows:

Step 1. All selected ground motions in a suite are scaled to a constant PGA, e.g., PGA $= 0.3\,g$.

Step 2. For a fixed damping ratio ζ, calculate GRS $\mathcal{S}_{\mathrm{A}}(f, \zeta)$ and tRS $\mathcal{S}_{\mathrm{A}}^{\mathrm{t}}(f, \zeta)$ for frequencies f uniformly spaced over the logarithmic scale of a required frequency range, e.g., from 0.1 to 100 Hz.

Step 3. Calculate amplification ratios

$$AR(f,\zeta) = \frac{S_A^t(f,\zeta)}{S_A(f,\zeta)}, \tag{4.6.3}$$

for all ground motions in the suite, and determine the median $AR_{50\%}$ and $AR_{84.1\%}$ with 50% and 84.1% NEP, respectively.

Step 4. Analyze the trend of the median amplification ratios $AR_{50\%}$.

Two examples are shown in Figures 4.5 and 4.6 to illustrate the trend of the amplification ratio AR for 5% damping ratios.

The first example shown in Figure 4.5 is based on the 49 horizontal ground motions recorded at B sites. The discrete points represent median $AR_{50\%}$ and $AR_{84.1\%}$ determined in Step 3 for 101 frequencies uniformly spaced over the logarithmic scale of the frequency range from 0.1 to 100 Hz. It can be observed that AR remains almost constant in the frequency range from 0.5 to 5 Hz, decreases almost linearly from 5 to 8 Hz, then decreases linearly with decreasing rates from 8 to 10 Hz, from 10 to 16 Hz, from 16 to 25 Hz, from 25 to 33 Hz, from 33 to 50 Hz, and finally approaches 1 for frequencies greater than 50 Hz. Furthermore, this figure reveals that the variations of AR remain almost constant from 0.5 to 5 Hz, increase from 5 to 25 Hz, decrease after 25 Hz, and reduce to almost zero near 50 Hz. Because of the large uncertainties in real ground motions, it is difficult to capture the variation of AR between 10 to 50 Hz, especially in the frequency range from 25 to 50 Hz in which its coefficient of variation reduces from large values to almost zero. Similar trends are also observed in other suites of horizontal ground motions for damping ratios less than 20%.

The second example shows the results based on the 49 vertical ground motions recorded at B sites in Figure 4.6. It can be observed that AR remains almost constant between 0.5 an 8 Hz, decreases linearly from 8 to 10 Hz, decreases linearly with decreasing rates from 10 to 15 Hz, from 15 to 25 Hz, from 25 to 33 Hz, from 33 to 50 Hz, and finally approaches 1 for frequencies greater than 50 Hz. Moreover, it is seen that the variations of AR remain almost constant from 0.5 to 8 Hz, increase in the frequency range from 8 to 33 Hz, decrease after 33 Hz, and reduce to almost zero near 50 Hz. Similar to horizontal ground motions, because of the large uncertainties in real ground motions, it is difficult to capture the variation of AR

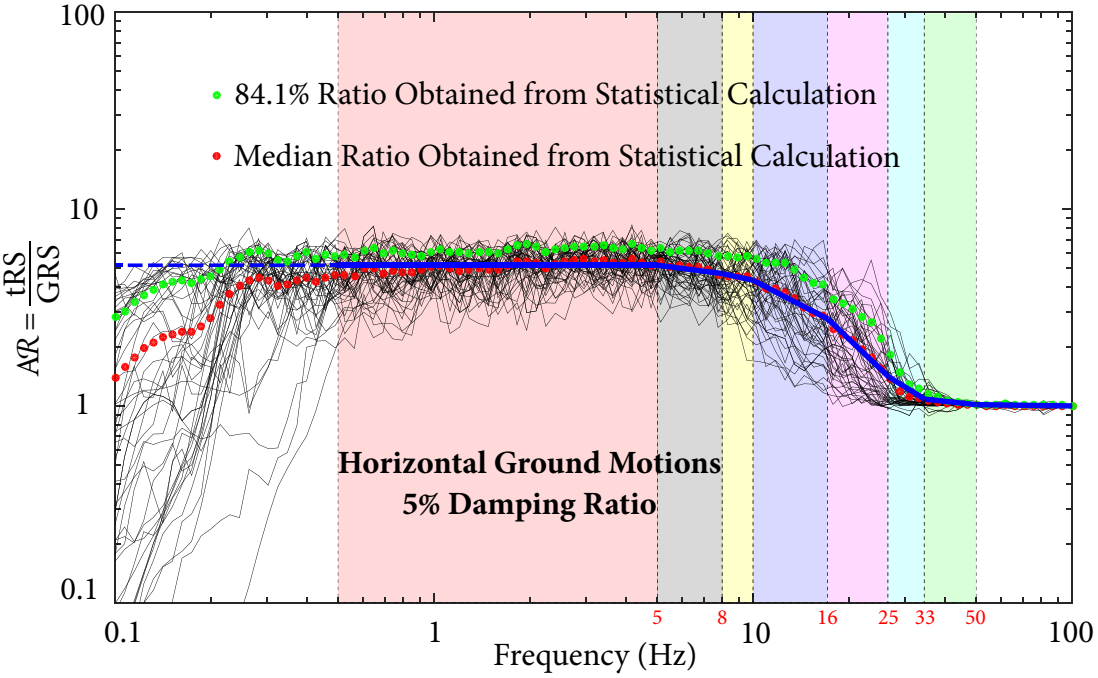

Figure 4.5 Ratio of tRS to GRS for the 49 horizontal ground motions at B sites

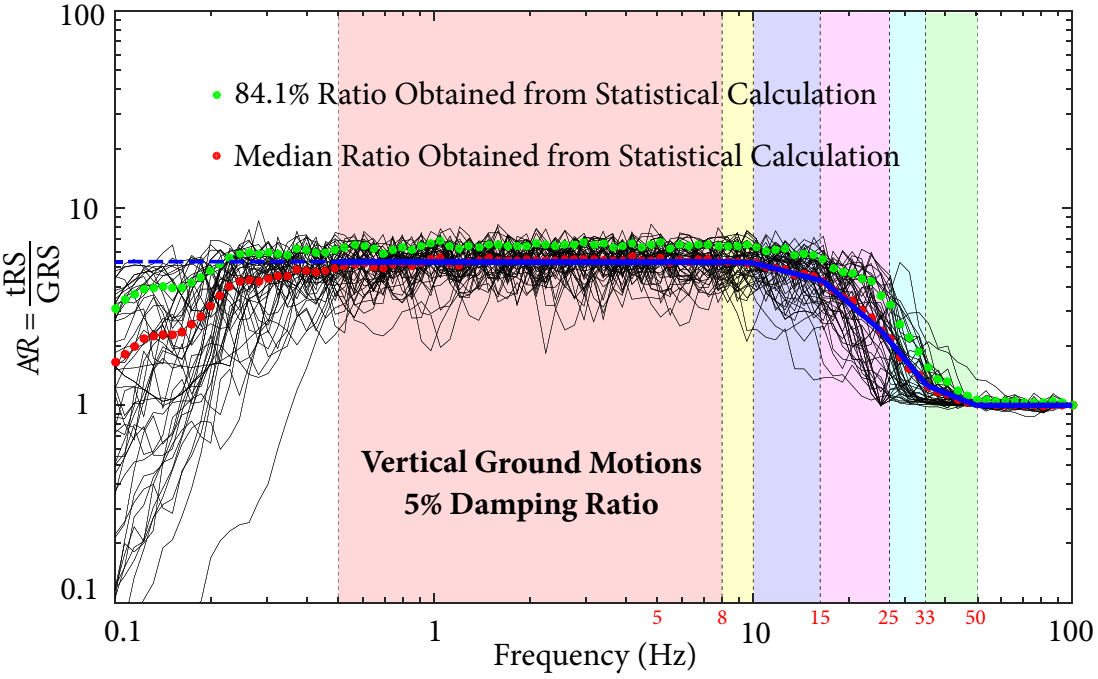

Figure 4.6 Ratio of tRS to GRS for the 49 vertical ground motions at B sites

between 10 and 50 Hz, especially between 33 and 50 Hz, in which the coefficient of variation reduces from large values to almost zero. Similar trends are also observed in other suites of vertical ground motions under damping ratios less than 20%.

Comparison between the trends of Figures 4.5 and 4.6 reveals that the components of ground motions—horizontal component and vertical component—affect the statistical relationships between tRS and GRS. Thus, it is necessary to establish the statistical relationships between tRS and GRS separately for horizontal and vertical motions.

Step 5. In the frequency ranges from 0.5 to 5 Hz for horizontal motions and from 0.5 to 8 Hz for vertical motions, the amplification ratio AR is almost constant; all random tRS and all random GRS are grouped together, respectively, and one regression analysis is performed.

In frequency ranges from 0.1 to 0.5 Hz and from 5 to 50 Hz for horizontal motions, and from 0.1 to 0.5 Hz and from 8 to 50 Hz for vertical motions, perform frequency-by-frequency regression analysis to all random tRS and all random GRS.

For frequencies greater than 50 Hz, $AR = 1$, i.e., tRS is considered to be equal to GRS without variation.

For frequency ranges from 25 to 50 Hz for horizontal ground motions and from 33 to 50 Hz for vertical ground motions, because the coefficient of variation of AR reduces from large values to zero, it is difficult to quantify these variations by statistical relationships. For real ground motions, tRS or GRS usually either reduce rapidly from large values to PGA or remain close to PGA over 25 to 50 Hz. If tRS at 25 Hz is connected linearly to tRS at 50 Hz, the resulting tRS is conservative. Considering the special variations of AR between 25 and 50 Hz, it is recommended to linearly interpolate tRS in the logarithmic-linear scale between 25 to 50 Hz in estimating horizontal and vertical tRS for $25 < f < 50$ Hz to avoid possible nonconservatism.

4.6.2 Statistical Relationship between Horizontal tRS and GRS

In this subsection, following the procedure presented in Section 4.6.1, statistical relationships between tRS and GRS for horizontal ground motions with 5% damping ratio are established, using the 28 horizontal ground motions for NUREG/CR-0098, the 49, 154, and 220 horizontal ground motions recorded at B, C, and D sites, respectively. For each suite of

ground motions, a total of 68 regression equations are obtained from the regression analysis. The 68 regression equations describe the horizontal statistical relationship between tRS and GRS over the frequency range from 0.1 to 100 Hz—defining the complete horizontal statistical relationship.

It will be quite complex if all 68 regression equations are applied to generate FRS using the direct spectra-to-spectra method. A simplified yet robust horizontal statistical relationship, suitable for engineering applications, is developed by considering the following factors:

1. Because frequencies lower than 0.5 Hz are not very important for structures and equipment in nuclear power plants and there are extremely large variations in the amplification ratio AR as shown in Figure 4.5, the horizontal statistical relationship for frequencies between 0.1 and 0.5 Hz is taken as that in the frequency range from 0.5 to 5 Hz.
2. In the frequency range from 5 to 50 Hz, horizontal statistical relationship at critical frequencies 8, 10, 16, 25, 33, and 50 Hz are used to characterize the horizontal statistical relationship over this frequency range.
3. For frequencies greater than 50 Hz, since the amplification ratio AF approaches 1, tRS are considered to be equal to GRS.

For each suite of horizontal ground motions, using the 50% NEP Newmark design spectrum as the input GRS, tRS with 50% and 84.1% NEP are calculated by the complete and simplified horizontal statistical relationships and are shown in Figure 4.7. Comparison between the tRS results reveals that the complete relationships are well approximated by the simplified relationships in estimating tRS over the frequency range from 0.5 to 100 Hz, except for the frequency range from 0.1 to 0.5 Hz. However, frequencies lower than 0.5 Hz are almost out of the frequency of interest for structures and equipment in nuclear power plants (USNRC, 2007B). The same conclusion is obtained for other damping ratios less than 20%. Hence, the simplified horizontal statistical relationships are suitable to replace the complete horizontal statistical relationships.

To investigate the effect of site conditions on the horizontal statistical relationships between tRS and GRS, tRS determined by the simplified horizontal statistical relationships

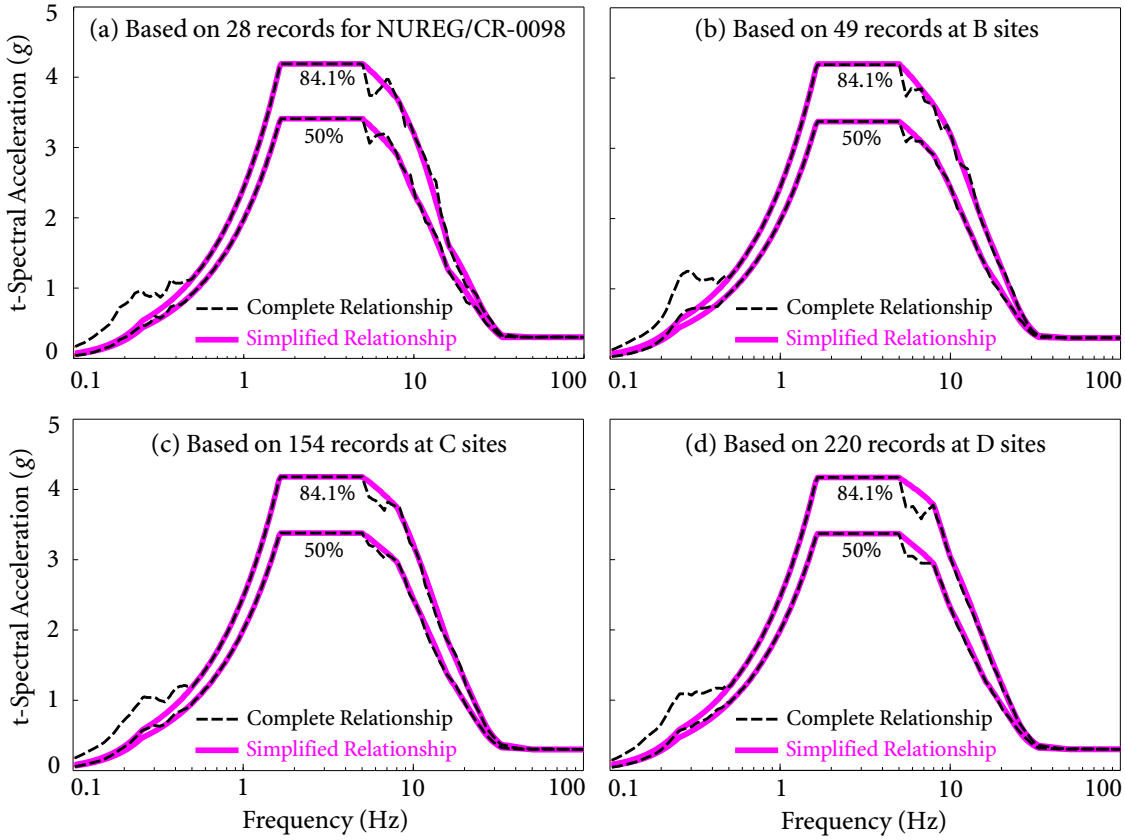

Figure 4.7 tRS based on different suites of horizontal ground motions

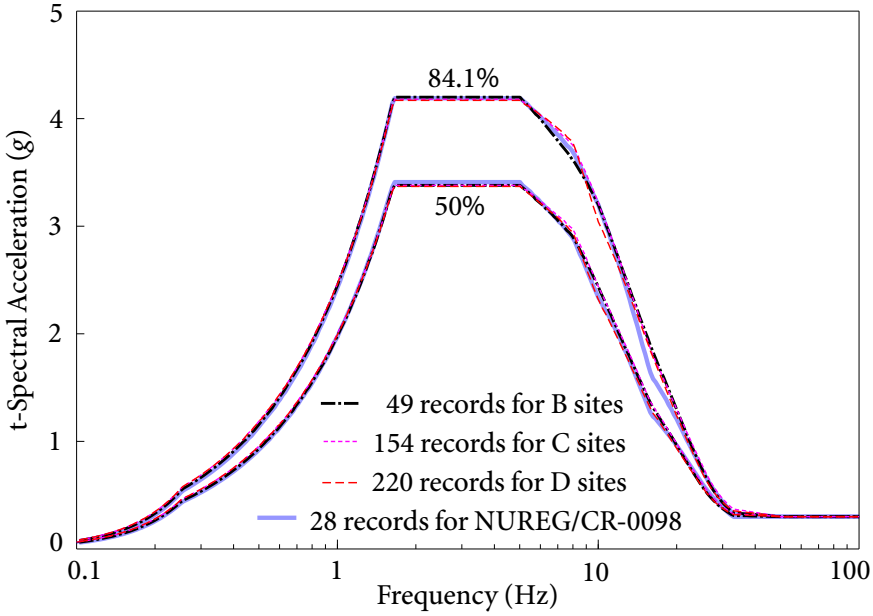

Figure 4.8 Comparison of tRS by horizontal relationships for various site conditions

for different site conditions shown in Figure 4.7 are compared in Figure 4.8. It is clearly seen that the differences among the tRS for different site conditions are very small. Thus, it is concluded that the influence of site conditions on the horizontal statistical relationships between tRS and GRS is small; this conclusion is valid for tRS with damping ratios less than 20%.

4.6.2.1 General Horizontal Statistical Relationship

Since site conditions have a negligible effect on the horizontal statistical relationship between tRS and GRS, the 28 horizontal ground motions used to construct design response spectrum in NUREG/CR-0098, the 49, 154, and 220 horizontal ground motions recorded at B, C, and D sites are combined into one suite of horizontal ground motions to obtain a more reliable statistical result. Using this suite of horizontal ground motions, simplified horizontal statistical relationships between tRS and GRS for 20 damping ratios (1%, 2%, 3%, . . . , 20%) are established; the regression coefficients in equation (4.6.1) of seven selected damping ratios are listed in Table 4.1.

Based on the regression coefficients for the 20 damping ratios, equations for regression coefficients against damping ratio are obtained by curve fitting using the least-square method. Samples of curve-fitting are shown in Figures 4.9 to 4.11. Equations for the regression coefficients from the curve fitting are listed in Table 4.2. This table presents only coefficients and standard deviations for critical frequencies; coefficients and standard deviations for other frequencies can be obtained using linear interpolation in the logarithmic-linear scale.

In developing a regression model, it is necessary to restrict the coverage of the regression model to some interval or region of values of the predictor variables (Neter *et al.*, 1996). The horizontal statistical relationship developed in this study is valid for GRS falling between the minimal and maximal values of predictor variable S_A used for regression analysis. An example of valid coverage of GRS for the horizontal statistical relationship for 5% damping ratio is shown in Figure 4.12. The horizontal design spectra in NUREG/CR-0098 (Newmark and Hall, 1978) with 5% damping ratio for soil sites constructed using the method proposed by Newmark and Hall (Hall, Mohraz, and Newmark, 1976; Newmark, Blume, and Kapur, 1973A; Newmark, Hall, and Mohraz, 1973B; Newmark and Hall, 1969), and horizontal design

Table 4.1 Coefficients of simplified horizontal statistical relationship for various damping ratios

f (Hz)	Damping Ratio ζ (%)																			
	1.0			3.0			5.0			7.0			10.0			15.0			20.0		
	c_1	c_2	$\sigma_{\ln S_A^t}$	c_1	c_2	$\sigma_{\ln S_A^t}$	c_1	c_2	$\sigma_{\ln S_A^t}$	c_1	c_2	$\sigma_{\ln S_A^t}$	c_1	c_2	$\sigma_{\ln S_A^t}$	c_1	c_2	$\sigma_{\ln S_A^t}$	c_1	c_2	$\sigma_{\ln S_A^t}$
0.1∼5	3.00	1.12	0.30	2.11	1.07	0.24	1.70	1.07	0.21	1.44	1.07	0.20	1.18	1.09	0.19	0.93	1.14	0.18	0.80	1.21	0.19
8	3.00	1.33	0.27	2.14	1.45	0.25	1.76	1.51	0.24	1.54	1.55	0.23	1.34	1.61	0.21	1.20	1.69	0.16	1.09	1.69	0.14
10	2.99	1.45	0.29	2.19	1.65	0.28	1.88	1.77	0.28	1.70	1.84	0.26	1.52	1.89	0.22	1.30	1.85	0.18	1.16	1.80	0.13
16	3.31	2.21	0.43	2.72	2.57	0.40	2.39	2.58	0.33	2.15	2.52	0.27	1.86	2.38	0.21	1.48	2.14	0.15	1.30	2.01	0.11
25	6.42	5.67	0.62	5.07	5.02	0.35	3.66	3.95	0.22	2.80	3.27	0.16	2.20	2.80	0.10	1.72	2.42	0.06	1.52	2.25	0.04
33	7.35	6.68	0.49	3.77	4.02	0.21	2.32	2.88	0.11	1.67	2.36	0.07	1.30	2.06	0.04	1.20	1.98	0.03	1.18	1.97	0.02
50∼100	0.0	1.00	0.0	0.0	1.00	0.0	0.0	1.00	0.0	0.0	1.00	0.0	0.0	1.00	0.0	0.0	1.00	0.0	0.0	1.00	0.0

Table 4.2 Equations for coefficients and standard deviations of horizontal statistical relationship

Frequency (Hz)	Coefficient c_1	Coefficient c_2	Standard deviation $\sigma_{\ln S_A^t}$
0.1∼5.0	$0.06(\ln\zeta)^2 - 0.92\ln\zeta + 3.03$	$0.02(\ln\zeta)^3 - 0.04(\ln\zeta)^2 - 0.02\ln\zeta + 1.12$	$-0.01(\ln\zeta)^2 - 0.05\ln\zeta + 0.30$
8.0	$0.10(\ln\zeta)^2 - 0.93\ln\zeta + 3.01$	$-0.01(\ln\zeta)^3 + 0.07(\ln\zeta)^2 + 0.03\ln\zeta + 1.35$	$-0.01(\ln\zeta)^3 + 0.02(\ln\zeta)^2 - 0.02\ln\zeta + 0.27$
10.0	$0.06(\ln\zeta)^2 - 0.80\ln\zeta + 2.99$	$-0.06(\ln\zeta)^3 + 0.21(\ln\zeta)^2 + 1.45$	$-0.01(\ln\zeta)^3 + 0.01(\ln\zeta)^2 + 0.28$
16.0	$-0.08(\ln\zeta)^2 - 0.45\ln\zeta + 3.32$	$-0.22(\ln\zeta)^2 + 0.58\ln\zeta + 2.24$	$0.02(\ln\zeta)^3 - 0.12(\ln\zeta)^2 + 0.07\ln\zeta + 0.43$
25.0	$0.39(\ln\zeta)^3 - 1.74(\ln\zeta)^2 + 0.16\ln\zeta + 6.33$	$0.35(\ln\zeta)^3 - 1.66(\ln\zeta)^2 + 0.77\ln\zeta + 5.58$	$0.02(\ln\zeta)^3 - 0.04(\ln\zeta)^2 - 0.21\ln\zeta + 0.60$
33.0	$0.21(\ln\zeta)^3 - 0.22(\ln\zeta)^2 - 3.16\ln\zeta + 7.23$	$0.20(\ln\zeta)^3 - 0.38(\ln\zeta)^2 - 2.15\ln\zeta + 6.58$	$0.04(\ln\zeta)^2 - 0.31\ln\zeta + 0.49$
50.0∼100.0	0	1	0

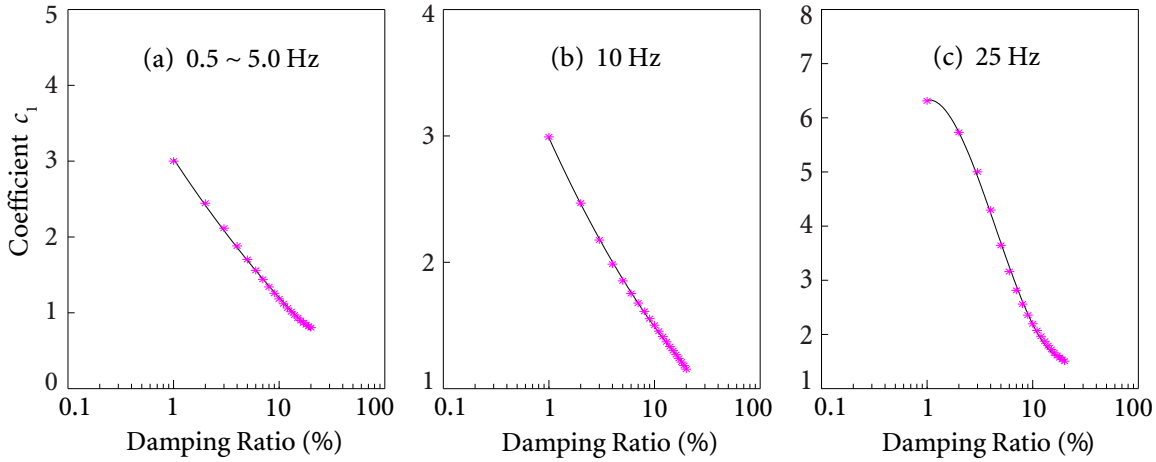

Figure 4.9 Curve-fitting to coefficient c_1 of horizontal statistical relationship

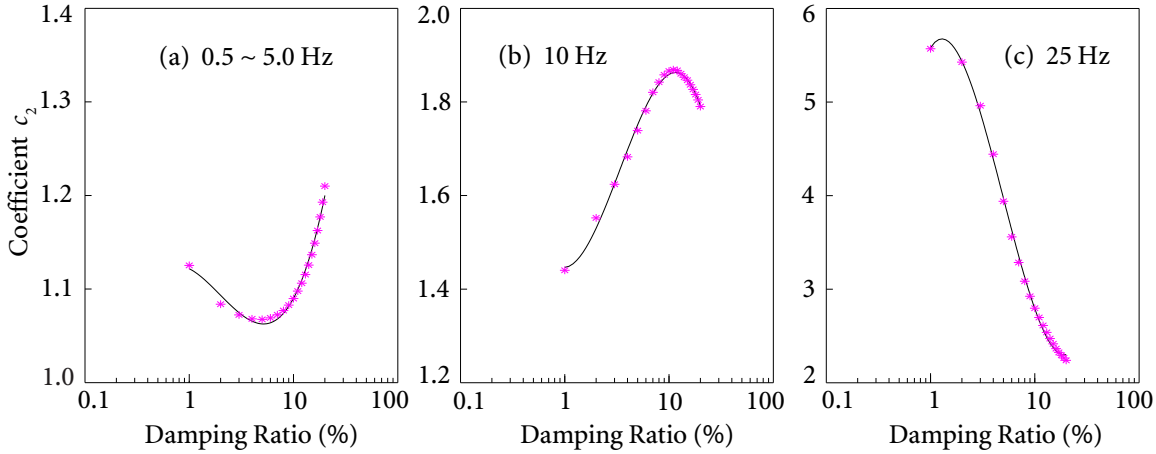

Figure 4.10 Curve-fitting to coefficient c_2 of horizontal statistical relationship

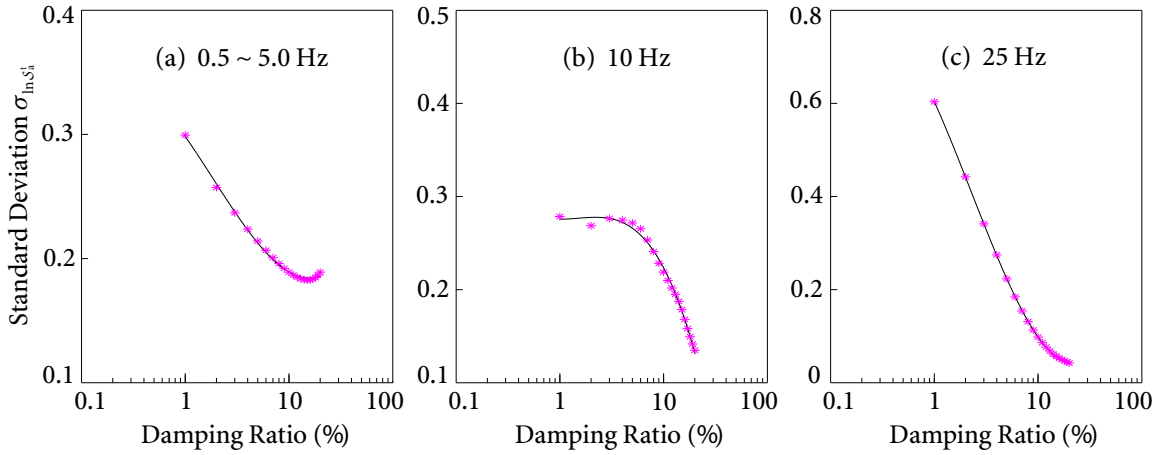

Figure 4.11 Curve-fitting to standard deviation of horizontal statistical relationship

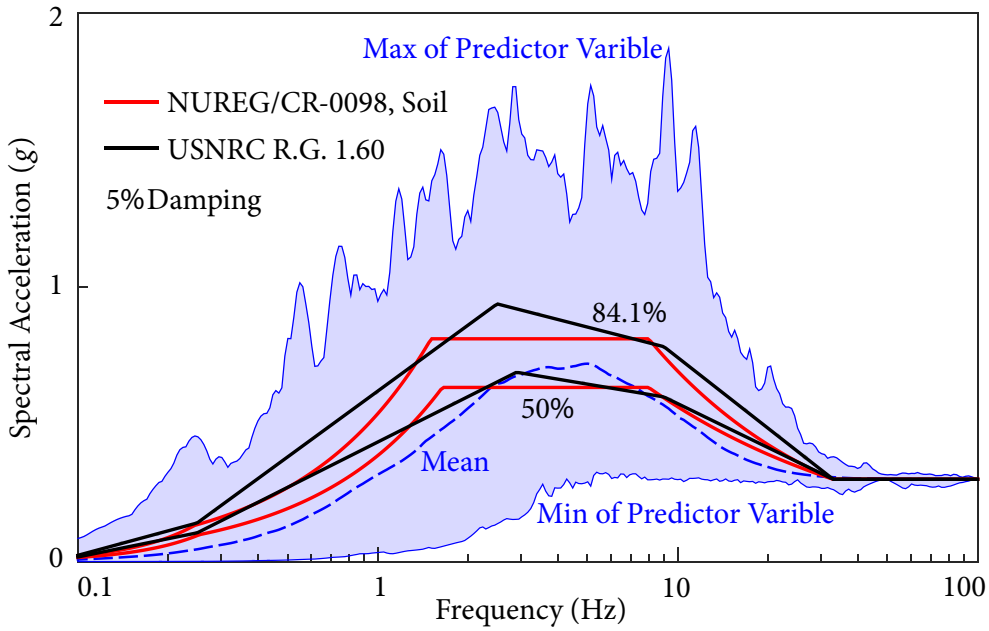

Figure 4.12 Valid coverage of GRS for the horizontal statistical relationship

spectra in USNRC R.G. 1.60 (USNRC, 2014) constructed by Blume *et al.* (Blume, Sharpe, and Dalal, 1973; Newmark, Blume, and Kapur, 1973A) are also shown for comparison. Note that USNRC R.G. 1.60 presents only the 84.1% NEP horizontal design response spectrum; the 50% NEP horizontal design response spectrum is taken from Newmark *et al.* (Newmark *et al.*, 1973A) with some adjustment.

It is clearly seen that the horizontal design spectra in NUREG/CR-0098 and USNRC R.G. 1.60 fall within the valid coverage of the horizontal statistical relationship. The differences between the horizontal design spectra in NUREG/CR-0098 and in USNRC R.G. 1.60 are small. Previous studies (Green, Gunberg, Parrish, *et al.*, 2007; McGuire, Silva, and Costantino, 2001; Silva, Youngs, and Idriss, 1999) have concluded that the differences between the spectral shapes of NUREG/CR-0098 and those of Uniform Hazard Spectra (UHS) in Western North America (WNA) are small, whereas the differences between spectral shapes of NUREG/CR-0098 and those of UHS in Central and Eastern North America (CENA) are large. Therefore, the horizontal statistical relationships developed in this study are suitable to estimate tRS corresponding to horizontal design spectra in NUREG/CR-0098

and USNRC R.G. 1.60, horizontal UHS in WNA, and any horizontal GRS falling inside the valid coverage of the horizontal statistical relationship.

4.6.2.2 Amplification Ratio Method for UHS with Significant High Frequency Components

For horizontal UHS with significant high frequency spectral accelerations, such as the standard UHS in CENA (Atkinson and Elgohary, 2007) shown in Figure 4.24, they may fall outside the valid coverage of horizontal statistical relationship. Motivated by Figure 4.5, an approach using the amplification ratio $AR = \text{tRS}/\text{GRS}$ is proposed to estimate tRS.

For $f \leqslant 50$ Hz, a constant amplification ratio is determined by

$$AR^{p}(f_{\text{h0}}, \zeta) = \frac{\mathcal{S}_{\text{A}}^{\text{t},p}(f_{\text{h0}}, \zeta)}{\mathcal{S}_{\text{A}}^{\text{mean}}(f_{\text{h0}}, \zeta)}, \tag{4.6.4}$$

where $AR^{p}(f_{\text{h0}}, \zeta)$ is the amplification ratio with NEP p, $f_{\text{h0}} = 5$ Hz, $\mathcal{S}_{\text{A}}^{\text{mean}}(f_{\text{h0}}, \zeta)$ is the mean value of predictor variable (i.e., mean value of spectral accelerations of the 451 horizontal ground motions used in regression analysis) at f_{h0}, and $\mathcal{S}_{\text{A}}^{\text{t},p}(f_{\text{h0}}, \zeta)$ is the tRS with NEP p calculated by equation (4.6.2) using $\mathcal{S}_{\text{A}}(f, \zeta) = \mathcal{S}_{\text{A}}^{\text{mean}}(f_{\text{h0}}, \zeta)$.

The mean value of horizontal predictor variable $\mathcal{S}_{\text{A}}^{\text{mean}}(f_{\text{h0}}, \zeta)$ at $f_{\text{h0}} = 5$ Hz for various damping ratios is determined and shown in Figure 4.13. Regression analysis gives the relationship between mean horizontal predictor variable (at 5 Hz) and damping ratio:

$$\mathcal{S}_{\text{A}}^{\text{mean}}(f_{\text{h0}}, \zeta) = 0.02\left[\ln(100\zeta)\right]^2 - 0.28\ln(100\zeta) + 1.14. \tag{4.6.5}$$

It is known that, the amplification ratio AR should be equal to 1 at 100 Hz. For frequencies between 50 and 100 Hz, tRS is obtained by linear interpolation in the logarithmic-logarithmic scale using known tRS at 50 and 100 Hz. Thus, for horizontal UHS with significant high frequency spectral accelerations, the corresponding tRS is determined as

$$\mathcal{S}_{\text{A}}^{\text{t},p}(f, \zeta) = \mathcal{S}_{\text{A}}^{\text{UHS}}(f, \zeta) \times AR^{p}(f_{\text{h0}}, \zeta), \quad f \leqslant 50\,\text{Hz}, \tag{4.6.6a}$$

$$\log_{10}\mathcal{S}_{\text{A}}^{\text{t},p}(f, \zeta) = \frac{\log_{10}\text{PGA} - \log_{10}\mathcal{S}_{\text{A}}^{\text{t},p}(50, \zeta)}{\log_{10}2} \cdot \log_{10} f + \frac{\log_{10}(\text{PGA})(\log_{10}2 - 2) + 2\log_{10}\mathcal{S}_{\text{A}}^{\text{t},p}(50, \zeta)}{\log_{10}2}, \quad 50\,\text{Hz} < f \leqslant 100\,\text{Hz}, \tag{4.6.6b}$$

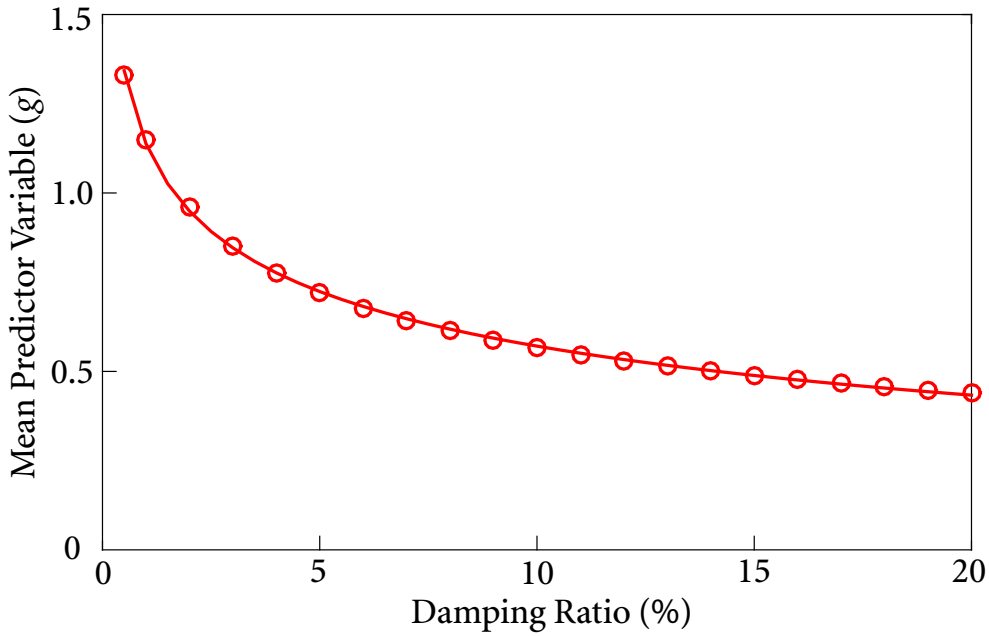

Figure 4.13 Mean horizontal predictor variable at 5 Hz for various damping ratios

where $S_A^{UHS}(f, \zeta)$ represents spectral acceleration of horizontal UHS.

4.6.3 Vertical Statistical Relationship between tRS and GRS

In this section, following the procedure to establish statistical relationship presented in Section 4.6.1, vertical statistical relationships between tRS and GRS for 5% damping ratio are established using 14 vertical ground motions used in Newmark's study (Newmark *et al.*, 1973B) for NUREG/CR-0098, the 49, 154, and 220 vertical ground motions recorded at B, C, and D sites, respectively.

For a suite of ground motions, a total of 62 regression equations are obtained from the regression analysis. The 62 regression equations describe the vertical statistical relationship between tRS and GRS over the frequency range from 0.1 to 100 Hz—defining the complete vertical statistical relationship. To provide simple and practical vertical statistical relationships between tRS and GRS, simplified vertical statistical relationships are established by considering the following factors:

1. Because frequencies lower than 0.5 Hz are very not important for structures and equipment in nuclear power plants, the vertical statistical relationship for frequencies from 0.1 to 0.5 Hz is taken as that in the frequency range from 0.5 to 8 Hz.
2. In the frequency range between 8 and 50 Hz, the vertical statistical relationship at critical frequencies 10, 15, 25, 33, and 50 Hz are used to characterize the relationship over this frequency range.
3. For frequencies greater than 50 Hz, as the amplification ratio AR is close to 1, tRS is considered to be equal to GRS.

Using the 50% NEP Newmark design spectrum as the input GRS, tRS with 50% and 84.1% NEP are determined by the complete and simplified vertical statistical relationships, respectively, and are shown in Figure 4.14. Comparison between the results reveals that the complete vertical statistical relationships are well approximated by the simplified vertical statistical relationships in estimating tRS over frequencies from 0.5 to 100 Hz. For frequency range from 0.1 to 0.5 Hz, there are some discrepancies; however, this frequency range is almost out of the frequency of interest for structures and equipment in nuclear power plants. The same conclusion can also be drawn for other damping ratios less than 20%. Therefore, the simplified vertical statistical relationships are suitable to replace the complete vertical statistical relationships.

To investigate whether site conditions have a significant effect on the vertical statistical relationships between tRS and GRS, tRS with 50% and 84.1% NEP determined by the simplified relationships for different site conditions corresponding to the 50% input GRS are compared, as shown in Figure 4.15. Comparison reveals that the differences among tRS with 50% and 84.1% NEP for different site conditions are small, except the tRS with 84.1% NEP for D sites, which is around 10% greater than other tRS in the intermediate frequency range. Influences of site conditions on vertical statistical relationships between tRS and GRS for other damping ratios less than 20% are also studied, and the same conclusion is obtained. Considering the 10% difference between the estimated tRS for soft sites (D sites) and for hard sites (mainly B and C sites), the vertical statistical relationships between tRS and GRS for hard sites and soft sites are established separately.

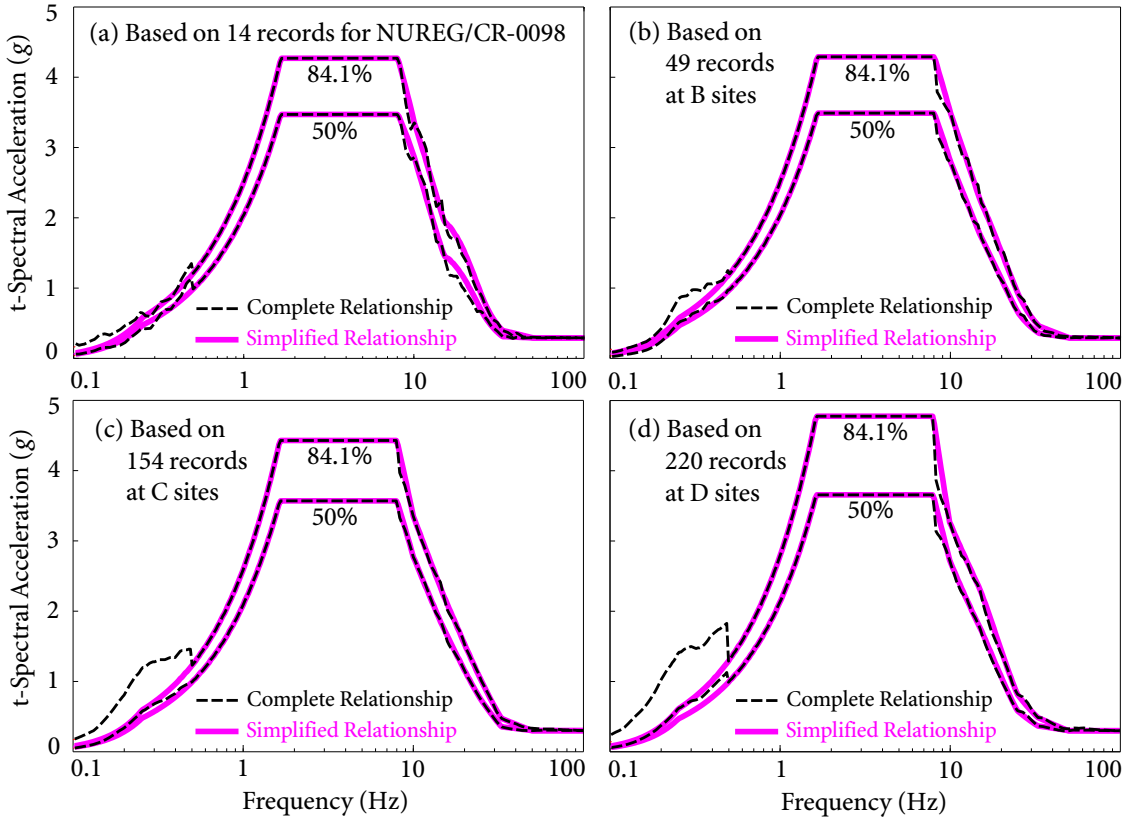

Figure 4.14 tRS based on different suites of vertical ground motions

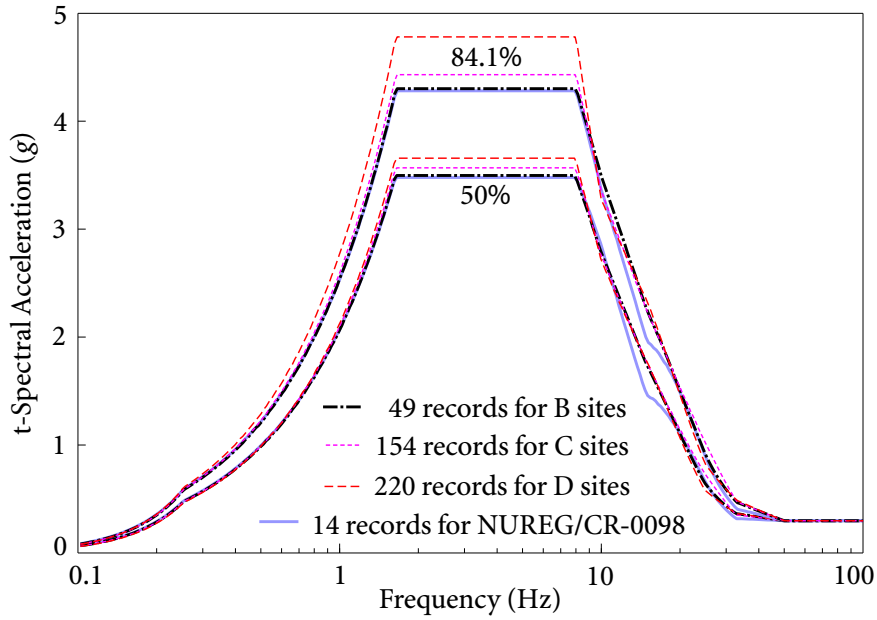

Figure 4.15 Comparison of tRS by vertical statistical relationships for various site conditions

4.6.3.1 General Vertical Statistical Relationship

To obtain more reliable vertical statistical relationships between tRS and GRS, the 14 vertical ground motions used in Newmark's study (Newmark *et al.*, 1973B) for NUREG/CR-0098, the 49 and 154 vertical ground motions recorded at B and C sites are combined into one suite of ground motions for hard sites, and the 220 vertical ground motions recorded at D sites are used for soft sites.

The procedure to establish the statistical relationship between tRS and GRS discussed in Section 4.6.1 is followed and the regression model in equation (4.6.1) is used. The simplified relationships between tRS and GRS for hard sites and soft sites with 20 damping ratios (1%, 2%, 3%, $\cdots$, 20%) are established, respectively, and the regression coefficients in equation (4.6.1) of seven selected damping ratios are shown in Tables 4.3 and 4.4.

Similar to the case of horizontal components, based on the regression coefficients for the 20 damping ratios, equations for regression coefficients against damping ratios are obtained by curve fitting using the least-square method and are listed in Tables 4.5 and 4.6, respectively, for hard and soft sites. For simplicity of practical applications, coefficients and standard deviations for only critical frequencies are presented in these tables; coefficients and standard deviations for other frequencies can be obtained using linear interpolation in the logarithmic scale for frequency. Samples of curve-fitting are shown in Figures 4.16 to 4.18 for hard sites, and in Figures 4.19 to 4.21 for soft sites.

The vertical statistical relationship should be valid for GRS falling within the minimal and maximal values of vertical predictor variable $\mathcal{S}_{\mathrm{A}}$. An example of valid coverage of GRS for the vertical statistical relationship with 5% damping ratio is presented in Figure 4.22. For comparison, Figure 4.22 also presents the 50% and 84.1% vertical design spectra in NUREG/CR-0098 (Newmark and Hall, 1978) with 5% damping ratio for soil sites constructed using the method proposed by Newmark and Hall (Hall, Mohraz, and Newmark, 1976; Newmark, Blume, and Kapur, 1973A; Newmark, Hall, and Mohraz, 1973B; Newmark and Hall, 1969), and the 50% and 84.1% vertical design spectrum in USNRC R.G. 1.60 (USNRC, 2014) constructed by Blume *et al.* (Blume, Sharpe, and Dalal, 1973; Newmark, Blume, and Kapur, 1973A). Note that USNRC R.G. 1.60 provides only 84.1% vertical design spec-

Table 4.3 Coefficients of simplified vertical statistical relationships for hard sites

f (Hz)	Damping Ratio ζ (%)																				
	1.0			3.0			5.0			7.0			10.0			15.0			20.0		
	c_1	c_2	$\sigma_{\ln \mathcal{S}_A^t}$	c_1	c_2	$\sigma_{\ln \mathcal{S}_A^t}$	c_1	c_2	$\sigma_{\ln \mathcal{S}_A^t}$	c_1	c_2	$\sigma_{\ln \mathcal{S}_A^t}$	c_1	c_2	$\sigma_{\ln \mathcal{S}_A^t}$	c_1	c_2	$\sigma_{\ln \mathcal{S}_A^t}$	c_1	c_2	$\sigma_{\ln \mathcal{S}_A^t}$
0.1∼8.0	3.06	1.15	0.28	2.17	1.09	0.23	1.76	1.08	0.21	1.49	1.07	0.21	1.21	1.08	0.20	0.93	1.11	0.19	0.78	1.17	0.20
10.0	3.07	1.23	0.20	2.19	1.28	0.19	1.80	1.35	0.19	1.58	1.42	0.20	1.37	1.48	0.19	1.14	1.51	0.16	1.00	1.52	0.14
15.0	3.04	1.35	0.26	2.20	1.54	0.25	1.85	1.66	0.25	1.66	1.75	0.23	1.48	1.80	0.21	1.32	1.83	0.17	1.23	1.84	0.14
25.0	3.28	2.28	0.6	2.64	2.53	0.43	2.33	2.55	0.33	2.14	2.53	0.27	1.94	2.48	0.20	1.62	2.28	0.13	1.45	2.16	0.09
33.0	3.87	3.29	0.65	3.42	3.56	0.39	2.90	3.27	0.28	2.39	2.89	0.23	1.88	2.50	0.16	1.36	2.09	0.10	1.20	1.96	0.07
50.0∼100	0.0	1.00	0.0	0.0	1.00	0.0	0.0	1.00	0.0	0.0	1.00	0.0	0.0	1.00	0.0	0.0	1.00	0.0	0.0	1.00	0.0

Table 4.4 Coefficients of simplified vertical statistical relationships for soft sites

f (Hz)	Damping Ratio ζ (%)																				
	1.0			3.0			5.0			7.0			10.0			15.0			20.0		
	c_1	c_2	$\sigma_{\ln \mathcal{S}_A^t}$	c_1	c_2	$\sigma_{\ln \mathcal{S}_A^t}$	c_1	c_2	$\sigma_{\ln \mathcal{S}_A^t}$	c_1	c_2	$\sigma_{\ln \mathcal{S}_A^t}$	c_1	c_2	$\sigma_{\ln \mathcal{S}_A^t}$	c_1	c_2	$\sigma_{\ln \mathcal{S}_A^t}$	c_1	c_2	$\sigma_{\ln \mathcal{S}_A^t}$
0.1∼8.0	3.1	1.17	0.32	2.22	1.11	0.28	1.8	1.10	0.27	1.53	1.10	0.26	1.26	1.11	0.26	0.98	1.14	0.25	0.84	1.20	0.24
10.0	3.06	1.24	0.22	2.18	1.32	0.18	1.78	1.35	0.18	1.53	1.38	0.18	1.28	1.39	0.18	1.06	1.42	0.16	0.88	1.37	0.14
15.0	3.02	1.40	0.24	2.15	1.47	0.27	1.75	1.51	0.28	1.53	1.55	0.25	1.31	1.57	0.23	1.11	1.60	0.18	1.01	1.64	0.15
25.0	3.20	2.62	0.73	2.70	2.84	0.48	2.51	2.88	0.34	2.34	2.82	0.27	2.12	2.68	0.22	1.81	2.45	0.17	1.59	2.28	0.12
33.0	3.17	2.62	0.58	3.05	3.19	0.39	2.79	3.15	0.28	2.45	2.93	0.22	2.15	2.73	0.15	1.80	2.46	0.11	1.58	2.29	0.08
50.0∼100	0.0	1.00	0.0	0.0	1.00	0.0	0.0	1.00	0.0	0.0	1.00	0.0	0.0	1.00	0.0	0.0	1.00	0.0	0.0	1.00	0.0

Table 4.5 Equations for coefficients and standard deviations of vertical statistical relationships for hard sites

Frequency (Hz)	Coefficient c_1	Coefficient c_2	Standard deviation $\sigma_{\ln S_A^t}$
0.5∼8.0	$0.04(\ln\zeta)^2 - 0.89\ln\zeta + 3.09$	$0.01(\ln\zeta)^4 - 0.06(\ln\zeta)^3 + 0.12(\ln\zeta)^2 - 0.12\ln\zeta + 1.15$	$0.01(\ln\zeta)^2 - 0.06\ln\zeta + 0.28$
10.0	$0.07(\ln\zeta)^2 - 0.90\ln\zeta + 3.08$	$-0.04(\ln\zeta)^3 + 0.19(\ln\zeta)^2 - 0.13\ln\zeta + 1.24$	$-0.01(\ln\zeta)^3 + 0.05(\ln\zeta)^2 - 0.05\ln\zeta + 0.2$
15.0	$0.10(\ln\zeta)^2 - 0.90\ln\zeta + 3.06$	$-0.03(\ln\zeta)^3 + 0.13(\ln\zeta)^2 + 0.08\ln\zeta + 1.35$	$-0.01(\ln\zeta)^3 + 0.01(\ln\zeta)^2 + 0.25$
25.0	$-0.03(\ln\zeta)^2 - 0.52\ln\zeta + 3.25$	$-0.03(\ln\zeta)^3 - 0.02(\ln\zeta)^2 + 0.29\ln\zeta + 2.28$	$0.01(\ln\zeta)^3 - 0.05(\ln\zeta)^2 - 0.12\ln\zeta + 0.60$
33.0	$0.17(\ln\zeta)^3 - 0.98(\ln\zeta)^2 + 0.51\ln\zeta + 3.83$	$0.17(\ln\zeta)^3 - 1.10(\ln\zeta)^2 + 1.28\ln\zeta + 3.26$	$0.01(\ln\zeta)^2 - 0.26\ln\zeta + 0.65$
50.0∼100	0	1	0

Table 4.6 Equations for coefficients and standard deviations of vertical statistical relationships for soft sites

Frequency (Hz)	Coefficient c_1	Coefficient c_2	Standard deviation $\sigma_{\ln S_A^t}$
0.5∼8.0	$0.04(\ln\zeta)^2 - 0.90\ln\zeta + 3.13$	$0.01(\ln\zeta)^3 - 0.03(\ln\zeta)^2 - 0.04\ln\zeta + 1.17$	$-0.04\ln\zeta + 0.32$
10.0	$0.05(\ln\zeta)^2 - 0.90\ln\zeta + 3.08$	$-0.02(\ln\zeta)^4 + 0.09(\ln\zeta)^3 - 0.14(\ln\zeta)^2 + 0.14\ln\zeta + 1.24$	$-0.01(\ln\zeta)^3 + 0.06(\ln\zeta)^2 - 0.09\ln\zeta + 0.22$
15.0	$0.09(\ln\zeta)^2 - 0.95\ln\zeta + 3.05$	$0.01(\ln\zeta)^4 - 0.07(\ln\zeta)^3 + 0.15(\ln\zeta)^2 - 0.03\ln\zeta + 1.40$	$-0.01(\ln\zeta)^3 - 0.01(\ln\zeta)^2 + 0.04\ln\zeta + 0.24$
25.0	$-0.08(\ln\zeta)^2 - 0.27\ln\zeta + 3.15$	$0.04(\ln\zeta)^4 - 0.25(\ln\zeta)^3 + 0.37(\ln\zeta)^2 + 0.06\ln\zeta + 2.63$	$0.01(\ln\zeta)^3 - 0.02(\ln\zeta)^2 - 0.24\ln\zeta + 0.74$
33.0	$-0.19(\ln\zeta)^2 + 3.21$	$0.07(\ln\zeta)^4 - 0.34(\ln\zeta)^3 + 0.17(\ln\zeta)^2 + 0.65\ln\zeta + 2.62$	$0.02(\ln\zeta)^3 - 0.07(\ln\zeta)^2 - 0.13\ln\zeta + 0.58$
50.0∼100.0	0	1	0

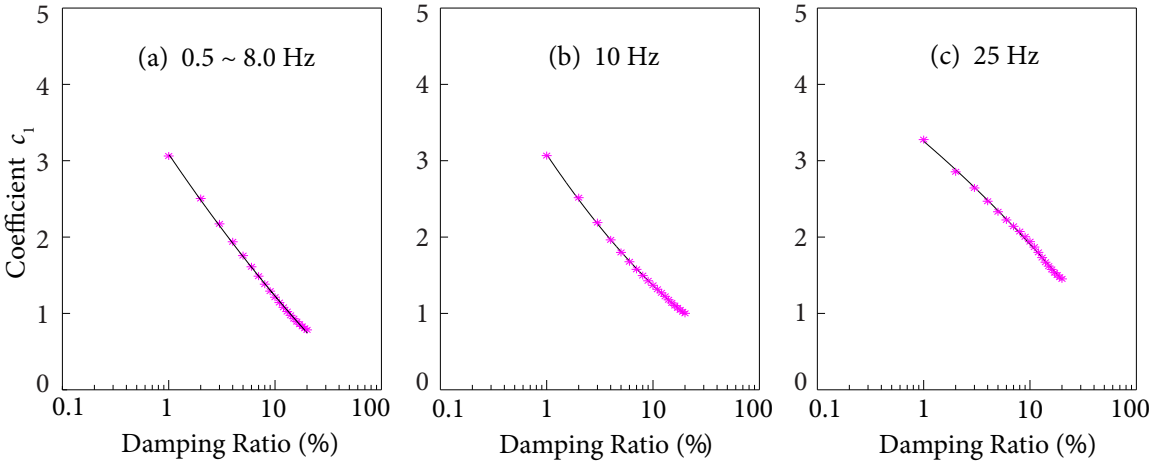

Figure 4.16 Curve-fitting to coefficient c_1 of vertical relationship for hard sites

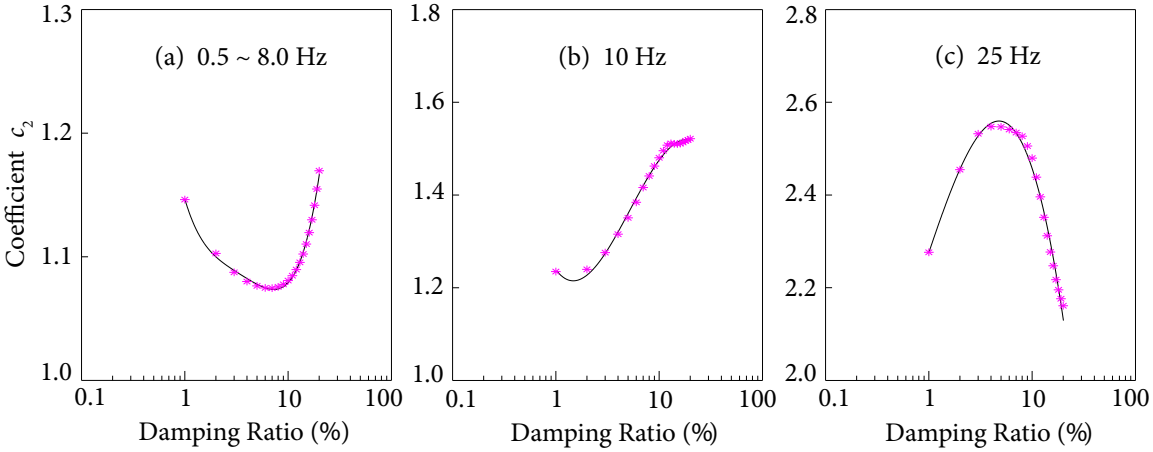

Figure 4.17 Curve-fitting to coefficient c_2 of vertical relationship for hard sites

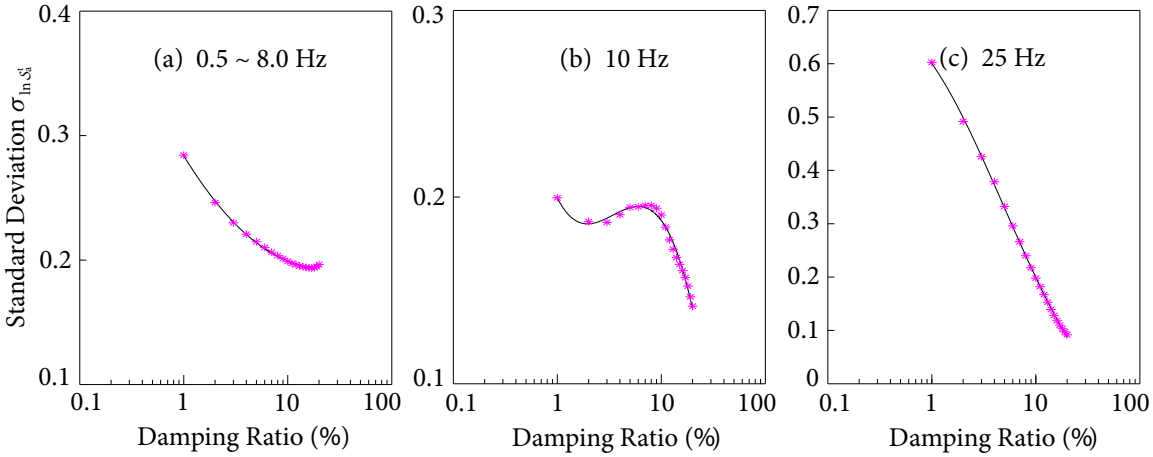

Figure 4.18 Curve-fitting to standard deviation of vertical relationship for hard sites

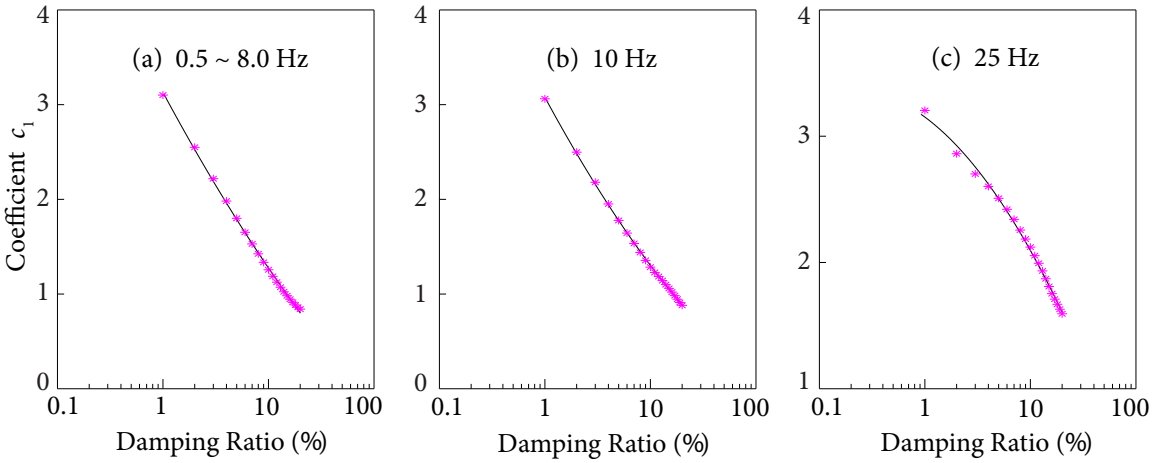

Figure 4.19 Curve-fitting to coefficient c_1 of vertical relationship for soft sites

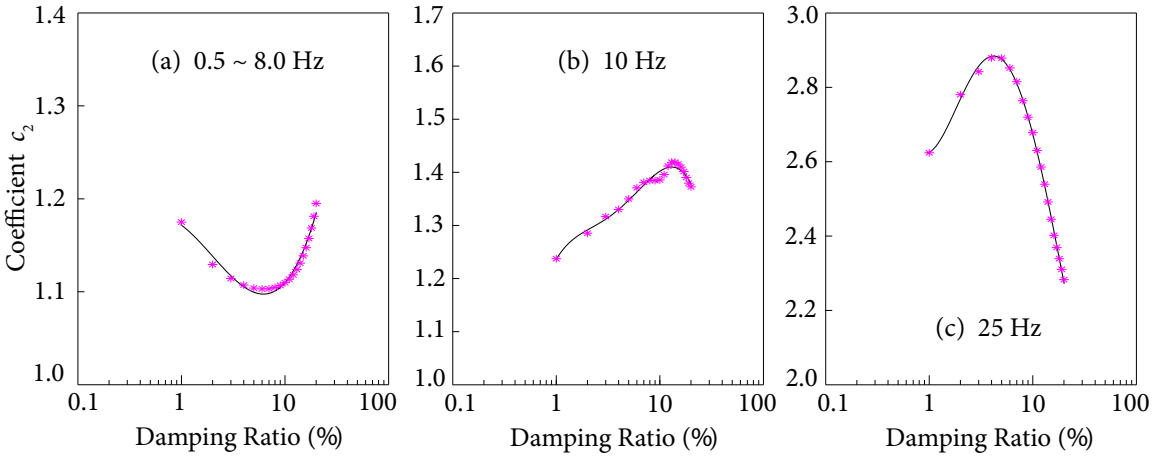

Figure 4.20 Curve-fitting to coefficient c_2 of vertical relationship for soft sites

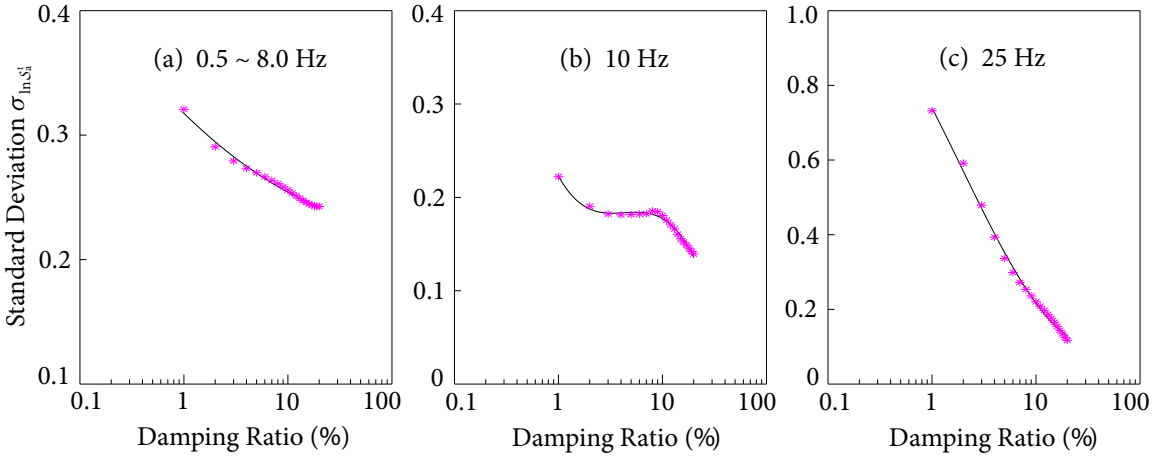

Figure 4.21 Curve-fitting to standard deviation of vertical relationship for soft sites

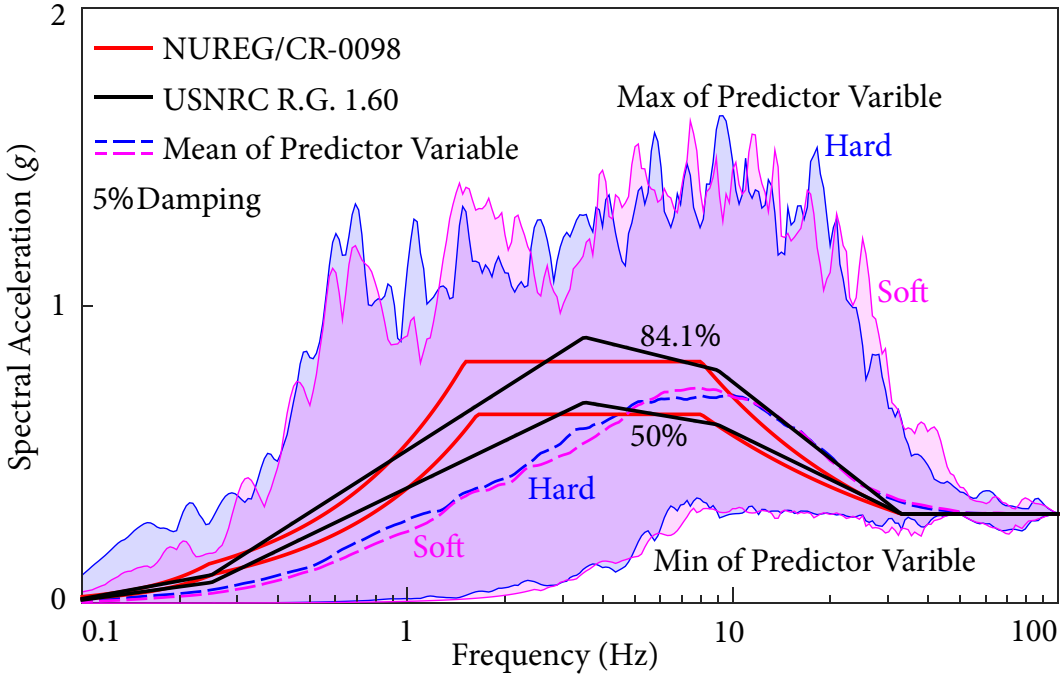

Figure 4.22 Valid coverage of GRS for the vertical statistical relationships

trum; the 50% vertical design spectrum is obtained by referring to the relationship between 84.1% and 50% horizontal design spectra in USNRC R.G. 1.60.

Similar to the horizontal case, the vertical statistical relationships are suitable for determining tRS corresponding to vertical design spectra in NUREG/CR-0098 and in USNRC R.G. 1.60, vertical UHS in WNA, and any GRS falling inside the valid coverage of the vertical statistical relationship.

4.6.3.2 Amplification Ratio Method for UHS with Significant High Frequency Components

For vertical UHS with significant high frequency spectral accelerations (e.g., UHS in CENA) such that they fall outside the valid coverage of vertical statistical relationship, the amplification ratio approach is applied to estimate tRS.

For frequency $f \leqslant 50$ Hz, a constant amplification ratio is determined as

$$AR^{p}(f_{v0},\zeta) = \frac{S_{A}^{t,p}(f_{v0},\zeta)}{S_{A}^{mean}(f_{v0},\zeta)}, \tag{4.6.7}$$

where $AR^{p}(f_{v0},\zeta)$ is the amplification ratio with NEP p, $f_{v0}=8$ Hz, $S_{A}^{mean}(f_{v0},\zeta)$ is the mean value of vertical predictor variable at 8 Hz, and $S_{A}^{t,p}(f_{v0},\zeta)$ is the tRS with NEP p calculated by equation (4.6.2) using $S_{A}(f,\zeta)=S_{A}^{mean}(f_{v0},\zeta)$.

The mean value of vertical predictor variable at 8 Hz for various damping ratios is shown in Figure 4.23 for hard sites and soft sites. From regression analyses, the relationships between mean vertical predictor variable at 8 Hz and damping ratio are

$$S_{A}^{mean}(f_{v0},\zeta)=\begin{cases}0.03\left[\ln(100\zeta)\right]^{2}-0.36\ln(100\zeta)+1.19, & \text{for hard sites;}\\ 0.04\left[\ln(100\zeta)\right]^{2}-0.38\ln(100\zeta)+1.24, & \text{for soft sites.}\end{cases} \tag{4.6.8}$$

For $f=100$ Hz, the amplification ratio $AR=1$. For frequencies between 50 and 100 Hz, tRS is approximated using linear interpolation in the logarithmic-logarithmic scale.

Hence, tRS in the vertical direction is estimated as

$$S_{A}^{t,p}(f,\zeta)=S_{A}^{UHS}(f,\zeta)\times AR^{p}(f_{v0},\zeta),\quad f\leqslant 50\text{ Hz}, \tag{4.6.9}$$

where $S_{A}^{UHS}(f,\zeta)$ is the vertical UHS. For $50\text{ Hz}<f\leqslant 100$ Hz, $S_{A}^{t,p}(f,\zeta)$ is obtained by linear interpolation in the logarithmic-logarithmic scale, given by equation (4.6.6b).

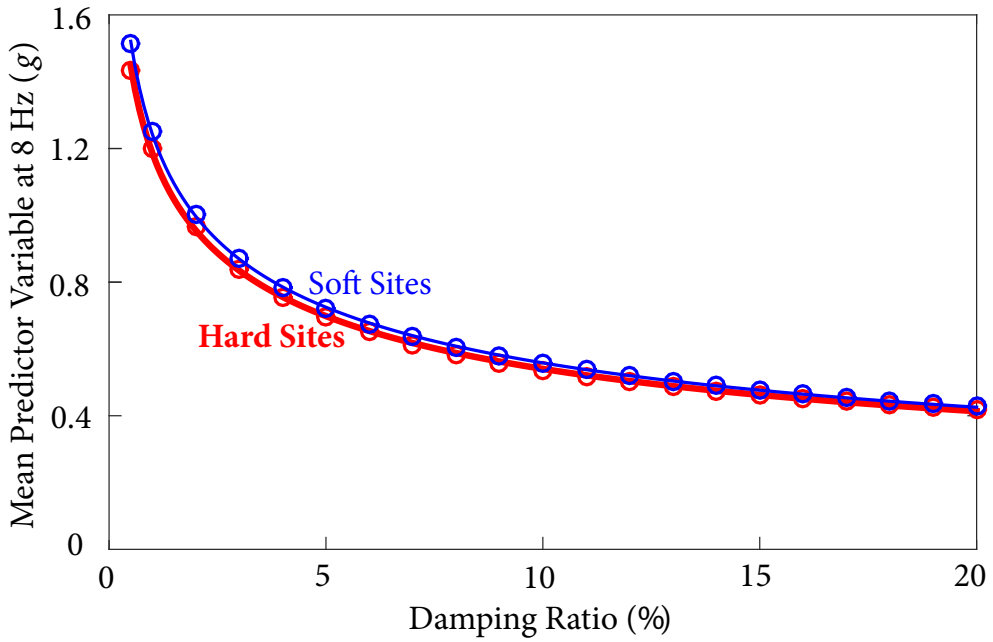

Figure 4.23 Mean vertical predictor variables at 8 Hz for various damping ratios

4.7 Examples of Estimating tRS

Two examples of estimating tRS by the statistical relationships between tRS and GRS and the amplification ratio method are presented in this section.

Example 1 – USNRC R.G. 1.60 Design Spectra

GRS are taken from the 5% horizontal and vertical design spectra in USNRC R.G. 1.60 (USNRC, 2014). 30 time histories compatible with the horizontal GRS and 30 time histories compatible with the vertical GRS are generated following Approach 2 of USNRC SRP 3.7.1 (USNRC, 2007B) using the Hilbert-Huang Transform method (Ni, Xie, and Pandey, 2011; Ni, Xie, and Pandey, 2013). The generated horizontal and vertical time histories all closely match their corresponding target GRS, as shown in Figures 4.24 and 4.25, respectively.

tRS of the 30 horizontal and 30 vertical time histories are calculated; tRS with 50% and 84.1% NEP are statistically calculated and used as benchmarks, as shown in Figures 4.24 and 4.25. In these figures, curves labelled "tRS from Statistical Relationship Directly" are tRS with 50% and 84.1% NEP calculated using the simplified statistical relationships. Considering the special variation over the frequency range between 25 and 50 Hz, tRS calculated using the statistical relationship are replaced by straight lines connecting tRS at 25 Hz to tRS at 50 Hz to avoid possible nonconservatism.

Horizontal GRS: From Figure 4.24, the following observations can be made.

- tRS with 50% NEP estimated by the horizontal statistical relationship closely matches the 50% NEP benchmark tRS except for the frequency range from 25 to 50 Hz.
- tRS with 84.1% NEP estimated by the horizontal statistical relationship closely matches the 84.1% NEP benchmark tRS over the frequency range from 0.3 to 8 Hz, displays some degree of conservatism from 8 to 20 Hz, and is slightly below the benchmark tRS from 20 to 25 Hz. Overall, the estimated tRS with 84.1% NEP is acceptable for frequencies lower than 25 Hz in comparison with the benchmark tRS.
- tRS with 50% and 84.1% NEP estimated by the horizontal statistical relationship are somewhat below their benchmark tRS for frequencies from 25 to 50 Hz. As seen in Figure 4.5, this is due to the special variation of AR over this frequency range.

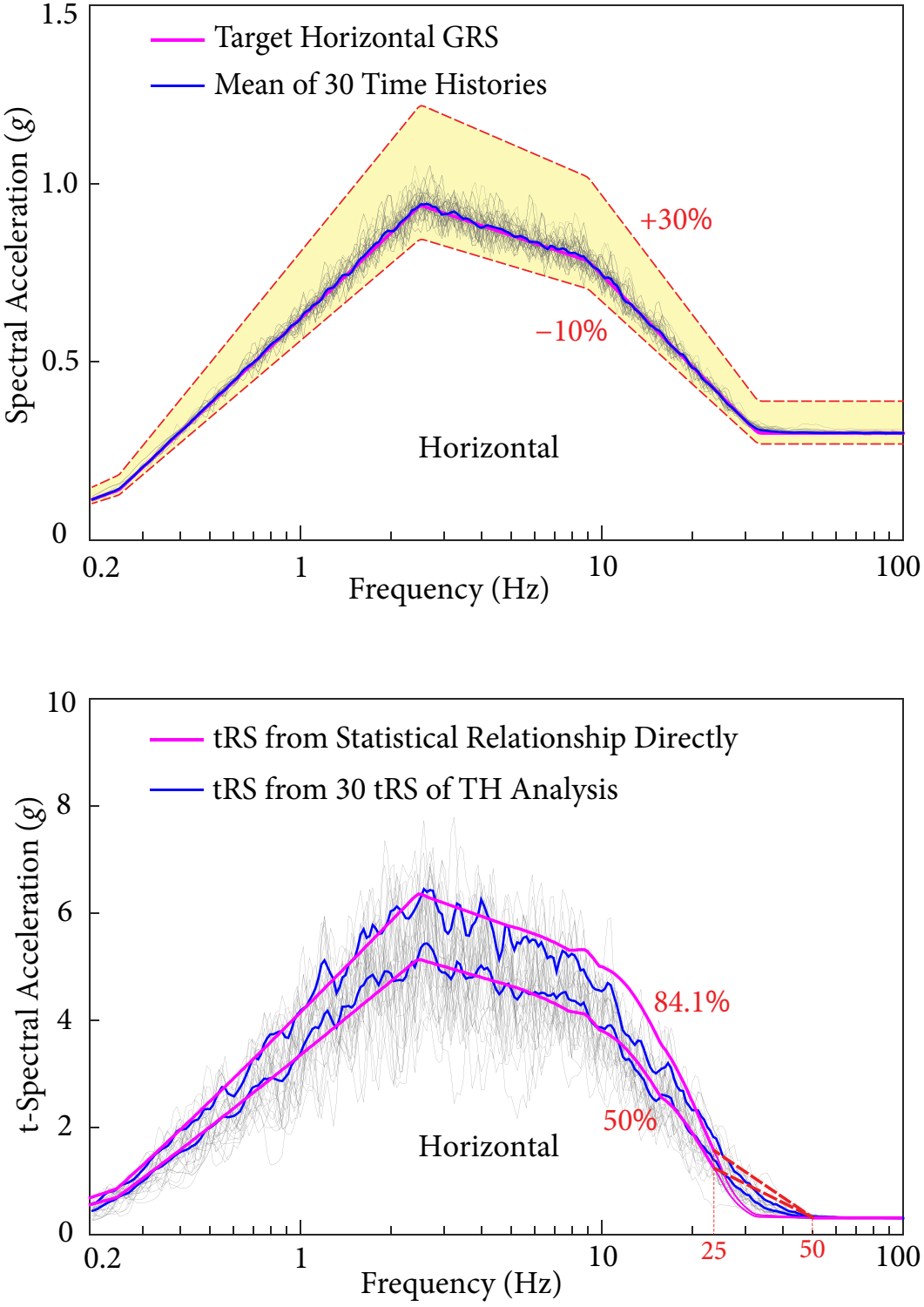

Figure 4.24 Comparison between horizontal tRS and GRS

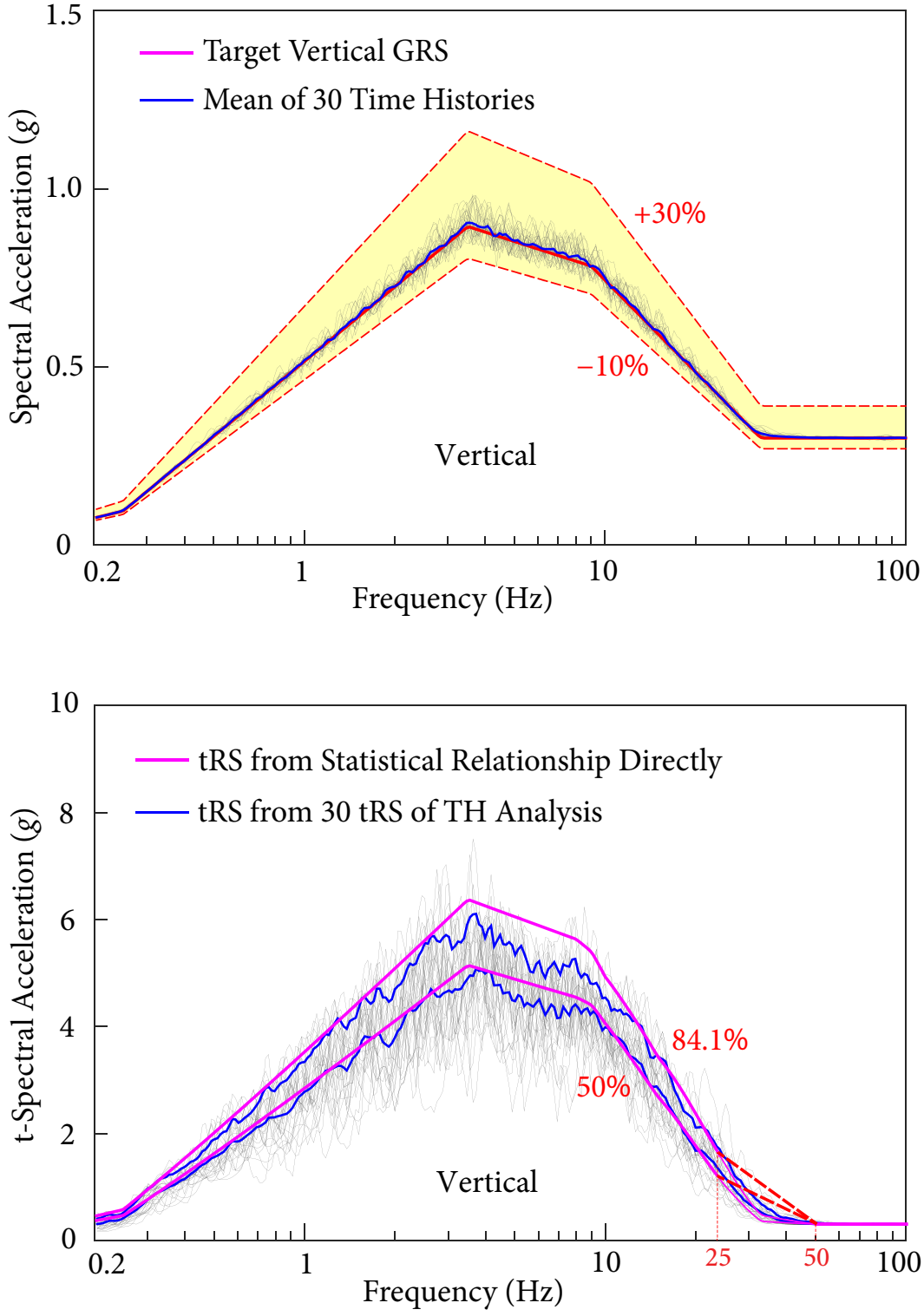

Figure 4.25 Comparison between vertical tRS and GRS

- The adjusted tRS over the frequency range from 25 to 50 Hz by linearly connecting tRS at 25 Hz to tRS at 50 Hz are more conservative than their corresponding benchmark tRS.

Vertical GRS: From Figure 4.25, the following observations can be made.

- tRS estimated by the vertical statistical relationship closely match the benchmark tRS over the frequency ranges from 0.3 to 4 Hz and from 8 to 25 Hz for 50% NEP, from 0.3 to 3 Hz and from 10 to 25 Hz for 84.1% NEP. The estimated tRS are conservative from 4 to 8 Hz for 50% NEP and from 3 to 10 Hz for 84.1% NEP.
- tRS with 50% and 84.1% NEP estimated by the vertical statistical relationship are somewhat below their benchmark tRS from 25 to 50 Hz, due to the special variation of AR over this frequency range as seen in Figure 4.6. The adjusted tRS by linearly connecting tRS at 25 and 50 Hz are more conservative than their corresponding benchmark tRS.

Comparison between Figures 4.24 and 4.25 reveals that the estimated horizontal tRS match the benchmark tRS better than the estimated vertical tRS do. This is because the horizontal design spectra in USNRC R.G. 1.60 was developed using 33 horizontal real ground motions (Blume, Sharpe, and Dalal, 1973; Newmark, Blume, and Kapur, 1973A; USNRC, 2014); whereas the vertical design spectra in USNRC R.G. 1.60 was obtained by empirically adjusting amplification factors of horizontal design spectra (USNRC, 2014), which may not fully reflect the characteristics of vertical ground motions. Because the vertical statistical relationships are established using real vertical ground motions in this study, discrepancy between estimated vertical tRS and benchmark vertical tRS cannot be avoided.

From this example, it is concluded that the horizontal and vertical statistical relationships between tRS and GRS developed in this study are acceptable in practice to estimate tRS and generate FRS for GRS falling within the valid coverage of the statistical relationship.

Example 2 – Standard UHS for CENA

The 5% standard UHS proposed by Atkinson and Elgohary (Atkinson and Elgohary, 2007) for CENA sites is taken as the horizontal GRS. 30 time histories compatible with the standard UHS are generated following the requirements of CSA N289.3 (CSA, 2010) using the Hilbert-Huang Transform method (Ni, Xie, and Pandey, 2011; Ni, Xie, and Pandey, 2013). As

shown in Figure 4.26, GRS of the 30 generated time histories closely match the target UHS. tRS of the 30 time histories are calculated; tRS with 50% and 84.1% NEP are statistically calculated and used as benchmarks, as shown in Figure 4.26.

It is clearly seen that the standard UHS dose not fall within the valid coverage of the horizontal statistical relationship in the high frequency range. Thus, the horizontal statistical relationship cannot be used to estimate tRS corresponding to the standard UHS; the amplification ratio method proposed in Section 4.6.2.2 is applied to estimate tRS. From Figure 4.26, the following observations can be made.

- The estimated tRS with 50% and 84.1% NEP match their corresponding benchmark tRS almost within a 5% relative error over the frequency range from 1 to 25 Hz, which is important for structures and components of nuclear power plants.
- The estimated tRS with 50% and 84.1% NEP match their corresponding benchmark tRS very well over the frequency range from 50 HZ to 100 Hz.
- The estimated tRS with 84.1% NEP is generally conservative in comparison with the benchmark tRS over the frequency range from 0.2 to 50 Hz.
- The estimated tRS with 50% and 84.1% NEP are larger than the corresponding benchmark tRS over the frequency range from 33 to 50 Hz for 50% NEP tRS, and over the frequency range from 25 to 50 Hz for 84.1% NEP tRS. However, the effect of this conservatism on FRS is negligible for structures and equipment in nuclear power plants (USNRC, 2007B).

The amplification ratios obtained from the amplification ratio method and calculated from 30 UHS-compatible time histories are presented in Figure 4.27. The 50% and 84.1% amplification ratios from 30 time histories are obtained by statistical calculation using the ratios of 30 tRS to the UHS. The small discrepancies between amplification ratios from the amplification ratio method and from the 30 UHS-compatible time histories cause the discrepancies between the estimated and the benchmark tRS in Figure 4.26.

From this example, it is concluded that the amplification ratio method developed in this study is acceptable to estimate tRS and to generate FRS for nuclear power facilities under

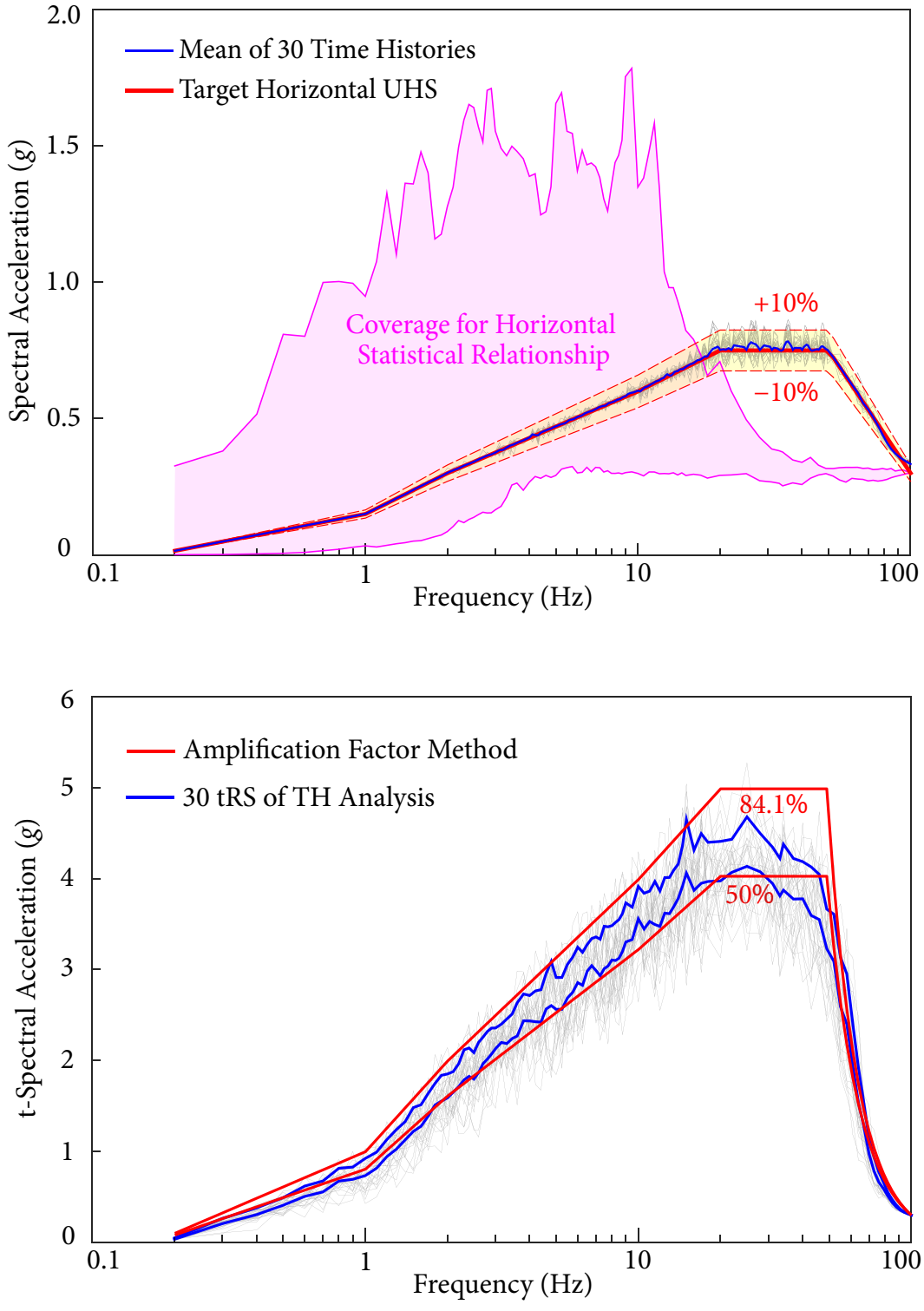

Figure 4.26 Comparison between horizontal tRS and UHS

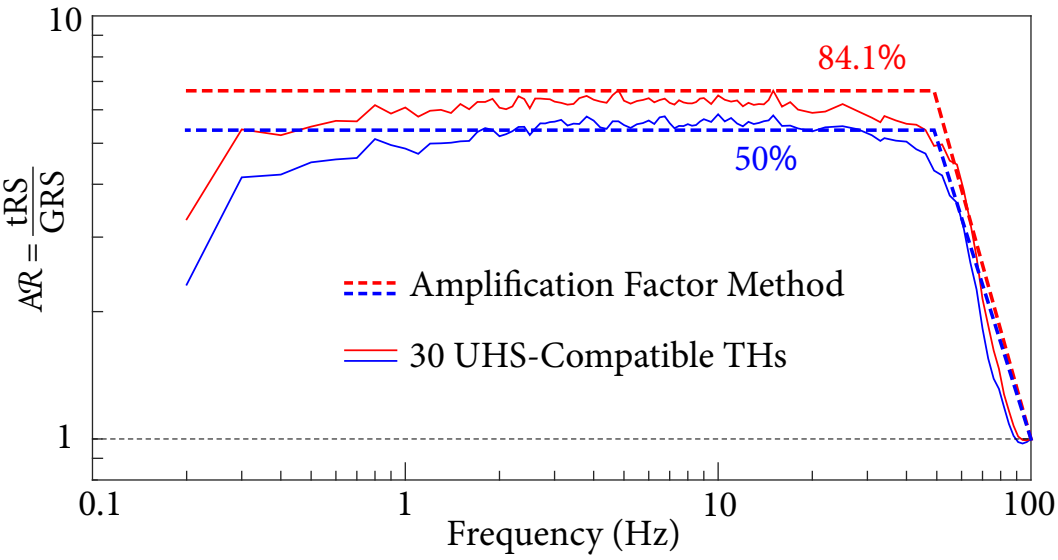

Figure 4.27 Amplification ratios of tRS corresponding to UHS

prescribed UHS with significant high frequency spectral accelerations, such as UHS in CENA.

4.8 Summary

In this chapter, the concept of t-response spectrum (tRS) is proposed. When generating probabilistic FRS considering the uncertainty from ground motions by the direct spectra-to-spectra method, statistical relationship between tRS and GRS is required.

Procedure for establishing the statistical relationship between tRS and GRS is discussed first. Because the trend of amplification ratio $AR = \mathcal{S}_A^t(f,\zeta)/\mathcal{S}_A(f,\zeta)$ is different for horizontal and vertical ground motions, horizontal and vertical statistical relationships are established separately using horizontal and vertical ground motions, respectively. Using a total of 451 horizontal and 437 vertical ground motions observed at different site categories, horizontal and vertical statistical relationships between tRS and GRS are established. For easy application of statistical relationships to generate FRS in practice, simplified statistical relationships are developed.

Simulation results show that the influence of site conditions on horizontal statistical relationship is negligible, whereas the influence of site conditions on vertical statistical relationship cannot be ignored. Thus, horizontal statistical relationship applicable to all site categories, and vertical statistical relationships applicable to hard sites and soft sites are constructed for various damping ratios. Through regression analysis, general equations for statistical relationships applicable to damping ratios less than 20% are established.

The horizontal and vertical statistical relationships developed in this study are suitable to estimate tRS for design spectra in USNRC R.G. 1.60 and NUREG/CR-0098, UHS in WNA, and any GRS falling inside the valid coverage of statistical relationships.

For UHS with significant high frequency spectral accelerations, such as those in CENA, they may fall outside the valid coverage of statistical relationships, especially for high frequencies. In such cases, the amplification ratio method is proposed to estimate tRS.

This chapter also presents complete statistical results for estimating tRS corresponding to any specified GRS. Two numerical examples demonstrate that the statistical relationships and the amplification ratio method give estimates of tRS either with very small errors or on the conservative side compared with benchmark tRS. The effective estimation of tRS, together with the direct spectra-to-spectra method, provides an efficient and accurate approach to generate probabilistic FRS considering the uncertainty from ground motions in various practical situations.

CHAPTER 5

Conclusions and Future Research

Performance-based seismic design (P-BSD) has been widely implemented in engineering. In P-BSD, an accurate and reliable prediction of failure probability of designing structures is required to obtain a most economic solution. To accurately predict failure probability of designing structures, accurate and realistic prediction of structure responses, for which realistic and reliable input response spectrum is an essential prerequisite, is required. Considering the problems with constructing input response spectrum, this study focuses on bridging the gap between P-BSD for nuclear facilities and realistic design response spectra. Several contributions for this objective have been made in this study, summarized as follows.

5.1 Modify Newmark Design Spectrum

Previous studies showed that Newmark design spectra exhibit lower amplitudes at high frequencies and higher amplitudes at low frequencies. Unreliable failure probability may be obtained if the Newmark design spectrum is used as design ground response spectrum to do P-BSD of structures or facilities standing on a target site, because the Newmark design spectrum may not represent the realistic earthquake characteristics of the site.

Using a wide range of ground motions recorded at three types of sites, i.e., B sites, C sites, and D sites, this study establishes a system of site design spectrum coefficients considering earthquake magnitudes and site categories. Using the site design spectrum coefficients to

modify the Newmark design spectrum resolves the problem of Newmark design spectrum. In this study, some conclusions are also drawn:

- Influences of the parameter V_{s30} on the ratios v/a and ad/v^2 are negligible, which may be due to the fact that V_{s30} is a weak proxy to seismic amplification of sites.
- Influence of source-to-site distance R on the ratios v/a and ad/v^2 is small, while the influence of earthquake magnitude M on these ratios is remarkable. The study also shows that the ratios v/a and ad/v^2 for large earthquakes ($M > 6$) are greater than those for small earthquakes ($M \leqslant 6$).
- For the same site category and damping ratio, spectrum amplification factors of large earthquakes are greater than those of small earthquakes except a few cases with high damping ratios. This further verifies the significant magnitude bias of spectrum amplification factors in Newmark's study.
- The ratios of the estimated spectral bounds to the spectral bounds for Newmark design spectra are calculated for different site categories and various damping ratios. It is found that the ratios are almost independent of damping values.

Examples of 5% damping-ratio Newmark design spectra and the modified Newmark design spectra by different coefficients at the non-exceedance level of 84.1% with PGA anchored at $0.3g$ are constructed. Discussions from these examples show that:

- For sites dominated by small earthquakes, Newmark design spectra and the modified Newmark design spectra by the coefficients in Mohraz's study are too conservative in the intermediate and the low frequency regions.
- For all site categories and earthquake magnitudes, Newmark design spectra tend to be lower at high frequencies and higher at low frequencies.
- For sites dominated by large earthquakes, the modified Newmark design spectra by coefficients in Mohras's study tend to be lower in the intermediate frequency region.
- The modified Newmark design spectra by coefficients in this study can better match the benchmark response spectra, especially for spectral values in the acceleration sensitive and the velocity sensitive regions. This is crucial because the fundamental frequencies of many critical structures fall within these two regions.

5.2 Propose Framework to Construct Soil UHS

This study also proposes a probabilistic framework to construct UHS at the soil surface. In this framework, the soil parameter variabilities, the nonlinear property of soils, and the vector-valued seismic site responses analysis comprehensively integrate into PSHA for soil sites. Using the probabilistic framework, reliable soil UHS can be constructed. Based on one example in this study, some conclusions are obtained:

- Spectral shapes and spectral amplitudes of rock UHS are greatly different from those of soil UHS. The rock UHS reflect characteristics of ground motions propagating from seismic sources to bedrock, while the soil UHS reflect characteristics of ground motions propagating from seismic sources to bedrock then to soil surface. Thus, the difference is caused by effects of the local soil deposit.
- The nonlinear responses of soils cannot be neglected, which could substantially affect spectral amplitudes and spectral shapes of the soil UHS.
- Seismic sources dominate the variability of the results of PSHA for soil sites, but the contribution of soil parameter variabilities should not be neglected, which could also affect spectral shapes and spectral amplitudes of UHS.
- The soil UHS may be constructed by the GMPEs which use the generic soil to roughly characterize the local soil conditions. However, the significant difference between the soil UHS by the modified GMPEs (base case) and the soil UHS by GMPEs (base case) shows that constructing soil UHS by GMPEs using the generic soil is not acceptable in practice.

5.3 Response Spectra for Equipment-Structure Resonance

This study proposes the concept of t-response spectrum. Contribution of the tuning cases to the uncertainty of FRS is studied, and the statistical relationship between tRS and GRS is established using a large number of ground motions recorded at different categories of sites. The statistical relationship between tRS and GRS is required to construct probabilistic FRS

considering the uncertainty from ground motions by the direct spectra-to-spectra method. Some conclusions are obtained from this study:

- Influence of site conditions on horizontal statistical relationship is negligible, whereas effect of site conditions on vertical statistical relationship cannot be ignored. Considering the influence of site conditions, horizontal statistical relationship suitable for all site conditions and vertical statistical relationships suitable for hard sites and soft sites are established, respectively.
- The horizontal and vertical statistical relationships are suitable to estimate tRS corresponding to design response spectra in USNRC R.G. 1.60 and NUREG/CR-0098, UHS in WNA, or any GRS falling inside the valid coverage of the statistical relationship.
- For UHS with significant high frequency spectral accelerations, such as UHS in CENA, the amplification ratio method deriving from the statistical relationship between tRS and GRS should be used.

Two numerical examples in this study demonstrate that the statistical relationships and the amplification ratio method give estimates of probabilistic tRS either with very small errors or on the conservative side compared with benchmark tRS. Using the statistical relationships between tRS and GRS developed in this study, the probabilistic FRS considering the uncertainty from ground motions could be generated using the direct spectra-to-spectra method with high efficiency.

5.4 Future Research

In seismic response analysis of structures or facilities, two methods are mainly used: the response spectrum analysis and the time history analysis. Advantages of the time history analysis are remarkable: it can analyze nonlinear seismic responses, consider the influence of phasing characteristics of ground motions on structural responses, and analyze irregular and high structures. Thus, the time history analysis is usually used in seismic design and analysis of structures, especially for critical structures, such as nuclear buildings.

In time history analysis, time histories spectrum-compatible with design response spectrum are required. Further studies need to study how to generate time histories compatible

with the design response spectrum, such as the modified Newmark design spectrum, soil UHS, and the probabilistic floor response spectrum.

Bibliography

Abrahamson, N. A. and Silva, W. J., 1997. Empirical response spectral attenuation relations for shallow crustal earthquakes. *Bulletin of the Seismological Society of America*, **68**(1), 94–127.

Adam, C. and Fotiu, P. A., 2000. Dynamic analysis of inelastic primary-secondary systems. *Engineering Structures*, **22**(1), 58–71.

Ambraseys, N., Smit, P., Douglas, J., *et al.*, 2004. Internet site for European strong-motion data. *Bollettino di Geofisica Teorica ed Applicata*, **45**(3), 113–129.

Ambraseys, N., Smit, P., Sigbjornsson, R., *et al.*, 2002. *Internet Site for European Strong-motion Data*. European Commission, Research-Directorate General, Environment and Climate Programme.

Amick, D. and Gelinas, R., 1991. The search for evidence of large prehistoric earthquakes along the atlantic seaboard. *Science*, **251**(4994), 655–658.

Anderson, J. C. and Trifunac, M. D., 1977. Uniform risk absolute acceleration spectra. *Advances in Civil Engineering through Engineering Mechanics, ASCE*, 332–335.

Anderson, J. G. and Trifunac, M. D., 1978. Uniform risk functionals for characterization of strong earthquake ground motion. *Bulletin of the Seismological Society of America*, **68**(1), 205–218.

Andrus, R. D., Zhang, J., Ellis, B. S., *et al.*, 2003. *Guide for Estimating the Dynamic Properties of South Carolina Soils for Ground Response Analysis*. Clemson University, Clemson, SC.

ANS, 2004. *Categorization of Nuclear Facility Structures, Systems, and Components for Seismic Design, Standard* ANSI/ANS-2.26. American Nuclear Society Standards Committee, La Grange Park, Illinois.

ANS, 2008. *American National Standard Probabilistic Seismic Hazards Analysis, Standard* ANSI/ANS-2.29-2008. American Nuclear Society, Illinois, USA.

Ardakan, S. T., 2006. *Probabilistic Seismic Assessment of Floor Acceleration Demands in Multi-Story Buildings*. PhD thesis, Stanford University.

ASCE, 2000. *Seismic Analysis of Safety-related Nuclear Structures and Commentary, Standard* ASCE 4-98. American Society of Civil Engineers, Reston, Virginia.

ASCE, 2005. *Seismic Design Criteria for Structures, Systems, and Components in Nuclear Facilities, Standard* ASCE/SEI 43-05. American Society of Civil Engineers, Reston, Virginia.

ASCE, 2010. *Minimum Design Loads for Buildings and Other Structures, Standard* ASCE/SEI 7-10. American Society of Civil Engineers, Reston, Virginia.

Asfura, A. and Kiureghian, A. D., 1986. Floor response spectrum method for seismic analysis of multiply supported secondary systems. *Earthquake Engineering and Structural Dynamics*, **14**(2), 245–265.

ASTM, 2011. *D2487 Standard Practice for Classification of Soils for Engineering Purposes (Unified Soil Classification System), Standard* ASTM D2487. American Society for Testing and Materials International, West Conshohocken, PA.

ATC, 1996. *Seismic Evaluation and Retrofit of Concrete Buildings, Standard* ATC-40. Applied Technology Council, Redwood City, California.

Atkinson, G. M. and Elgohary, M., 2007. Typical uniform hazard spectra for eastern north american sites at low probability levels. *Canadian Journal of Civil Engineering*, **34**(1), 12–18.

Baker, J. W. and Cornell, C. A., 2006. Spectral shape, epsilon and record selection. *Earthquake Engineering and Structural Dynamics*, **35**(9), 1077–1095.

Baker, J. W. and Jayaram, N., 2009. Correlation of spectral acceleration values from NGA ground motion models. *Earthquake Spectra*, **24**(1), 299–317.

Baker, J. W., 2010. Conditional mean spectrum: Tool for ground motion selection. *Journal of Structural Engineering*, **137**(3), 322–331.

Bazzurro, P. and Cornell, C. A., 2004A. Ground-motion amplification in nonlinear soil sites with uncertain properties. *Bulletin of the Seismological Society of America*, **94**(6), 2090–2109.

Bazzurro, P. and Cornell, C. A., 2004B. Nonlinear soil-site effects in probabilistic seismic-hazard analysis. *Bulletin of the Seismological Society of America*, **94**(6), 2110–2123.

Bertero, V. V., 1992. Major issues and future directions in earthquake-resistant design. In *Proceedings of the 10th World Conference on Earthquake Engineering*, Madrid, Spain.

Bertero, V. V., 2000. Performance-based seismic engineering: conventional vs. innovative approaches. In *Proceedings of the 12th World Conference on Earthquake Engineering*, volume 2074, New Zeeland.

Biot, B. A., 1941. A mechanical analyzer for the prediction of earthquake stresses. *Bulletin of the Seismological Society of America*, **31**(2), 151–171.

Biot, M. A., 1933. Theory of elastic systems vibrating under transient impulse with an application to earthquake-proof buildings. *Proceedings of the National Academy of Sciences of the United States of America*, **19**(2), 262–268.

Blume, J. A., Sharpe, R. L., and Dalal, J. S., 1973. *Recommendations for Shape of Earthquake Response Spectra,* WASH-1254. U.S. Atomic Energy Commission, Washington D.C.

Bommer, J. J. and Acevedo, A. B., 2004. The use of real earthquake accelerograms as input to dynamic analysis. *Journal of Earthquake Engineering*, **8**(S1), 43–91.

Boore, D. M. and Atkinson, G. M., 2008. Ground-motion prediction equations for the average horizontal component of PGA, PGV, and 5%-damped PSA at spectral periods between 0.01 s and 10.0 s. *Earthquake Spectra*, **24**(1), 99–138.

Bozorgnia, Y. and Bertero, V. V., 2004. *Earthquake Engineering: from Engineering Seismology to Performance-based Engineering.* CRC press, Boca Raton, Florida.

Campbell, K. W. and Bozorgnia, Y., 2003. Updated near-source ground-motion (attenuation) relations for the horizontal and vertical components of peak ground acceleration and acceleration response spectra. *Bulletin of the Seismological Society of America*, **93**(1), 314–331.

Castellaro, S., Mulargia, F., and Rossi, P. L., 2008. Vs30: Proxy for seismic amplification? *Seismological Research Letters*, **79**(4), 540–543.

Chopra, A. K., 2011. *Dynamics of Structures*. Prentice Hall New Jersey, New Jersey, United States.

Clough, R. W. and Penzien, J., 2003. *Dynamics of Structures (third edition)*. Computers and Structures, Inc., Berkeley, CA.

Committee, SEAOC Vision 2000, 1995. *Performance Based Seismic Engineering of Buildings*. Structural Engineers Association of California, Sacramento, California.

Cornell, C. A. and Krawinkler, H., 2000. Progress and challenges in seismic performance assessment. *PEER Center News*, **3**(2), 1–4.

Cornell, C. A., 1968. Engineering seismic risk analysis. *Bulletin of the Seismological Society of America*, **58**(5), 1583–1606.

Cramer, C. H., 2003. Site-specific seismic-hazard analysis that is completely probabilistic. *Bulletin of the Seismological Society of America*, **93**(4), 1841–1846.

CSA, 2010. *Design Procedures for Seismic Qualification of Nuclear Power Plants, Standard* CSA-N289.3-10. Canadian Standard Association (CSA), Mississauga, Ontario.

DOE, 2002. *Natural Phenomena Hazards Assessment Criteria, Standard* DOE-STD-1023-2002. U.S. Department of Energy, Washington D.C.

Dunbar, W. S. and Charlwood, R. G., 1991. Empirical methods for the prediction of response spectra. *Earthquake Spectra*, **7**(3), 333–353.

EPRI, 1986. *Seismic Hazard Methodology for the Central and Eastern United States,* EPRI NP-4726. Electric Power Research Institute, Palo Alto, California.

Faccioli, E., Santoyo, E., and Leon, J. L., 1973. Microzonation criteria and seismic response studies for the city of managua. In *Proceedings of Earthquake Engineering Research Institute: Managua, Nicaragua, Earthquake of December*, volume 23, 271–291.

FEMA, 1997. *NEHRP Guidelines for the Seismic Rehabilitation of Buildings, Standard* FEMA 273. Federal Emergency Management Agency, Washington D.C.

FEMA, 2000. *Prestandard and Commentary for the Seismic Rehabilitation of Buildings, Standard* FEMA 356. Federal Emergency Management Agency, Washington D.C.

Goltz, J. D., 1994. The northridge, california earthquake of january 17, 1994: General reconnaissance report. In *Technical Report NCEER*, number 94-0005. US National Center for Earthquake Engineering Research.

Green, R. A., Gunberg, K., Parrish, K., *et al.*, 2007. A simple uniform hazard design spectral shape for rock sites. *Seismological Research Letters*, **78**(2), 323–343.

Halchuk, S. and Adams, J., 2004. Deaggregation of seismic hazard for selected Canadian cities. In *Proceedings of the 13th World Conference on Earthquake Engineering*, Vancouver, Canada.

Hall, W. J., Mohraz, B., and Newmark, N. M., 1976. *Statistical Studies of Vertical and Horizontal Earthquake Spectra,* NUREG-0003. U.S. Nuclear Regulatory Commission, Urbana, Illinois.

Hall, W. J., 1982. Observations on some current issues pertaining to nuclear power plant seismic design. *Nuclear Engineering and Design*, **69**(3), 365–378.

Hancock, J. and Bommer, J. J., 2007. Using spectral matched records to explore the influence of strong-motion duration on inelastic structural response. *Soil Dynamics and Earthquake Engineering*, **27**(4), 291–299.

Hashash, Y. M. A., Groholski, D. R., Phillips, C. A., *et al.*, 2011. *DEEPSOIL 5.0, User Manual and Tutorial.* University of Illinois at Urbana-Champaign, Champaign, Illinois.

Hashash, Y. M. A. and Park, D., 2001. Nonlinear one-dimensional seismic ground motion propagation in the mississippi embayment. *Engineering Geology*, **62**(1), 185–206.

Housner, G. W., 1959. Behavior of structures during earthquakes. *Journal of the Engineering Mechanics Division, ASCE*, **85**(EM4), 109–129.

Housner, G. W., 1970. *Design Spectrum*. Prentice-Hall, Inc., Englewood Cliffs, New Jersey.

IBC, 2000. *2000 International Building Code*. International Code Council, Falls Church, Virginia.

IBC, 2012. *2012 International Building Code*. International Code Council, Washington D.C.

Idriss, I. M., Dobry, R., and Sing, R. D., 1978. Nonlinear behavior of soft clays during cyclic loading. *Journal of Geotechnical and Geoenvironmental Engineering*, **104**(ASCE 14265), 1427–1447.

Igusa, T. and Kiureghian, A. D., 1985. Generation of floor response spectra including oscillator-structure interaction. *Earthquake Engineering and Structural Dynamics*, **13**(5), 661–676.

Iwan, W. D., 1967. On a class of models for the yielding behavior of continuous and composite systems. *Journal of Applied Mechanics*, **34**(3), 612–617.

Jayaram, N. and Baker, J. W., 2008. Statistical tests of the joint distribution of spectral acceleration values. *Bulletin of the Seismological Society of America*, **98**(5), 2231–2243.

Jeanpierre, F. and Livolant, M., 1977. Direct calculation of floor response spectra from the fourier transform of ground movement-application to the superphenix fast reactor project. *Nuclear Engineering and Design*, **41**(1), 45–51.

Johnson, R. A., 1991. *Applied Multivariate Statistical Analysis*. Springer-Verlag, New York.

Kappos, A., 2001. *Dynamic Loading and Design of Structures*. CRC Press, New York.

Kennedy, R. P., 1984. *Engineering Characterization of Ground Motion-Task I,* NUREG/CR-3805. U.S. Nuclear Regulatory Commission, Washington D.C.

Kennedy, R. P., 1989. *Comments on Proposed Revisions to Standard Review Plan Seismic Provisions*. Brookhaven National Laboratory, Upton, New York.

Kondner, R. L., 1963. *A Hyperbolic Stress-Strain Formulation for Sands*. Northwestern University, Evanston, Illinois.

Kramer, S. L., 1996. *Geotechnical Earthquake Engineering*. Prentice-Hall, New Jersey.

Lee, V. M. and Trifunac, M. D., 2010. Should average shear-wave velocity in the top 30 m of soil be used to describe seismic amplification? *Soil Dynamics and Earthquake Engineering*, **30**(11), 1250–1258.

Lilhanand, K., Wing, D. W., and Tseng, W. S., 1985. Systematic evaluations of probabilistic floor response spectrum generation. In *Proceedings of the 8th International Conference on Structural Mechanics in Reactor Technology*, Brussels, Belgium.

Li, B., Ni, S-H., Xie, W-C., and Pandey, M. D., 2012. Probabilistic seismic hazard analysis considering nonlinear soil effects and variability of soil parameters. In *Proceedings of the 22nd International Conference on Structural Mechanics in Reactor Technology*, San Francisco, California, USA.

Li, W., 2010. *Nonlinear Effects in Ground Motion Simulations: Modeling Variability, Parametric Uncertainty and Implications in Structural Performance Predictions*. Ph. D. thesis, Georgia Institute of Technology.

Lumb, P., 1966. The variability of natural soils. *Canadian Geotechnical Journal*, **3**(2), 74–97.

Malhotra, P. K., 2006. Smooth spectra of horizontal and vertical ground motions. *Bulletin of the Seismological Society of America*, **96**(2), 506–518.

McGuire, R. K., Silva, W. J., and Costantino, C. J., 2001. *Technical basis for Revision of Regulatory Guidance on Design Ground Motions: Hazard- and Risk-Consistent Ground Motion Spectra Guidelines,* NUREG/CR-6728. U.S. Nuclear Regulatory Commission, Washington D.C.

McGuire, R. K., 1995. Probabilistic seismic hazard analysis and design earthquakes: closing the loop. *Bulletin of the Seismological Society of America*, **85**(5), 275–1284.

Mohraz, B., 1976. A study of earthquake response spectra for different geological conditions. *Bulletin of the Seismological Society of America*, **66**(3), 915–935.

Mohraz, B., 1978. Comments on earthquake response spectra. *Nuclear Engineering and Design*, **45**(2), 489–495.

Mohraz, B., 1992. Recent studies of earthquake ground motion and amplification. In *Proceedings of the Tenth World Conference on Earthquake Engineering*, volume 11, 6695–704.

Neter, J., Kutner, M., Wasserman, W., *et al.*, 1996. *Applied Linear Regression Models*. McGraw-Hill, Chicago, Illinois.

Newmark, N. M., Blume, J. A., and Kapur, K. K., 1973A. Seismic design spectra for nuclear power plants. *Journal of the Power Division*, **99**(2), 287–303.

Newmark, N. M., Hall, W. J., and Mohraz, B., 1973B. *A Study of Vertical and Horizontal Earthquake Spectra*. U.S. Atomic Energy Commission, Washington D.C.

Newmark, N. M. and Hall, W. J., 1978. *Development of Criteria for Seismic Review of Selected Nuclear Power Plants,* NUREG/CR-0098. Newmark Consulting Engineering Services, Urbana, Illinois.

Newmark, N. M. and Hall, W. J., 1982. *Earthquake Spectra and Design*. Earthquake Engineering Research Institute, Berkeley, California.

Newmark, N. and Hall, W. J., 1969. Seismic design criteria for nuclear reactor facilities. In *Proceedings 4th World Conference on Earthquake Engineering, Santiago, Chile*, volume 4, 37–50.

Ni, S-H., Xie, W-C., and Pandey, M. D., 2011. Tri-directional spectrum-compatible earthquake time-histories for nuclear energy facilities. *Nuclear Engineering and Design*, **241**(8), 2732–2743.

Ni, S-H., Xie, W-C., and Pandey, M. D., 2013. Generation of spectrum-compatible earthquake ground motions considering intrinsic spectral variability using Hilbert-Huang transform. *Structural Safety*, **42**, 45–53.

Ni, S. H., Zhang, D. Y., Xie, W. C., and Pandey, M. D., 2012. Vector-valued uniform hazard spectra. *Earthquake Spectra*, **28**(4), 1549–1568.

ONR, 2014. *Nuclear Safety Technical Assessment Guide, Standard* NS-TAST-GD-013. Office for Nuclear Regulation, United Kingdom.

Padgett, J. E. and DesRoches, R., 2007. Sensitivity of seismic response and fragility to parameter uncertainty. *Journal of Structural Engineering*, **133**(12), 1710–1718.

Paskalov, A. and Reese, S., 2003. Deterministic and probabilistic floor response spectra. *Soil Dynamics and Earthquake Engineering*, **23**(7), 605–618.

PEER, 2010. *Report for the PEER Ground Motion Database Web Application*. Pacific Earthquake Engineering Research Center, Berkeley, California.

Petersen, M. D., Frankel, A. D., Harmsen, S. C., *et al.*, 2008. *Documentation for the 2008 Update of the United States National Seismic Hazard Maps*. U.S. Geological Survey, Reston, Virginia.

Regnier, J., Bonilla, F., and Bertrand, E., 2008. Variability of one-dimensional soil amplification estimates at four sites of the French permanent accelerometer network (RAP). In *Proceedings of the 14th World Conference on Earthquake Engineering*, Beijing, China.

Riddell, R. and Newmark, N. M., 1979. *Statistical Analysis of the Response of Nonlinear Systems Subjected to Earthquakes*. Department of Civil Engineering, University of Illinois at Urbana-Champaign, Urbana, Illinois.

Ritcher, C. F. Elementary seismology, 1958.

Rogers, J. D., Karadeniz, D., and Chung, J. W., 2007. The effect of site conditions on amplification of ground motion in the St. Louis area. In *Proceedings of the 4th International Conference on Earthquake Geotechnical Engineering*, Thessaloniki, Greece.

Scanlan, R. H., 1974. Earthquake time histories and response spectra. *Journal of the Engineering Mechanics Division*, **100**(4), 635–655.

Seifried, A. E. and Baker, J. W., 2014. Spectral variability and its relationship to structural response estimated from scaled and spectrum-matched ground motions. In *Proceedings of the Tenth U.S. National Conference on Earthquake Engineering*, Anchorage, Alaska.

Silva, W. J., Youngs, R. R., and Idriss, I. M., 1999. Development of design response spectral shapes for Central and Eastern US (CEUS) and Western US (WUS) rock site conditions. In *Proceedings of the OECE-NEA Workshop on Engineering Characterization of Seismic Input*, 15–17.

Singh, M. P., 1975. Generation of seismic floor spectra. *Journal of the Engineering Mechanics Division*, **101**(5), 593–607.

Singh, M. P., 1980. Seismic design input for secondary systems. *Journal of the Engineering Mechanics Division*, **106**(2), 505–517.

SPC, 1997. *Code for Seismic Design of Nuclear Power Plants, Standard* GB 50276-97. Standards Press of China, Beijing, P. R. China.

Stewart, J. P., Chiou, S-J, Bray, J. D., *et al.*, 2001. *Ground Motion Evaluation Procedures for Performance-Based Design*. Pacific Earthquake Engineering Research Center, University of California, Berkeley.

Streeter, V. L., Wylie, E. B., and Richart, F. E., 1974. Soil motion computations by characteristics method. *Journal of the Geotechnical Engineering Division*, **100**(3), 247–263.

Talwani, P. and Cox, J., 1985. Paleoseismic evidence for recurrence of earthquakes near charleston, south carolina. *Science*, **229**(4711), 379–381.

Toro, G. R., 1993. *Probabilistic Model of Soil-profile Variability*. Electric Power Research Institute, Palo Alto, California.

Trifunac, M. D., 1976. Preliminary empirical model for scaling fourier amplitude spectra of strong ground acceleration in terms of earthquake magnitude, source-to-station distance, and recording site conditions. *Bulletin of the Seismological Society of America*, **66**(4), 1343–1373.

Trifunac, M. D., 1989. Dependence of fourier spectrum amplitudes of recorded earthquake accelerations on magnitude, local soil conditions and on depth of sediments. *Earthquake Engineering and Structural Dynamics*, **18**(7), 999–1016.

Tsai, C. C. P., 2000. Probabilistic seismic hazard analysis considering nonlinear site effect. *Bulletin of the Seismological Society of America*, **90**(1), 66–72.

USNRC, 1978. *Development of Floor Design Response Spectra for Seismic Design of Floor-supported Equipment or Components, Standard* R.G. 1.122. U.S. Atomic Energy Commission, Washington D.C.

USNRC, 1994. *Revised Livermore Seismic Hazard Estimates for Sixty-Nine Nuclear Power Plant Sites East of the Rocky Mountains,* NUREG-1488. U.S. Nuclear Regulatory Commission, Washington D.C.

USNRC, 1997. *Identification and Characterization of Seismic Sources and Determination of Safe Shutdown Earthquake Ground Motion, Standard* NUREG R.G. 1.165. U.S. Nuclear Regulatory Commission, Washington D.C.

USNRC, 2007a. *A Performance-based Approach to Define the Site-specific Earthquake Ground Motion, Standard* NUREG R.G. 1.208. U.S. Nuclear Regulatory Commission, Washington D.C.

USNRC, 2007b. *Standard Review Plan-Seismic Design Parameters, Standard* SRP 3.7.1. U.S. Nuclear Regulatory Commission, Washington D.C.

USNRC, 2007c. *Standard Review Plan-Seismic System Analysis, Standard* SRP 3.7.2. U.S. Nuclear Regulatory Commission, Washington D.C.

USNRC, 2014. *Design Response Spectra for Seismic Design of Nuclear Power Plants, Standard* NUREG R.G. 1.60 (Revision 2). U.S. Nuclear Regulatory Commission, Washington D.C.

Villaverde, R., 1997. Seismic design of secondary structures: state of the art. *Journal of Structural Engineering*, **123**(8), 1011–1019.

Villaverde, R., 2009. *Fundamental Concepts of Earthquake Engineering*. CRC Press, Baton Raton, Florida.

Wills, C. J., Petersen, M., Bryant, W. A., *et al.*, 2000. A site-conditions map for california based on geology and shear-wave velocity. *Bulletin of the Seismological Society of America*, **90**(6B), S187–S208.

Zhang, J., Andrus, R. D., and Juang, C. H., 2005. Normalized shear modulus and material damping. *Journal of Geotechnical and Geoenvironmental Engineering*, **131**(1), 453–464.